# Large scale dynamics of integrable systems

Yoshimura, Takato

*Awarding institution:*
King's College London

# Large scale dynamics of integrable systems


Takato Yoshimura
King's College London

A thesis submitted for the degree of *Doctor of Philosophy*

February, 2020

# Abstract

In this thesis, we consider a hydrodynamic approach to study the out-of-equilibrium dynamics of integrable systems, termed generalized hydrodynamics (GHD). The theory goes beyond the conventional hydrodynamics by accounting for an infinite number of conserved charges in integrable systems. This seemingly formidable task is achieved by making use of Thermodynamic Bethe ansatz, whereby the hydrodynamic equations are cast into continuity equations for the distribution of quasi-particles. The idea is then illustrated using a particular nonequilibrium protocol through which the power of GHD becomes evident. Subsequently we explore several aspects of GHD, which includes the equivalence between GHD and hydrodynamics of certain classical systems, and also the application of GHD to low-temperature dynamics. An analytical derivation of one of the key ingredients in GHD will also be provided.

# Acknowledgements

First and foremost of all, my deepest gratitude goes to my supervisor, Benjamin Doyon. You are the person who taught me aesthetics we need to have if we wish to do good works in theoretical physics. Having had you as my supervisor is one of the luckiest things that have happened to my life, and I am truly grateful for it.

I was also greatly benefited by my visit at IPhT Saclay in 2018, and would like to thank Hubert Saleur for hosting me. It has also been a pleasure to work and interact with my fellow colleagues and friends there, in particular with Kemal Bidzhiev and Dinh-Long Vu.

# Contents

# Chapter 1

# Introduction

When we want to study properties of a many-body system, it is always tempting to think that we can understand it by decomposing the system into elementary constituents and investigate them. This kind of approach or attitude in understanding physical substances is called *reductionism*, and is the fundamental philosophy in elementary particle physics. Reductionism approach has yielded unquestionable depth and scope of insights into physics, but in fact is not always the best way to decipher physical phenomena. For instance, it is typically not able to characterize *emergent phenomena* [1] of the matter, which are in general caused by constituent matters (e.g. excitations) behave collectively in an emergent fashion, and consequently present novel properties that are not predictable by merely looking at those elementary components of the system. Those emergent phenomena that could be overlooked by reductionism might be instead captured by looking at the system from the macroscopic point of view. This perspective is particularly useful when we study physical systems that are in equilibrium, in which situation all the configurations of elementary constituents are expected to be realized in the equal probability whenever their energies are the same. This allows the system as a whole to be treated as a statistical ensemble (i.e. stationary measure under the time-evolution), and forms the foundation of statistical mechanics. This principle turns out to be generically applicable to any systems with a large degrees of freedom at equilibrium, and has served as a universal tool in dealing with such systems since it was initiated by Boltzmann in 19th century.

Once the system departs from equilibrium, however, the situation becomes drastically different. Statistical mechanics is no longer able to predict physical properties of the system, and case-by-case investigations are needed. In general, barring some exceptions[1], it is believed that there is no universal prescription to deal with out-of-equilibrium systems in the sense of statistical mechanics, and exact results are hard to obtain, despite of

[1]It would be worth mentioning that, in fact, we have a rather powerful tool to study nonequilibrium steady states in a universal way called *macroscopic fluctuation theory* [2]. This theory is primarily developed for driven diffusive systems, and is able to predict fluctuations of the system from its hydrodynamics.

ubiquity of far from equilibrium situations. That said so, it is still highly desired to establish concrete understandings on how many-body systems relax to stationary states, and see if the resulting stationary states are prescribed by statistical mechanics. In the realm of quantum many-body systems, this line of research has been active in the last decades due largely to advances in experiments that can create effectively isolated systems with unprecedented precision, and monitor the time-evolution of such isolated systems [3–7]. This is made possible by manipulating and probing ultra-cold atom gases, and remarkably, by tuning interaction properly, the resulting gases can be modeled by a variety of quantum many-body systems. Therefore the ultra-cold atom experiments serve as *quantum simulator*, and provide invaluable opportunities for the ideas developed in theory to be tested. Of course, the utility of those experiments is not limited to examine the properties of relaxation, and encompasses from studies on prethermalization to realization of the Kondo system in an optical trap [8–10].

## 1.1 Thermalization in isolated non-integrable quantum systems

From theoretical perspective, the modern interest in the mechanism of thermalization in quantum systems was initiated when the concept of *eigenstate thermalization hypothesis* (ETH) was proposed by Deutsch and Srednicki in 90s [11, 12]. Although it pertained to theoretical interests at the time, the spectacular advances in experiments in the 2000s have led to the revival of the interest, and since then has come to the fore [13–18]. Let us elaborate a bit on the statement of ETH.

A common wisdom of thermodynamics tells us that a thermalized state can be characterized by just a few numbers of parameters such as the inverse temperature $\beta$, chemical potential $\mu$ etc. It is generally believed (with some rare exceptions [19]) that the dynamics of an isolated non-integrable many-body system locally relaxes to such an thermalized state in some way under the unitary time evolution. For instance, one can characterize relaxation by looking at expectation values of observables $\langle \mathcal{O} \rangle$ that are expected to reach some stationary values under time-evolution. There are several ways to establish an approach towards a thermalization in a non-integrable system, one of which being ETH. ETH states that thermalization actually occurs at the level of each eigenstate (i.e. the diagonal matrix elements of an operator is equivalent to its microcanonical average with respect to relevant energy scales). This implies that, even if an initial state is prepared as a superposition of eigenstates, the long-time asymptotics of the expectation value of the operator will eventually be prescribed by microcanonical ensemble [13]. To be more precise, suppose that our initial state is a superposition of the orthonormal eigenstate $|\psi_\alpha\rangle$, i.e. $|\psi(0)\rangle = \sum_\alpha c_\alpha |\psi_\alpha\rangle$ with $H|\psi_\alpha\rangle = E_\alpha |\psi_\alpha\rangle$ and $\sum_\alpha |c_\alpha|^2 = 1$. Furthermore, we assume that the distribution of $c_\alpha$ is sufficiently narrow so that the energy variance $\Delta E = \sqrt{\langle H^2 \rangle - \langle H \rangle^2}$ satisfies $\Delta E \ll \langle H \rangle$. Then the average of a time-evolved generic

operator $A$ with respect to the state is $\langle\psi(t)|A|\psi(t)\rangle = \sum_{\alpha,\beta} c_\alpha^* c_\beta e^{\mathrm{i}(E_\alpha - E_\beta)t} A_{\alpha\beta}$, where $A_{\alpha\beta} = \langle\psi_\alpha|A|\psi_\alpha\rangle$. After the relaxation, the value $\langle\psi(t)|A|\psi(t)\rangle$ is expected to reach its long-time average

$$\bar{A} = \lim_{\tau\to\infty} \frac{1}{\tau}\int_0^\tau \mathrm{d}t \langle\psi(t)|A|\psi(t)\rangle = \sum_\alpha |c_\alpha|^2 A_{\alpha\alpha}, \tag{1.1}$$

which takes the form of a diagonal ensemble $\bar{A} = \mathrm{Tr}(\rho_{\mathrm{DE}} A)$, where $\rho_{\mathrm{DE}} = \sum_\alpha |c_\alpha|^2 |\psi_\alpha\rangle\langle\psi_\alpha|$. A caveat here is that the ensemble is explicitly depending on the distribution of the initial state $c_\alpha$. This is in contradiction with the universality of thermalized ensembles, and ETH resolves the dichotomy by providing the connection of the diagonal ensemble with the microcanonical ensemble. For a given energy average $e = \langle H\rangle$ and a small energy scale $\Delta e$ that vanishes in the thermodynamic limit, the microcanonical ensemble of the operator $A$ reads

$$\langle A\rangle_{\mathrm{mc}}(e) = \frac{1}{\mathcal{N}(e,\Delta e)} \sum_{\alpha: E_\alpha \in I} A_{\alpha\alpha}, \tag{1.2}$$

where $I = [e-\Delta e, e+\Delta e]$ is the energy window centred at $e$, and $\mathcal{N}(e,\Delta e)$ is the number of eigenstates that are within the window. Now, ETH speculates that the diagonal element $A_{\alpha\alpha}$ is a smooth function of $E_\alpha$, and is same as the microcanonical average up to an exponentially decaying term in system size [13, 20]. That is, the following holds for every $\alpha$

$$A_{\alpha\alpha} \simeq \langle A\rangle_{\mathrm{mc}}(E_\alpha). \tag{1.3}$$

This statement has a far-reaching consequence. Let us Taylor expand $A_{\alpha\alpha}$ around the mean value $e$:

$$A_{\alpha\alpha} \simeq \langle A\rangle_{\mathrm{mc}}(e) + (E_\alpha - e)\left.\frac{\partial A_{\alpha\alpha}}{\partial E_\alpha}\right|_{E_\alpha=e} + \frac{1}{2!}(E_\alpha - e)^2 \left.\frac{\partial^2 A_{\alpha\alpha}}{\partial E_\alpha^2}\right|_{E_\alpha=e}, \tag{1.4}$$

where we used (1.3) in the first term, and also assume that $\partial^n A_{\alpha\alpha}/\partial E_\alpha^n|_{E_\alpha=e}$ are $\alpha$-independent for any $n > 0$. Then plugging this into (1.1), we obtain

$$\bar{A} \simeq \langle A\rangle_{\mathrm{mc}}(e) + \frac{1}{2!}(\Delta E)^2 \left.\frac{\partial^2 A_{\alpha\alpha}}{\partial E_\alpha^2}\right|_{E_\alpha=e}. \tag{1.5}$$

Since we assumed that the variance is sufficiently small and it is typically subextensive, one therefore establishes the equivalence between the diagonal ensemble and the mircocanonical ensemble $\bar{A} = \langle A\rangle_{\mathrm{mc}}(e)$ for large system sizes and sufficiently narrow initial distributions of $E_\alpha$.

In general the above consideration applies to any non-integrable systems for which we have a few number of conserved charges. We are then interested in the question as to whether ETH is still valid or not in integrable systems. The answer is a little

tricky; the *weak* ETH still holds but the *strong* ETH generically breaks down in integrable systems[2] [23]. Here, the weak ETH refers to the case where there are some eigenstates $|\psi_r\rangle$ for which (1.3) is not satisfied, whereas the strong ETH means that we have no such eigenstate that invalidates (1.3).

## 1.2 Lack of thermalization in intgerable systems

In the previous section, we argued that generically an isolated non-integrable quantum system is thermalized in the course of time evolution, and its mechanism can be explained by ETH. This is in stark contrast with the case in integrable systems: it is known that thermalization is in fact absent in integrable systems [3, 24]. Thermalization is prohibited due to the presence of an infinite number of conserved charges in integrable systems. The lack of thermalization was at first observed in a famous quantum Newton's cradle experiment [3]. A protocol employed in the experiment was simple: authors observed a dynamics starting from an initial kick (Bragg pulse) that separates a single cloud of $^{87}$Rb atoms into two clouds in a cigar-like trap with a confining potential. Remarkably, what they observed was a persistent collisions of two split clouds of $^{87}$Rb in the confining potential. In such a situation, one typically expects that, after some short transient time involving dephasing, two colliding clouds of atoms would soon reach to some stationary state that is dictated by a Gibbs ensemble. This was not quite what happened in their experiments, and the absence of thermalization was then attributed to the fact that the model effectively describes the dynamics of the $^{87}$Rb, the Lieb-Liniger model, is integrable [25–27].

Theoretical investigations have also revealed that, despite of the lack of thermalization, integrable systems do relax to some stationary state, which turns out to be not characterized by the conventional Gibbs ensemble [28]. This novel equilibrated state is called *generaized Gibbs ensemble* (GGE), and can be thought of as a generalization of the Gibbs ensemble in a sense that the ensemble incorporates all the available conserved charges in the system, on top of the standard ones such as the hamiltonian and the $U(1)$ charge. Hence, contrary to a standard Gibbs ensemble $\rho \sim e^{-\beta(H-\mu N)}$, a GGE takes its generalized form $\rho \sim e^{-\sum_i \beta_i Q_i}$, where $Q_i$ are available conserved charges, and $\beta_i$ are associated Lagrange multipliers. It is also possible to consider a generalized version of the microcanocial ensemble, which was dubbed generalized microcanonical ensemble (GME). It then allows us to justify a relaxation to GGE by generalizing the ETH with the aid of GME [29]. The validity of GGE has been tested analytically and numerically (see e.g. [28] and references therein) since the introduction of GGE [24], and later it was realized that, in order to have a complete characterization of a GGE, one has to include newly-discovered *quasi-local charges* [30–32] as well as ordinary local conserved charges.

[2] Strong ETH actually breaks down in some non-integrable models as well, e.g. quantum scars [21, 22]. In integrable systems, however, there are more such states.

Here the term *quasi-local* refers to the fact that these charges are not local (having a finite region of support) but still their quasi-locality is guaranteed by some conditions on their size with respect to the Hilbert-Schmidt norm [32].

## 1.3 Transport phenomena and hydrodynamics

The arbitrariness of nonequilibrium states makes it hard to build a coherent theory for such states, but there is a class of nonequilibrium states that admits in-depth theoretical investigations: nonequilibrium steady states (NESSs). A NESS is characterized as an inhomogeneous stationary state, and is a nonequilibrium state that is nontrivial enough, but still close to equilibrium states (i.e. homogeneous stationary states). It often arises in the context of transport phenomena, and can be realized both in open and closed systems. Since transport phenomena are the most experimentally relevant out-of-equilibrium situations, it is of great importance to develop a solid understanding on the nature of NESSs.

A prominent tool to study transport phenomena is *hydrodynamics*. The modern history of hydrodynamics goes back to the 18th century when Euler wrote down the celebrated Euler equation for the first time. The equation was introduced so that it describes the motion of dissipationless fluid-like objects, but later on, it was realized that generically any many-body systems, both quantum and classical, follow the Euler equation whenever they vary spatially in a sufficiently smooth fashion. This is equivalent to saying that hydrodynamics is a universal tool that in general governs the low-energy (long-wavelength) dynamics of many-body systems [33]. It is remarkable that the dynamics of both quantum and classical systems are expected to be captured by the same (classical) hydrodynamics in large scale. In particular, in quantum systems, the mechanism of how initial quantum correlations are washed away and ensuing emergence of hydrodynamics have been largely elusive and attracts much attentions [34–38]. Even in the classical systems, the emergence of hydrodynamics has only been rigorously proven in few systems such as the hard-rod gas [39]. Due to its universality and predictive power, hydrodynamics has been so far applied to a numerous variety of models ranging from classical systems such as the hard-rod system [39] and the stochastic exclusion process [40] to quantum systems such as superfluids [41, 42], graphene [43, 44], and quantum integrable systems [45, 46].

The primary assumption in using hydrodynamics to study the dynamics of a many-body system is the propagation of *local equilibrium*. On the crudest length scale (Euler scale), at each time slice, one can regard the system as a local equilibrium state with the spatio-temporal Lagrange multipliers $\beta^i(\vec{x}, t)$. This means that the dynamics has to be gentle enough not to agitate the system to deviate from local equilibrium in the course of time-evolution. It is in general believed that such a situation is realized at late times in the dynamics, which is largely controlled by slow modes such as conserved charges. Although being an approximation, hydrodynamic description of the dynamics is a drastic simplification compared to microscopically tracking the time-evolution, and encodes

essential information of the dynamics. A virtue of the hydrodynamics is that the degree of approximation can be controlled in the light of *derivative expansion* (for the precise formulation of hydrodynamics and derivative expansion, see the section 3.1), which is an expansion of the hydrodynamic current in terms of spatial derivatives of averages of charge densities. The full effect of diffusion and dissipation can be extracted by including the second term in the expansion, and generally the higher derivative terms are irrelevant for the dynamics. The hydrodynamic equation accounting for both ballistic and diffusion (viscosity) contributions is called *Navier-Stokes* equation. The strength of diffusion is controlled by transport coefficients, which can always be written as equilibrium correlation functions via Kubo formulae. Upon linearizing hydrodynamics with respect to a static background, one can obtain the linearized hydrodynamic equation that governs the equilibrium dynamical correlation functions $S_{ij}(x,t) = \langle \mathfrak{q}_i(x,t)\mathfrak{q}_j(0,0)\rangle^c$, where $\mathfrak{q}_i$ is the density of the conserved charge $Q_i$, which is a primary quantity that characterizes the dynamics of the system [47, 48]. Hydrodynamics has a strong predictive power on its behavior for large $x$ and $t$, according to which we can classify the transport type of the charge. In experiments, the dynamical spin structure factor, which is the Fourier transformed quantity $S_{00}(k,\omega) = \int \mathrm{d}x\mathrm{d}t\, e^{\mathrm{i}\omega t - \mathrm{i}kx} S_{00}(x,t)$, can be measured using inelastic neutron scattering (INS), and has played an important role in examining dynamical properties of quantum spin systems [49].

Typically in higher dimensions, the system supports diffusive transport. At the level of linearized hydrodynamics, this implies that $S_{ij}(x,t)$ propagates ballistically with diffusive broadening (i.e. the width of $S_{ij}(x,t)$ spreads as $t^{1/2}$). However, the situation in lower dimensions, and in particular in one dimension, turns out to be rather peculiar; it is known that the low dimensionality constrains the dynamics severely, and consequently results in the *divergence* of diffusion constants. This phenomenon is called *superdiffusion*, and is known to result in the anomalous broadening of $S_{ij}(x,t)$ as $t^\alpha$, where $\alpha > 1/2$. This implies the breakdown of the conventional linearized hydrodynamics, and calls for a new theory that predicts the large time asymptotics of $S_{ij}(x,t)$ correctly. A minimum and natural generalization of the linearized hydrodynamics is to include the second order terms in the fluctuation od the linearizing field $\delta\mathfrak{q}_i$ . Typically a noise term, which is supposed to account for the effect of microscopic degrees of freedom that is traced out in writing hydrodynamic equations, is also added. The resulting hydrodynamics was formulated by Spohn [47], and was dubbed *nonlinear fluctuating hydrodynamics* (NLFHD) [47,48,50,51]. Surprisingly enough, NLFHD is capable of describing a variety of superdiffusion types such as the one corresponding to $\alpha = 3/2$ (Karder-Parisi-Zhang scaling) and the one $\alpha = 5/4$ (Lévy scaling), and is nowadays regarded as a universal, if phenomenological, tool to study superdiffusion in one-dimensional (classical) many body systems.

## 1.4 Transport in integrable systems

Despite of possessing rather peculiar properties, transport phenomena in quantum integrable systems have attracted an large amount of interests amongst other transport phenomena over the past decades. Although it is natural to expect that transport type in integrable systems would be generically ballistic due to the presence of stable quasiparticles, there had been some efforts to figure out if other type of transport, such as normal (diffusive) transport, could ever exist in such systems [52–55]. This decades-long question was finally settled down in [56, 57], where it was demonstrated that diffusive transport can generally exist in integrable systems. Being said so, a quantitative understanding was still missing in these studies, and the exact computations of relevant quantities such as the Drude weight and the diffusion constant was still out of reach. Meanwhile the quest for obtaining analytic results on these quantities was pushed forward in the context of open quantum systems, initiated by the seminal works [58, 59] in which the exact nonequilibrium steady state (NESS) in the boundary-driven XXZ spin 1/2 chain was constructed in terms of matrix product states. Note also that this type of solutions that take the form of matrix product ansatz (MPA) has also been used for quite a while in order to construct the NESS in classical exclusion processes, one of which being the paradigmatic *asymmetric simple exclusion process* [60, 61]. This was the first instance where an exact NESS was obtained in quantum systems, and the MPA method has been successfully applied to other models such as the Fermi-Hubbard chain [62] and the $SU(3)$ spin-1 Lai-Sutherland model [63] for which particle contents are more complicated. The MPA approach, however, works only for integrable systems that are driven by boundary Lindblad operators, and is presumably not to be able to characterize NESSs generated in isolated systems. For instance, one of the representative protocols to study NESSs in isolated systems is the partitioning protocol[3], in which two semi-halves of a system are prepared with two global parameters initially, and simultaneously joined together. A universal way to characterize transport phenomena in integrable systems had to await the invention of a hydrodynamic approach to study the dynamics of integrable systems, which was finally proposed in 2016 by two works [45, 46], the former of which is coauthored by the author of this thesis.

## 1.5 Aim of the thesis

As we have emphasized in the previous section, we have witnessed considerable interests and progress in understanding transport phenomena in integrable systems in the last decades. However, only until recently, there was no universal tool that can be applied

[3]This is essentially equivalent to the Riemann problem in the study of hydrodynamics, but following the custom in quantum many-body systems, we call it partitioning protocol in the context of transport in quantum and classical many-body systems.

to any transport setups in integrable systems (except, of course, the trivial case: free systems). Indeed, one can exploit integrability to carry out microscopic computations to monitor nonequilibrium dynamics, but this is often plagued by computational difficulties, and is highly dependent on each particular case in question. In view of this situation, it is therefore of paramount importance to establish a versatile and universal tool to study transport phenomena integrable systems. Motivated by this status quo, the aim of our recent works is to invent and develop a hydrodynamic theory that is capable of describing any inhomogeneous dynamics in integrable systems regardless of initial conditions. This is in fact a very natural idea by merely appealing to the predictive power and universality in hydrodynamics as was advocated in the section 1.3 (see Chapter 4 for the detail), and the resulting theory, named *generalized hydrodynamics* (GHD), is nowadays acknowledged as a primary tool to investigate large scale dynamics of integrable systems. In this thesis, we shall introduce and present some of the key ideas and results in these works. In formulating GHD, we crucially rely on thermodynamic Bethe ansatz (TBA), which is a standard tool to study the thermodynamics of integrable systems, and the theory will be presented in the language of TBA.

This thesis is organized as follows.

In Chapter 2, we review the idea of integrability in the context of relativistic integrable field theories. We first introduce the standard approach to study the thermodynamics, i.e. TBA, which was first proposed for the Lieb-Liniger model [64], and later for relativistic integrable field theories [65]. Some of the quantities defined in the course of this thesis, such as the density of quasi-particles, would play fundamental roles in GHD. We then move on to rederive the thermodynamics of integrable systems from a completely different perspective: combinatorics. This will be largely based on a recent work [66], and the approach turns out to be instrumental in proving one of the core ideas in GHD [67]. Having elaborated on two methods to evaluate thermodynamics of integrable systems, we shall present some important aspects of form factors, which are elementary matrix elements of local operators, and serve as building blocks of integrable systems. We then spell out how combinatorics can be useful in proving the celebrated LeClair-Mussardo formula [68], which is the form factor expansion of local operators in the infinite volume. A special case of the density of a conserved charge is supplemented as well.

In Chapter 3, we review the basics of hydrodynamics built on the assumption of the propagation of local equilibrium. A full hydrodynamic equation that also takes the viscosity effects into account is obtained from the derivative expansion. We then closely examine the effect of ballistic and diffusive contributions by deriving a dynamical equation for the equilibrium correlation function valid at large scale in $x$ and $t$.

Chapter 4 consists of four subchapters each of which is dedicated to the review of one of

the papers coauthored by the author of this thesis. Each subchapter is followed by its original paper.

In subchapter 4.1, we introduce the theory of generalized hydrodynamics. In doing so, we first summarize recent developments of the theory that illustrate how diverse and impactful the theory is. We then demonstrate how to implement the idea of hydrodynamics in integrable systems. The crucial part is to conjecture the form of the mean value of current operators using TBA, with which the hydrodynamic equation for integrable systems, dubbed GHD equation, readily follows. Having obtained it, the application of GHD to the partitioning protocol and an extension to the case where external potentials are present are briefly discussed. The exposition is based on a joint work with Olalla Calstro-Alvaredo and Benjamin Doyon [45].

In subchapter 4.2, we prove the conjectured form of the average of currents by means of graph theory. The idea is expected to be universally applicable to any Bethe solvable systems, and for simplicity we exemplify it by studying diagonally-scattering relativistic quantum field theories. The content presented here is based on a work with Dinh-Long Vu [67].

Subchapter 4.3 contains a discussion on the analogy between GHD and hydrodynamics of classical hard-rod gases. Prompted by this intriguing observation, we then show how one can alter the microscopic dynamics of hard-rod gases so that the resulting kinetics gives rise to the same hydrodynamics as GHD at large scale. We thereby establish the correspondence between the hydrodynamics of quantum integerable systems and that of classical rigid objects. This correspondence is also practically useful in simulating GHD using molecular dynamics, which turns out to be quite efficient. This subchapter is based on a work in collaboration with Jean-Sébastien Caux and Benjamin Doyon [69].

A specialization of GHD to the case of low-temperature is discussed in subchapter 4.4. There, focusing on gapless integrable systems whose ground states are Luttinger liquids, it is found that the GHD equation is simplified and takes a form of a finite-component hydrodynamics, as long as the system stays near to the ground state. In spite of the fact that the hyrdoynamics is finite-component, it is noted and elucidated why the system never suffers from gradient catastrophe (shocks). Furthermore, we remark that the number of components is just two before the system starts developing any sharp structure (which dissolves eventually), and in that case the hydrodynamics can be recast into the form of conventional hydrodynamics. Thus for the first time we justify the use of conventional hydrodynamics in a particular situation when studying the dynamics of (gapless) integrable systems. These findings are obtained in a joint work with Benjamin Doyon, Jérôme Dubail, and Robert Konik [70].

In Chapter 5, we provide conclusions and outlooks on future directions.

# Chapter 2

# Integrability in (1+1)-dimensional quantum field theories

## 2.1 Thermodynamic Bethe ansatz in integrable quantum field theories

### 2.1.1 $L$- and $R$-channel quantization

In this section, we introduce the notion of thermmodynamic Bethe ansatz (TBA), which is a way to systematically study thermodynamics of Bethe solvable systems. The idea of TBA was firstly introduced in a work by Yang and Yang [64] where they studied thermodynamics of the Lieb-Liniger model [71]. Our exposition will closely follow the paper by A. B. Zamolodchikov [65].

Let us consider a (1+1)-dimensional relativistic euclidian quantum field theory defined on a rectangular with lengths $R$ and $L$. We eventually impose periodic boundary condition to the plane in both directions under which the place becomes a torus. Let us for now do so in just one direction, along which we quantize the system. We have two possible choices for the periodic boundary condition, which we call $R$ and $L$ channel respectively, as depicted in Fig.2.1. In the $L$-channel, we quantize the system along the circumference $R$ on which the Hilbert space of the system is defined. On the other hand, in the $R$-channel, we quantize the system along the axis $L$. The partition functions for both channels are then given by, respectively,

$$Z(R, L) = \mathrm{Tr}\, e^{-LH_R} \tag{2.1}$$

$$Z(R, L) = \mathrm{Tr}\, e^{-RH_L}. \tag{2.2}$$

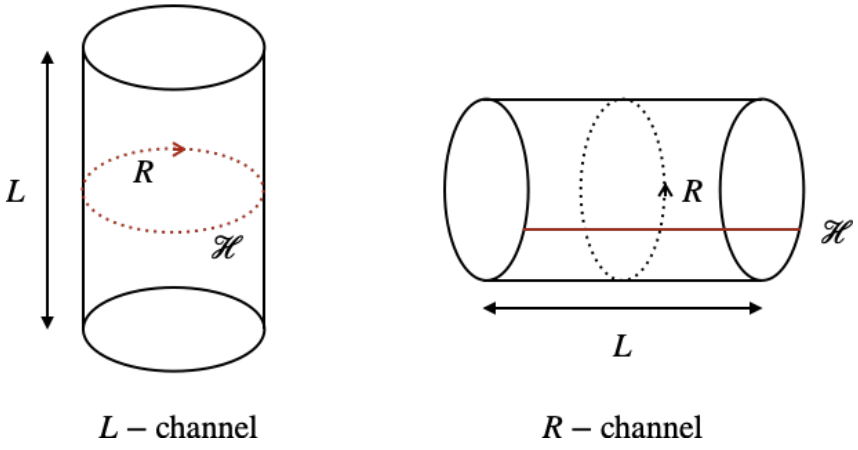


Figure 2.1: Two different quantizations.

Let us take a limit $R \ll L$ under which they behave as

$$Z(R, L) \simeq e^{-LE_0(R)} \tag{2.3}$$

$$Z(R, L) \simeq e^{-LRf(R)}. \tag{2.4}$$

The former asymptotics follows immediately, as (2.2) is clearly dominated by the lowest eigenvalue of $H_R$ when $R \ll L$. The latter is obtained by noting that, in the $R$-channel, we can interpret the system as a one-dimensional quantum system defined on the $L$-axis at finite temperature $1/R$. Then the partition function in the $R$-channel (2.2) asymptotically equals to (2.4) where $f(R)$ is the free energy of the quantum system.

$R$-channel quantization can be easily generalized to thermodynamics involving many conserved charges (i.e. GGEs). More precisely, one can consider a system governed by the generalized hamiltonian $\tilde{H} = \sum_i \beta_i Q_i$, and ask its thermodynamics. By the same argument as above, the partition function then asymptotically becomes $Z = \mathrm{Tr}\, e^{-\sum_i \beta_i Q_i} \simeq e^{-L\tilde{f}(\vec{\beta})}$, where $\tilde{f}(\vec{\beta})$ is the generalized free energy. In what follows we will study the thermodynamics of the system quantized in the $R$-channel.

### 2.1.2 Bethe wave function

Consider an integrable relativistic quantum field theory whose spectrum consists of $n$ species of particle of the mass $m_a, a = 1, \cdots, n$. The correlation length of the system, a typical length scale over which particles interact, is then set by the smallest mass $\xi = 1/m_1$. It is known that integrability, or equivalently the existence of an infinite number of conservation laws, strongly constraints the kinetics of a system by enforcing scatterings to be elastic [65, 72]. As a result, the set of momenta is always preserved upon each scattering process, prohibiting annihilations and creations of particles (i.e. inelastic scattering). Furthermore, the existence of an infinite number of conserved charges ensures

that all the many-body scattering processes in integrable systems are always factorized into the series of two-body scatterings, hence the wave functions before and after the collisions differ only by multiplcations of the two-body scattering matrices.

To better understand the nature of scatterings in the system, we consider the simplest case, namely the system that admits elastic scatterings with no backscattering (i.e. no reflection upon collisions) only, and has one particle species. Let us further suppose that we have $N$ relativistic particles with well-separated positions $x_{i_1} \ll x_{i_2} \ll \cdots \ll x_{i_N}$ (more precisely, $|x_i - x_j| \gg \xi$ for any $i \neq j$) and momenta $p_{i_1}, p_{i_2}, \cdots, p_{i_N}$. We denote such a configuration as $\{i_1, \cdots, i_N\}$, i.e. $i$ is an arbitrary permutation of the integer set $1, \cdots, N$. Since each particle is far apart each other, the corresponding wave function $\Psi(\{x\}, \{p\})$ is simply a plane wave

$$\Psi(\{x\}, \{p\}) = e^{\mathrm{i}\sum_{j=1}^{N} p_{i_j} x_{i_j}}. \tag{2.5}$$

Now, what would happen if two adjacent particles at positions $x_{i_k}$ and $x_{i_{k+1}}$ approach to each other? In this case, the plane wave (2.5) is no longer correct due to interactions and possible creation of virtual particles. Note that, since particles at $x_{i_k}$ and $x_{i_{k+1}}$ are still far from the rest of particles, we can actually focus on the scattering event involving just these two particles and ignore the effects arising from the interaction with other particles. No back scattering means that, upon the collision, the configuration is simply rearranged as $\{i_1, \cdots, i_k, i_{k+1}, \cdots, i_N\} \to \{i_1, \cdots, i_{k+1}, i_k, \cdots, i_N\}$. Hence the only actual change is the multiplication of the two-body $S$-matrix $S(p_{i_k}, p_{i_{k+1}})$. Remember that $S(p, q)$ can be written as $S(p, q) = e^{\mathrm{i}\delta(p,q)}$, where $\delta(p, q) \in \mathbb{R}$ is the scattering phase.

The above mechanism of elastically scattering particles with no backscattering yields a significant consequence. Suppose that we impose the periodic boundary condition with circumference $L$ to the system. We then let a probe particle with momentum $p_i$ go around the system, which amounts to the successive scatterings with $N - 1$ particles on the ring. This of course results in the product of corresponding scattering matrices, while the probe particle itself picks up a phase $e^{\mathrm{i}p_i L}$ in the wave function after the travel. Periodic boundary condition requires that the initial wave function be the same as that after the collisions, hence we obtain the Bethe equations

$$e^{\mathrm{i}p_i L} \prod_{j \neq i} S(p_i, p_j) = 1, \quad i = 1, \cdots, N. \tag{2.6}$$

It is also convenient to introduce rapidities $\theta$ that parameterize energies and momenta as $E_k = E(\theta_k) = m \cosh \theta_k$ and $p_k = p(\theta_k) = m \sinh \theta_k$. Thanks to Lorentz invariance of the system, the $S$-matrix becomes a function of the difference of rapidities $S(p_i, p_j) = S(\theta_i - \theta_j)$. The Bethe equation (2.6) can then be cast into the form of the Bethe-Yang equations

$$L p_k + \sum_{j \neq k} \phi(\theta_k - \theta_j) = 2\pi n_k, \quad i = 1, \cdots, N, \tag{2.7}$$

where $\phi(\theta_k - \theta_j) = -\mathrm{i}\log S(\theta_k - \theta_j)$ and $n_k$ are quantum numbers that are either integers or half-integers depending on the parity of $N$. It was proven by C. N. Yang and C. P. Yang that the Bethe-Yang equations (2.7) have a unique solution, and is characterized by the set of integers (or half-integers) $(n_1, \cdots, n_N)$ The exact form of the $S$-matrix is generically model dependent, but its value at $\theta_i = \theta_j$ is determined by the statistics of the model. Unitarity of a system demands $S(\theta)S(-\theta) = 1$, hence we have two possible values for $S(0)$, i.e. $S(0) = \pm 1$. Bethe ansatz with the choice $S(0) = -1$ is called fermionic Bethe ansatz [65] regardless of the underlying statistics of the system, and leads to a wave-function that is antisymmetric in their coordinates with the same rapidity in this case. If elementary particles of a system are of bosonic type, then the antisymmetric nature of the wave function nevertheless entails fermionic behavior of the particles; each quantum number $n_i$ has to be different. On the other hand, if elementary particles are fermions, then there is no restriction on the configurations of $n_i$. As for the choice $S(0) = 1$, the situation is simply other way around with respect to bosons and fermions. In this thesis we will stick to the fermionic Bethe ansatz.

### 2.1.3 Thermodynamic Bethe ansatz

Typically we are interested in the limit where the system size $L$ and the number of particle $N$ are very large. In fermioninc TBA, it is always the case that $\phi(\theta)$ is a monotonically increasing function. Accordingly it is readily seen that when $n_j > n_k$, then $\theta_j > \theta_k$, and in particular if $n_j = n_k$ then $\theta_j = \theta_k$. To study the distribution of the Bethe roots $n_i$, it is useful to introduce a function $p(x)$ where $x \in \mathbb{R}$ that satisfies the following equation which is closely related to (2.7):

$$p(\theta(x)) + \frac{1}{L}\sum_{j=1}^{N} \phi(\theta(x) - \theta_j) = 2\pi x, \tag{2.8}$$

where $p(\theta)$ is momentum, and $\theta(x)$ is a monotonically increasing function of $x$. The equation reduces to the Bethe-Yang equation when $x = n_i/L$ where $n_i \in (n_1, \cdots, n_N)$ is one of the quantum numbers in (2.7), i.e.

$$\theta\left(\frac{n_i}{L}\right) = \theta_i. \tag{2.9}$$

The function $\theta(m/L)$ with an unoccupied integer $m \notin (n_1, \cdots, n_N)$ can then be considered as the rapidity of a hole. We, therefore, for a given window of $x$, have a set of integers each of which corresponds to either a particle or a hole. Since adjacent rapidities are distributed with the width $\theta_j - \theta_{j+1} \sim 1/L$ in (2.7), it is reasonable to define the total density $\rho_{\mathrm{tot}}(\theta(x)) = \mathrm{d}x(\theta)/\mathrm{d}\theta$ with which (2.8) implies

$$p'(\theta(x)) + \frac{1}{L}\sum_{j=1}^{N} \varphi(\theta(x) - \theta_j) = 2\pi\rho_{\mathrm{tot}}(\theta(x)), \tag{2.10}$$

where $\varphi(\theta) = \mathrm{d}\phi(\theta)/\mathrm{d}\theta$. Note that the total density is simply a sum of the density of particles and holes: $\rho_{\mathrm{tot}}(\theta) = \rho_{\mathrm{p}}(\theta) + \rho_{\mathrm{h}}(\theta)$. The thermodynamic limit of (2.10) then immediately follows as

$$p'(\theta) + \int \mathrm{d}\theta' \rho_{\mathrm{p}}(\theta')\varphi(\theta - \theta') = 2\pi\rho_{\mathrm{tot}}(\theta). \tag{2.11}$$

The relation between $\rho_{\mathrm{tot}}, \rho_{\mathrm{p}}$ and $\rho_{\mathrm{h}}$ can be determined by the following considerations. A thermodynamic state is specified by how macroscopic number of particles and holes are distributed according to $\rho_{\mathrm{p}}$ and $\rho_{\mathrm{h}}$. For instance, we have $L\rho_{\mathrm{p}}(\theta)\mathrm{d}\theta$ and $L\rho_{\mathrm{h}}(\theta)\mathrm{d}\theta$ particles and holes, respectively, for a given small interval $\mathrm{d}\theta$. Then, the number of ways to allocate these particles and holes to $L\rho_{\mathrm{tot}}(\theta)\mathrm{d}\theta$ available vacancies is

$$\mathrm{d}S = \frac{(L\rho_{\mathrm{tot}}(\theta)\mathrm{d}\theta)!}{(L\rho_{\mathrm{p}}(\theta)\mathrm{d}\theta)!(L\rho_{\mathrm{h}}(\theta)\mathrm{d}\theta)!}, \tag{2.12}$$

which is asymptotically true subject to $1/mL \ll \mathrm{d}\theta \ll 1$. This is nothing but the thermodynamic entropy for an infinitesimal interval $\mathrm{d}\theta$, and using the Stirling's formula $\log n! = n\log n - n + \mathcal{O}(\log n)$, we can obtain the leading contribution to the full thermodynamic entropy [64]

$$S[\rho_{\mathrm{tot}}, \rho_{\mathrm{p}}] = L\int \mathrm{d}\theta(\rho_{\mathrm{tot}}\log\rho_{\mathrm{tot}} - \rho_{\mathrm{p}}\log\rho_{\mathrm{p}} - \rho_{\mathrm{h}}\log\rho_{\mathrm{h}}). \tag{2.13}$$

In order to unveil the relation between the densities, we recall that, in the thermodynamic limit, the free energy $f[\rho_{\mathrm{tot}}, \rho_{\mathrm{p}}] = E[\rho_{\mathrm{p}}] - TS[\rho_{\mathrm{tot}}, \rho_{\mathrm{p}}]$ has to be minimized with respect to $\rho_{\mathrm{tot}}$ and $\rho_{\mathrm{p}}$, where $T = 1/R$. Since the energy $E[\rho_{\mathrm{p}}]$ is given by

$$E[\rho_{\mathrm{p}}] = \int \mathrm{d}\theta\rho_{\mathrm{p}}(\theta)E(\theta), \tag{2.14}$$

we can vary $\rho_{\mathrm{p}}$ and determine a condition on $\rho_{\mathrm{p}}$ and $\rho_{\mathrm{tot}}$ that minimizes the free energy, which amounts to the following consistency relation [64, 73]

$$n(\theta) = \frac{1}{1 + e^{\epsilon(\theta)}} = \frac{\rho_{\mathrm{p}}(\theta)}{\rho_{\mathrm{tot}}(\theta)} \tag{2.15}$$

where the pseudo-energy $\epsilon(\theta)$ satisfies the Yang-Yang equation

$$\epsilon(\theta) = RE(\theta) - \int \frac{\mathrm{d}\theta'}{2\pi}\varphi(\theta - \theta')\log(1 + e^{-\epsilon(\theta')}). \tag{2.16}$$

Notice that $n(\theta)$ plays a role of the Fermi weight in a free fermion system where the energy is renormalized due to the interaction. The free energy of the system is now expressed nicely in terms of the pseudo-energy [64, 73]

$$f = -\frac{1}{R}\int \frac{\mathrm{d}\theta}{2\pi}p'(\theta)\log(1 + e^{-\epsilon(\theta)}), \tag{2.17}$$

from which the partition function of the system reads, according to (**??**),

$$Z = \exp\left[L \int \frac{\mathrm{d}\theta}{2\pi} E'(\theta) \log(1 + e^{-\epsilon(\theta)})\right]. \tag{2.18}$$

The energy density average of the system is obtained from the free energy as

$$\langle E \rangle = \frac{\partial(Rf)}{\partial R} = \int \frac{\mathrm{d}\theta}{2\pi} E'(\theta) n(\theta) \frac{\partial \epsilon(\theta)}{\partial R}, \tag{2.19}$$

where $\partial\epsilon(\theta)/\partial R = \rho_{\mathrm{tot}}(\theta)$ satisfies the integral equation

$$\rho_{\mathrm{tot}}(\theta) = \frac{1}{2\pi} \cosh\theta + \int \frac{\mathrm{d}\theta'}{2\pi} \varphi(\theta - \theta') n(\theta') \rho_{\mathrm{tot}}(\theta'). \tag{2.20}$$

The free energy (2.17) and the explicit form of the pseudo-energy (2.16) completely fixes the thermodynamics of a given relativistic integrable system. When the density $d = N/L$ is fixed, then we also have a conservation of the total number of particles which also has to be taken into account when minimizing the free energy. The trick is simple: we can simply replace $E[\rho_{\mathrm{p}}]$ with $E[\rho_{\mathrm{p}}] - \mu N[\rho_{\mathrm{p}}]$, which gives rise to the pseudo-energy with a source term being $R(E(\theta) - \mu)$.

In general, we can consider a GGE state where higher conserved charges are involved. For example, when the system is equilibrated with a GGE $\rho \sim e^{-\sum_i \beta^i Q_i}$, the pseudo-energy takes a generalized form [74]

$$\epsilon(\theta) = \sum_i \beta^i h_i(\theta) - \int \frac{\mathrm{d}\theta'}{2\pi} \varphi(\theta - \theta') \log(1 + e^{-\epsilon(\theta')}), \tag{2.21}$$

where $h_i(\theta)$ is the one-particle eigenvalue of the conserved charge $Q_i$: $Q_i|\theta\rangle = h_i(\theta)|\theta\rangle$. Accordingly we also define the generalized free energy $f = -\int \frac{\mathrm{d}\theta}{2\pi} p'(\theta) \log(1 + e^{-\epsilon(\theta)})$, and with the one-particle eigenvalue $h_i(\theta)$, we can express the average of the conserved charge $Q_i$ as

$$\langle \mathfrak{q}_i \rangle = \frac{\partial f}{\partial \beta_i} = \int \frac{\mathrm{d}\theta}{2\pi} p'(\theta) n(\theta) h_i^{\mathrm{dr}}(\theta), \tag{2.22}$$

where $\mathfrak{q}_i$ is defined by $Q_i = \int \mathrm{d}x\, \mathfrak{q}_i(x)$. Here we introduced the *dressing* operation, which is defined for any function of $\theta$ as

$$f^{\mathrm{dr}}(\theta) = f(\theta) + \int \frac{\mathrm{d}\alpha}{2\pi} \varphi(\theta, \alpha) n(\alpha) f^{\mathrm{dr}}(\alpha). \tag{2.23}$$

Note that in the integral-operator language, the dressing operation can also be understood as the application of $(1 - \varphi n)^{-1}$, i.e. $f^{\mathrm{dr}}(\theta) = ((1 - \varphi n)^{-1} f)(\theta)$. Expanding (2.23) and

plugging it into (2.22), it is readily seen that we can also have an alternative expression for the charge density average

$$\langle \mathfrak{q}_i \rangle = \int \frac{\mathrm{d}\theta}{2\pi} (p')^{\mathrm{dr}}(\theta) n(\theta) h_i(\theta) = \int \mathrm{d}\theta \rho_{\mathrm{p}}(\theta) h_i(\theta). \tag{2.24}$$

Therefore, defining the bilinear form for arbitrary functions $f(\theta)$ and $g(\theta)$ as

$$(f, g) = \int \frac{\mathrm{d}\theta}{2\pi} f^{\mathrm{dr}}(\theta) n(\theta) g(\theta), \tag{2.25}$$

we can express the charge density average in a symmetric way

$$\langle \mathfrak{q}_i \rangle = (p', h_i) = (h_i, p'). \tag{2.26}$$

In section 2.3, we will see that the particular form of the (connected) form factor of the densities of conserved charges $\mathfrak{q}_i$ underlies this symmetry.

It should be stressed that the structure of TBA we just found actually holds in any known Bethe-solvable quantum systems, whether spin chains or field theories, and whether relativistic or non-relativistic [64, 65, 73, 75–80]. An alternative way to study the thermodynamics of integrable systems is the quantum transfer-matrix method [81, 82].

## 2.2 TBA from combinatorics

### 2.2.1 Partition function in terms of the Gaudin determinant

In this section, we shall see that TBA can also be derived from combinatorics, which is a completely different perspective than the one presented above. The underlying idea was introduced in the original works [83–86], but the exposition here will largely follow the recent works [66, 87, 88]. Let us first recall the definition of the partition function

$$Z(R, L) = \mathrm{Tr}\, e^{-RH_L} = \sum_{M=0}^{\infty} \frac{1}{M!} \sum_{n_1, \cdots, n_M} e^{-RE(n_1, \cdots, n_M)}, \tag{2.27}$$

The sum here is in fact overcounting; assuming the bosonic statistics of the system under consideration, in the fermionic TBA, coinciding quantum numbers are not allowed. As such, implementing this condition, the correct spectral decomposition for the partition function is

$$Z(R, L) = \sum_{M=0}^{\infty} \frac{1}{M!} \sum_{n_1, \cdots, n_M} \prod_{j<k}^{M} (1 - \delta_{n_j, n_k}) e^{-RE(n_1, \cdots, n_M)} \tag{2.28}$$

$$= 1 + \sum_{n} e^{-RE(n)} + \frac{1}{2!} \sum_{n_1, n_2} e^{-RE(n_1, n_2)} - \frac{1}{2!} \sum_{n} e^{-RE(n, n)} + \cdots . \tag{2.29}$$

It is easy to see that the sum (2.29) covers all the terms each of which involves a Boltzmann weight of the form $e^{-RE(n_1^{r_1},\cdots,n_m^{r_m})}$ with a fixed number of quasiparticles $M = r_1 + \cdots + r_m$. Here, $n_k^{r_k}$ symbolically implies that there are $r_k$ quasiparticles with the quantum number $n_k$, hence $E(n_k^{r_k})$ corresponds to the total energy of these quasiparticles. We can interpret that a Bolztmann weight $e^{-RE(n_1^{r_1},\cdots,n_m^{r_m})}$ corresponds to a configuration of a set of $M$ quasiparticles with $m$ clusters where the number of quasiparticles in each cluster is $r_m$. Note that quasiparticles in a same cluster has the same velocity, hence do not interact each other (see Fig. 2.2). Having this in mind, the expansion of the Kronecker delta in

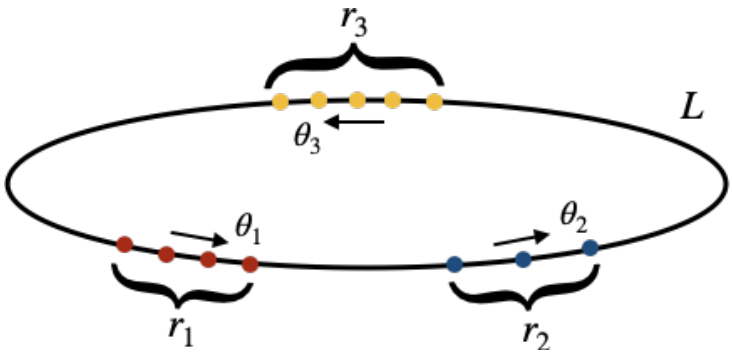


Figure 2.2: Clusters of quasiparticles.

(2.28) gives an alternative expression of the partition function

$$Z(R,L) = \sum_{m=0}^{\infty} \frac{(-1)^m}{m!} \sum_{n_1,\cdots,n_m} \sum_{r_1,\cdots,r_m} (-1)^{r_1+\cdots+r_m} C_{r_1,\cdots,r_m} e^{-RE(n_1^{r_1},\cdots,n_m^{r_m})}, \tag{2.30}$$

where $C_{r_1,\cdots,r_m}$ is a to-be-determined factor, which is purely combinatorial. The combinatorial factor $C_{r_1,\cdots,r_m}$ can be fixed by merely invoking the free fermion case: in free fermions, thanks to the Wick's theorem, we have

$$\begin{aligned} Z(R,L) = \det_{\mathcal{H}_{1\mathrm{P}}}\left(1 + e^{-RH_{1\mathrm{P}}}\right) &= \exp\left[\sum_{r=1}^{\infty} \frac{(-1)^r}{r} \mathrm{Tr}_{\mathcal{H}_{1\mathrm{P}}} e^{-rRH_{1\mathrm{P}}}\right] \\ &= \exp\left[\sum_{n} \sum_{r=1}^{\infty} \frac{(-1)^r}{r} e^{-rRE(n)}\right], \end{aligned} \tag{2.31}$$

where $\mathcal{H}_{1\mathrm{P}}$ is the one-particle Hilbert space and $H_{1\mathrm{P}} = \sum_n E(n)|n\rangle\langle n|$ is the one-particle Hamiltonian, and in the second equality we used $\det e^X = e^{\mathrm{Tr}X}$ that is valid for any linear operator $X$. The last expression can be expanded, yielding

$$Z(R,L) = 1 + \sum_{m=1}^{\infty} \frac{(-1)^m}{m!} \sum_{n_1,\cdots,n_m} \sum_{r_1,\cdots,r_m} \frac{(-1)^{r_1+\cdots+r_m}}{r_1 \cdots r_m} \sum_{j=1}^{m} e^{-r_j RE(n_j)}, \tag{2.32}$$

from which we infer

$$C_{r_1,\cdots,r_m} = \frac{1}{r_1 \cdots r_m}. \tag{2.33}$$

We therefore observe that the insertion of the Kronecker delta (2.28) amounts to the clustering of particles with same rapidities. Then the numerical factor $(-1)^r/r$ accounts for the Fermi statistics of the system, and also $\mathbb{Z}_r$ symmetry of the identical particles within each cluster.

The goal now is to achieve the exact resummation over the quantum numbers and multiplicities with the combinatorial factor $C_{r_1,\cdots,r_m}$ in (2.30). We first note that the quantum numbers $n_i$ in (2.30) and the associated rapidities $\theta_i$ do not satisfy the usual Bethe equation (2.6). Fixing the number of clusters $m$, suppose we let a test quasiparticle with momentum $p_j$ travel around the system. During the travel the quasiparticle will undergo $\sum_k r_k - 1$ scatterings with other quasiparticles, yielding the following modified Bethe equations

$$e^{-\mathrm{i}Lp_j} = \prod_{k\neq j} S(\theta_j - \theta_k)^{r_k} S(0)^{r_j - 1}. \tag{2.34}$$

Since we are working with fermionic TBA we have $S(0) = -1$, and accordingly the following generalized Bethe-Yang equation follows

$$\psi_j(\theta_1^{r_1}, \cdots, \theta_m^{r_m}) := p_j L + \sum_{k\neq j}^{m} r_k \phi(\theta_j - \theta_k) + \pi(r_j - 1) = 2\pi n_j. \tag{2.35}$$

Now, we want to take the thermodynamic limit of (2.30), and in particular, pass from the summations over quantum numbers to the integration over rapidities. We first replace the summations $\sum_{n_i}$ with the integrations $\int \mathrm{d}\psi_i/2\pi$ (we can do so, as $\psi$ is of order $L$)

$$Z(R,L) = \sum_{m=0}^{\infty} \frac{(-1)^m}{m!} \int \frac{\mathrm{d}\psi_1}{2\pi} \cdots \frac{\mathrm{d}\psi_m}{2\pi} \sum_{r_1,\cdots,r_m} \frac{(-1)^{r_1+\cdots+r_m}}{r_1 \cdots r_m} e^{-RE(\psi_1^{r_1},\cdots,\psi_m^{r_m})}. \tag{2.36}$$

We then perform a change of variables from $\psi_i$ to $\theta_i$ using (2.35), yielding

$$Z(R,L) = \sum_{m=0}^{\infty} \frac{(-1)^m}{m!} \int \frac{\mathrm{d}\theta_1}{2\pi} \cdots \frac{\mathrm{d}\theta_m}{2\pi} \mathcal{G}(\theta_1^{r_1}, \cdots, \theta_m^{r_m}) \sum_{r_1,\cdots,r_m} \frac{(-1)^{r_1+\cdots+r_m}}{r_1 \cdots r_m} \prod_{j=1}^{m} e^{-Rr_j E(\theta_j)}, \tag{2.37}$$

where $\mathcal{G} = \det G$ is the Gaudin determinant, which is a determinant of a $m \times m$ Gaudin matrix

$$\begin{aligned} G_{jk} &= \frac{\partial}{\partial \theta_j} \psi_k(\theta_1^{r_1}, \cdots, \theta_m^{r_m}) \\ &= \Big( (Lp'(\theta_j) + \sum_{l=1}^{m} r_l \varphi(\theta_j - \theta_l) \Big) \delta_{jk} - r_j \varphi(\theta_k - \theta_j). \end{aligned} \tag{2.38}$$

For the later convenience, it is in fact useful to introduce the rescaled Gaudin matrix $\hat{G}_{jk} = G_{jk} r_k$ so that we can express $\hat{G}_{jk}$ in terms of the Laplace matrix $\hat{\varphi}_{jk}$ as

$$\hat{G}_{jk} = Lp'(\theta_j) r_j \delta_{jk} + \hat{\varphi}_{jk}, \tag{2.39}$$

where

$$\hat{\varphi}_{jk} = \sum_{l=1}^{m} r_j r_l \varphi(\theta_j - \theta_l)\delta_{jk} - r_k r_j \varphi(\theta_k - \theta_j). \tag{2.40}$$

### 2.2.2 Matrix tree theorem

At first glance, carrying out the integrations and summations in (2.37) is a formidable task, especially due to the appearance of the Gaudin matrix. It turns out, however, that the very form of the Gaudin matrix is what facilitates such computations by appealing to the matrix tree theorem. In order to introduce the notion of the matrix tree theorem, let us recall some basics of graph theory.

**Definition 2.2.1** (Graphs)**.** *A graph is a set of vertices and edges $(V, E)$. If each edge of a given graph is directed, the graph is called a directed graph. If some numerical value is assigned to each edge of a graph, then the graph is called a weighed graph.*

**Definition 2.2.2** (Trees and forests)**.** *A tree is a connected graph without cycles. A forest is a set of trees. If vertices of a tree cover all the available vertices in a given graph, then the tree is called a spanning tree. A spanning forest is defined in a similar way.*

In our considerations we are only interested in directed and weighted graphs, so let us introduce the definition of Laplacian matrices of these graphs.

**Definition 2.2.3** (Laplacian matrix)**.** *Given a weighed directed graph with $n$ vertices, let us assume that a weight $\omega_{jk}$ is assigned to each directed edge that is outgoing from the vertex $k$ and incoming to the vertex $j$. Then the Laplacian matrix of the graph is defined as*

$$L_{jk} = \delta_{jk} \sum_{l \neq j}^{n} \omega_{jl} - (1 - \delta_{jk})\omega_{jk}. \tag{2.41}$$

*If we interpret the weights $\omega_{ij}$ as currents, then the Laplacian matrix $L_{jk}$ represents all the incoming currents to $j$ when $j = k$, and a negative current on the edge $\langle jk \rangle$ when $j \neq k$.*

Having these objects defined, let us present the most important theorem for us to calculate the partition function (2.37).

**Definition 2.2.4** (Weighed matrix tree theorem)**.** *Let $\alpha$ be a subset of an integer set $\{1,\dots,n\}$, and $L$ be a Laplacian matrix defined by (2.41). Denoting the principal minor of $L$ obtained by subtracting its $\alpha$-rows and $\alpha$-columns as $\mathcal{L}(\alpha|\alpha)$, the principal minor is then given by [89]*

$$\mathcal{L}(\alpha|\alpha) = \sum_{F\in\mathcal{F}_\alpha}\prod_{l\in F}\omega_l, \tag{2.42}$$

*where $l\in F$ is an edge in a forest $F$, and $\mathcal{F}_\alpha$ is a set of forests each of which contains exactly $|\alpha|$ trees rooted at vertices of $\alpha$.*

It is illuminating to illustrate the theorem using the case of $n=3$, for which the Laplacian matrix (2.41) reads

$$L = \begin{pmatrix} \omega_{12}+\omega_{13} & -\omega_{12} & -\omega_{13} \\ -\omega_{21} & \omega_{21}+\omega_{23} & -\omega_{23} \\ -\omega_{31} & -\omega_{32} & \omega_{31}+\omega_{32} \end{pmatrix}. \tag{2.43}$$

First, one of the rank-2 principal minors $\mathcal{L}(1|1)$ is given by

$$\mathcal{L}(1|1) = \omega_{21}\omega_{31}+\omega_{21}\omega_{32}+\omega_{23}\omega_{31}. \tag{2.44}$$

Since $|\alpha|=1$, the directed forests we have for $\mathcal{L}(1|1)$ are directed trees rooted at 1 (see Fig. 2.3). If, on the other hand, we choose $\alpha=\{2,3\}$, then the rank-1 principal minor $\mathcal{L}(\{2,3\}|\{2,3\})$ is simply

$$\mathcal{L}(\{2,3\}|\{2,3\}) = \omega_{12}+\omega_{13}. \tag{2.45}$$

The associated forests are depicted in Fig. 2.4.

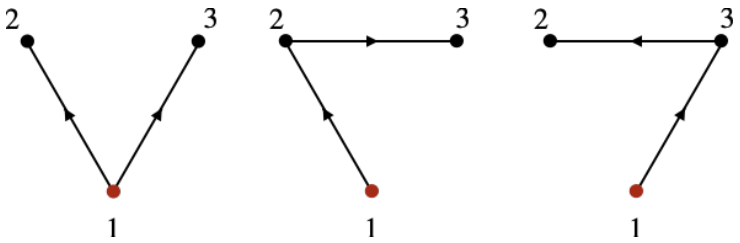


Figure 2.3: Forests corresponding to $\mathcal{L}(1|1)$.

Now, let us apply the matrix tree theorem to the Gaudin determinant $\mathcal{G}=\hat{\mathcal{G}}/\prod_i r_i$, where $\hat{\mathcal{G}}=\det\hat{G}$. Noting that $\hat{\mathcal{G}}$ can be written as a sum of minors

$$\hat{\mathcal{G}} = \sum_{\alpha\subset\{1,\cdots,m\}}\prod_{i\in\alpha} Lp'(\theta_i)r_i\mathcal{L}(\alpha|\alpha), \tag{2.46}$$

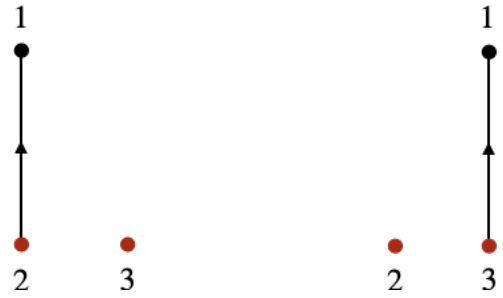


Figure 2.4: Forests corresponding to $\mathcal{L}(\{2,3\}|\{2,3\})$.

where now the weight is $\omega_{jk} = r_j r_k \varphi_{jk}$, the weighed matrix tree theorem (2.42) allows us to write the Gaudin determinant as a sum of forests

$$\mathcal{G} = \prod_{j=1}^{m} \frac{1}{r_j} \sum_{\alpha \subset \{1,\cdots,m\}} \prod_{i \in \alpha} L p_i' r_i \sum_{F \in \mathcal{F}_\alpha} \prod_{\langle jk \rangle \in F} r_j r_k \varphi_{jk}, \tag{2.47}$$

where $p_i' = p'(\theta_i)$ and $\varphi_{jk} = \varphi(\theta_j - \theta_k)$.

### 2.2.3 Resummation over forests

We are now in a position to carry out the exact resummation in (2.37) by means of the weighed matrix tree theorem. Plugging (2.47) into (2.37), we have [66]

$$\begin{aligned} Z(R,L) &= \sum_{m=0}^{\infty} \frac{(-1)^m}{m!} \sum_{r_1,\cdots,r_m} \int \prod_{j=1}^{m} \frac{\mathrm{d}\theta_j}{2\pi} \frac{\left(-e^{RE_j}\right)^{r_j}}{r_j^2} \sum_{\alpha \subset \{1,\cdots,m\}} \prod_{i \in \alpha} L p_i' r_i \sum_{F \in \mathcal{F}_\alpha} \prod_{\langle jk \rangle \in F} r_j r_k \varphi_{jk} \\ &= \sum_{m=0}^{\infty} \frac{1}{m!} \sum_{\alpha \subset \{1,\cdots,m\}} \prod_{j \in \alpha} \sum_{(\theta_j, r_j)} \frac{L p_j' (-1)^{r_j - 1}}{r_j} e^{-r_j R E_j} \prod_{k \in \bar{\alpha}} \sum_{(\theta_k, r_k)} \frac{(-1)^{r_k - 1}}{r_k^2} e^{-r_k R E_k} \\ &\quad \times \sum_{F \in \mathcal{F}_\alpha} \prod_{\langle jk \rangle \in F} r_j r_k \varphi_{jk}, \end{aligned} \tag{2.48}$$

where $E_j = E(\theta_j)$, $\bar{\alpha}$ is the complement of $\alpha$, and $\sum_{(\theta_j, r_j)} = \int \frac{\mathrm{d}\theta_j}{2\pi} \sum_{r_j}$. In each forest, we have three ingredients that constitute them; roots, vertices, and edges. We assign numerical values to them according to Fig. 2.5. With this rule in mind, let us explicitly write down the first few terms that appear in the expansion:

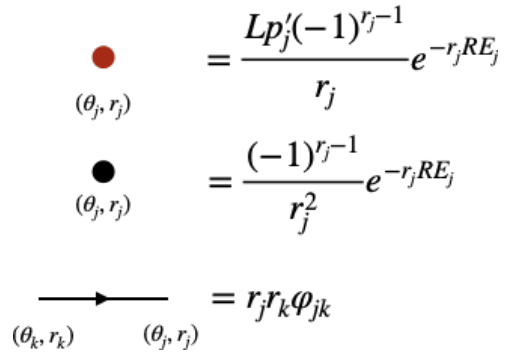


Figure 2.5: Feynman rules for roots, vertices, and edges.

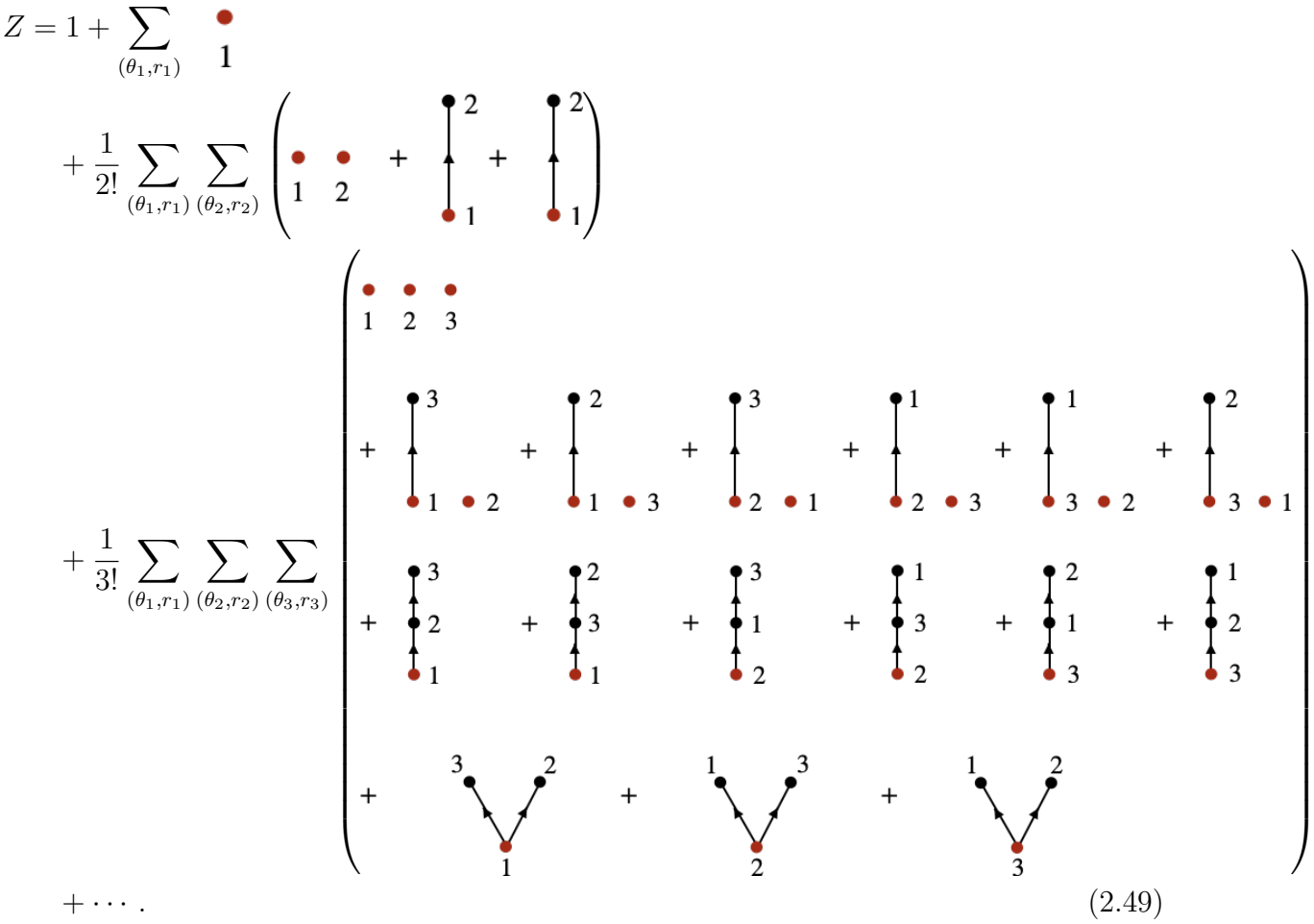


(2.49)

We then immediately observe that, upon integrations, we are left with forests

accompanied by the symmetry factor of each tree

$Z = 1 +$ 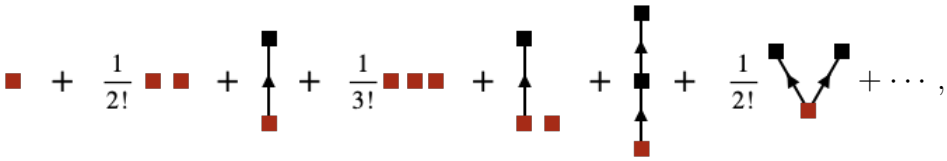 $+ \cdots ,$ (2.50)

where the box dots imply that the integrations over rapidities and summations over the multiplicities are already taken. The higher terms (forests) generally take the following form

$$\frac{1}{n_1!} V_1^{n_1} \cdots \frac{1}{n_N!} V_N^{n_N} \tag{2.51}$$

where $V_i$ is a value of the tree labeled by $i$, and $n_i$ is the number of its copy so that $1/n_i!$ serves as the global symmetry factor of the tree within a given forest. The partition function can be then written as a sum of these forests, which in turn exponentiates as in disconnected diagrams in quantum field theories:

$$\begin{aligned} Z &= \sum_{N=0}^{\infty} \sum_{\substack{n_1, n_2, \cdots, \\ \sum_j n_j = N}} \frac{1}{n_1!} V_1^{n_1} \cdots \frac{1}{n_N!} V_N^{n_N} = \exp(V_1 + V_2 \cdots) \\ &= \exp \left( \right. \text{ 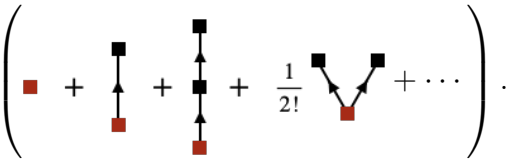 } \left. \right) . \end{aligned} \tag{2.52}$$

Notice that the diagrams in the exponential come with their internal symmetry factors. By pulling out the factor $Lp'r$ from the roots (red dots), we can cast $\log Z$ into the integration and summation over generating functions [66]

$$\log Z = L \int \frac{\mathrm{d}\theta}{2\pi} p'(\theta) \sum_{r=1}^{\infty} r Y_r(\theta), \tag{2.53}$$

where $Y_r(\theta)$ is the generating function of directed trees that are rooted at $(\theta, r)$ (see Fig. 2.6).

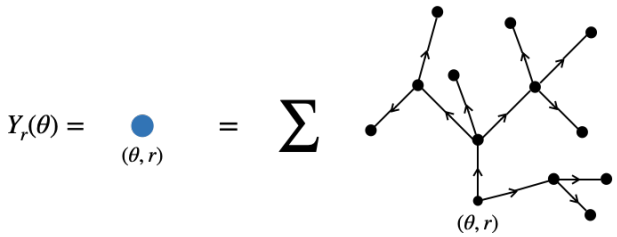


Figure 2.6: Generating function of the trees rooted at $(\theta, r)$.

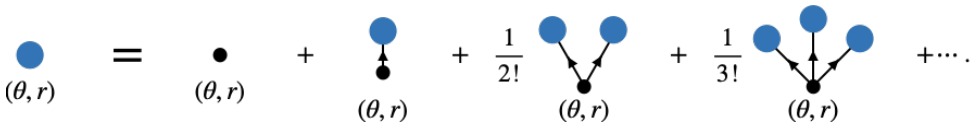


Figure 2.7: Schwinger-Dyson equation for $Y_r(\theta)$.

Note that the root of each tree in the summation in Fig. 2.6 has the same weight as other vertices. Then the generating function $Y_r(\theta)$ is expected to satisfy the self-consistency condition depicted in Fig. 2.7, which can be interpreted as the Schwinger-Dyson equation in the language of quantum field theory.

Recalling the Feynman rules Fig. 2.5, the diagrammatic equation Fig. 2.7, which can actually be interpreted as the Schwinger-Dyson equation for $Y_r(\theta)$, can be cast into the following integration equation

$$\begin{aligned} Y_r(\theta) &= \frac{(-1)^{r-1}}{r^2} e^{-rRE(\theta)} \sum_{n=0}^{\infty} \frac{1}{n!} \left( \sum_s \int \frac{\mathrm{d}\theta'}{2\pi} sr\varphi(\theta' - \theta) Y_s(\theta') \right)^n \\ &= \frac{(-1)^{r-1}}{r^2} \left( e^{-RE(\theta)} e^{\sum_s \int \frac{\mathrm{d}\theta'}{2\pi} sr\varphi(\theta'-\theta) Y_s(\theta')} \right)^r . \end{aligned} \tag{2.54}$$

This equation can be further simplified. Noting that, for $r = 1$ we have

$$Y_1(\theta) = e^{-RE(\theta)} e^{\sum_s \int \frac{\mathrm{d}\theta'}{2\pi} s\varphi(\theta'-\theta) Y_s(\theta')}, \tag{2.55}$$

the second line in (2.54) can be recast into

$$Y_r(\theta) = \frac{(-1)^{r-1}}{r^2} (Y_1(\theta))^r . \tag{2.56}$$

Since this implies

$$\sum_r r Y_r(\theta) = \log(1 + Y_1(\theta)), \tag{2.57}$$

The equation (2.55) now becomes an integral equation involving $Y_1(\theta)$ only

$$Y_1(\theta) = e^{-RE(\theta)} e^{\int \frac{\mathrm{d}\theta'}{2\pi} \varphi(\theta'-\theta) \log(1+Y_1(\theta'))}. \tag{2.58}$$

Defining $Y_1(\theta) = e^{-\epsilon(\theta)}$, this is nothing but the Yang-Yang equation (2.16). Finally, according to (2.53), this gives the partition function of the system up to some exponential correction

$$\log Z = L \int \frac{\mathrm{d}\theta}{2\pi} p'(\theta) \log(1 + Y_1(\theta)) + \mathcal{O}(e^{-L}). \tag{2.59}$$

It is remarkable that two completely different approaches, one is maximizing the free energy, and another is to directly compute the standard definition of the partition function (2.27), yield exactly the same results.

## 2.3 Form factors in integrable systems

### 2.3.1 Axioms for the elementary form factors

In this section, we review fundamental properties of the building blocks in integrable relativistic quantum field theories: form factors (see e.g. [90]). Let us suppose that the theory we consider has one particle species of mass $m$, and has no internal degrees of freedom. Let us also assume that the theory is supported on an infinitely extended geometry. It is worth emphasizing that the infinite-volume limit is taken in the following consideration unless otherwise stated. This results in the existence of kinematic and dynamical poles that will be prescribed by some of the axioms below; the connection between the infinite and finite volume form factors will be presented in the next subsection. The Hilbert space of a generic (1+1)-D relativistic quantum field theory has natural bases: asymptotic *in* and *out* states $|\theta_1, \cdots, \theta_n\rangle^{in,out}$ parameterized by rapidities $\theta$, which in turn diagonalize all the conserved charges if the model is integrable (to fix the basis, we use the *out* state, i.e. the ordering $\theta_1 < \cdots < \theta_n$). The *form factors* of a local operator $\mathcal{O}$ of the model is then defined by

$$F_{n+m}(\theta_1, \cdots, \theta_n | \eta_1 \cdots, \eta_m) = \langle \theta_1, \cdots, \theta_n | \mathcal{O}(0) | \eta_1, \cdots, \eta_m \rangle. \tag{2.60}$$

This type of object appears whenever we express physical quantities in terms of the Källén-Lehmann spectral representation. For instance, the thermal correlation function $\langle \mathcal{O}_1(x,t)\mathcal{O}_2(0,0)\rangle$ can be expanded as

$$\begin{aligned}\langle \mathcal{O}_1(x,t)\mathcal{O}_2(0,0)\rangle &= \frac{1}{Z}\mathrm{Tr}\left(e^{-\beta H}\mathcal{O}_1(x,t)\mathcal{O}_2(0,0)\right) \\ &= \frac{1}{Z}\sum_{n,m=0}^{\infty}\frac{1}{n!m!}\int\prod_{j=1}^{n}\frac{\mathrm{d}\theta_j}{2\pi}\int\prod_{k=1}^{m}\frac{\mathrm{d}\eta_k}{2\pi} e^{-\beta\sum_j E(\theta_j)} e^{\mathrm{i}(\sum_j E(\theta_j) - \sum_k E(\theta_k))t} \\ &\quad \times e^{-\mathrm{i}(\sum_j P(\theta_j) - \sum_k P(\theta_k))x} |F_{n+m}(\theta_1, \cdots, \theta_n | \eta_1 \cdots, \eta_m)|^2. \end{aligned} \tag{2.61}$$

Form factors can be in fact decomposed further into the more elementary blocks called *elementary form factors*

$$F_n(\theta_1, \cdots, \theta_n) = \langle \mathrm{vac} | \mathcal{O}(0) | \theta_1, \cdots, \theta_n \rangle. \tag{2.62}$$

Decomposition into those pieces can be achieved by making use of the crossing relations

$$\begin{aligned} &F_{n+m}(\theta_1,\cdots,\theta_n|\eta_1\cdots,\eta_m) \\ &= F_{n+m}(\theta_1,\cdots,\theta_{n-1}|\theta_n+\mathrm{i}\pi,\eta_1\cdots,\eta_m)+\sum_{k=1}^{m}\Bigg(2\pi\delta(\theta_n-\eta_k)\prod_{l=1}^{k-1}S(\eta_l-\eta_k) \\ &\quad\times F_{n+m-1}(\theta_1,\cdots,\theta_{n-1}|\eta_1\cdots,\eta_{k-1},\eta_{k+1},\cdots,\eta_m)\Bigg) \end{aligned} \tag{2.63}$$

The elementary form factors are expected to satisfy the following axioms [90]:
1. Relativistic invariance

$$F_n(\theta_1+\eta,\cdots,\theta_n+\eta)=e^{s\eta}F_n(\theta_1,\cdots,\theta_n) \tag{2.64}$$

where $s$ is the spin of the operator $\mathcal{O}$.
2. Watson's equations

$$\begin{aligned} F_n(\theta_1,\cdots,\theta_k,\theta_{k+1},\cdots,\theta_n) &= S(\theta_k-\theta_{k+1}) \\ &\quad\times F_n(\theta_1,\cdots,\theta_{k+1},\theta_k,\cdots,\theta_n) \end{aligned} \tag{2.65}$$

$$F_n(\theta_1+2\pi\mathrm{i},\cdots,\theta_n)=F_n(\theta_2,\cdots,\theta_n,\theta_1) \tag{2.66}$$

3. Kinematic poles

$$-\operatorname*{i\,Res}_{\theta\to\theta'}F_{n+2}(\theta+\pi\mathrm{i},\theta',\theta_1,\cdots,\theta_n)=\Bigg(1-\prod_{k=1}^{n}S(\theta-\theta_k)\Bigg)F_n(\theta_1,\cdots,\theta_n). \tag{2.67}$$

Note that if our model has bound states, there are additional *dynamical* poles on the imaginary axis within the strip $0<\operatorname{Im}\theta_{ij}<\pi$. We further assume that form factors are meromorphic functions except poles that are dictated by the axioms mentioned. In what follows, for brevity, we shall focus on the case with one particle species.

### 2.3.2 Finite volume form factors

As we saw in the previous section, in the infinite-volume limit, elementary form factors are generically plagued by poles (singularities) when two rapidities approach together. This often gives rise to computational issues in the form factor expansions, and therefore better be regularized. One natural way to do so is to consider a system with the finite volume $L$ [91–96]. Contrary to the infinite-volume case, each state in the system can be characterized by specifying quantum numbers, i.e. $|n_1,\cdots,n_N\rangle$, where $\{n_i\}$ satisfy the Bethe-Yang equations (2.6). The spectral expansion (2.61) in terms of quantum numbers

now read

$$\begin{aligned}\langle \mathcal{O}_1(x,t)\mathcal{O}_2(0,0)\rangle_L &= \frac{1}{Z}\mathrm{Tr}\left(e^{-RH}\mathcal{O}_1(x,t)\mathcal{O}_2(0,0)\right)_L \\ &= \frac{1}{Z}\sum_{N,M=0}^{\infty}\frac{1}{N!M!}\sum_{\{n_j\}}\sum_{\{m_k\}} e^{-R\sum_j E(\theta_j)}e^{\mathrm{i}(\sum_j E(\theta_j)-\sum_k E(\theta_k))t} \\ &\quad\times e^{-\mathrm{i}(\sum_j P(\theta_j)-\sum_k P(\theta_k))x}|\langle n_N,\cdots,n_1|\mathcal{O}(0,0)|m_1,\cdots,m_M\rangle|^2. \quad (2.68)\end{aligned}$$

In the thermodynamic limit, (2.68) becomes (2.61) up to the exponentially decaying correction in system size $\mathcal{O}(e^{-\mu L})$, where $\mu$ is a positive, model dependent constant [93]. Then, changing the variables from the quantum numbers $\{n_i\}$ to rapidities $\{\theta\}$ as in (2.37), we can relate states $|n_1,\cdots,n_N\rangle_L$ and $|\theta_1,\cdots,\theta_N\rangle_L$ as

$$|n_1,\cdots,n_N\rangle_L = \frac{1}{\sqrt{\mathcal{G}(\theta_1,\cdots,\theta_N)}}|\theta_1,\cdots,\theta_N\rangle_L, \quad (2.69)$$

where $\mathcal{G}(\theta_1,\cdots,\theta_N)$ is the Gaudin determinant (2.47). This further implies that, using the crossing relation

$$\langle n_N,\cdots,n_1|\mathcal{O}(0,0)|m_1,\cdots,m_M\rangle = \frac{F_{N+M}(\theta_1+\mathrm{i}\pi,\cdots,\theta_N+\mathrm{i}\pi,\eta_1\cdots,\eta_M)}{\sqrt{\mathcal{G}(\theta_1,\cdots,\theta_N)\mathcal{G}(\eta_1,\cdots,\eta_M)}}+\mathcal{O}(e^{-\mu L}), \quad (2.70)$$

as long as there is no overlap between the two rapidity sets $\{\theta\}$ and $\{\eta\}$. If there is at least one common rapidity, then it gives rise to the appearance of *disconnected terms*. For interacting systems[1], there are only two situations where such term arise: one is where the two sets $\{n_i\}$ and $\{m_j\}$ are exactly the same, i.e., $N=M$ and

$$\{n_1,\cdots,n_N\} = \{m_1,\cdots,m_M\}. \quad (2.71)$$

Obviously this gives a diagonal matrix element, on which object we elaborate in the next section. Another case is where both states are parity-symmetric

$$\{n_1,\cdots,n_N\} = \{-n_N,\cdots,-n_1\}, \quad \{m_1,\cdots,m_M\} = \{-m_M,\cdots,-m_1\}, \quad (2.72)$$

for which further details can be found in [94].

### 2.3.3 Diagonal matrix elements and LeClair-Mussardo formula

Diagonal matrix elements of a local field $\langle \overleftarrow{\theta}|\mathcal{O}(0)|\overrightarrow{\theta}\rangle$, where we introduced the shorthanded notation $|\overrightarrow{\theta}\rangle = |\theta_1,\cdots,\theta_n\rangle$ (and $\langle\overleftarrow{\theta}| = \langle\theta_n,\cdots,\theta_1|$), play a crucial role in computing the thermal average of the local field. According to the crossing relation (2.63),

[1] In free models, we could also have a disconnected term when there are a subset of $\{n_i\}$ and $\{m_j\}$ that are equal.

the relevant form factor for this object is [93]

$$F_{2n}(\theta_1+\pi\mathrm{i},\theta_2+\pi\mathrm{i},\cdots,\theta_n+\pi\mathrm{i},\theta_n,\cdots,\theta_2,\theta_1), \tag{2.73}$$

which is ill-defined due to the presence of kinematic poles. In order to better understand the singularity structure of the form factor (2.73), let us regularize it as follows:

$$\begin{aligned} &F_{2n}(\theta_1+\pi\mathrm{i}+\delta_1,\theta_2+\pi\mathrm{i}+\delta_2,\cdots,\theta_n+\pi\mathrm{i}+\delta_n,\theta_n,\cdots,\theta_2,\theta_1) \\ &\quad=\prod_{i=1}^{n}\frac{1}{\delta_i}\sum_{i_1=1}^{n}\sum_{i_2=1}^{n}\cdots\sum_{i_n=1}^{n}f_{i_1,i_2,\cdots,i_n}(\theta_1,\cdots,\theta_n)\delta_{i_1}\delta_{i_2}\cdots\delta_{i_n}+\cdots, \end{aligned} \tag{2.74}$$

where $f_{i_1,i_2,\cdots,i_n}(\theta_1,\cdots,\theta_n)$ is completely symmetric with respect to a rearrangement of indices, and "$\cdots$" refers to all the terms that vanish upon taking $\{\delta_i\}\to 0$ in any order. Notice that the value of the form factor (2.74) depends on the order of limits $\{\delta_i\}\to 0$, hence the order has to be properly specified so as to obtain a meaningful value. There are two common ways to eliminate such singularities: one is to keep only finite terms by getting rid of all the terms that are divergent when taking $\{\delta_i\}\to 0$ in (2.74). This prescription gives the finite unique result that is irrelevant to the order of limits $\{\delta_i\}\to 0$, yielding the *connected* form factor [68, 94]

$$F^{\mathrm{c}}_{2n}(\theta_1,\cdots,\theta_n)=\mathrm{FP}\lim_{\{\delta_k\}\to 0}F_{2n}(\theta_1+\pi\mathrm{i}+\delta_1,\cdots,\theta_n+\pi\mathrm{i}+\delta_n,\theta_n,\cdots,\theta_1). \tag{2.75}$$

Another one is to take a uniform limit such that $\delta_i=\delta\to 0$ for all $i$ that gives rise to the finite *symmetric* form factor [94]

$$F^{\mathrm{s}}_{2n}(\theta_1,\cdots,\theta_n)=\lim_{\{\delta_k\}=\delta\to 0}F_{2n}(\theta_1+\pi\mathrm{i}+\delta,\cdots,\theta_n+\pi\mathrm{i}+\delta,\theta_n,\cdots,\theta_1). \tag{2.76}$$

It was proven in [94] that, in terms of these form factors, the finite-volume diagonal matrix element $\langle\overleftarrow{\theta}\,|\mathcal{O}(0)|\,\overrightarrow{\theta}\,\rangle_L$ can be written as

$$\begin{aligned} \langle\overleftarrow{\theta}\,|\mathcal{O}(0)|\,\overrightarrow{\theta}\,\rangle_L&=\sum_{\substack{\alpha\subset\{1,\cdots,n\}\\ \alpha\neq\varnothing}}F^{\mathrm{s}}_{2|\alpha|}(\{\theta_i\}_{i\in\alpha})\mathcal{G}(\{\theta_i\}_{i\in\bar{\alpha}})+\mathcal{O}(e^{-\mu L}) \\ &=\sum_{\substack{\alpha\subset\{1,\cdots,n\}\\ \alpha\neq\varnothing}}F^{\mathrm{c}}_{2|\alpha|}(\{\theta_i\}_{i\in\alpha})\mathcal{G}(\alpha|\alpha)+\mathcal{O}(e^{-\mu L}), \end{aligned} \tag{2.77}$$

where $\mathcal{G}(\alpha|\alpha)$ is the principal minor of the Gaudin matrix, as before. Notice that, in fact, the second equality is satisfied without the exponential correction $\mathcal{O}(e^{-\mu L})$, i.e.

$$\sum_{\substack{\alpha\subset\{1,\cdots,n\}\\ \alpha\neq\varnothing}}F^{\mathrm{s}}_{2|\alpha|}(\{\theta_i\}_{i\in\alpha})\mathcal{G}(\{\theta_i\}_{i\in\bar{\alpha}})=\sum_{\substack{\alpha\subset\{1,\cdots,n\}\\ \alpha\neq\varnothing}}F^{\mathrm{c}}_{2|\alpha|}(\{\theta_i\}_{i\in\alpha})\mathcal{G}(\alpha|\alpha) \tag{2.78}$$

holds for whatever system size $L$. Therefore, it is possible to write a symmetric form factor $F^{\rm s}_{2n}(\theta_1,\cdots,\theta_n)$ just in terms of connected form factors $F^{\rm c}_{2n}(\theta_1,\cdots,\theta_n)$ only by taking a limit $L\to 0$:

$$F^{\rm s}_{2n}(\theta_1,\cdots,\theta_n)=\sum_{\substack{\alpha\subset\{1,\cdots,n\}\\ \alpha\neq\varnothing}}\mathcal{L}(\alpha|\alpha)F^{\rm c}_{2|\alpha|}(\{\theta_i\}_{i\in\alpha}). \tag{2.79}$$

To show this, we first note that the determinant $\mathcal{G}(\{\theta_i\}_{i\in\bar\alpha})$ can be represented in the following way

$$\mathcal{G}(\{\theta_i\}_{i\in\bar\alpha})=\sum_{\substack{I\subset\bar\alpha\\ I\neq\varnothing}}\mathcal{L}(I|I)\prod_{i\in I}Vp'(\theta_i), \tag{2.80}$$

Since $I$ is always a non-empty set, (2.80) necessarily vanishes when $L\to 0$ except when $\bar\alpha=\varnothing$, i.e. $\alpha=\{1,\cdots,n\}$. Hence the LHS of (2.78) becomes that of (2.79) under the limit. Together with an immediate observation that $\mathcal{G}(\alpha|\alpha)\to\mathcal{L}(\alpha|\alpha)$ with $L\to 0$, the relation (2.79) is established.

Having these in mind, we are now in a position to introduce the LeClair-Mussardo formula [68]. The formula is a variant of Källén-Lehmann spectral representation for the thermal (or GGE) average of a local operator $\mathcal{O}$, and is valid only in the infinite volume limit. It reads [68]

$$\langle\mathcal{O}\rangle=\frac{1}{Z}\mathrm{Tr}\,(e^{-RH}\mathcal{O})=\sum_{l=0}^{\infty}\Big(\prod_{k=1}^{l}\int\frac{\mathrm{d}\theta_k}{2\pi}n(\theta_k)\Big)F^{\rm c}_{2l}(\mathcal{O};\theta_1,\cdots,\theta_k) \tag{2.81}$$

where $Z$ is the partition function, and the filling function $n(\theta)$ is given by (2.15). This is a remarkable simplification in computing the thermal average of a local operator, but it still requires us to compute the connected form factor, which in general is very hard. Further, even if one manages to do so, carrying out the resummation is, in most cases, not feasible. Therefore, in practice, the formula is used with truncating after some terms; if excitation over the vacuum is small enough, this provides a fairly good approximation of the average.

We shall derive the formula combinatorially below. To start, let us first write down the finite-volume one-point function

$$\begin{aligned}\langle O\rangle_L&=\frac{1}{Z}\sum_{M=0}\frac{1}{M!}\sum_{n_1,\cdots,n_M}\sum_{j<k}^{M}(1-\delta_{n_j,n_k})e^{-RE(n_1,\cdots,n_M)}\langle n_M,\cdots,n_1|O|n_1,\cdots,n_M\rangle\\&=\frac{1}{Z}\sum_{m=0}^{\infty}\frac{(-1)^m}{m!}\sum_{n_1,\cdots,n_m}\sum_{r_1,\cdots,r_m}\frac{(-1)^{r_1+\cdots+r_m}}{r_1\cdots r_m}\\&\quad\times e^{-RE(n_1^{r_1},\cdots,n_m^{r_m})}\langle n_m^{r_m},\cdots,n_1^{r_1}|O|n_1^{r_1},\cdots,n_m^{r_m}\rangle.\end{aligned} \tag{2.82}$$

This becomes, in the thermodynamic limit,

$$\langle O\rangle = \frac{1}{Z}\sum_{m=0}^{\infty}\frac{(-1)^m}{m!}\int\frac{\mathrm{d}\theta_1}{2\pi}\cdots\frac{\mathrm{d}\theta_m}{2\pi}\sum_{r_1,\cdots,r_m}\frac{(-1)^{r_1+\cdots+r_m}}{r_1\cdots r_m} \times\prod_{j=1}^{m}e^{-Rr_jE(\theta_j)}\langle\theta_m^{r_m},\cdots,\theta_1^{r_1}|O|\theta_1^{r_1},\cdots,\theta_m^{r_m}\rangle \tag{2.83}$$

Notice that the matrix element entering in the expression actually differs from the standard one $\langle\overleftarrow{\theta}|\mathcal{O}(0)|\overrightarrow{\theta}\rangle_L$ up to the multiplicities for rapidities. Motivated by the Takács-Pozsgay formula (2.77), it was postulated in [93] that a similar formula holds even with the multiplicities:

$$\langle\theta_m^{r_m},\cdots,\theta_1^{r_1}|O|\theta_1^{r_1},\cdots,\theta_m^{r_m}\rangle = \sum_{\substack{\alpha\subset\{1,\cdots,m\}\\ \alpha\neq\varnothing}}F^{\mathrm{c}}_{2|\alpha|}(\{\theta_i\}_{i\in\alpha})\mathcal{G}(\alpha|\alpha) \tag{2.84}$$

Then, noting that

$$\begin{aligned}\hat{\mathcal{G}}(\alpha|\alpha)=\det(\hat{D}(\alpha|\alpha)+L(\alpha|\alpha)))&=\sum_{I\subset\bar{\alpha}}\mathcal{L}(\alpha\cup I|\alpha\cup I)\prod_{j\in I}Lp_j'r_j\\ &=\sum_{I\subset\bar{\alpha}}\sum_{F\in\mathcal{F}_{\alpha\cup I}}\prod_{j\in I}Lp_j'r_j\prod_{\langle jk\rangle\in F}r_jr_k\varphi_{jk},\end{aligned} \tag{2.85}$$

where $\hat{D}_{ij}=Lp_i'r_i\delta_{ij}$, the one point function (2.83) can be written as

$$\begin{aligned}\langle O\rangle = \frac{1}{Z}\sum_{m=0}^{\infty}\frac{1}{m!}\sum_{r_1}\int\frac{\mathrm{d}\theta_1}{2\pi}\frac{(-1)^{r_1-1}e^{-r_1RE(\theta_1)}}{r_1^2}\cdots\sum_{r_m}\int\frac{\mathrm{d}\theta_m}{2\pi}\frac{(-1)^{r_m-1}e^{-r_mRE(\theta_m)}}{r_m^2}\\ \times\sum_{\alpha\subset\{1,\cdots,m\}}\prod_{j\in\alpha}r_j^2F^{\mathrm{c}}_{2|\alpha|}(\{\theta_i\}_{i\in\alpha})\sum_{I\subset\bar{\alpha}}\sum_{F\in\mathcal{F}_{\alpha\cup I}}\prod_{j\in I}Lp_j'r_j\prod_{\langle jk\rangle\in F}r_jr_k\varphi_{jk}.\end{aligned} \tag{2.86}$$

Forests in the forest expansion in (2.86) are slightly more complicated than those showing up in (2.48). Each forest is made of directed trees rooted at vertices $\alpha\cup I$ where $\alpha\subset\{1,\cdots,m\}$ and $I\subset\bar{\alpha}$. These trees can be further grouped into those rooted at $I$ and $\alpha$, the latter of which can be regarded as a decoration of a single vertex with $|\alpha|$ lines growing out: see Fig. 2.8. Summing over the forests those two subforests are factorized, and as a consequence, the former consisting of vacuum diagrams are canceled out by the partition function in (2.86). We are thus left with the diagrams depicted in Fug.2.9, where the symmetry factor of each tree is taken into account as usual. It is immediate to write down the expression corresponding to these diagrams, yielding

$$\langle\mathcal{O}\rangle=\sum_{m=0}^{\infty}\frac{1}{m!}\int\prod_{j=1}^{m}\frac{\mathrm{d}\theta_j}{2\pi}\sum_{r_j}r_j^2Y_{r_j}(\theta_j)F^{\mathrm{c}}_{2m}(\theta_1,\cdots,\theta_m). \tag{2.87}$$

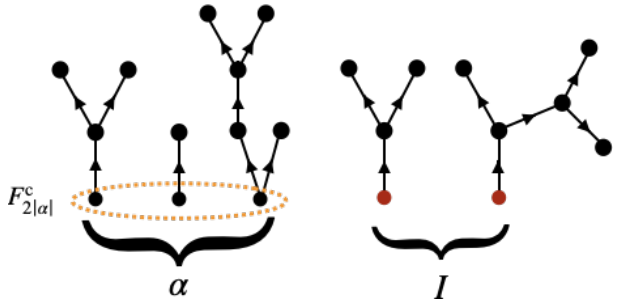


Figure 2.8: A typical forest appearing in (2.86). It can be divided into subforests comprising vacuum diagrams and a vertex $F^{\rm c}_{2|\alpha|}$ with $|\alpha|$ lines growing out of it each of which is connected to a tree.

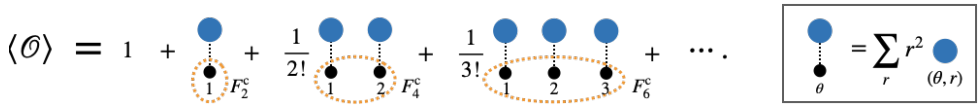


Figure 2.9: Tree expansion of a thermal one-point function. A blue dot is the generating function of the trees rooted at a particular vertex, as defined in Fig. 2.6.

This is nothing but the LeClair-Mussardo forumla (2.81), since

$$\sum_r r^2 Y_r(\theta) = \frac{Y_1(\theta)}{1+Y_1(\theta)} = n(\theta). \tag{2.88}$$

As stated above, it is in general hard to obtain exact connected form factors, but there are some known observables whose connected form factors are explicitly determined. One of such example is the densities of the conserved charges, $\mathfrak{q}$, for which the connected form factor reads

$$F^{\rm c}_{2n,\mathfrak{q}}(\theta_1,\cdots,\theta_n) = h(\theta_1)\varphi_{1,2}\cdots\varphi_{n-1,n}p'(\theta_n) + \text{perm}, \tag{2.89}$$

where perm. is understood as permutations with respect to the integer set $\{1,\cdots,n\}$. This was conjectured by Saleur in [97], and can be in fact obtained easily combinatorially [66]. We first realize that its finite volume matrix element is trivially given by

$$\langle \theta_m^{r_m},\cdots,\theta_1^{r_1}|\mathfrak{q}|\theta_1^{r_1},\cdots,\theta_m^{r_m}\rangle = \frac{1}{L}\sum_{j=1}^m r_j h(\theta_j)\mathcal{G}(\{\theta_i\}_{i\in\{1,\cdots,m\}}). \tag{2.90}$$

Plugging it into (2.83), we then realize that the resulting forest expansion merely generates all possible forests each of which contains a tree in which $r_j h(\theta_j)/L$ is inserted at one of the vertices. In each forest, trees without the insertion constitute the vacuum trees as usual. This results in the factorisation of the set of trees with insertions and forests without insertions, the latter of which are cancelled out by the partition function. We then end up with the spanning trees each of which is inserted $r_j h(\theta_j)/L$ at an arbitrary

vertex. Notice that we can think of each tree as a consequence of decorating the vertices belonging to the unique spine growing out from the root down to the inserted vertex. As a consequence, the sum over such spanning trees can be expanded as in Fig. 2.10. Pulling

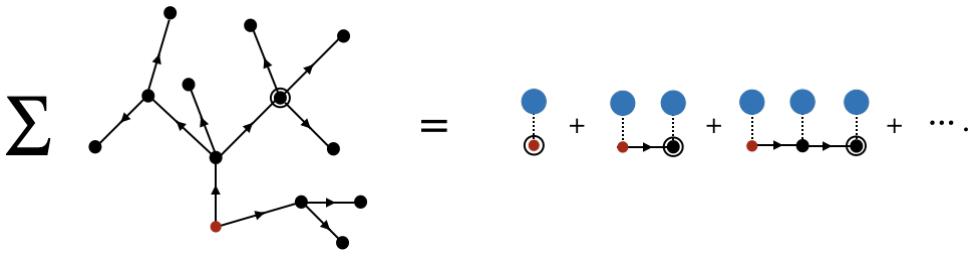

Figure 2.10: Tree expansion of a thermal one-point function for the density of a conserved charge. The black circle indicates the vertex at which the extra factor is inserted.Note that global symmetric factors are absent, as the trees are marked.

out the factor $Lrp'$ from each red vertex, the expansion can be written as

$$\begin{aligned}\langle \mathfrak{q} \rangle &= \sum_r \int \frac{\mathrm{d}\theta}{2\pi} p'(\theta) r^2 Y_r(\theta) h(\theta) \\ &\quad + \sum_{r_1,r_2} \int \frac{\mathrm{d}\theta_1}{2\pi} \frac{\mathrm{d}\theta_2}{2\pi} p'(\theta_1) r_1^2 Y_{r_1}(\theta_1) \varphi(\theta_2,\theta_1) r_2^2 Y_{r_2}(\theta_2) \cdots \\ &= \sum_{n=1}^{\infty} \int \prod_{j=1}^{n} \frac{\mathrm{d}\theta_j}{2\pi} n(\theta_j) p'(\theta_n) \varphi(\theta_n,\theta_{n-1}) \cdots \varphi(\theta_2,\theta_1) h(\theta_1), \end{aligned} \tag{2.91}$$

which implies (2.89). In fact we can carry out the exact resummation for (2.91), yielding (2.22), namely

$$\langle \mathfrak{q} \rangle = \int \frac{\mathrm{d}\theta}{2\pi} p'(\theta) n(\theta) h^{\mathrm{dr}}(\theta), \tag{2.92}$$

From the last line of (2.91), it is obvious that the expression is invariant under swapping $p'$ and $h$, hence (2.26) follows.

# Chapter 3

# Hydrodynamics

## 3.1 Derivative expansion

The underlying condition for the validity of hydrodynamics is usually referred to *local equilibrium* and its stable propagation, in a manner of which local equilibrium is achieved at each time slice. The emergent mesoscopic region in space (and time) within which equilibrium is effectively realized is called *fluid cell* [33, 45], and we claim that hydrodynamic approximation is valid whenever the system evolves with maintaining the local equilibrium. Fluid cells are supposed to be large enough so that thermodynamics can be locally applied to each of them, but still small enough compared to macroscopic scales such as the variation of the density of the fluid. The emergence of fluid cells is also called the *separation of scale*, and is the only working assumption that underpins the use of hydrodynamics. Technically, the assumption of local equilibrium and its stable propagation is implemented through the hydrodynamic equations. To illustrate the idea, let us consider the slow dynamics of a locally interacting many-body system. Let us further suppose that the system has $N$ conservation laws with conserved charges $Q_i$, $i = 1, \cdots, N$. Accordingly we have the associated density of the conserved charges $\mathfrak{q}_i$ (i.e. $Q_i = \int \mathrm{d}x\, \mathfrak{q}_i(x,0)$ ) and the current $\mathfrak{j}_i$ that satisfy the continuity equation

$$\partial_t \mathfrak{q}_i(x,t) + \partial_x \mathfrak{j}_i(x,t) = 0. \tag{3.1}$$

The corresponding continuity equation for the average of $\mathfrak{q}_i$ and $\mathfrak{j}_i$ can then be written down:

$$\partial_t \langle \mathfrak{q}_i(x,t) \rangle + \partial_x \langle \mathfrak{j}_i(x,t) \rangle = 0, \tag{3.2}$$

where the average $\langle \cdots \rangle$ is taken with respect to the initial density operator $\rho_{\mathrm{ini}}$. When the system is varying on a large scale both in time and space, the assumption of local equilibrium is implemented as follows [98]: the average of any observable $\mathcal{A}(x,t)$ can be expressed just in terms of $\langle \mathfrak{q}_i(\cdot,t) \rangle$. Namely, for every $\mathcal{A}(x,t)$, there is a functional of $\mathfrak{q}_i(\cdot,t) = \langle \mathfrak{q}_i(\cdot,t) \rangle$ such that

$$\langle \mathcal{A}(x,t) \rangle = \mathcal{F}[\vec{\mathfrak{q}}(\cdot,t)], \tag{3.3}$$

where $\mathfrak{q}_i(\cdot,t)$ refers to the average charge density in the vicinity of space $x$. Equivalently, we can also write $\mathcal{A}(x,t)$ as a derivative expansion

$$\langle \mathcal{A}(x,t)\rangle = \mathfrak{A}[\vec{\mathfrak{q}}(x,t)] + \sum_j \mathfrak{B}[\vec{\mathfrak{q}}(x,t)]\partial_x \mathfrak{q}_j(x,t) + \mathcal{O}(\partial_x^2 \mathfrak{q}_j(x,t)). \tag{3.4}$$

This is clearly a drastic simplification in computing the space-time dependent observable averages in an inhomogeneous state; in order to calculate the average of an observable at $(x,t)$, one only needs to know the averages of the conserved charges within the fluid cell containing $x$. The rationale behind (3.3) is that the dynamics of many-body systems is generically expected to be governed by the slow modes like conserved charges when the system varies gently, and as such the dynamics of observables are largely constrained by that of conserved charges.

For our purpose, we apply the derivative expansion to the current average:

$$\langle \mathfrak{j}_i(x,t)\rangle = \mathfrak{F}_i[\vec{\mathfrak{q}}(x,t)] - \sum_j \mathfrak{D}_i{}^j[\vec{\mathfrak{q}}(x,t)]\partial_x \mathfrak{q}_j(x,t) + \mathcal{O}(\partial_x^2 \mathfrak{q}_j(x,t)). \tag{3.5}$$

Some comments are in order. First, the first term in (3.5), $\mathfrak{F}_i[\vec{\mathfrak{q}}(x,t)]$, is called the *equations of state*, and is completely fixed by the thermodynamics of the model. This is the leading term in the derivative expansion, and the hydrodynamic theory with the derivative expansion truncated after this term is called *Euler hydrodynamics*. The second term is what we call the *constitutive relation*, and is responsible for the diffusive effect arising in the fluids motion. This term accounts for the subleading effect in the derivative expansion, and therefore can be neglected when one considers the dynamics on a sufficiently large scale. It, however, becomes important when the fluid develops a fine structure, or when the leading contribution vanishes for some reason (e.g. symmetry) [46, 98, 99].

Let us first consider the case where the diffusive correction is ignorable, i.e. Euler scale[1]. The hydrodynamic equation can be cast into the following quasi-convective form

$$\partial_t \mathfrak{q}_i(x,t) + \sum_j A_i{}^j[\vec{\mathfrak{q}}(x,t)]\partial_x \mathfrak{q}_j(x,t) = 0, \tag{3.6}$$

where $A_i{}^j[\vec{\mathfrak{q}}(x,t)] = \partial \mathfrak{F}_i[\vec{\mathfrak{q}}(x,t)]/\partial \mathfrak{q}_j(x,t)$ is the flux Jacobian matrix. The fluid variable $\mathfrak{q}_i(x,t)$ is a natural and physical variable that originates from the density of the conserved charges. In fact, at the Euler scale, states, and in particular the average of a local observable $\langle \mathcal{A}(x,t)\rangle$, can be fully fixed by the spatio-temporal lagrange multipliers $\beta^i(x,t)$ [33, 100]:

$$\langle \mathcal{A}(x,t)\rangle = \frac{1}{Z(x,t)}\mathrm{Tr}\left(e^{-\sum_j \beta^j(x,t)Q_j}\mathcal{A}(0,0)\right), \quad Z(x,t) = \mathrm{Tr}\left(e^{-\sum_j \beta^j(x,t)Q_j}\right). \tag{3.7}$$

[1] A mathematically precise definition of the Euler scale can be found, for instance, in [100].

Hence this relation induces a map $\vec{\beta}(x,t) \mapsto \vec{\mathfrak{q}}(x,t)$, which is expected to be bijective. This allows us to cast the Euler equation (3.6) into the equation for $\beta^i(x,t)$, which reads

$$\partial_t \beta^i(x,t) + \sum_j (A^{\mathrm{T}})^i{}_j(x,t)\partial_x \beta^j(x,t) = 0. \tag{3.8}$$

Those are however not the most convenient fluid coordinates for some purposes. It is sometimes better and more transparent to work with another fluid coordinate called *normal mode* $\vec{n}$ whose Jacobian matrix for the nonlinear transformation $\vec{\mathfrak{q}} \mapsto \vec{n}$ diagonalizes the flux Jacobian matrix $A$

$$\sum_{k,l} \frac{\partial n_i(x,t)}{\partial \mathfrak{q}_k(x,t)} A_k{}^l \frac{\partial n_l(x,t)}{\partial \mathfrak{q}_j(x,t)} = \mathrm{diag}\,(v_i^{\mathrm{eff}})\delta_i{}^j, \tag{3.9}$$

where $v_i^{\mathrm{eff}}(x,t)$, which we call effective velocity, are the eigenvalues of $A$. Accordingly the hydrodynamic equation in terms of the normal mode takes the diagonalized form

$$\partial_t n_i(x,t) + v_i^{\mathrm{eff}}(x,t)\partial_x n_i(x,t) = 0. \tag{3.10}$$

We therefore see that the matrix $A$ and its eigenvalues completely determine the nature of ballistic transport. It is however important to note that the existence of such nonlinear transformation is not always guaranteed[2]. That said so, we can easily see that stable normal modes can always exist when the system is close to equilibrium. Suppose that we can linearize (3.6) with respect to a homogeneous background. Then the linearized equation becomes

$$\partial_t \mathfrak{q}_i(x,t) + \sum_j A_i{}^j[\vec{\mathfrak{q}}_{\mathrm{sta}}]\partial_x \mathfrak{q}_j(x,t) = 0, \tag{3.11}$$

where $\mathfrak{q}_{\mathrm{sta}}$ is the equilibrium average with respect to the uniform background. With the linear transformation $n_i = \sum_j R_i{}^j \mathfrak{q}_j$ where $RAR^{-1} = \mathrm{diag}(v_i^{\mathrm{eff}})$, we can transform (3.11) into the equation for the normal mode

$$\partial_t n_i(x,t) + v_i^{\mathrm{eff}}\partial_x n_i(x,t) = 0. \tag{3.12}$$

Let us also remark that, in fact, the flux Jacobian matrix $A$ is intimately related to a quantity that has played a pivotal role in the context of transport phenomena: the Drude weight. The Drude weight matrix $D_{ij}$ is defined as

$$D_{ij} = \lim_{t\to\infty} \frac{1}{2t} \int_{-t}^{t} \mathrm{d}s \int \mathrm{d}x \langle \mathfrak{j}_i(x,s)\mathfrak{j}_j(0,0)\rangle^c, \tag{3.13}$$

[2]In the case of integrable systems, the special structure of its hydrodynamic equation admits such transformation, hence the normal modes [45, 46, 101]

which, provided that $t \to \infty$ limit exists, also can be cast into

$$D_{ij} = \lim_{t\to\infty} \int \mathrm{d}x \langle \mathfrak{j}_i(x,t)\mathfrak{j}_j(0,0)\rangle^c. \tag{3.14}$$

Remarkably, Drude weight can be written as

$$D_{ij} = (BC^{-1}B)_{ij} = (ACA^{\mathrm{T}})_{ij}, \tag{3.15}$$

where $B_{ij}$ and the susceptibility matrix $C_{ij}$ are defined by

$$B_{ij} = \int \mathrm{d}x \langle\, \mathfrak{q}_i(x,0)\mathfrak{j}_j(0,0)\rangle^c, \quad C_{ij} = \int \mathrm{d}x\, S_{ij}(x,0) \tag{3.16}$$

with the equilibrium correlation function $S_{ij}(x,t) = \langle \mathfrak{q}_i(x,t)\mathfrak{q}_j(0,0)\rangle^c$. Note that we used $B_{ij} = (AC)_{ij} = (CA^{\mathrm{T}})_{ij}$ in the last expression in (3.15), which can be shown as follows. First, recall that the following holds for any homogeneous and stationary state

$$\langle \mathfrak{j}_i(x,t)\mathfrak{q}_j(0,0)\rangle^c = \langle \mathfrak{q}_i(x,t)\mathfrak{j}_j(0,0)\rangle^c, \tag{3.17}$$

which implies $B_{ij} = \partial\langle \mathfrak{j}_j\rangle/\partial\beta_i = \partial\langle \mathfrak{j}_i\rangle/\partial\beta_j = B_{ji}$. Then, using the chain rule the relation follows from the definition of $A_i^{\ j}$ and $C_{ij}$.

To show (3.15), let us introduce the idea of *hydrodynamic projection* [100,102]. Among possible implementations, what we present here is called a stronger version of hydrodynamic projection. The underlying idea is that, in the long-wavelength limit, any physical state can be projected onto the time-invariant subspace spanned by conserved charges. More precisely, let us consider an equilibrium correlator $S_{\mathcal{AB}}(x,t) = \langle \mathcal{A}(x,t)\mathcal{B}(0,0)\rangle^c$ for two arbitrary local operators $\mathcal{A}$ and $\mathcal{B}$, and its Fourier transformation $S_{\mathcal{AB}}(k,t) = \int \mathrm{d}x\, e^{\mathrm{i}kx} S_{\mathcal{AB}}(x,t)$. Furthermore we define its Euler scaling limit as

$$S^{\mathrm{Eur}}_{\mathcal{AB}}(kt) = \lim_{\substack{k\to 0,\, t\to\infty \\ kt:\text{fixed}}} S_{\mathcal{AB}}(k,t). \tag{3.18}$$

The hydrodynamic projection is then implemented as the following *assumption*: $S^{\mathrm{Eur}}_{\mathcal{AB}}(kt)$ can be decomposed as

$$S^{\mathrm{Eur}}_{\mathcal{AB}}(kt) = \sum_{i,j,l,m} S^{\mathrm{Eur}}_{\mathcal{A}i}(kt) C^{ij} S_{jl}(kt) C^{lm} S^{\mathrm{Eur}}_{m\mathcal{B}}(kt), \tag{3.19}$$

where $C^{ij} = (C^{-1})_{ij}$. In hydrodynamics, objects of the form $f_{\mathcal{AB}} = \lim_{t\to\infty} \int \mathrm{d}x\, S_{\mathcal{AB}}(x,t)$ often appear for which hydrodynamic projection offers a simple decomposition

$$f_{\mathcal{AB}} = \sum_{i,j} S^{\mathrm{Eur}}_{\mathcal{A}i}(0) C^{ij} S^{\mathrm{Eur}}_{j\mathcal{B}}(0), \tag{3.20}$$

which reminds us of an insertion of the identity of resolution in the spectral decomposition. Now, applying this formula to the Drude weight, we immediately find that $D_{ij} = (BC^{-1}B)_{ij}$.

## 3.2 Effect of diffusion

When the diffusion term is included in the hydrodynamic equation, we have the so-called *Navier-Stokes equation*

$$\partial_t \mathfrak{q}_i(x,t) + \sum_j A_i{}^j[\vec{\mathfrak{q}}(x,t)]\partial_x \mathfrak{q}_j(x,t) = \partial_x \sum_j \mathfrak{D}_i{}^j[\vec{\mathfrak{q}}(x,t)]\partial_x \mathfrak{q}_j(x,t). \tag{3.21}$$

To better appreciate the effect of the diffusion term, it is instructive to consider the propagation of an initial perturbation. For that purpose, let us consider the time-evolution of the equilibrium correlator $S_{ij}(x,t)$. In order to derive an evolution equation for this object, let us assume that our initial state is a slowly varying state $\rho_{\rm ini} = \exp(\sum_k \int \mathrm{d}x\, \beta_k(x)\mathfrak{q}_k(x,0))/Z$, where $Z$ is the partition function of the initial state. Then, by differentiating $\langle \mathfrak{q}_i(x,t)\rangle$ with respect to $\beta_j(y)$, we obtain $\langle \mathfrak{q}_i(x,t)\mathfrak{q}_j(0,0)\rangle^c_{\rm ini}$ whose average is evaluated with respect to $\rho_{\rm ini}$. Taking the uniform limit $\beta_i(x) \to \beta_i$ for all $i$, we then have the equilibrium average $\langle \mathfrak{q}_i(x,t)\mathfrak{q}_j(0,0)\rangle^c$. We perform the similar manipulation to (3.21), and noting that $\partial_x \mathfrak{q}_i(x,t) = 0$ when evaluated with the uniform Lagrange multipliers $\beta_i$, we end up with the following equation

$$\partial_t S_{ij}(x,t) + \sum_k \Big( A_i{}^k[\vec{\mathfrak{q}}_{\rm sta}]\partial_x - \mathfrak{D}_i{}^k[\vec{\mathfrak{q}}_{\rm sta}]\partial_x^2 \Big) S_{kj}(x,t) = 0. \tag{3.22}$$

This equation now takes the form of the heat equation, thus has a closed solution. Suppose that we choose our initial state as $S_{ij}(x,0) = C_{ij}\delta(x,0)$. Then the solution of (3.22) is given in terms of a Fourier transformation

$$S_{ij}(x,t) = \int \frac{\mathrm{d}k}{2\pi} e^{\mathrm{i}kx} \Big( e^{-(\mathrm{i}kA + k^2\mathfrak{D})t} C \Big)_{ij}. \tag{3.23}$$

Notice that the solution is valid only for $t > 0$, and not true for $t < 0$. This is because, provided the Navier-Stokes equation is correct for $t < 0$, it cannot emerge from the initial condition $\rho_{\rm ini}$, which is a state prepared at $t = 0$, i.e. time later than $t < 0$. Nonetheless we can still deduce the equation $S_{ij}(x,t)$ satisfies when $t < 0$ by invoking the $\mathcal{PT}$*-symmetry*. $\mathcal{PT}$-symmetry can be implemented in various ways to a given system, but has to be represented by an anti-unitary transformation that preserves Hamiltonian and momentum operator. It is in fact very natural to assume the symmetry, which is expected to be possessed by most physical system (see e.g. [103] for a review of $\mathcal{PT}$-symmetric systems in general). Here we assume the stronger version of it, namely we assume that all the conserved charges $Q_i$ are $\mathcal{PT}$-symmetric, and that local observables are transformed into local observables under $\mathcal{PT}$ transformation. These conditions then impose a constraint as to how $\mathcal{PT}$-transformation acts onto densities of conserved charges $\mathfrak{q}_i$, which turns out to be, upon appropriately fixing the inherent gauge degrees of freedom

in $\mathfrak{q}_i$[3],

$$\mathcal{PT}\mathfrak{q}_i(x,t)(\mathcal{PT}) = \mathfrak{q}_i(-x,-t). \tag{3.24}$$

We then perform the $\mathcal{PT}$-transformation to $S_{ij}(x,t)$, which gives $S_{ij}(x,t) = S_{ij}(-x,-t)$. As a consequence, (3.22) yields [98]

$$\left[\partial_t + \sum_k \left(A_i{}^k[\vec{\mathfrak{q}}_{\rm sta}]\partial_x + \mathfrak{D}_i{}^k[\vec{\mathfrak{q}}_{\rm sta}]\partial_x^2\right)\right] S_{kj}(x,t) = 0, \tag{3.25}$$

which is now only valid for $t < 0$. This allows us to derive the full $S_{ij}(x,t)$ defined for any $t$ with the initial condition $S_{ij}(x,0) = C_{ij}\delta(x,0)$:

$$S_{ij}(x,t) = \int \frac{\mathrm{d}k}{2\pi} e^{\mathrm{i}kx} \left(e^{-(\mathrm{i}kAt + k^2\mathfrak{D}|t|)}C\right)_{ij}. \tag{3.26}$$

The physical meaning of it becomes even clearer if instead we look at the correlators of normal modes, i.e. $S^\sharp_{ij}(x,t) = \langle (R\vec{\mathfrak{q}})_i(x,t)(R\vec{\mathfrak{q}})_j(0,0)\rangle^c$. We normalize the normal modes so that $\int \mathrm{d}x S^\sharp_{ij}(x,t) = \delta_{ij}$, which entails $RCR^{\mathrm{T}} = 1$. Accordingly the normal mode correlator reads

$$S^\sharp_{ij}(x,t) = \int \frac{\mathrm{d}k}{2\pi} e^{\mathrm{i}kx} \left(e^{-(\mathrm{i}kA^\sharp t + k^2\mathfrak{D}^\sharp|t|)}\right)_{ij}, \tag{3.27}$$

where $A^\sharp_{ij} = \sum_{k,l,m} R_i{}^k A^l_k (R^{-1})_l{}^m \delta_{mj} = v^{\rm eff}_i \delta_{ij}$ and $\mathfrak{D}^\sharp_{ij} = \sum_{k,l,m} R_i{}^k \mathfrak{D}^l_k (R^{-1})_l{}^m \delta_{mj}$. The diffusion matrix in the normal mode basis $\mathfrak{D}^\sharp_{ij}$ obviously couples each normal mode to another, but we anticipate that, for large $t$, the cross-coupling accounted for by the non-diagonal components of $\mathfrak{D}^\sharp_{ij}$ becomes negligible. This *decoupling principle* is motivated by the fact that each normal mode has its propagation velocity $v^{\rm eff}$ (assumed to be non-degenerate), wherefore correlation between two distinctive modes become substantially small in the large time limit. Hence we expect that, for large $t$,

$$S^\sharp_{ij}(x,t) \simeq \delta_{ij} \int \frac{\mathrm{d}k}{2\pi} e^{\mathrm{i}kx} e^{-(\mathrm{i}kv^{\rm eff}_i t + k^2 \mathfrak{D}^\sharp_{ii}|t|)} = \frac{1}{\sqrt{4\pi \mathfrak{D}^\sharp_{ii}|t|}} \exp\left[-\frac{(x - v^{\rm eff}_i t)^2}{4\mathfrak{D}^\sharp_{ii}|t|}\right], \tag{3.28}$$

where we assumed that the diagonal components $\mathfrak{D}^\sharp_{ii}$ are positive for all $i$. We are finally in a position to examine how the diagonal correlator $S^\sharp_{ii}(x,t)$ with the initial delta-function profile $S^\sharp_{ii}(x,0) = \delta(x)$ propagates across the system. First, when we ignore the effect of diffusion, we immediately see that the correlator keeps its form in the course of time-evolution, i.e. $S^\sharp_{ii}(x,t) = \delta(x - v^{\rm eff}t)$. The role played by diffusion is then to broaden the sharp profile so that the width of the peak spreads as $\sim t^{\frac{1}{2}}$. Namely, in the presence of diffusion, $S^\sharp_{ii}(x,t)$ represents a peak propagating ballistically with broadening diffusively [47].

[3]We always have a freedom to add a total derivative term to $\mathfrak{q}_i$ and $\mathfrak{j}_i$ by making sure that, after these additions, they still satisfy the continuity equations.

# Chapter 4

# Generalized hydrodynamics

## 4.1 Basic formalism of generalized hydrodynamics

In this section, we review the paper [45] supplemented by some topics discussed in [104]. My main contribution in [45] are the (sketchy) proofs of the current average formula (presented in the appendix D) and analysis on the Lieb-Liniger model.

As we discussed in the section 3.1, the idea of hydrodynamics has been applied to, even within the realm of mechanical many-body systems, a plethora of both quantum and classical systems. It had not been, however, applied to integrable systems until 2016 in the works [45,46] in which the Euler scale hydrodynamics of integrable systems was proposed for the first time. Its validity for the spin-1/2 XXZ chain was also checked against stringent numerical simulation by the time dependent density matrix renormalization group (tDMRG) in [46]. Initiated by these two works, the idea of hydrodynamics for integrable systems, later coined *generalized hydrodynamics*[1] (GHD), has been an extremely active subject since then, revealing its remarkable structures as well as far-reaching predictive power that is useful in describing the dynamics of ultra-cold atoms confined in one dimension.

Before going into the detail of the theory, let us summarize the developments of GHD so far and its current status. After the invention of the theory, it was soon extended so that it can incorporate the effect of external potentials [104]. This made the theory into a prominent tool to theoretically study the dynamics of the Lieb-Liniger gas in the inhomogeneous potential, which is expected to describe the actual ultra-cold atom experiments. Furthermore, it was also realized that there is a remarkable correspondence with the hydrodynamics of the classical hard-rod gases [69], which will be elaborated in the section 4.3. This has allowed us to simulate GHD efficiently by means of molecular dynamics even in the presence of external forces [105,106]. Meanwhile, instead of simulating GHD, a way to directly solve the GHD equation was also sought. It turned out that the

[1] This name was chosen following the nomenclature in integrable systems, i.e. in the same spirit as how GGE was termed.

conventional method of characteristics can actually be applied to the GHD equation in two different, but closely-related manners [107, 108].

These investigations indeed aimed at understanding and solving the hydrodynamics of integrable systems at the Euler scale, which is the largest possible hydrodynamic scale in space and time. By simply appealing to the nature of quasi-particle excitations that propagate ballistically, it is tempting to conclude that all the large scale dynamics in integrable systems follow the GHD equation. However, as we mentioned in the introduction already, there are known cases where ballistic transport is absence, and rather, diffusive transport is realized. One of the most prominent examples is the spin transport in the gapped XXZ spin-1/2 chain where all the conserved charges are spin-flip invariant except the $z$-component of spin $S^z$, rendering the spin Drude weight being zero [56, 57, 98, 99, 109–112]. Hence it is of prime importance, and also a natural extension as a hydrodynamic theory, to know how to implement the diffusion corrections to the original Euler scale GHD equation. This enterprise actually requires us to work out computations involving a rather nontrivial correlation function. Being said so, it was recently realized that one can actually assess the correlation function with the aid of thermodynamic form factors[2] [114, 115], and it was confirmed that the so-obtained diffusion constants agree with tDMRG numerics as well as reproduce the known diffusion corrections of the hard rod gases [98]. With the diffusive corrections, we have therefore obtained the full Navier-Stokes equation for integrable systems. It was also realized later that the diffusion constants in integrable systems actually constitute a nontrivial contribution to the whole diffusion constants in a generic non-integrable system with ballistic components [116, 117]. So far GHD has been applied to a wide range of models from classical integrable systems such as the classical hard-rod gases [118, 119], the classical sinh-Gordon model [120], and the classical Toda chain [121–124] to quantum integrable systems such as the Lieb-Liniger model [45, 70, 105, 108], the XXZ spin 1/2 chain [46, 99, 112, 125–127], the Fermi-Hubbard model [128], and the sine-Gordon model [129].

NESS currents are one of the primary quantities to look at in hydrodynamics. They can be, however, also obtained as a byproduct by studying the *fluctuation* of the transferred charge. A common pathway to study fluctuation is the large deviation theory, or equivalently, the full counting statistics [130]. Of particular interest in the latter is the cumulant generating function that encodes all the information of fluctuation including the currents. The cumulant generating function in integrable systems was explicitly derived [102, 131] in a way that is somewhat related to the macroscopic fluctuation theory [2]. The validity of the cumulant generating function was confirmed for the hard rod gases by computing the first few cumulants obtained by the generating function and comparing

[2]Thermodynamic form factors are the generalization of standard form factors in a sense that the standard ones are matrix elements for excitations over the vacuum, while the thermodynamic ones involve excitations on top of the thermodynamic macro states. A program to rationalize the thermodynamic form factor approach in the same spirit as the conventional form factor approach has been put forward recently [113], but large parts of it has not yet been well grounded.

against Monte-Carlo simulations [131].

In the context of ultra-cold atom experiments, the actual setup used in the quantum Newton's cradle experiment was demonstrated using GHD for the Lieb-Liniger model in [105]. There, the lack of thermalization after two clouds of the Lieb-Liniger gases colliding each other was indeed observed as in the experiment. In fact, it is reasonable to expect that if we wait long enough (longer than the time scale accessible by state-of-the-art experiments), then inhomogeneity of the trap induces integrability-breaking and eventual relaxation to a Gibbs state. This was note quite what we observed: because the GHD equation has actually infinitely many conserved quantities even in the presence of trapping potentials (not in the sense of Bethe ansatz), an equilibration to a Gibbs state could not be captured by GHD. It is also noteworthy that the validity of GHD was recently experimentally confirmed using 87Rb gases on an atom chip [106]. Importantly, in the experiment, it was explicitly demonstrated that the experimental data agrees more with the prediction by GHD than with that by conventional hydrodynamics, thereby invalidating the use of conventional hydrodynamics in describing the dynamics of one dimensional ultra-cold atom gases in general.

Following [45,104], let us first introduce the basic formalism of the Euler scale GHD. At the Euler scale, according to the principle of derivative expansion (3.5), we can completely fix the hydrodynamic problem by providing the equations of state: relations connecting averages of currents to averages of densities. In integrable systems, the thermodynamic Bethe ansatz (TBA) formulation, introduced in the section 2.1, of GGE averages offers a powerful way of obtaining these equations of state. In this formulation, the most natural objects are the quasi-particles. Recall that quasi-particles are parametrized by their internal quantum numbers $a$ (parametrizing the spectrum of the model) and a continuous rapidity $\theta$. Note that $\theta$ will be identified with the velocity in Galilean systems or the rapidity in relativistic systems. Furthermore, the model can also have additional internal degrees of freedoms (flavor), which results in non-diagonal scatterings. Integrable systems with these additional degrees of freedoms, such as the sine-Gordon model and the Fermi-Hubbard model, are known to be solved by the nested TBA, and it has been checked that generalized hydrodynamics can be naturally applied to these systems as well. For brevity, we shall consider the simplest case in the following considerations, i.e. a generic quantum integrable system possessing single species (of fermionic type) only with diagonal scatterings. The fundamental object that complete the full specification of the model is the differential scattering $\varphi(\theta, \theta')$, describing the scattering between particles. By relativistic or Galilean invariance, it depends on the rapidities or velocities only through their differences $\theta - \theta'$.

The basic ingredient needed to specify the full hydrodynamic states at the Euler scale is, according to (3.6), the equations of state $\langle \mathfrak{j}_i \rangle_\rho = \mathfrak{F}[\langle \vec{\mathfrak{q}}_i \rangle_\rho]$, i.e. the thermodynamic relation between the average of densities $\mathfrak{q}_i$ of conserved charges $Q_i = \int \mathrm{d}x\, \mathfrak{q}_i(x,0)$ and the average of associated currents $\mathfrak{j}_i$. Here the average is taken with respect to an arbitrary GGE $\rho \sim e^{-\sum_i \beta_i Q_i}$. A cornerstone of GHD is that, one can actually express both $\langle \mathfrak{q}_i \rangle_\rho$

and $\langle \mathfrak{j}_i \rangle_\rho$ in terms of quasi-particle basis. The TBA expression of $\langle \mathfrak{q}_i \rangle_\rho$ was derived in the section 2.3.3, and we shall present the derivation of the current averages in the next section. Let us simply cite the results here; to reiterate, the average charge densities $\langle \mathfrak{q}_i \rangle_\rho$, in the infinite volume limit, have a remarkably concise form [65, 66, 97]

$$\langle \mathfrak{q}_i \rangle_\rho = \int \mathrm{d}\theta \rho_{\mathrm{p}}(\theta) h_i(\theta), \tag{4.1}$$

where $\rho_{\mathrm{p}}(\theta)$ is the density of particle determined by (2.15), (2.16), and (2.20), and $h_i(\theta)$ is the one-particle eigenvalue of the conserved charge $Q_i$: $Q_i|\theta\rangle = h_i(\theta)|\theta\rangle$. Note that this is the only quantity entering in the expression that has information about $Q_i$. By contrast, although the LeClair-Mussardo-Saleur formula (4.1) has been known for decades (and also follows straightforwardly from TBA), it was not known until 2016 was how to express the current average $\langle \mathfrak{j}_i \rangle_\rho$ in the similar manner. A proposal was then made in [45, 46], reading

$$\langle \mathfrak{j}_i \rangle_\rho = \int \mathrm{d}\theta \rho_{\mathrm{p}}(\theta) v^{\mathrm{eff}}(\theta) h_i(\theta), \tag{4.2}$$

where the *effective velocity* $v^{\mathrm{eff}}(\theta)$ is given by

$$v^{\mathrm{eff}}(\theta) = \frac{(E')^{\mathrm{dr}}(\theta)}{(p')^{\mathrm{dr}}(\theta)}, \tag{4.3}$$

and where $E(\theta)$ and $p(\theta)$ are the energy and momentum of a particle at velocity or rapidity $\theta$, and the dressing operation was defined in (2.23). We emphasize that the current average formula (4.2) is true only at the Euler scale; when diffusion corrections are taken into account, the current average also includes the subleading term as per (3.5). Notice that the averages of densities $\langle \mathfrak{q}_i \rangle_\rho$ and currents $\langle \mathfrak{j}_i \rangle_\rho$ differ only by the appearance of $v^{\mathrm{eff}}(\theta)$ in the latter. These relations are independent of the state itself, and they characterize the family of GGE states for a given model. In this sense, the form of the effective velocity can be regarded as the GGE equations of state, and could be alternatively represented as [45]

$$v^{\mathrm{eff}}(\theta) = v^{\mathrm{gr}}(\theta) + \int \mathrm{d}\alpha \, \frac{\varphi(\theta,\alpha)\, \rho_{\mathrm{p}}(\alpha)}{p'(\theta)} \, (v^{\mathrm{eff}}(\alpha) - v^{\mathrm{eff}}(\theta)) \tag{4.4}$$

with the group velocity $v^{\mathrm{gr}}(\theta) := E'(\theta)/p'(\theta)$. This expression is more physically suggestive, as we can clearly see that the first term represents the velocity of a freely propagating particle while the second term accounts for the renormalization due to the interaction / scatterings with other particles. In the subsequent section, we will present a kinetic derivation of (4.4), which allows us to understand it as a consequence of scatterings among soliton-like particles.

We are now in a position to spell out the Euler equation for integrable systems. Plugging (4.1) and (4.2) into (3.2), and using the completeness of the set of $h_i(\theta)$[3], one arrives

[3]It is commonly believed that the functions $h_i(\theta)$ associated to pseudolocal charges form a complete set of basis of $L^2$-space [132]

at the following equation

$$\partial_t \rho_{\rm p}(\theta) + \partial_x (v^{\rm eff}(\theta)\rho_{\rm p}(\theta)) = 0. \tag{4.5}$$

This is the *GHD equation*, and serves as the fundamental dynamical equation that completely characterizes the dynamics of integrable systems at the Euler scale. The fluid variable $\rho_{\rm p}$ is indeed physically motivated, as it is directly connected to conservation laws of the system, but one could work as well with another variable. A particularly useful one is the *normal mode* $n(\theta)$ for which (4.5) can be cast into the diagonalized form

$$\partial_t n(\theta) + v^{\rm eff}(\theta)\partial_x n(\theta) = 0. \tag{4.6}$$

The flux Jacobian matrix [119] associated to the transformation $\rho_{\rm p}(\theta) \mapsto n(\theta)$ is given by

$$A(\theta,\alpha) = \int {\rm d}\beta (R^{-1})(\theta,\beta) v^{\rm eff}(\beta) R(\beta-\alpha), \tag{4.7}$$

where $R(\theta-\alpha)$ is the transformation matrix

$$R(\theta-\alpha) = \frac{\partial n(\theta)}{\partial \rho_{\rm p}(\alpha)} = \frac{n(\theta)}{\rho_{\rm p}(\alpha)}\big(\delta(\theta-\alpha) - \frac{n(\theta)}{2\pi}\varphi(\theta-\alpha)\big). \tag{4.8}$$

Notice that, employing the integral operatorial notation, we can also write the matrix $A$ simply as $A = R^{-1} v^{\rm eff} R$. We also normalize $R$, which is the left eigenvector of $A$, as $R = 1 - nT$ where $T = \varphi/(2\pi)$.

In order to illustrate how GHD works, let us apply it to solve one of the cleanest nonequilibrium setups: partitioning protocol. This is a protocol to generate a NESS by gluing two identical systems that are initially thermalized at different temperatures (or, more generally, initially prepared with different global parameters such as the chemical potential). Supposing that initially Lagrange multipliers $\vec{\beta}_{R,L}$ are used to prepare two halves of the system, the initial condition can be implemented as the asymptotic condition

$$\lim_{x\to\pm\infty} \langle \vec{\mathfrak{q}}(x,0)\rangle_{\rm ini} = \langle \vec{\mathfrak{q}}\rangle_{\vec{\beta}_{R,L}}. \tag{4.9}$$

With this initial condition, we can expect that the system becomes scale invariant under a rescaling $(x,t) \mapsto (ax,at)$ for $a \in \mathbb{R}$, and accordingly the solution of (4.6) depends on rays $\xi = x/t$ only. Therefore we can rewrite (4.6) as

$$(v^{\rm eff}(\theta) - \xi)\partial_\xi n(\theta) = 0, \tag{4.10}$$

which can be solved as [45, 46]

$$n(\theta) = n_L(\theta)\Theta(\theta-\theta_*) + n_R(\theta)\Theta(\theta_*-\theta), \tag{4.11}$$

where $\Theta(\theta)$ is the step function, and $\theta_*$ is a function of $\xi$. The value of $\theta_*(\xi)$ at which $n(\theta)$ has a jump is determined by the relation $v^{\rm eff}(\theta_*) = \xi$. Equivalently, defining $r_\xi(\theta) = E'(\theta) - \xi p'(\theta)$, $\theta_*$ is the zero of $r_\xi^{\rm dr}(\theta)$, i.e. $r_\xi^{\rm dr}(\theta_*) = 0$. Unfortunately it is not possible to calculate $\theta_*$ analytically, but numerical iteration allows us to determine it with the desired precision. To be more precise, we can fix it as follows: for the first iteration, we start with $\theta_*$ in the free case, i.e. $\theta_* = v^{-1}(\xi)$ (in the case of relativistic systems $v^{-1}(\xi) = \arctan(\xi)$, while in the nonrelativistic case, $v^{-1}(\xi) = \xi$), and plug it into (4.11). We then use it to compute $r_\xi^{\rm dr}(\theta)$ and numerically calculate its zero, i.e. new $\theta_*$. Since $r_\xi^{\rm dr}(\theta)$ is a monotonically increasing function in $\theta$, we anticipate that $r_\xi^{\rm dr}(\theta)$ always admits the unique zero for each $\xi$. We then repeat this procedure until the value of $\theta_*$ converges. We numerically find that indeed the value of $\theta_*$ converges rather quickly, and its precision can be controlled by the number of iterations. In [45], we analyzed energy and charge transport in the Lieb-Liniger model and sinh-Gordon model, and obtained the results that are consistent with particular limits and known inequality that bounds the allowed value of energy NESS currents [133].

So far we have considered the case where there is no external force that drives the system. In fact, GHD equation can naturally incorporate the effect of external forces [104]. For instance, let us consider the Lieb-Liniger model, which is a prototypical integrable system and is often used to characterize the dynamics of ultra-cold atom gases. The model is a nonrelativistic system whose Hamiltonian reads

$$H = \int \mathrm{d}x \big(\frac{1}{2m}\partial_x\psi^\dagger\partial_x\psi + \frac{c}{2}\psi^\dagger\psi^\dagger\psi\psi\big), \tag{4.12}$$

where $c > 0$ is the coupling constant. Suppose a Lieb-Liniger gas is put in an external potential $V(x)$ that couples to the density of the system $\mathfrak{q}_0$. The Hamiltonian for the trapped Lieb-Liniger model is then given by

$$H_{\rm force} = H + \int \mathrm{d}x\, V(x)\mathfrak{q}_0(x). \tag{4.13}$$

One can then show that, as long as the trap is varying in a slowly enough fashion (so that higher derivative terms in the derivative expansion with respect to $V$ can be neglected), the Euler scale dynamics of the system can be described by a hydrodynamic equation that generalizes GHD equation, reading

$$\partial_t\rho_{\rm p}(\theta) + \partial_t(v^{\rm eff}(\theta)\rho_{\rm p}(\theta)) - \frac{\partial_x V}{m}\partial_\theta\rho_{\rm p}(\theta) = 0. \tag{4.14}$$

The equation can also be cast into the normal mode

$$\partial_t n(\theta) + v^{\rm eff}(\theta)\partial_x n(\theta) - \frac{\partial_x V}{m}\partial_\theta n(\theta) = 0. \tag{4.15}$$

These equations can be further generalized to the case of potentials coupling to arbitrary conserved charges. For their derivations and further details, one can refer to [104].

These equations have a far-reaching power in predicting the dynamics of the trapped integrable systems, and in particular, the Lieb-Liniger model. Indeed, in ultra-cold atom experiments, the Lieb-Liniger model is often used to describe $^{87}$Rb gases trapped in some external potential. A prominent example would be the famous quantum Newton's cradle experiment where authors observed the dynamics of two clouds of $^{87}$Rb gases trapped in an (almost) harmonic potential. This kind of situation is where the above equations become most useful and powerful, and we exploited them to study such situations in [105].

# Emergent hydrodynamics in integrable quantum systems out of equilibrium

Olalla A. Castro-Alvaredo,[1] Benjamin Doyon,[2] and Takato Yoshimura[2]

[1] *Department of Mathematics, City, University of London, Northampton Square EC1V 0HB, U.K.*
[2] *Department of Mathematics, King's College London, Strand WC2R 2LS, UK*

Understanding the general principles underlying strongly interacting quantum states out of equilibrium is one of the most important tasks of current theoretical physics. With experiments accessing the intricate dynamics of many-body quantum systems, it is paramount to develop powerful methods that encode the emergent physics. Up to now, the strong dichotomy observed between integrable and non-integrable evolutions made an overarching theory difficult to build, especially for transport phenomena where space-time profiles are drastically different. We present a novel framework for studying transport in integrable systems: hydrodynamics with infinitely-many conservation laws. This bridges the conceptual gap between integrable and non-integrable quantum dynamics, and gives powerful tools for accurate studies of space-time profiles. We apply it to the description of energy transport between heat baths, and provide a full description of the current-carrying non-equilibrium steady state and the transition regions in a family of models including the Lieb-Liniger model of interacting Bose gases, realized in experiments.

## I. INTRODUCTION

Many-body quantum systems out of equilibrium give rise to some of the most important challenges of modern physics [1]. They have received a lot of attention recently, with experiments on quantum heat flows [2, 3], generalized thermalization [4, 5] and light-cone effects [6]. The leading principle underlying non-equilibrium dynamics is that of local transport carried by conserved currents. Deeper understanding can be gained from studying non-equilibrium, current-carrying steady states, especially those emerging from unitary dynamics [7]. This principle gives rise to two seemingly disconnected paradigms for many-body quantum dynamics. On the one hand, taking into account only few conservation laws, emergent hydrodynamics [8–12] offers a powerful description where the physics of fluids dominates [13–18]. On the other hand, in integrable systems, the infinite number of conservation laws are known to lead to generalized thermalization [19–21] (there are many fundamental works on the subject, see the review [22]), and the presence of quasi-local charges has been shown to influence transport [23, 24] (see the review [25]). However, except at criticality [26, 27] (see the review [28]), no general many-body emergent dynamics has been proposed in the integrable case; with the available frameworks, these two paradigms seem difficult to bridge. The study of pre-thermalization or pre-relaxation under small integrability breaking [22, 28–30], the elusive quantum KAM theorem [31, 32], the development of perturbation theory for non-equilibrium states, and the exact treatment of non-equilibrium steady states and of non-homogeneous quantum dynamics in unitary interacting integrable models remain difficult problems.

In this paper, using the recent advances on generalized thermalization and developing further aspects of integrability, we propose a solution to such problems by deriving a general theory of hydrodynamics with infinitely-many conservation laws. The theory, applicable to a large integrability class, is derived solely from the fundamental tenet of emerging hydrodynamic: local entropy maximization (often referred to as local thermodynamic equilibrium) [33–37]. Focussing on quantum field theory (QFT) in one space dimension, we then study a family of models that include the paradigmatic Lieb-Liniger model [38] for interacting Bose gases, explicitly realized in experiments [4, 5, 39–41]. We concentrate on far-from-equilibrium states driven by heat baths in the partitioning protocol [7, 26, 27, 42] (see Fig. 1). We provide currents and full space-time profiles which are in principle experimentally accessible, beyond linear response and for arbitrary interaction strengths. We make contact with the physics of rarefaction waves, and with the concept of quasi-particle underlying integrable dynamics.

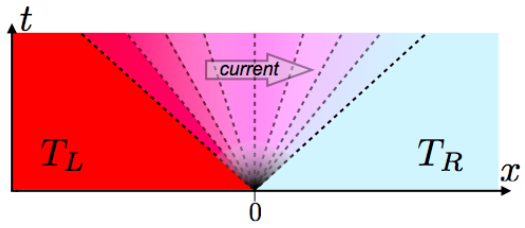


FIG. 1. The partitioning protocol. With ballistic transport, a current emerges after a transient period. Dotted lines represent different values of $\xi = x/t$. If a maximal velocity exists (e.g. due to the Lieb-Robinson bound), initial reservoirs are unaffected beyond it (light-cone effect). The steady state lies at $\xi = 0$.

*Note added:* After a first version of this paper appeared as a preprint, similar dynamical equations as those derived here were independently obtained in the integrable XXZ Heisenberg chain by assuming, in addition to local entropy maximization, an underlying kinetic theory [43]. Solutions to these equations of the same type as those considered here were constructed and confirmed by numerical simulations.

## II. SETUP

Let two semi-infinite halves (which we refer to as the left and right reservoirs) of a homogeneous, short-range one-dimensional quantum system be independently thermalized, say at temperatures $T_L$ and $T_R$. Let this initial state $\langle\cdots\rangle_{\rm ini}$ be evolved unitarily with the Hamiltonian $H$ representing the full homogeneous system. One may then investigate the steady state that occurs at large times (see e.g. [28]),

$$\mathtt{O}^{\rm sta} := \lim_{t\to\infty} \langle e^{{\rm i}Ht} O e^{-{\rm i}Ht}\rangle_{\rm ini}, \quad O \text{ local observable.} \quad (1)$$

If the limit exists, it is a maximal-entropy steady state involving, in principle, all (quasi-)local conserved charges of the dynamics $H$ (see (4) below). Generically, the dynamics only admits a single conserved quantity, $H$ itself: this means that, due to diffusive processes, ordinary Gibbs thermalization occurs. However, when conserved charges exist that are odd under time reversal, the steady state may admit nonzero stationary currents. This indicates the presence of ballistic transport, and the emergence of a current-carrying state that is far from equilibrium (breaking time-reversal symmetry). This is the partitioning protocol for building non-equilibrium steady states. See Fig. 1.

The study of such non-equilibrium steady states has received a large amount of attention recently (see [28] and references therein). They form a uniquely interesting set of states: they are simple enough to be theoretically described, yet encode nontrivial aspects of non-equilibrium physics. They naturally occur in the universal region near criticality described by QFT, where ballistic transport emerges thanks to continuous translation invariance; and in integrable systems, where it often arises thanks to the infinite family of conservation laws.

Works [26, 27] open the door to their study at strong-coupling critical points with unit dynamical exponent, obtaining in particular the full universal time evolution. The steady state was found to be homogeneous within a light cone, with the energy current being

$$\mathtt{j}^{\rm sta} = \frac{\pi c k_B^2}{12\hbar}(T_L^2 - T_R^2) \quad (2)$$

where $c$ is the central charge of the conformal field theory (CFT) (below we set $k_B = \hbar = 1$). This result arises from the independent thermalization of emerging left- and right-moving energy carriers (chiral separation). It was numerically verified [44] and agrees with recent heat-flow experiments [2]. It was generalized using hydrodynamic methods to higher-dimensional critical points [13, 14, 17, 18] and to deviations from criticality [15, 16, 18]. Under conditions that are fulfilled in universal near-critical regions, inequalities that generalize (2) can be derived [28, 45] (here with unit Lieb-Robinson velocity [46])

$$\frac{\mathtt{e}^L - \mathtt{e}^R}{2} \geq \mathtt{j}^{\rm sta} \geq \frac{\mathtt{k}^L - \mathtt{k}^R}{2} \quad (3)$$

where $\mathtt{e}^{L,R}$ and $\mathtt{k}^{L,R}$ are, respectively, the energy densities and the pressures in the left and right reservoirs[1].

Many further results exist in free-particle models (see [28] and references therein), where independent thermalization of right- and left-movers still hold. In contrast, however, only conjectures and approximations are available for interacting integrable models [47–49]. In addition, a striking dichotomy is observed between integrable situations and hydrodynamic-based results: for instance, conformal hydrodynamics is expected to emerge in strong-coupling CFT [13, 14], leading to shock structures, but generically fails in free-particle conformal models [50], where transition regions are smooth. This points to the stark effect of integrability on non-equilibrium quantum dynamics, still insufficiently understood with available techniques.

## III. EMERGING HYDRODYNAMICS IN QUANTUM SYSTEMS

Let us recall the basic concepts underlying the hydrodynamic description of many-body quantum systems, and its use in the setup described above (similar concepts exist in many-body classical systems).

Let $Q_i$, $i \in \{1, 2, \ldots, N\}$ be local conserved quantities in involution. These are integrals of local densities $q_i(x,t)$, and the conservation laws take the form $\partial_t q_i(x,t) + \partial_x j_i(x,t) = 0$, where $j_i$ are the associated local currents. A Gibbs ensemble is a maximal-entropy ensemble under conditions fixing all averaged local conserved densities. It is described by a density matrix

$$\rho = e^{-\sum_i \beta_i Q_i} / {\rm Tr}\big[e^{-\sum_i \beta_i Q_i}\big], \quad (4)$$

where $\beta_i$ are the associated potentials. For instance, $Q_1$ is taken as the Hamiltonian, and $\beta_1$ is the inverse temperature. We will denote $\underline{\beta} = (\beta_1, \beta_2, \ldots, \beta_N)$ the vector representing this state, and $\langle\cdots\rangle_{\underline{\beta}}$ the averages.

Clearly, the Gibbs averages of local densities $\mathtt{q}_i = \langle q_i\rangle_{\underline{\beta}}$ (these are independent of space and time by homogeneity and stationarity) may be seen as defining a map from states to averages, $\underline{\beta} \mapsto \underline{\mathtt{q}}$. This is expected to be a bijection: the set of averages fully determines the set of potentials. Therefore, the current averages $\mathtt{j}_i = \langle j_i\rangle_{\underline{\beta}}$ are functions of the density averages,

$$\underline{\mathtt{j}} = \underline{\mathcal{F}}(\underline{\mathtt{q}}). \quad (5)$$

These are the equations of state, and are model-dependent. The averages $\underline{\mathtt{q}}$ can be generated by differentiation of the (specific, dimensionless) free energy $f_{\underline{\beta}}$.

[1] The second inequality in (3) was shown in [45], with the goal of establishing the existence of current-carrying non-equilibrium steady states. The first was suggested to BD by M. J. Bhaseen shortly afterwards, and can be shown in the same manner.

Similarly, one can show [28] (see Appendix A) that there exists a function $g_{\underline{\beta}}$ that, likewise, generates the currents,

$$\underline{\mathtt{q}} = \nabla_{\underline{\beta}} f_{\underline{\beta}}, \quad \underline{\mathtt{j}} = \nabla_{\underline{\beta}} g_{\underline{\beta}}. \tag{6}$$

A hydrodynamics description of quantum dynamics is expected to emerge at large space-time scales. This has been exploited, in the present setup, in [13–18]. The emergence of hydrodynamics is solely based on the assumption of local entropy maximization (or local thermodynamic equilibrium[2]). Technically, this is the assumption that averages of local quantities $\langle O(x,t)\rangle$ tend uniformly enough, at large times, to averages evaluated in local Gibbs ensembles $\langle O\rangle_{\underline{\beta}(x,t)}$ with space-time dependent potentials $\underline{\beta}(x,t)$. Physically, this is a consequence of *separation of scales*, as follows (see for instance [37]).

Assume that, after some time, physical properties vary only on space-time scales that are much larger than microscopic scales. This may be referred to as the "local relaxation time". From that time on, microscopic processes such as particle collisions or inter-site interactions give rise to fast, local relaxation: the reaching of a (approximate) steady state on space-time scales small compared to variations but large enough for thermodynamics to be applicable. By Boltzmann's phase-space argument, these local steady states are obtained from entropy maximization, and as usual maximization is under the conditions provided by conservation laws (properties of the microscopic dynamics). That is, on each space-time "fluid cell" a Gibbs state is (very nearly) reached. Neighboring Gibbs states are different, but their variations are small. This is local entropy maximization.

Assume local entropy maximization. On each fluid cell, the Gibbs state is initially characterized by the values of the conserved densities at the local-relaxation time. The large-scale dynamics is thereon obtained from conservation laws, as follows. Consider microscopic conservation in integral form, $\int_{x_1}^{x_2} \mathrm{d}x \left(q_i(x,t_2) - q_i(x,t_1)\right) + \int_{t_1}^{t_2} \mathrm{d}t \left(j_i(x_2,t) - j_i(x_1,t)\right) = 0$. Since averages of densities and currents, after the local relaxation time, take the form $\langle q_i(x,t)\rangle = \langle q_i\rangle_{\underline{\beta}(x,t)}$ and $\langle j_i(x,t)\rangle = \langle j_i\rangle_{\underline{\beta}(x,t)}$ uniformly enough, we have

$$\int_{x_1}^{x_2} \mathrm{d}x \left(\underline{\mathtt{q}}(x,t_2) - \underline{\mathtt{q}}(x,t_1)\right) + \int_{t_1}^{t_2} \mathrm{d}t \left(\underline{\mathtt{j}}(x_2,t) - \underline{\mathtt{j}}(x_1,t)\right) = 0 \tag{7}$$

where $\underline{\mathtt{q}}(x,t) = \langle \underline{q}\rangle_{\underline{\beta}(x,t)}$ and $\underline{\mathtt{j}}(x,t) = \langle \underline{j}\rangle_{\underline{\beta}(x,t)}$. Here, integrals may be taken to cover a *macroscopic number of fluid cells*: these become macroscopic conservation equations. Macroscopic conservation equations can be re-written in differential form, with differentials representing small variations amongst fluid cells:

$$\partial_t \underline{\mathtt{q}}(x,t) + \partial_x \underline{\mathtt{j}}(x,t) = 0. \tag{8}$$

These are the pure hydrodynamic (Euler-type) equations, representing the slow, large-scale quantum dynamics of conserved densities and currents flowing amongst neighboring cells.

The problem of emergence of hydrodynamics in many-body systems is one of the most important unsolved problem of modern mathematical physics. Although there are few proofs of emergence of hydrodynamics, there is strong evidence for the validity of emerging Euler equations in many situations; see the books [33–37], and the recent paper [51] for a study of emerging Euler equations in classical anharmonic chains.

Combined with the equations of state (5), Euler equations (8) give

$$\partial_t \underline{\mathtt{q}}(x,t) + J(\underline{\mathtt{q}}(x,t))\partial_x \underline{\mathtt{q}}(x,t) = 0 \tag{9}$$

where $J(\underline{\mathtt{q}}) := \nabla_{\underline{\mathtt{q}}} \underline{\mathtt{j}}$ is an $N$ by $N$ matrix, the Jacobian matrix of the transformation from densities to currents,

$$J(\underline{\mathtt{q}})_{ij} = \partial \mathcal{F}_i(\underline{\mathtt{q}})/\partial \mathtt{q}_j. \tag{10}$$

Equations (9) are the emergent pure hydrodynamic equations in quasi-linear (or characteristic) form [12]. The complete model dependence, including all quantum effects, is encoded, besides the number $N$ of conserved quantities, in the Jacobian $J(\underline{\mathtt{q}})$.

The density averages $\underline{\mathtt{q}}$, like the potentials $\underline{\beta}$, correspond to a set of state coordinates. One may choose any other set of state coordinates $\underline{\mathtt{n}}$, with $\underline{\mathtt{q}} = \underline{\mathcal{F}}^{\mathtt{q}}(\underline{\mathtt{n}})$ and $\underline{\mathtt{j}} = \underline{\mathcal{F}}^{\mathtt{j}}(\underline{\mathtt{n}})$. A similar equation is obtained,

$$\partial_t \underline{\mathtt{n}}(x,t) + J(\underline{\mathtt{n}}(x,t))\partial_x \underline{\mathtt{n}}(x,t) = 0, \tag{11}$$

where $J(\underline{\mathtt{n}}) = \left(\nabla_{\underline{\mathtt{n}}} \underline{\mathtt{q}}\right)^{-1} \nabla_{\underline{\mathtt{n}}} \underline{\mathtt{j}}$. Observe that $J(\underline{\mathtt{n}})$ and $J(\underline{\mathtt{q}})$ are related to each other by a similarity transformation: $J(\underline{\mathtt{n}}) = \left(\nabla_{\underline{\mathtt{n}}} \underline{\mathtt{j}}\right)^{-1} J(\underline{\mathtt{q}})|_{\underline{\mathtt{q}}=\underline{\mathcal{F}}^{\mathtt{q}}(\underline{\mathtt{n}})} \nabla_{\underline{\mathtt{n}}} \underline{\mathtt{j}}$. Therefore, the spectrum of $J(\underline{\mathtt{n}})$ is independent of the choice of coordinates, and is a fundamental property of the model. We will denote this spectrum by $\{v_i^{\mathrm{eff}}(\underline{\mathtt{n}}), i = 1, \ldots, N\}$.

Choosing coordinates $\underline{\mathtt{n}}$ that diagonalize $J(\underline{\mathtt{n}})$ one obtains

$$\partial_t \mathtt{n}_i(x,t) + v_i^{\mathrm{eff}}(\underline{\mathtt{n}}(x,t))\partial_x \mathtt{n}_i(x,t) = 0. \tag{12}$$

These express the vanishing of the convective derivatives, representing the constancy of each fluid mode $\mathtt{n}_i(x,t)$ on fluid cells. The eigenvalues $v_i^{\mathrm{eff}}(\underline{\mathtt{n}}(x,t))$ are therefore interpreted as the *propagation velocities* of these normal modes. The normal modes interact with each other only through the propagation velocities, which is generically a function of all state coordinates.

Let us now apply the above to the solution of the partitioning problem. For clarity of the following discussion,

[2] The phrase "local thermodynamic equilibrium" is often used to describe the fluid cells, however it might be slightly misleading as it seems to suppose that fluid cells are in equilibrium; in order to have nontrivial hydrodynamics this however is not the case, as one needs the presence of nonzero ballistic currents, breaking time-reversal symmetry.

we come back to the $\mathtt{q}$-coordinates (but it is easy to generalize to any coordinates $\mathtt{n}$). Consider the large-scale limit $(x,t)\mapsto(ax,at)$, $a\to\infty$. Because (9) is invariant under this scaling, in the limit, if it exists, the solution is also invariant. Thus we may assume *self-similar solutions* $\underline{\beta}(x,t)=\underline{\beta}(\xi)$ where $\xi=x/t$, and (9) becomes an eigenvalue equation,

$$(J(\underline{\mathtt{q}})-\xi\mathbf{1})\partial_\xi\underline{\mathtt{q}}=0. \tag{13}$$

The initial condition is determined by the state at the local relaxation time (at which the fluid-dynamics description starts to be valid). This state is unknown, as it depends on the full quantum dynamics, but its asymptotic at large $|x|$ is identical to that of the original state. In the large-scale solution, the initial condition $t\to 0^+$ is implemented as asymptotic conditions as $\xi\to\pm\infty$. Therefore it only depends on the asymptotic form of the initial state, and we impose

$$\lim_{\xi\to\pm\infty}\underline{\mathtt{q}}(\xi)=\lim_{x\to\pm\infty}\langle\underline{q}(x,0)\rangle_{\rm ini}. \tag{14}$$

In the present setup, these involve Gibbs states at potentials $\underline{\beta}^{R,L}$:

$$\lim_{x\to\pm\infty}\langle\underline{q}(x,0)\rangle_{\rm ini}=\langle\underline{q}\rangle_{\underline{\beta}^{R,L}} \tag{15}$$

and the steady-state averages are given by

$$\underline{\mathtt{q}}^{\rm sta}:=\underline{\mathtt{q}}(\xi=0),\quad \underline{\mathtt{j}}^{\rm sta}:=\underline{\mathtt{j}}(\xi=0). \tag{16}$$

The solution to the eigenvalue equation (13) and initial conditions (14) provides the exact large-scale asymptotic form of the full quantum solution, along any ray $x=\xi t$ (see Fig. 1). The eigenvalue equation (13) represents the small changes of averages along various rays, due to the exchange of conserved charges amongst fluid cells. The set of eigenvalues of $J(\underline{\mathtt{q}})$ – the available propagation velocities in the state characterized by the averages $\underline{\mathtt{q}}$ – form a finite, discrete set for finite $N$.

Solutions to (13), (14) are typically composed of regions of constant $\underline{\mathtt{q}}$-values separated by transition regions [12]. Transition regions may be of two types: either shocks (weak solutions), where $\underline{\mathtt{q}}$-values display finite jumps, or rarefaction waves, where they form a smooth solution to (13). Rarefaction waves, the most natural type of solution, cannot, generically, cover the full space between two reservoirs. Indeed, (13) specifies that the curve traced by the solution in the $\underline{\mathtt{q}}$-plane must at all points be tangent to an eigenvector of $J(\underline{\mathtt{q}})$. Since eigenvectors – and available propagation velocities – form a discrete set, smooth variations of $\underline{\mathtt{q}}$ along the curve imply a unique choice of eigenvector at each point (except possibly at points where eigenvalues cross). Thus, the curve is completely determined by its initial point, and cannot join two arbitrary reservoir values. That is, in ordinary pure hydrodynamics, shocks are often required.

## IV. HYDRODYNAMICS WITH INFINITELY MANY CURRENTS

In integrable systems, there are infinitely many local conservation laws. In fact, this space is enlarged to that of "pseudolocal" conservation laws, where the densities $q_i(x,t)$ and currents $j_i(x,t)$ are supported on extended spacial regions with weight decaying fast enough away from $x$. This enlargement plays an important role in non-equilibrium quantum dynamics [20, 21, 23–25]. Under maximal-entropy principles, Gibbs states are then replaced by generalized Gibbs ensembles (GGE) [19, 21, 22]: formally the limit $N\to\infty$ of the density matrix (4), involving all basis elements in the space of conserved pseudolocal charges. We choose $Q_1=H$ (the Hamiltonian) and $Q_2=P$ (the momentum operator).

Under the influence of infinitely many conservation laws, the picture of local entropy maximization is still expected to hold: all physical principles underlying it stay unchanged, the only difference being the use of GGEs instead of Gibbs ensembles. This, along with the emergence of self-similar solutions in the partitioning protocol, are our working hypotheses; see Appendix B for a discussion. The emergence of a generalized type of hydrodynamics was proven in the classical hard-rod problem [37, 52], whose relation with the present quantum problem we will study in a future work. The emergence of self-similar solutions was observed numerically in the quantum XXZ chain in [53]. In free-particle quantum models, hydrodynamic ideas and related semi-classical approximations, as well as ray-dependent local entropy maximization, were studied in various works, see [54–59].

Looking for a full solution to the infinity of equations (9), (13) and (14), an appropriate choice of state variables is crucial. A powerful way is to recast them into the quasi-particle language underlying the thermodynamic Bethe ansatz (TBA) method for integrable systems [60]. Using this language, we derive the exact GGE equations of state, and the ensuing *generalized hydrodynamics* equation. We determine the exact normal modes and propagation velocities, and obtain full ray-dependent solutions.

### A. GGE equations of state

We assume that the spectrum of stable quasi-particles is composed of a single quasi-particle species of mass $m$ (see Appendix C for a many-particle generalization). The dispersion relation is encoded via a parametrization $E(\theta)$, $p(\theta)$ of the energy and momentum: in the relativistic case $\theta$ is the rapidity, $E(\theta):=m\cosh(\theta)$, $p(\theta):=m\sinh(\theta)$, and in the Galilean case $\theta$ is the velocity, $E(\theta):=m\theta^2/2$, $p(\theta):=m\theta$. In integrable models, scattering is elastic and factorizes into two-particle processes, and a model is fully specified by giving the elastic two-particle scattering amplitude $S(\theta_1-\theta_2)$. The differential scattering phase is defined as $\varphi(\theta)=-\mathrm{i}\,\mathrm{d}\log S(\theta)/\mathrm{d}\theta$. We denote by $h_i(\theta)$ the one-particle eigenvalue of the conserved charge $Q_i$; in

particular $h_1(\theta) = E(\theta)$ and $h_2(\theta) = p(\theta)$.

Let us first recall the basic ingredients of TBA. Three related quantities play important roles: the quasi-particle density $\rho_{\rm p}(\theta)$, the state density $\rho_{\rm s}(\theta)$, and the quasi-particle occupation number $n(\theta) := \rho_{\rm p}(\theta)/\rho_{\rm s}(\theta)$. The functions $\rho_{\rm p}(\theta)$ and $n(\theta)$ are two different sets of state coordinates; each can be used to fully characterize the GGE. The former specifies all average densities in a simple way:

$$\mathtt{q}_i = \int \mathrm{d}\theta\, \rho_{\rm p}(\theta) h_i(\theta). \tag{17}$$

This can in fact be seen as a definition of $\rho_{\rm p}(\theta)$. Here and below, integrations are over $\mathbb{R}$.

As a consequence of interactions, quasi-particle and state densities are related to each other. Using the Bethe ansatz, one finds the following *constitutive relation* [60]:

$$2\pi\, \rho_{\rm s}(\theta) = p'(\theta) + \int \mathrm{d}\alpha\, \varphi(\theta-\alpha)\rho_{\rm p}(\alpha) \tag{18}$$

where $p'(\theta) = \mathrm{d}p(\theta)/\mathrm{d}\theta$. This relation gives rise to a nonlinear relation between the state coordinates $\rho_{\rm p}(\theta)$ and $n(\theta)$. The transformation from the former to the latter is direct from the above definitions. In the opposite direction, the transformation is effected by

$$2\pi\, \rho_{\rm p}(\theta) = n(\theta)\, (p')^{\rm dr}\,(\theta) \tag{19}$$

where the "dressing" operation $h \mapsto h^{\rm dr}$ is defined by the solution to the linear integral equation

$$h^{\rm dr}(\theta) = h(\theta) + \int \frac{\mathrm{d}\gamma}{2\pi} \varphi(\theta-\gamma)\, n(\gamma)\, h^{\rm dr}(\gamma). \tag{20}$$

The potentials $\underline{\beta}$ can be recovered: the occupation number is related to the one-particle eigenvalue $w(\theta) = \sum_i \beta_i h_i(\theta)$ of the charge $\sum_i \beta_i Q_i$ in the GGE (4) via the so-called pseudo-energy $\epsilon_w(\theta)$ [60, 61]:

$$\begin{aligned} n(\theta) &= \frac{1}{1+\exp\left[\epsilon_w(\theta)\right]} \\ \epsilon_w(\theta) &= w(\theta) - \int \frac{\mathrm{d}\gamma}{2\pi} \varphi(\theta-\gamma) \log(1+e^{-\epsilon_w(\gamma)}). \end{aligned} \tag{21}$$

The above ingredients give exact average densities as functions of GGE states. However, they do not provide expressions for average currents as functions of state coordinates, and for equations of states. Hence they are not sufficient in order to develop generalized hydrodynamics.

We solve this problem by obtaining the following expressions:

$$\mathtt{q}_i = \int \frac{\mathrm{d}p(\theta)}{2\pi} n(\theta) h_i^{\rm dr}(\theta), \quad \mathtt{j}_i = \int \frac{\mathrm{d}E(\theta)}{2\pi} n(\theta) h_i^{\rm dr}(\theta) \tag{22}$$

where $h_i^{\rm dr}(\theta)$ is the dressed one-particle eigenvalue. These expressions emphasize the role of relativistic or Galilean symmetry: the sole difference between GGE averages of charge densities and currents is the integration measure, determined by the dispersion relation.

The first equation in (22) is well known and is a consequence of (17) and (19). In integral-operator notation (with measure $\mathrm{d}\theta/(2\pi)$), the dressing operation is

$$h^{\rm dr} = (1-\varphi\mathcal{N})^{-1} h \tag{23}$$

where $\mathcal{N}$ is diagonal with kernel $2\pi\, n(\theta)\delta(\theta-\alpha)$, and $\varphi$ has kernel $\varphi(\theta-\alpha)$. Therefore, introducing the symmetric operator $\mathcal{U} = \mathcal{N}(1-\varphi\mathcal{N})^{-1}$ and the bilinear form $a\cdot b = \int \mathrm{d}\theta/(2\pi)\, a(\theta)b(\theta)$, we have

$$\mathtt{q}_i = h_i \cdot \mathcal{U}\, p' = p' \cdot \mathcal{U}\, h_i \tag{24}$$

which leads to the first equation of (22).

The second equation in (22) is new. It may be proven, in the relativistic case, using relativistic crossing symmetry, and then obtained by the non-relativistic limit in the Galilean case. In the relativistic case, crossing symmetry says that local currents $j_i$, in the cross-channel, are local densities $q_i$; therefore the current expression in (22) is obtained from that of the density under an appropriate exchange of energy and momentum. Let $\mathcal{C}$ be the crossing transformation $(x,t) \mapsto (\mathrm{i}t, -\mathrm{i}x)$, implemented on rapidities by $\theta \mapsto \mathrm{i}\pi/2 - \theta$. Note that it squares to the identity, $\mathcal{C}^2 = 1$. Let us denote by $q[h]$ and $j[h]$ the density and current operators, respectively, associated to a one-particle eigenvalue $h(\theta)$. Then the statement that local currents $j_i$, in the cross-channel, are local densities $q_i$ translates into $\mathcal{C}(j[h]) = \mathrm{i}q[h^C]$ where $h^C(\theta) = h(\mathrm{i}\pi/2-\theta)$. Let us also denote by $\langle\mathcal{O}\rangle_w$ the average of observables $\mathcal{O}$ in the state characterized by $w(\theta)$. Then $\langle\mathcal{C}(\mathcal{O})\rangle_w = \langle\mathcal{O}\rangle_{w^C}$ where $w^C(\theta) = w(\mathrm{i}\pi/2-\theta)$. Using $\langle j[h]\rangle_w = \langle\mathcal{C}(\mathcal{C}(j[h]))\rangle_w = \mathrm{i}\langle q[h^c]\rangle_{w^C}$ and the expression for $\mathtt{q}_i = \mathtt{q}[h_i]$ in Equation (22), we obtain that for $\mathtt{j}_i = \mathtt{j}[h_i]$. An alternative proof, using the machinery of integrable systems, is presented in Appendix D.

Expressions (22) have interesting consequences. First, using $\mathtt{j}_i = h_i \cdot \mathcal{U}\, E'$ where $E'(\theta) = \mathrm{d}E(\theta)/\mathrm{d}\theta$ in (22), the average current may also be written in terms of a current spectral density $\rho_{\rm c}(\theta)$:

$$\mathtt{j}_i = \int \mathrm{d}\theta\, \rho_{\rm c}(\theta) h_i(\theta), \tag{25}$$

which takes the forms

$$2\pi\, \rho_c(\theta) = n(\theta)\, (E')^{\rm dr}(\theta) = 2\pi\, v^{\rm eff}(\theta)\rho_{\rm p}(\theta). \tag{26}$$

Here $v^{\rm eff}(\theta)$ is the *effective velocity*, defined by

$$v^{\rm eff}(\theta) := \frac{(E')^{\rm dr}\,(\theta)}{(p')^{\rm dr}\,(\theta)}. \tag{27}$$

The effective velocity depends on the state via the occupation number entering the dressing operation, and brings out the quasi-particle interpretation of the current expression: since $\rho_c(\theta) = v^{\rm eff}(\theta)\rho_{\rm p}(\theta)$, quasi-particles are

seen as moving at effective velocities $v^{\rm eff}(\theta)$, influenced by the state in which they move.

Second, one may extract explicit GGE equations of state from expressions (22). The equations of states are necessary and sufficient relations between densities and currents, guaranteeing the existence of $n(\theta)$ such that both relations in (22) hold for all $h_i(\theta)$. Assume that $\mathtt{q}_i$ and $\mathtt{j}_i$ are averages in a state, not necessarily a GGE. In complete generality, both are linear functionals of $h(\theta)$, hence we may still write (17) and (25) for some quasi-particle density $\rho_{\rm p}(\theta)$ and current spectral density $\rho_{\rm c}(\theta)$. GGE equations of states can therefore be written as relations between $\rho_{\rm p}(\theta)$ and $\rho_{\rm c}(\theta)$, necessary and sufficient for the existence of $n(\theta)$ such that (22) hold. One can show that these relations are

$$\frac{\rho_{\rm c}(\theta)}{\rho_{\rm p}(\theta)} = \frac{E'(\theta) + \int {\rm d}\alpha\, \varphi(\theta-\alpha)\rho_{\rm c}(\alpha)}{p'(\theta) + \int {\rm d}\alpha\, \varphi(\theta-\alpha)\rho_{\rm p}(\alpha)}. \qquad (28)$$

These relations are independent of the state: they hold in any GGE, in the model described by the differential scattering phase $\varphi(\theta-\alpha)$. They characterize the set of doublets of functions $(\rho_{\rm p}, \rho_{\rm c})$ describing available GGEs for this integrable model. The proof of (28) is obtained by isolating $n(\theta)$ in both (19) and (26), in the forms $2\pi(\mathcal{N}^{-1}-\varphi)\rho_{\rm p} = p'$ and $2\pi(\mathcal{N}^{-1}-\varphi)\rho_{\rm c} = E'$, and equating the resulting expressions.

Finally, recalling (26), the left hand side of (28) is $v^{\rm eff}(\theta)$. Simple manipulations of (28) then give a linear integral equation for the effective velocity $v^{\rm eff}(\theta)$ in terms of quasi-particle densities:

$$v^{\rm eff}(\theta) = v^{\rm gr}(\theta) + \int {\rm d}\alpha\, \frac{\varphi(\theta-\alpha)\,\rho_{\rm p}(\alpha)}{p'(\theta)}\,(v^{\rm eff}(\alpha) - v^{\rm eff}(\theta)) \qquad (29)$$

where $v^{\rm gr}(\theta) = E'(\theta)/p'(\theta)$ is the group velocity. In this form, the equations of state of integrable systems are seen as equations specifying an effective velocity of quasi-particles, as a modification of the group velocity.

We note that the effective velocity derived here agrees with that proposed in [62][3]. This is interesting, as our derivation is based on comparing current spectral density to quasi-particle density, while the concept proposed in [62] is based on stationary-phase arguments.

### B. Generalized hydrodynamics

The basic equation of generalized pure hydrodynamics is derived from (8) along with the quasi-particle expressions (17) and (25). The fact that the space of pseudolocal charges is complete [21] suggests that these hold for a complete set of functions $h_i(\theta)$, and thus (here and below we suppress explicit $x,t$ dependences for lightness of notation):

$$\partial_t \rho_{\rm p}(\theta) + \partial_x \rho_{\rm c}(\theta) = 0. \qquad (30)$$

Using the equations of state (28), this is an integro-differential system for the space-time dependent state characterized by the particle densities $\rho_{\rm p}(\theta)$.

Alternatively, using the effective-velocity formulation (26) and (29), Equation (30) may be written as

$$\partial_t \rho_{\rm p}(\theta) + \partial_x\big(v^{\rm eff}(\theta)\rho_{\rm p}(\theta)\big) = 0. \qquad (31)$$

This is the conservation form of generalized hydrodynamics. It is a density-type conservation equation, and identifies $\rho_{\rm p}(\theta)$ as a conserved fluid density.

The state coordinates $\rho_{\rm p}(\theta)$ are, however, not the most convenient. We show that the occupation numbers $n(\theta)$ *diagonalize the Jacobian* $J(\underline{\mathtt{n}})$ in the quasi-linear form (11): the space-time dependent occupation number $n(\theta)$ satisfies the following integro-differential system, the vanishing of the convective derivative of $n(\theta)$:

$$\partial_t n(\theta) + v^{\rm eff}(\theta)\partial_x n(\theta) = 0. \qquad (32)$$

Here (27) may be used to express the effective velocity in terms of $n(\theta)$. Hence, $n(\theta)$ are the normal modes of generalized hydrodynamics, and further, the eigenvalues – the propagation velocities – are exactly the effective velocities $v^{\rm eff}(\theta)$.

The proof of (32) is as follows. Using the integral-operator relations $2\pi\rho_{\rm p} = \mathcal{U}p'$ and $2\pi\rho_{\rm c} = \mathcal{U}E'$, we have $(\partial_t\mathcal{U})\,p' + (\partial_x\mathcal{U})\,E' = 0$. Taking derivatives, $\partial_{x,t}\mathcal{U} = (1-\mathcal{N}\varphi)^{-1}(\partial_{x,t}\mathcal{N})(1-\varphi\mathcal{N})^{-1}$, and we obtain

$$\partial_t\mathcal{N}\,(1-\varphi\mathcal{N})^{-1}p' + \partial_x\mathcal{N}\,(1-\varphi\mathcal{N})^{-1}E' = 0 \qquad (33)$$

which gives (32) using (23).

Observe that using (31) and (32), it is simple to show that the state density $\rho_{\rm s}(\theta)$, as well as the hole density $\rho_{\rm h}(\theta) := \rho_{\rm s}(\theta) - \rho_{\rm p}(\theta)$, also satisfy the *same density-type conservation equation* (31) (this was noted in [43]). Further, as a consequence, the *entropy density* [60],

$$s(\theta) := \rho_{\rm s}(\theta)\log\rho_{\rm s}(\theta) - \rho_{\rm p}(\theta)\log\rho_{\rm p}(\theta) - \rho_{\rm h}(\theta)\log\rho_{\rm h}(\theta), \qquad (34)$$

also satisfies this conservation equation, $\partial_t s(\theta) + \partial_x\big(v^{\rm eff}(\theta)s(\theta)\big) = 0$. Conservation of entropy density is a fundamental property of perfect fluids, as no viscosity effects are taken into account.

In the large-scale limit the equation for the ray-dependent ($\xi$-dependent) occupation number $n(\theta)$ simplifies to

$$(v^{\rm eff}(\theta) - \xi)\,\partial_\xi n(\theta) = 0.$$

This is the eigenvalue equation (13) in the occupation-number coordinates (which diagonalize the Jacobian), and its solution gives $\underline{\mathtt{q}}(\xi)$ and $\underline{\mathtt{j}}(\xi)$ via (22), (20).

One can show that the solution for the non-equilibrium, ray-dependent occupation number $n(\theta)$ is the discontinuous function

$$n(\theta) = n^L(\theta)\Theta(\theta-\theta_\star) + n^R(\theta)\Theta(\theta_\star-\theta) \qquad (35)$$

[3] Note that in [62], $v^{\rm eff}(\theta)$ is written in a form similar to, but different from (27), using a different definition of dressing.

where $\Theta(\cdots)$ is Heavyside's step function. The position of the discontinuity $\theta_\star$ depends on $\xi$ and is self-consistently determined by $v^{\rm eff}(\theta_\star)=\xi$; equivalently, it is the zero of the dressed, boosted momentum $p_\xi(\theta):=p(\theta-\eta)$ where $\xi=\tanh\eta$ (relativistic case) or $\xi=\eta$ (Galilean case),

$$p_\xi^{\rm dr}(\theta_\star)=0. \tag{36}$$

The GGE occupation numbers $n^{L,R}(\theta)$ entering (35) guarantee that the asymptotic conditions on $\xi$ correctly represent the asymptotic baths as per (14). They are obtained using (21) with $w=w^{L,R}(\theta)$ the one-particle eigenvalues characterizing the GGE of the left and right asymptotic reservoirs; for instance, with reservoirs at temperatures $T_{L,R}$, we have $w^{L,R}(\theta)=T_{L,R}^{-1}\,E(\theta)$.

Indeed, the solution (35) of the scaled problem holds since $v^{\rm eff}(\theta)$ is monotonic and covers the full range of $\theta$ (which is $[-1,1]$ in the relativistic case and $\mathbb{R}$ in the Galilean case): therefore there is a unique solution to $v^{\rm eff}(\theta)=\xi$, thus a unique jump; and $\theta_\star$ is monotonic with $\xi$, hence the asymptotic conditions are correctly implemented.

The system of integral equations (22), (20), (35) and (36) can be solved numerically using Mathematica, yielding extremely accurate results. Integral equations in (21) and (20) can be solved iteratively, a procedure that converges fast [60]. The hydrodynamic solution is obtained by first constructing the thermal occupation numbers $n^{L,R}(\theta)$ (21). Then, the non-equilibrium occupation number is evaluated by solving the system (35), (36): one first chooses $\theta_\star=\eta$ in order to construct $n(\theta)$, and then evaluates $p_\xi^{\rm dr}(\theta)$. The zero of $p_\xi^{\rm dr}(\theta)$ is numerically found – we observed that $p_\xi^{\rm dr}(\theta)$ always has a single zero. The process is repeated until the zero is stable – we observed that this is a convergent procedure. Finally, the non-equilibrium occupation number is used in (22), (20). The solving time increases slowly with the numerical precision demanded, thus this allows arbitrary-precision results.

The solution presented may be interpreted as a single *space-covering rarefaction wave*, in the sense that it is a solution to the eigenvalue equation (13) where all physical observables $\mathtt{q}_i$, $\mathtt{j}_i$ are continuous and interpolate between the two reservoirs. With relativistic dispersion relation, the solution is smooth within the light cone, beyond which the states are constant and equal to the initial baths' states; while in the Galilean case, the solution is generically smooth on the whole space. In this solution, every normal mode $n(\theta)$, seen as a function of $\xi$ for fixed $\theta$, is discontinuous exactly at its propagation velocity. Every normal mode therefore displays a "contact discontinuity" (a discontinuity without entropy production) [12]. Hence, the rarefaction wave may be seen as being composed of infinitely many contact discontinuities. In contrast to the finite-dimensional case, this single rarefaction wave can account for *generic reservoirs*, and no shock need to develop. This is because in the infinite-dimensional case, the eigenvalues of $J(\underline{\mathtt{n}})$ form a continuum: all propagation velocities $v^{\rm eff}(\theta)$ are available as conserved charges guarantee a large number of stable excitations, providing an additional continuous parameter tuning the smooth state trajectory and guaranteeing its correct asymptotic-reservoir values. Since weak solutions (shocks) are not necessary to connect the asymptotic reservoirs, they do not appear.

## V. ANALYSIS AND DISCUSSION

Concentrating on pure thermal transport, we have analyzed the above general system of equations for two related models: the relativistic integrable sinh-Gordon model and its non-relativistic limit [63, 64], the (repulsive) Lieb-Liniger model. We have also verified that our hydrodynamic equations reproduce the known results for the case of free particles.

### A. The relativistic sinh-Gordon model

One of the simplest integrable relativistic QFT with non-trivial interactions is the sinh-Gordon model. It is defined by the Lagrangian [65, 66]:

$$\mathcal{L}_{\rm shG}=\frac{1}{2}(\partial_\mu\phi)^2-\frac{m^2}{\beta^2}\cosh(\beta\phi), \tag{37}$$

where $\phi$ is the sinh-Gordon field and $m$ is the mass of the single particle in the spectrum. The model is integrable and therefore the only non-trivial scattering matrix is that associated to two-particle scattering. It is given by [67–69]

$$S(\theta)=\frac{\tanh\frac{1}{2}\left(\theta-\frac{\mathrm{i}\pi B}{2}\right)}{\tanh\frac{1}{2}\left(\theta+\frac{\mathrm{i}\pi B}{2}\right)}. \tag{38}$$

The parameter $B\in[0,2]$ is the effective coupling constant which is related to the coupling constant $\beta$ in the Lagrangian by

$$B(\beta)=\frac{2\beta^2}{8\pi+\beta^2}, \tag{39}$$

under CFT normalization [70]. The $S$-matrix is obviously invariant under the transformation $B\to 2-B$, a symmetry which is also referred to as weak-strong coupling duality, as it corresponds to $B(\beta)\to B(\beta^{-1})$ in (39). The point $B=1$ is known as the self-dual point. At the self-dual point the TBA differential scattering phase is simply

$$\varphi_{\rm shG}(\theta)=-\mathrm{i}\frac{\mathrm{d}}{\mathrm{d}\theta}\log S(\theta)=\frac{2}{\cosh\theta}. \tag{40}$$

Contrary to the Lieb-Liniger model which we will discuss later, the general features of any quantities of interest in the sinh-Gordon model are very similar for any values of the coupling $B$. For this reason, in this paper

| $\beta_L$ | $\mathtt{j}^{\rm sta}$ | $\frac{\mathtt{e}^L-\mathtt{e}^R}{2}$ | $\frac{\mathtt{k}^L-\mathtt{k}^R}{2}$ |
|---|---|---|---|
| $10^{-5}$ | $2.5661\times10^9$ | $2.5701\times10^9$ | $2.5624\times10^9$ |
| $10^{-4}$ | $2.5450\times10^7$ | $2.5522\times10^7$ | $2.5386\times10^7$ |
| $10^{-3}$ | 250665.6 | 252117.9 | 249421.1 |
| $10^{-2}$ | 2424.9 | 2461.8 | 2396.4 |
| $10^{-1}$ | 22.0 | 23.3 | 21.1 |
| 1 | 0.126 | 0.181 | 0.101 |

TABLE I. The functions $\mathtt{j}^{\rm sta}$, $\frac{\mathtt{e}^L-\mathtt{e}^R}{2}$ and $\frac{\mathtt{k}^L-\mathtt{k}^R}{2}$ over a wide range of values of $\beta_L$. The bounds (3) are always met.

we will concentrate our analysis solely on the self-dual point in the understanding that similar results hold for other values of $B$.

We have evaluated the energy density $\mathtt{e} := \mathtt{q}_1$, energy current $\mathtt{j} := \mathtt{j}_1$ and pressure $\mathtt{k} := \mathtt{j}_2$. Typical profiles are shown in Figs. 2, 3. Fig. 2 shows smooth interpolation within the light cone between the asymptotic baths at $\xi = -1$ and $\xi = 1$ (the speed of light is set to 1). Fig. 3 shows how, as temperatures rise, the current approaches the plateau (2) predicted by CFT [26, 27]. Further, in Fig. 4, the relative deviation of the steady-state current from its bounds (3) is shown. The bounds are extremely tight, pointing to the strength of this constraint and confirming that the proposed solution is correct. The bounds are indeed so tight that it is difficult to distinguish some points in parts of Fig. 4. To better appreciate this, we present the numerical values of the points displayed in Fig. 4 (divided by $\beta_L^2$) in Table I.

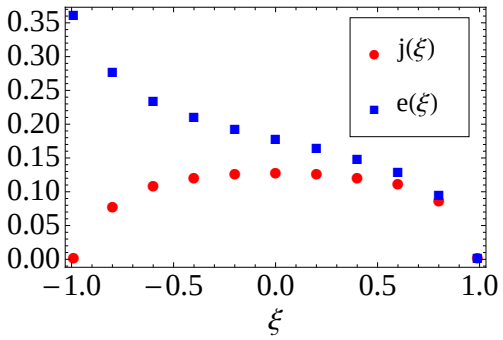


FIG. 2. The functions $\mathtt{j}(\xi)$ (dots) and $\mathtt{e}(\xi)$ (squares) for $\beta_L = 1$ and $\beta_R = 30$ in the sinh-Gordon model.

The numerical data have been obtained by solving the integral equations recursively until convergence is reached. Sources of error are the discretization and finite range of $\theta$ for numerical integration. Adjusting the number of divisions and the range, we estimate the error to be less than 0.1%.

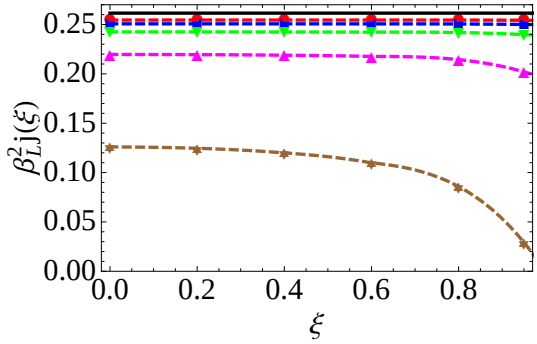


FIG. 3. The functions $\beta_L^2\mathtt{j}(\xi > 0)$ for $\beta_R = 30\beta_L$ and $\beta_L = 10^{-p}$ with $p = 0$ (stars), 1 (standing triangles), 2 (inverted triangles), 3 (squares) and 4 (circles). The continuous bold line represents the conformal value $\beta_L^2\mathtt{j}(\xi) = \frac{\pi}{12}\left(1-\frac{1}{900}\right)$ which, as expected is reached at high temperatures. Dashed curves are interpolations.

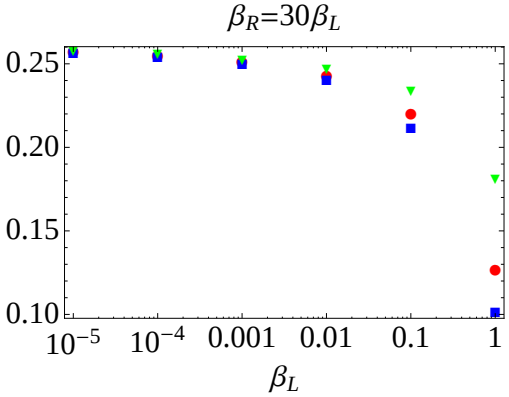


FIG. 4. Verification of the inequalities (3) in the sinh-Gordon model. Displayed are the functions $\beta_L^2\mathtt{j}^{\rm sta}$ (circles), $\beta_L^2(\mathtt{e}^L - \mathtt{e}^R)/2$ (triangles) and $\beta_L^2(\mathtt{k}^L - \mathtt{k}^R)/2$ (squares).

### B. The Lieb-Liniger model

The Lieb-Liniger (LL) model, in the repulsive regime ($\lambda > 0$), can be regarded as a non-relativistic limit of the sinh-Gordon model, as shown in [63, 64]. The Hamiltonian of the model is given by

$$H_{\rm LL} = \int {\rm d}x \Big( \frac{1}{2m}\partial_x\psi^\dagger\partial_x\psi + \lambda\psi^\dagger\psi^\dagger\psi\psi \Big). \qquad (41)$$

This is obtained from the Hamiltonian of the sinh-Gordon model by a double limit

$$c \to \infty,\ \beta \to 0;\ \beta c = 4\sqrt{\lambda}, \qquad (42)$$

where $c$ is the speed of light (which was implicit in (37))[4]. This limit can be performed within the TBA formalism

[4] This is the only equation in the present paper where the speed of light $c$ appears explicitly. Everywhere else $c$ denotes the central

[64], and accordingly, the density and current averages $\mathtt{q}_i$, $\mathtt{j}_i$ are given by (22), with the non-relativistic dispersion relation. There, the occupation number is given by $n_{\rm LL}(\theta) = 1/(1+e^{\epsilon_w(\theta)})$, and the pseudo-energy $\epsilon_w(\theta)$ and the dressed one-particle eigenvalues $h_i^{\rm dr}(\theta)$ are defined in the same manner as in Equations (21) and (20) (where $\theta = p/m$ is the velocity), with scattering matrix given by

$$S_{LL}(\theta) = \frac{\theta - 2\lambda i}{\theta + 2\lambda i}, \tag{43}$$

and corresponding differential scattering phase

$$\varphi_{\rm LL}(\theta) = \frac{4\lambda}{\theta^2 + 4\lambda^2}. \tag{44}$$

A uniform chemical potential $\mu$ is introduced, associated to the conserved charge $Q_0$ that counts the number of quasi-particles (with $h_0(\theta) = 1$). The energy current is chosen to be the current associated to of charge $H - \mu Q_0$,

$$\mathtt{j} := \mathtt{j}_1 - \mu \mathtt{j}_0 \qquad \text{(LL model)}. \tag{45}$$

Below we present some numerical results for several values of the coupling $\lambda$ and for $m = 1$.

Current profiles obtained for $\lambda = 3$ and various values of $\mu$ are displayed in Fig. 5. The main difference between the relativistic and non-relativistic cases is the lack, in the latter, of any sharp light-cone effect. Nevertheless, at low temperatures $T_{L,R} \ll \mu$, Luttinger Liquid physics emerges [71], including an emerging light-cone due to the Fermi velocity. This can be seen in Fig. 5: a plateau forms whose height is again in agreement with the general CFT result (2). The plateau lies between nearly symmetric values $\xi/v_F \approx \pm 1$ fixed by the Fermi velocity $v_F$. Thermal occupation numbers $n^{L,R}(\theta)$ are very sharply supported between Fermi points $\pm\theta_F^{L,R}$ with $\theta^{L,R} \gtrsim \sqrt{2\mu/m}$, and the Fermi velocity, which depends on $\xi$ very weakly, is the effective velocity $v^{\rm eff}(\theta_F^R)$ associated to the lowest temperature ($T_R < T_L$ in the present example). In agreement with general CFT results [26, 27], a light cone thus builds up (despite the model having no intrinsic maximal velocity), and the full state is in fact homogeneous between the Fermi velocities.

In the LL model the coupling constant may take any values between 0 and $\infty$ and the limits $\lambda \to 0$ and $\lambda \to \infty$ are of particular interest.

For $\lambda \to 0$ the differential scattering phase (44) becomes heavily peaked around $\theta = 0$. Formally, $\lim_{\lambda\to 0} \varphi_{LL}(\theta) = 2\pi\delta(\theta)$. The resulting TBA equations, with this differential scattering phase, admit no solution for the pseudoenergy if $\mu > 0$, but for $\mu < 0$ they can be solved exactly and reproduce the free Boson solution (for which $\mu > 0$ would make no physical sense). In particular the energy current takes the free Boson form,

$$\lim_{\lambda\to 0} \mathtt{j}(\xi) = \frac{1}{\beta_R^2}\int_{\alpha_R}^{\infty} d\theta\, \frac{\theta}{e^\theta - 1} - \frac{1}{\beta_L^2}\int_{\alpha_L}^{\infty} d\theta\, \frac{\theta}{e^\theta - 1}, \tag{46}$$

where $\alpha_{L,R} = \beta_{L,R}(\frac{\xi^2}{2} - \mu)$. In Fig. 6 we compare numerical values for $\lambda = 0.05$ and $\mu = -1$ to this analytical expression. The agreement is very good, confirming that a free Boson theory is smoothly recovered in this limit. With $\mu > 0$, as $\lambda$ becomes small the TBA equations gradually breakdown. How this occurs is subtle, and will be discussed in [81].

The qualitative change in behaviour of the TBA solutions as $\lambda \to 0$ is related to the two distinct regimes observed at small values of $\lambda$ [72]. Consider the dimensionless coupling $\gamma := 2m\lambda/\mathtt{q}_0$ (where we recall that $\mathtt{q}_0$ is the gas density, which may be taken in the initial baths for instance) and the reduced temperature $\tau := 2mT/\mathtt{q}_0^2$. The "decoherent regime", with large phase and density fluctuations, occurs for $\gamma \lesssim \min(\tau^2, \sqrt{\tau})$. In this regime, ideal Bose gas physics is recovered, and we have indeed verified that the inequality is satisfied in the parameter space where good agreement with (46) is observed (small $\lambda$, negative $\mu$). On the other hand, the "Gross-Pitaevskii regime" occurs for $\tau^2 \lesssim \gamma \lesssim 1$, a quasi-condensate with large phase fluctuations but suppressed density fluctuations. It is such quasi-condensate physics that strongly affects TBA solutions as $\lambda \to 0$ with $\mu > 0$.

The other interesting limit is $\lim_{\lambda\to\infty} \varphi_{LL}(\theta) = 0$. In this case we can also find an analytical expression for the current:

$$\lim_{\lambda\to\infty} \mathtt{j}(\xi) = \frac{1}{\beta_R^2}\int_{\alpha_R}^{\infty} d\theta\, \frac{\theta}{e^\theta + 1} - \frac{1}{\beta_L^2}\int_{\alpha_L}^{\infty} d\theta\, \frac{\theta}{e^\theta + 1}. \tag{47}$$

This corresponds to a free Fermion, in agreement with the expected Tonks-Girardeau physics occuring in the regime $\gamma \gtrsim \max(1, \sqrt{\tau})$ [72]. For $\xi \approx 0$ and $\mu\beta_{L,R} \gg 1$ it is easy to show that the integral above gives $\frac{\pi}{12}(\beta_L^{-2} - \beta_R^{-2})$ so that we recover the CFT result for the current with $c = 1$ (Dirac Fermion). Fig. 7 shows a comparison between numerical values of the current for $\lambda = 50$ and the formula above.

Let us now consider the particle current. Naturally, in the LL model, equilibrium states at higher temperatures have lower particle densities. Therefore, although the energy current flows from the left to the right in the present setup (with $T_L > T_R$), the initial particle density imbalance would naively suggest a particle flow from the right (higher density) to the left (lower density). The *opposite* occurs: Fig. 9 shows that the particle current is positive, hence flows form the left to the right. This means that the fluid flow produced by the temperature difference drags particles with enough force to counteract the particle imbalance and bring particles towards the higher-density bath. The fact that heat carries particles along its motion is a *thermoelectric effect*. It has been experimentally demonstrated in a quasi-two-dimensional fermionic cold atoms channel [3], and theoretically shown

charge. As both are standard notations, we opted to use the name $c$ for both.

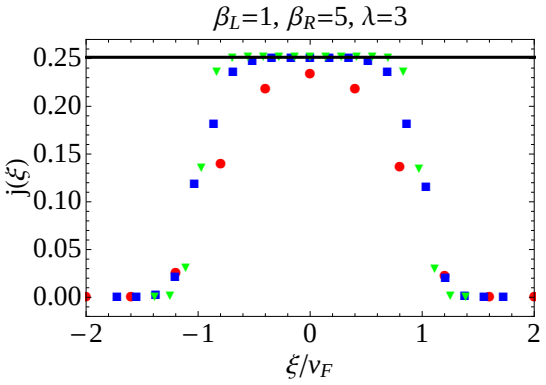


FIG. 5. Energy current in the Lieb-Liniger model for low temperatures, $\lambda = 3$ and chemical potentials $\mu = 3$ (circles), $\mu = 6$ (squares) and $\mu = 10$ (triangles). The CFT value $\frac{\pi}{12}\left(1-\frac{1}{25}\right)$ (bold horizontal line) is reached for high values of $\mu$. By plotting the currents against $\xi/v_F$ we observe the collapse of the various curves, which becomes better as $\mu$ increases. The regions where plateaux emerge are roughly $\xi/v_F \in [-1,1]$ with $v_F \approx 2.5, 2.9, 3.6$.

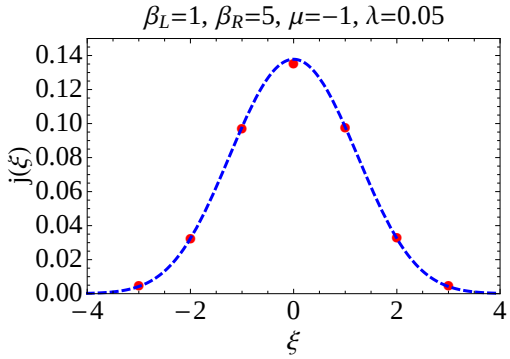


FIG. 6. Energy current in the Lieb-Liniger model for low temperatures, small coupling and negative chemical potential (circles). The dashed curve represents the current (46) for the same temperatures and chemical potential.

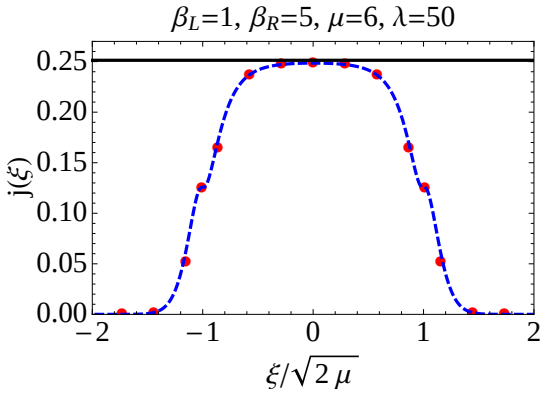


FIG. 7. Energy current in the Lieb-Liniger model for low temperatures, large coupling and chemical potential $\mu = 6$ (circles). Local stationary points occur at $\alpha_{L,R} = 0$, that is $\xi = \pm\sqrt{2\mu} = \pm 3.46$ (the Fermi velocity). The dashed curve represents the current (47) for the same temperatures and chemical potential, whose profile is not dissimilar to the plots shown in Fig. 5. As before, the bold horizontal line is the CFT value $\frac{\pi}{12}\left(1-\frac{1}{25}\right)$. The agreement is extremely good.

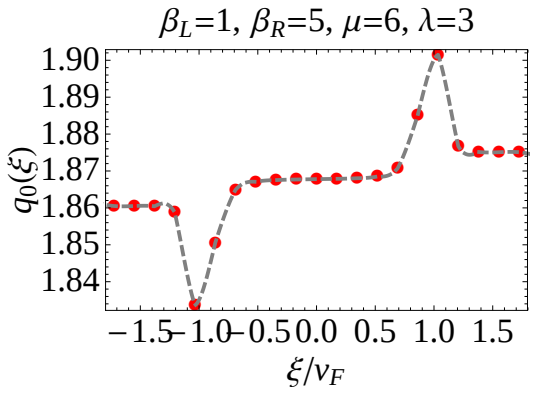


FIG. 8. A characteristic profile of the Lieb-Liniger particle density for $T_{L,R} \ll \mu$, $\lambda = 3$ and $\mu = 6$. The local maxima/minima are located around $\xi = \pm v_F$. The dashed curve is an interpolation.

in CFT in dimensions higher than one [17]. It is nontrivial in integrable models, as the large amount of conservation laws allows for independent currents to coexist, and our result gives the first theoretical prediction of this effect in the integrable one-dimensional Bose gas.

An additional consequence of the thermoelectric effect is that the particle density $\mathtt{q}_0(\xi)$ shows particle accumulation around $v_F$ and depletion around $-v_F$ (see Fig. 8). For instance, the start of the dip can be explained by the fact that, in any local spacial region originally in the left reservoir, the first particles to start moving towards the right are those on the right of the region, escaping and thus depleting it. Since time evolution at fixed position is obtained by scanning Fig. 8 from left to right, this explains the initial dip on the left. This depleting effect continues as long as the outgoing current on the right of the region is higher then the incoming current on its left – that is, until the region lies in the steady state. However, as time goes on, the effective local temperature decreases, and this tends to increase the particle density. This effect eventually overtakes the depleting effect, accounting for the rebounce to the higher steady-state value. The behavior of the current $\mathtt{j}_0$ in Fig. 9 is then a consequence of the continuity equation $\xi\partial_\xi \mathtt{q}_0 = \partial_\xi \mathtt{j}_0$.

This is a nonuniversal effect, not present in the density $\mathtt{q}_1(\xi) - \mu\mathtt{q}_0(\xi)$ controlled by low-energy processes, where the physics of chiral separation dominates and monotonic transition regions occur.

### C. General features

The form of the non-equilibrium occupation number indicates that quasi-particles are thermalized according to the initial GGE's, in a way that depends on the ra-

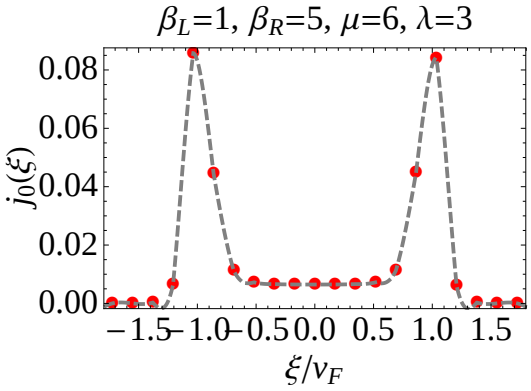


FIG. 9. A characteristic profile of the Lieb-Liniger particle current for $T_{L,R} \ll \mu$, $\lambda = 3$ and $\mu = 6$. The local maxima/minima are located around $\xi = \pm v_F$. The dashed curve is an interpolation.

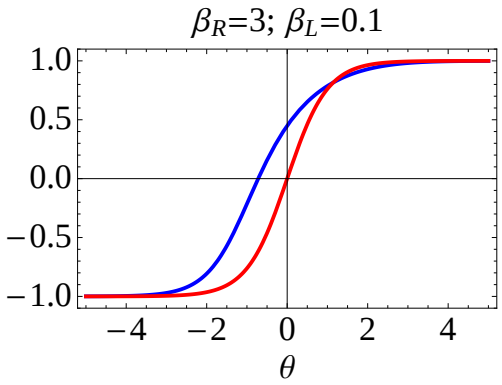


FIG. 10. Effective velocity in the sinh-Gordon model for $\xi = 0$. Displayed are the effective velocity $v^{\rm eff}(\theta)$ (blue line) and the bare relativistic velocity $\tanh\theta$ (red line).

pidity. It connects with the picture, proposed in [26, 47], according to which in the steady state ($\xi = 0$), quasi-particles traveling towards the right (left) are thermalized according to the left (right) reservoir. However, in the present solution, what determines the traveling direction is the *effective velocity* in the steady state: quasi-particles with positive (negative) dressed velocities, reaching the point $x = 0$ at large times, will have travelled mostly towards the right (left) (after a relatively small transient). In the sinh-Gordon model with $T_L > T_R$, the effective velocity behaves as in Fig. 10. We observe that it is greater than the bare velocity $\tanh\theta$ for small or negative rapidities, and smaller for large positive rapidities. This is in agreement with the intuition according to which the quasi-particles are effectively carried by the flow, which transports them towards the right, for small enough rapidities, but slowed down by dominant "friction" effects of thermal fluctuations at large rapidities. A similar effects occur in the Lieb-Liniger model.

The generalized hydrodynamic result differs from previous proposals in interacting integrable models [47–49] (while all results agree in noninteracting cases). The original proposal [47] was later shown [45] to break the second inequality in (3), while the second proposal [48], based on similar ideas, gave slight disagreements with numerical simulations. The conjecture [49] which corresponds to taking $\theta_\star = 0$ in our framework, seems to give good agreement with numerical simulations. This may be due to the fact that taking $\theta_\star = 0$, gives very small errors in wide temperature ranges, of the order of 0.5-1% (we have confirmed this numerically).

## VI. CONCLUSIONS

In this paper we developed a hydrodynamic theory for infinitely-many conservation laws, and applied it to the study of heat flows in experimentally relevant integrable models. It would be interesting to study further the non-equilibrium physics of the Lieb-Liniger model, including the effects of the Gross-Pitaevskii quasi-condensate and transport between different regimes. The emerging physical picture and solution we have given can be applied to any Bethe-ansatz integrable model, where infinitely-many conservation laws exist and a quasi-particle description is available. This includes quantum chains (see [43]), as continuity of space on which the microscopic theory lies is not needed for emerging hydrodynamics. It also includes relativistic models with non-diagonal scattering such as the sine-Gordon model, where, for instance, our TBA construction may be generalized along the lines of the famous approach of Destri and de Vega [74, 75]. Of course, the hydrodynamic ideas do not require a quasi-particle description, and it might be possible to develop generalized hydrodynamics using a variety of techniques from integrability. We note that it is remarkable that independent quasi-particle mode thermalization agrees, in integrable models, with local entropy maximization. The dynamical equations derived can be used to describe more general situations in ultracold gases such as the release from a trap (see e.g. [73]). This new theory and its extensions, including viscosity effects and forcing, should also allow for efficient studies of integrability breaking and related problems in any dimensionality, as well as for exact descriptions of dynamics in smooth trapping potentials [4] at arbitrary coupling strength.

**Acknowledgments.**
We thank Denis Bernard, M. Joe Bhaseen, Jean-Sébastien Caux, Fabian Essler, Mauricio Fagotti and Eric Lutz for discussions, and especially Bruno Bertini and Lorenzo Piroli for sharing their preliminary ideas and Pasquale Calabrese for encouraging us to pursue this research. OAC-A and BD are grateful to SISSA, Trieste, Italy, for support during a visit where this work started. TY thanks the Takenaka Scholarship Foundation for a scholarship.

### Appendix A: Current generators

Let $\langle\cdots\rangle_{\underline{\beta}}$ be the state given by Equation (4), and $\langle a(x)b(y)\rangle^{\rm c}_{\underline{\beta}} := \langle a(x)b(y)\rangle_{\underline{\beta}} - \langle a(x)\rangle_{\underline{\beta}}\langle b(y)\rangle_{\underline{\beta}}$ the connected correlation functions. These are time-independent and functions of the difference $x-y$ only. Let us assume that connected correlation functions of conserved densities and currents vanish *faster* than the inverse distance $|x-y|$. Then,

$$\begin{aligned}\int {\rm d}x\, \langle q_m(x) j_n(0)\rangle^{\rm c} &= \int {\rm d}x\, \langle j_n(0) q_m(x)\rangle^{\rm c} \\ &= \int {\rm d}x\, \langle j_n(x) q_m(0)\rangle^{\rm c} \\ &= -\int {\rm d}x\, x\, \langle \partial_x j_n(x) q_m(0)\rangle^{\rm c} \\ &= \int {\rm d}x\, x\, \langle \partial_t q_n(x) q_m(0)\rangle^{\rm c} \\ &= -\int {\rm d}x\, x\, \langle q_n(x) \partial_t q_m(0)\rangle^{\rm c} \\ &= \int {\rm d}x\, x\, \langle q_n(x) \partial_y j_m(y)\rangle^{\rm c}|_{y=0} \\ &= -\int {\rm d}x\, x\, \partial_x \langle q_n(x) j_m(0)\rangle^{\rm c} \\ &= \int {\rm d}x\, \langle q_n(x) j_m(0)\rangle^{\rm c}. \end{aligned} \tag{A1}$$

In the first line we used the fact that $\int {\rm d}x\, q_m(x)$ is a conserved quantity and thus commutes with the density matrix $\rho$; in the second we used space translation invariance, in the third integration by parts and the fast-enough vanishing of correlation functions; in the fourth current conservation; in the fifth time-translation invariance; in the sixth current conservation, in the seventh space-translation invariance; and in the eight integration by parts. Therefore,

$$\frac{\partial}{\partial \beta_m} \mathtt{j}_n = \frac{\partial}{\partial \beta_n} \mathtt{j}_m \tag{A2}$$

and thus

$$\mathtt{j}_m = \frac{\partial}{\partial \beta_m} g_{\underline{\beta}} \tag{A3}$$

showing Equation (6).

In the TBA context, we note that expressions (22) show the existence of appropriate free energies $f_w$ and $g_w$ generating densities and currents, respectively, as in (6). Indeed they may be re-written as

$$\mathtt{q}_i = \int {\rm d}\theta\, h_i(\theta) \frac{\delta f_w}{\delta w(\theta)},\ f_w = -\int \frac{{\rm d}p(\alpha)}{2\pi} \log(1+e^{-\epsilon_w(\alpha)}) \tag{A4}$$

and

$$\mathtt{j}_i = \int {\rm d}\theta\, h_i(\theta) \frac{\delta g_w}{\delta w(\theta)},\ g_w = -\int \frac{{\rm d}E(\alpha)}{2\pi} \log(1+e^{-\epsilon_w(\alpha)}). \tag{A5}$$

It then follows that that functional $w(\theta)$-derivatives of these free energies give the quasi-particle and current densities, $\rho_{\rm p}(\theta) = \delta f_w/\delta w(\theta)$ and $\rho_{\rm c}(\theta) = \delta g_w/\delta w(\theta)$.

### Appendix B: Emergence of generalized hydrodynamics

The only principle at the basis of hydrodynamics, and of the derivation we provide, is that of the emergence of local generalized thermalization (local entropy maximization). Technically, this is the assumption that averages of local quantities $\langle \mathcal{O}(x,t)\rangle$ tend uniformly enough, at large $x$ and $t$, to averages evaluated in GGEs (infinite-volume, maximal-entropy states, under conditions on infinitely-many conservation laws), with space-time-dependent potentials. This assumption is sufficient to derive the explicit dynamics for all single-point averages of local conserved densities and currents: no ad-hoc kinetic principle is needed.

In the case of infinitely-many conservation laws, one delicate point is the consideration of quasi-local densities and currents, which are involved in generalized thermalization. Such a quantity is not supported on a finite region, but on an extended region, with a weight (as measured by, for instance, the overlap with any other local observable) that decays away from a point. However, since hydrodynamics is concerned with large-scale space-time regions (the fluid cells), it is natural to consider them on the same footing. This is implicitly done in the derivation presented in this paper by assuming a completeness property of conservation laws.

Another delicate point concerns the definition of GGEs itself. In finite systems, such states depend on the boundary conditions imposed, and in general, these boundary conditions may still have an effect in the infinite-volume limit. For instance, walls simply preclude any nonzero potential associated to the momentum operator, as they break translation invariance. Nevertheless, given a set of allowed conserved charges, at large volumes, boundary conditions have little effect on local averages of conserved currents and densities (as they do not affect specific free energies). Further, periodic boundary conditions, at the basis of the TBA formalism, appear to provide the maximal set of conserved charges. It is in fact possible to construct GGEs directly in infinite volumes [21]. We expect local thermalization, and the full set of available conserved charges, to be correctly described by such constructions; and we expect these to agree with the TBA formalism used here.

We finally mention that the classical hard-rod problem, proven to give rise to a form of hydrodynamics [37, 52], has strong connections with the integrable systems investigated here, which we will investigate in a future work.

### Appendix C: Many-particle spectrum

The theory developed here is directly applicable to any integrable model whose two-particle scattering is diagonal in the internal space. Let the spectrum be composed of $\ell$ particles, of masses $m_a$, $a = 1, \dots, \ell$, and assume that their scattering is diagonal. In this case, the TBA equations can still be applied [60, 76]: the differential scattering phase is replaced by a matrix of functions $\varphi_{ab}(\theta-\gamma)$, and the one-particle eigenvalue of $Q_i$ will be denoted by $h_i(\theta; a)$. The solution $\underline{\mathtt{q}}(\xi)$, $\underline{\mathtt{j}}(\xi)$ of the generalized hydrodynamic problem is:

$$\begin{aligned}\mathtt{q}_i(\xi) &= \sum_a \int \frac{\mathrm{d}p(\theta;a)}{2\pi} n(\theta;a) h_i^{\mathrm{dr}}(\theta;a)\\ \mathtt{j}_i(\xi) &= \sum_a \int \frac{\mathrm{d}E(\theta;a)}{2\pi} n(\theta;a) h_i^{\mathrm{dr}}(\theta;a)\end{aligned} \tag{C1}$$

where $p(\theta;a) = m_a \sinh\theta$ and $E(\theta;a) = m_a\cosh\theta$, and

$$h_i^{\mathrm{dr}}(\theta;a) = h_i(\theta;a) + \int \frac{\mathrm{d}\gamma}{2\pi} \sum_b \varphi_{a,b}(\theta-\gamma)\, n(\gamma;b)\, h_i^{\mathrm{dr}}(\gamma;b). \tag{C2}$$

The non-equilibrium occupation number $n(\theta;a)$ is given by the discontinuous function

$$n(\theta;a) = n^L(\theta;a)\Theta(\theta-\theta_\star(a)) + n^R(\theta;a)\Theta(\theta_\star(a)-\theta) \tag{C3}$$

where each particle $a$ is associated to a different discontinuity at position $\theta_\star(a)$. These positions are self-consistently determined by the zeroes of the dressed, boosted momenta of particles $a$; with $p_\xi(\theta;a) := m_a \sinh(\theta-\eta)$ (relativistic) or $m_a\theta$ (non-relativistic):

$$p_\xi^{\mathrm{dr}}(\theta_\star(a);a) = 0, \quad a = 1, \dots, \ell. \tag{C4}$$

Again the thermal occupation numbers $n^{L,R}(\theta;a)$ entering (C3) guarantee that the asymptotic conditions on $\xi$ correctly represent the asymptotic baths as per Equation (14). They are obtained using the TBA equations in terms of the pseudo-energies $\epsilon_w(\theta;a)$ [60, 76],

$$\begin{aligned} n^{L,R}(\theta;a) &= \frac{1}{1+\exp\left[\epsilon_{w^{L,R}}(\theta;a)\right]} \\ \epsilon_w(\theta;a) &= w(\theta;a) - \\ &\quad - \int \frac{\mathrm{d}\gamma}{2\pi} \sum_b \varphi_{a,b}(\theta-\gamma)\log(1+e^{-\epsilon_w(\gamma;b)}).\end{aligned} \tag{C5}$$

Here $w^{L,R}(\theta;a) = \sum_i \beta_i^{L,R} h_i(\theta;a)$ are the one-particle eigenvalues of the charge $\sum_i \beta_i^{L,R} Q_i$ characterizing the GGE of the left and right asymptotic reservoirs.

### Appendix D: Current averages

An alternative proof of Equations (22) may be given using the technology of integrable systems, which has the advantage of generalizing to flows generated by any conserved charge instead of just the Hamiltonian. For completeness we present here the main arguments. The idea is to prove expression (22) for current averages $\mathtt{j}_i$ given the expression for density averages $\mathtt{q}_i$. This is akin to extending the LeClair-Mussardo formula (LM formula) [77] so that it incorporates the infinite number of conserved charges, and applying it to the current with the aid of form factors (FFs). We shall use the notation introduced in [78]. Following the derivation in [78] we generalize the LM formula for a one-point function of a generic local operator $\mathcal{O}(x,t)$,

$$\langle \mathcal{O}(x,t)\rangle = \sum_{\ell=0}^{\infty} \frac{1}{\ell!}\left(\prod_{k=1}^{\ell}\frac{\mathrm{d}\theta_k}{2\pi} n(\theta_k)\right) \langle \overleftarrow{\theta}\,|\mathcal{O}(0)|\,\overrightarrow{\theta}\rangle_{\mathrm{c}}, \tag{D1}$$

where $|\,\overrightarrow{\theta}\rangle = |\theta_1, \cdots, \theta_\ell\rangle$ (and $\langle\overleftarrow{\theta}\,| = \langle\theta_\ell, \cdots, \theta_1|$ is its hermitian conjugate) and diagonal matrix elements (DMEs) in the sum are connected (the meaning of being "connected" will be described below). Here $n(\theta)$ is the same occupation number as that involved in (21), (22), (20). It is then immediate to see that an expression for the density average $\mathtt{q}_i$ with the one-particle eigenvalue $h_i(\theta)$ proved by Saleur [79] is modified to

$$\begin{aligned}\mathtt{q}_i = m\sum_{\ell=0}^{\infty}\left(\prod_{k=1}^{\ell}\frac{\mathrm{d}\theta_k}{2\pi} n(\theta_k)\right) \\ \times \varphi(\theta_{12})\cdots\varphi(\theta_{\ell-1,\ell}) h_i(\theta_1)\cosh\theta_\ell,\end{aligned} \tag{D2}$$

where $\varphi(\theta_{ij}) = \varphi(\theta_i-\theta_j)$. Observe that this is indeed in agreement with the expression in (22). The expression (D2) can be derived using the DMEs of $q_i(x,t)$ given by

$$\begin{aligned}\langle\overleftarrow{\theta}\,|q_i|\,\overrightarrow{\theta}\rangle_{\mathrm{c}} = m\varphi(\theta_{12})\varphi(\theta_{23})\cdots\varphi(\theta_{\ell-1,\ell}) \\ \times h_i(\theta_1)\cosh\theta_\ell + \text{permutations}.\end{aligned} \tag{D3}$$

Similarly, once we evaluate DMEs for the current $j_i(x,t)$, we can construct its average $\mathtt{j}_i$. The expression in (22), that we want to show, will then follow if the DMEs of the currents are obtained from those of the densities by the replacement of $\cosh\theta_n$ with $\sinh\theta_n$

$$\begin{aligned}\langle\overleftarrow{\theta}\,|j_i|\,\overrightarrow{\theta}\rangle_{\mathrm{c}} = m\varphi(\theta_{12})\varphi(\theta_{23})\cdots\varphi(\theta_{\ell-1,\ell}) \\ \times h_i(\theta_1)\sinh\theta_\ell + \text{permutations}.\end{aligned} \tag{D4}$$

Before embarking upon showing it, we elaborate on the definitions of connected and symmetric DMEs. Formally they are given by, respectively, [80]

$$\begin{aligned}\langle\overleftarrow{\theta}\,|\mathcal{O}|\,\overrightarrow{\theta}\rangle_{\mathrm{c}} &:= F^{\mathrm{c}}_{2\ell}(\mathcal{O},\,\overrightarrow{\theta}) \\ &:= \mathrm{FP}\lim_{\delta_k\to 0} F_{2\ell}(\mathcal{O};\,\overrightarrow{\theta}+\mathrm{i}\pi+\overrightarrow{\delta},\,\overleftarrow{\theta}),\end{aligned} \tag{D5}$$

$$\begin{aligned}\langle\overleftarrow{\theta}\,|\mathcal{O}|\,\overrightarrow{\theta}\rangle_{\mathrm{s}} &:= F^{\mathrm{s}}_{2\ell}(\mathcal{O},\,\overrightarrow{\theta}) \\ &:= \lim_{\delta\to 0} F_{2\ell}(\mathcal{O};\,\overrightarrow{\theta}+\mathrm{i}\pi+\delta,\,\overleftarrow{\theta})\end{aligned} \tag{D6}$$

where FP means "finite part" [78], $\overrightarrow{\delta} = (\delta_1, \cdots, \delta_\ell)$, and the FF $F_\ell(\mathcal{O};\,\overrightarrow{\theta})$ is defined by

$$F_\ell(\mathcal{O};\,\overrightarrow{\theta}) = \langle \mathrm{vac}|\mathcal{O}(0)|\,\overrightarrow{\theta}\rangle. \tag{D7}$$

Notice that with a limit such as in (D5), where the parameters $\delta_k$ differ in each component, different orders of limits lead to different results which may be singular; this is because when $\delta_k \to 0$, the FF (D5) becomes singular due to kinematic poles. It is in order to circumvent this ambiguity that one defines connected and symmetric FF's. The connected FF is a finite part, which simply prescribes to set to zero terms with singularities in $\delta_k$ [78], whereas the symmetric FF is defined by sending all parameters to zero simultaneously.

It was pointed out in [80] that any multi-particle symmetric FF can be written solely in terms of the connected FFs. For instance, for a two-particle state, the connected FF $F_4^{\rm c}(\mathcal{O};\theta_1,\theta_2)$ and the symmetric FF $F_4^{\rm s}(\mathcal{O};\theta_1,\theta_2)$ satisfy

$$F_4^{\rm c}(\mathcal{O};\theta_1,\theta_2) = F_4^{\rm s}(\mathcal{O};\theta_1,\theta_2) - \varphi(\theta_{12})F_2(\mathcal{O};\theta_1) - \varphi(\theta_{21})F_2(\mathcal{O};\theta_2), \tag{D8}$$

where $F_2(\mathcal{O};\theta) = F_2^{\rm c}(\mathcal{O};\theta) = F_2^{\rm s}(\mathcal{O};\theta)$ (in the case of a single parameter $\delta_1$, there is no singularity, hence no ambiguity). Applying this relation to $j_i$, we have

$$F_4^{\rm c}(j_i;\theta_1,\theta_2) = F_4^{\rm s}(j_i;\theta_1,\theta_2) - \varphi(\theta_{12})F_2(j_i;\theta_1) - \varphi(\theta_{21})F_2(j_i;\theta_2). \tag{D9}$$

This can be expressed in terms of FFs of the density $q_i$ thanks to the conservation law $\partial_t q_i + \partial_x j_i = 0$, which entails

$$F_{2\ell}^{\rm s}(j_i;\overrightarrow{\theta}) = \frac{\sum_{k=1}^{\ell}\sinh\theta_k}{\sum_{k=1}^{\ell}\cosh\theta_k}F_{2\ell}^{\rm s}(q_i;\overrightarrow{\theta}). \tag{D10}$$

Hence putting (D10) into (D9) yields

$$F_4^{\rm c}(j_i;\theta_1,\theta_2) = m\varphi(\theta_{12})h_i(\theta_1)\sinh\theta_2 + \{\theta_1 \leftrightarrow \theta_2\}, \tag{D11}$$

which is consistent with (D4). It is readily seen that for multi-particle states similar arguments hold, and thus we obtain (D4). Finally the generalized LM formula for the current gives

$$\mathtt{j}_i = m\sum_{\ell=0}^{\infty}\Big(\prod_{k=1}^{\ell}\frac{{\rm d}\theta_k}{2\pi}n(\theta_k)\Big) \times \varphi(\theta_{12})\cdots\varphi(\theta_{\ell-1,\ell})h_i(\theta_1)\sinh\theta_\ell. \tag{D12}$$

This exactly coincides with (22). Similar arguments give rise to current averages associated to flows $\mathrm{i}[Q_k, q_i] + \partial_x j_i^{(k)} = 0$ with respect to any local conserved quantity $Q_k$ (with odd spin):

$$\mathtt{j}_i^{(k)} = \int\frac{{\rm d}h_k(\theta)}{2\pi}n(\theta)h_i^{\rm dr}(\theta). \tag{D13}$$

A full derivation will be given in [81].


[1] J. Eisert, M. Friesdorf, C. Gogolin, "Quantum many-body systems out of equilibrium", Nature Phys. **11**, 124 (2015).

[2] S. Jezouin et al, "Quantum limit of heat flow across a single electronic channel", Science **342**, 601 (2013).

[3] J.-P. Brantut et al., "A thermoelectric heat engine with ultracold atoms", Science Reports **342**, 713 (2013)

[4] T. Kinoshita, T. Wenger, D.S. Weiss, "A quantum Newton's cradle", Nature **440**, 900 (2006).

[5] T. Langen et al, "Experimental observation of a generalized Gibbs ensemble" Science **348**, 207 (2015).

[6] M. Cheneau et al, "Light-cone-like spreading of correlations in a quantum many-body system", Nature **481**, 484 (2012).

[7] D. Ruelle, "Natural nonequilibrium states in quantum statistical mechanics", J. Stat. Phys. **98**, 57 (2000).

[8] P. Nozieres, D. Pines, *"The Theory of Quantum Liquids"*, Benjamin, New York, 1966.

[9] S. Jeon, L. G. Yaffe, "From quantum field theory to hydrodynamics: Transport coefficients and effective kinetic theory", Phys. Rev. **D 53**, 5799 (1996).

[10] A. G. Abanov, "Hydrodynamics of correlated systems. Emptiness formation probability and random matrices", in *Applications of Random Matrices in Physics*, vol. 221 of the series NATO Science Series II: Mathematics, Physics and Chemistry, 139-161 (2006).

[11] E. Bettelheim, A. G. Abanov, P. Wiegmann, "Quantum Shock Waves - the case for non-linear effects in dynamics of electronic liquids", Phys. Rev. Lett. **97**, 246401 (2006).

[12] A. Bressan, "Hyperbolic conservation laws: an illustrated tutorial", in: *Modelling and Optimisation of Flows on Networks*, Lecture Notes in Mathematics, **2062**, 157-245 (2013).

[13] J. Bhaseen, B. Doyon, A. Lucas, K. Schalm, "Far from equilibrium energy flow in quantum critical systems", Nature Physics **11**, 509 (2015).

[14] H.-C. Chang, A. Karch, A. Yarom, "An ansatz for one dimensional steady state configurations", J. Stat. Mech. **2014**, P06018 (2014).

[15] D. Bernard, B. Doyon, "A hydrodynamic approach to non-equilibrium conformal field theories", J. Stat. Mech. **2016**, 033104 (2016).

[16] R. Pourhasan, "Non-equilibrium steady state in the hydro regime", J. High Energ. Phys. **02**, 005 (2016).

[17] A. Lucas, K. Schalm, B. Doyon, M. J. Bhaseen, "Shock waves, rarefaction waves and non-equilibrium steady states in quantum critical systems", Phys. Rev. **D 94**, 025004 (2016).

[18] M. Spillane, C. P. Herzog, "Relativistic hydrodynamics and non-equilibrium steady states", preprint `arXiv:1512.09071`.

[19] M. Rigol, V. Dunjko, V. Yurovsky, M. Olshanii, "Relaxation in a completely integrable many-body quantum system: an ab initio study of the dynamics of the highly excited states of 1D lattice hard-core bosons", Phys. Rev. Lett. **98**, 050405 (2007)

[20] E. Ilievski J. De Nardis, B. Wouters, J.-S. Caux, F. H. L. Essler, T. Prosen, "Complete generalized Gibbs ensemble

in an interacting theory", Phys. Rev. Lett. **115**, 157201 (2015).

[21] B. Doyon, "Thermalization and pseudo-locality in extended quantum systems", preprint arXiv:1512.03713.

[22] F. Essler, M. Fagotti, "Quench dynamics and relaxation in isolated integrable quantum spin chains", to appear in: J. Stat. Mech., special issue on *Nonequilibrium dynamics in integrable quantum systems*, preprint arXiv:1603.06452.

[23] T. Prosen, "Open XXZ spin chain: non-equilibrium steady state and a strict bound on ballistic transport", Phys. Rev. Lett. **106**, 217206 (2011).

[24] T. Prosen, E. Ilievski, "Families of quasilocal conservation laws and quantum spin transport", Phys. Rev. Lett. **111**, 057203 (2013).

[25] E. Ilievski, M. Medenjak, T. Prosen, L. Zadnik, "Quasilocal charges in integrable lattice systems", to appear in: J. Stat. Mech., special issue on *Nonequilibrium dynamics in integrable quantum systems*, preprint arXiv:1603.00440.

[26] D. Bernard, B. Doyon, "Energy flow in non-equilibrium conformal field theory.", J. Phys. **A 45**, 362001 (2012).

[27] D. Bernard, B. Doyon, "Non-equilibrium steady-states in conformal field theory", Ann. Henri Poincaré **16**, 113-161 (2015).

[28] D. Bernard, B. Doyon, "Conformal field theory out of equilibrium: a review", to appear in: J. Stat. Mech., special issue on *Nonequilibrium dynamics in integrable quantum systems*, preprint arXiv:1603.07765.

[29] M. Moeckel, S. Kehrein, "Interaction Quench in the Hubbard Model", Phys. Rev. Lett. **100**, 175702 (2008).

[30] B. Bertini, F. H. L. Essler, S. Groha, N. J. Robinson, "Prethermalization and thermalization in models with weak integrability breaking", Phys. Rev. Lett. **115**, 180601 (2015).

[31] L.E. Reichl, "The search for a quantum KAM theorem", Found. Phys. **17**, 689 (1987).

[32] G.P. Brandino, J.-S. Caux, R.M. Konik, "Glimmers of a quantum KAM theorem: insights from quantum quenches in one-dimensional Bose gases", Phys. Rev. **X 5**, 041043 (2015).

[33] P. Glansdorff, I. Prigogine, I, *Thermodynamic Theory of Structure, Stability, and Fluctuations*, Wiley-Interscience, London, 1971.

[34] R. Balescu, *Equilibrium and Non-equilibrium Statistical Mechanics*, John Wiley & Sons, New York, 1975.

[35] J. Keizer, *Statistical Thermodynamics of Nonequilibrium Processes*, Springer-Verlag, New York, 1987.

[36] F. Schloegl, *Probability and Heat: Fundamentals of Thermostatistics*, Freidr. Vieweg & Sohn, Brausnchweig, 1989.

[37] H. Spohn, *Large Scale Dynamics of Interacting Particles*, Springer-Verlag, Berlin Heidelberg, 1991.

[38] E. H. Lieb, W. Liniger, "Exact analysis of an interacting Bose gas. I. The general solution and the ground state", Phys. Rev. **130**, 1605 (1963).

[39] T. Kinoshita, T. Wenger, D. S. Weiss, "Observation of a one-dimensional Tonks-Girardeau gas", Science **305**, 1125 (2004).

[40] B. Paredes et al, "Tonks-Girardeau gas of ultracold atoms in an optical lattice", Nature **429**, 277 (2004).

[41] A. H. van Amerongen et al, "Yang-Yang thermodynamics on an atom chip", Phys. Rev. Lett. **100**, 090402 (2008).

[42] H. Spohn, J. L. Lebowitz, "Stationary non-equilibrium states of infinite harmonic systems", Commun. Math. Phys. **54**, 97 (1977).

[43] B. Bertini, M Collura, J. De Nardis, M Fagotti, "Transport in out-of-equilibrium XXZ chains: exact profiles of charges and currents", preprint arXiv:1605.09790.

[44] C. Karrasch, R. Ilan, J. E. Moore, "Nonequilibrium thermal transport and its relation to linear response", Phys. Rev. **B 88**, 195129 (2013).

[45] B. Doyon, "Lower bounds for ballistic current and noise in non-equilibrium quantum steady states", Nucl. Phys. **B 892**, 190 (2015).

[46] E. H. Lieb, D. W. Robinson, "The finite group velocity of quantum spin systems", Commun. Math. Phys. **28**, 251 (1972).

[47] O. Castro-Alvaredo, Y. Chen, B. Doyon, M. Hoogeveen, "Thermodynamic Bethe ansatz for non-equilibrium steady states: exact energy current and fluctuations in integrable QFT", J. Stat. Mech. **2014**, P03011 (2014).

[48] A. De Luca, J. Viti, L. Mazza, D. Rossini, "Energy transport in Heisenberg chains beyond the Luttinger liquid paradigm", Phys. Rev. **B 90**, 161101(R) (2014).

[49] X. Zotos, "A TBA description of thermal transport in the XXZ Heisenberg model", preprint arXiv:1604.08434.

[50] B. Doyon, A. Lucas, K. Schalm, M. J. Bhaseen, "Non-equilibrium steady states in the Klein-Gordon theory", J. Phys. **A 48**, 095002 (2015).

[51] C. B. Mendl, H. Spohn, "Shocks, rarefaction waves, and current fluctuations for anharmonic chains", preprint arXiv:1607.05205.

[52] C. Boldrighini, R. L. Dobrushin, Yu. M. Sukhov, "One-dimensional hard rod caricature of hydrodynamics", J. Stat. Phys. **31**, 577 (1983).

[53] T. Sabetta, G. Misguich, "Nonequilibrium steady states in the quantum XXZ spin chain", Phys. Rev. **B 88**, 245114 (2013).

[54] T. Antal, P. L. Krapivsky, A. Rákos, "Logarithmic current fluctuations in nonequilibrium quantum spin chains", Phys. Rev. **E 78**, 061115 (2008).

[55] P. Wendenbaum, M. Collura, D. Karevski, "Hydrodynamic description of hard-core bosons on a Galileo ramp", Phys. Rev. **A 87**, 023624 (2013)

[56] M. Collura, D. Karevski, "Quantum quench from a thermal tensor state: boundary effects and generalized Gibbs ensemble", Phys. Rev. **B 89**, 214308 (2014).

[57] M. Collura, G. Martelloni, "Non-equilibrium transport in $d$-dimensional non-interacting Fermi gases", J. Stat. Mech. (2014) P08006.

[58] J. Viti, J.-M. Stéphan, J. Dubail, M. Haque, "Inhomogeneous quenches in a fermionic chain: exact results", preprint arXiv:1507.08132 (2015).

[59] B. Bertini and M. Fagotti, "Determination of the non-equilibrium steady state emerging from a defect", preprint arXiv:1604.04276 (2016).

[60] A. Zamolodchikov, "Thermodynamic Bethe ansatz in relativistic models. Scaling three state Potts and Lee-Yang models", Nucl. Phys. **B 342**, 695–720 (1990).

[61] J. Mossel, J.-S. Caux, "Generalized TBA and generalized Gibbs", J. Phys. **A 45**, 255001 (2012).

[62] L. Bonnes, F. H. L. Essler, A. M. Läuchli, ""Light-cone" dynamics after quantum quenches in spin chains", Phys. Rev. Lett. **113**, 187203 (2014).

[63] M. Kormos, G. Mussardo, A. Trombettoni, "Expectation values in the Lieb-Liniger Bose gas", Phys. Rev. Lett. **103**, 210404 (2009).

[64] M. Kormos, G. Mussardo, A. Trombettoni, "One-dimensional Lieb-Liniger Bose gas as nonrelativistic limit

of the sinh-Gordon model", Phys. Rev. **A 81**, 043606 (2010).

[65] A. E. Arinshtein, V. A. Fateev, A. B. Zamolodchikov, "Quantum S-matrix of the (1 + 1)-dimensional Toda chain", Phys. Lett. **B 87** 389–392 (1979).

[66] A. V. Mikhailov, M. A. Olshanetsky, A. M. Perelomov, "Two-dimensional generalized Toda lattice", Commun. Math. Phys. **79** 473–488 (1981).

[67] I. Ya. Arafeva, V. E. Korepin, "Scattering in two-dimensional model with Lagrangian $L = 1/\gamma(1/2(\partial_m uu)^2 + m^2(\cos u - 1))$", Pis'ma Zh. Eksp. Teor. Fiz. **20**, 680 (1974).

[68] S. N. Vergeles, V. M. Gryanik, "Two-dimensional quantum field theories having exact solutions", Yad. Fiz. **23**, 1324–1334 (1976).

[69] B. Schroer, T. T. Truong, P. H. Weisz, "Towards an explicit construction of the sine-Gordon theory", Phys. Lett. **B 63** 422–424 (1976).

[70] A. B. Zamolodchikov, Al. B. Zamolodchikov, "Factorized S-matrices in two-dimensions as the exact solutions of certain relativistic quantum field models", Ann. Phys. **120** 253–291 (1979).

[71] M. A. Cazalilla et al, "One dimensional bosons: From condensed matter systems to ultracold gases", Rev. Mod. Phys. **83**, 1405 (2011).

[72] K. V. Kheruntsyan, D. M. Gangardt, P. D. Drummond, G. V. Shlyapnikov, "Pair correlations in a finite-temperature 1D Bose gas", Phys. Rev. Lett. **91**, 040403 (2003).

[73] I. Bloch, J. Dalibard, W. Zwerge, "Many-body physics with ultracold gases", Rev. Mod. Phys. **80**, 885 (2008)

[74] C. Destri, H. De Vega, "New thermodynamic Bethe ansatz equations without strings", Phys. Rev. Lett. **69**, 2313 (1992)

[75] C. Destri, H. De Vega, "Unified approach to thermodynamic Bethe ansatz and finite size corrections for lattice models and field theories", Nucl. Phys. **B 438** 413 (1995).

[76] T. R. Klassen, E. Melzer, "The Thermodynamics of purely elastic scattering theories and conformal perturbation theory", Nucl. Phys. **B 350**, 635–689 (1991).

[77] A. LeClair, G. Mussardo, "Finite temperature correlation functions in integrable QFT", Nucl. Phys. **B 552**, 624–642 (1999).

[78] G. Mussardo, "Infinite-time average of local fields in an integrable quantum field theory after a quantum quench", Phys. Rev. Lett. **111**, 100401 (2013).

[79] H. Saleur, "A comment on finite temperature correlations in integrable QFT", Nucl. Phys. **B 567**, 602–610 (2000).

[80] B. Pozsgay, G. Takacs, "Form factors in finite volume II: disconnected terms and finite temperature correlators", Nucl. Phys. **B 788** 209–251 (2008).

[81] O. A. Castro-Alvaredo, B. Doyon, T. Yoshimura, in preparation.

## 4.2 Mean values of the current of conserved charges

In this section, we review the work [67]. My personal contribution is to provide some of the key ideas of the proof (e.g. to work with the symmetric form factors in order to get the connected form factor of the current). In fact, the main logic of the proof is based on the sketchy proof I provided in [45]. The idea on the proof of the finite matrix-element of the current is entirely my own.

The simple form of the Euler scale current average (4.2) suggests that it might also be proven in the light of graph theory as in the charge density averages. It turns out that it is indeed possible to achieve it, at least in the case of the diagonally-scattering relativistic systems, in a rather simple way. Below, invoking the LeClair-Mussardo formula, we outline how one can obtain the connected form factor of the current. For the complete derivation, see [67]. As a by-product, this will also allow us to derive the finite-volume matrix element of the current.

In order to calculate the connected form factor of the current, we take the following steps. First, we compute the symmetric form factor of the charge densities by using (2.79). We then transform them into that of currents by means of the continuity equations. By following the same logic by which we obtained the symmetric form factor of the charge densities backward, we finally obtain the connected form factor of the currents.

To start, let us examine (2.79). By merely invoking that $\mathcal{L}(\alpha|\alpha)$ is a sum of spanning forests rooted at vertices belonging to the set $\alpha$, and that $F^{\mathrm{c}}_{2|\alpha|}(\{\theta_i\}_{i\in\alpha})$ is a sum of spines equipped with vertices from $\alpha$, with two ends being $p'$ and $h$. Then what is done in the right hand side in (2.79) is the merger of these two objects, i.e. the decoration of the spines by planting trees at each vertex. This results in the spanning trees with $n$ vertices with $p'$ and $h$ inserted at two arbitrary positions in each tree. Any double counting of the same tree is avoided here, since each tree is now labeled and each spine comes with a different permutation. Therefore the symmetric form factor can be written as

$$F^{\mathrm{s}}_{2n,\mathfrak{q}}(\theta_1,\cdots,\theta_n)=\sum_{j=1}^{n}h(\theta_j)\sum_{k=1}^{n}p'(\theta_k)\sum_{T\in\mathcal{T}}\prod_{e\in T}\varphi_e. \tag{4.16}$$

Next, recalling the continuity equations at the operator level $\partial_t\mathfrak{q}+\partial_x\mathfrak{j}=0$, we realize that the following relation holds between the symmetric form factor of $\mathfrak{q}$ and $\mathfrak{j}$:

$$F^{\mathrm{s}}_{2n,\mathfrak{j}}(\theta_1,\cdots,\theta_n)=\frac{\sum_k E'(\theta_k)}{\sum_k p'(\theta_k)}F^{\mathrm{s}}_{2n,\mathfrak{q}}(\theta_1,\cdots,\theta_n). \tag{4.17}$$

Combining (4.16) and (4.17), we immediately obtain

$$F^{\mathrm{s}}_{2n,\mathfrak{j}}(\theta_1,\cdots,\theta_n)=\sum_{j=1}^{n}h(\theta_j)\sum_{k=1}^{n}E'(\theta_k)\sum_{T\in\mathcal{T}}\prod_{e\in T}\varphi_e. \tag{4.18}$$

Now, thanks to the connectedness and the absence of cycles in each tree, we can extract a unique spine that interpolates $E'$ and $h$ in each tree. This precisely amounts to the same decomposition into the sum of spanning trees and spines we had for $F^{\mathrm{s}}_{2n,\mathfrak{q}}(\theta_1,\cdots,\theta_n)$, except that $p'$ is now replaced by $E'$. This implies that the connected form factor of $\mathfrak{j}$ is

$$F^{\mathrm{c}}_{2n,\mathfrak{j}}(\theta_1,\cdots,\theta_n)=h(\theta_1)\varphi_{1,2}\cdots\varphi_{n-1,n}E'(\theta_n)+\text{perm.} \tag{4.19}$$

Plugging this into the LeClair-Mussardo formula (2.81), we obtain the current average formula

$$\langle\mathfrak{j}\rangle_\rho=\int\frac{\mathrm{d}\theta}{2\pi}(E')^{\mathrm{dr}}(\theta)n(\theta)h(\theta)=\int\mathrm{d}\theta\rho_{\mathrm{p}}(\theta)v^{\mathrm{eff}}(\theta)h(\theta). \tag{4.20}$$

Next, let us turn to the finite-volume matrix element of the current operator $\mathfrak{j}$. It turns out that it has a neat expression, reading

$$\langle\theta_n,\cdots,\theta_1|\mathfrak{j}|\theta_1,\cdots,\theta_n\rangle_L=\mathcal{G}(\theta_1,\cdots,\theta_n)\sum_{i,j=1}^n E'(\theta_j)G^{-1}_{ji}h(\theta_i), \tag{4.21}$$

where $G^{-1}$ is the inverse of the $n\times n$ Gaudin matrix and $\mathcal{G}=\det G$ is the Gaudin determinant. To prove it, let us first recall that, according to the Pozsgay-Takács formula (2.77), the finite-volume diagonal matrix element of the current operator $\mathfrak{j}$ can be written in terms of its connected form factor as

$$\langle\theta_n,\cdots,\theta_1|\mathfrak{j}|\theta_1,\cdots,\theta_n\rangle_L=\sum_{I\subset\{1,\cdots,n\}}F^{\mathfrak{j}}_{2|I|,c}(\{\theta_i\}_{i\in I})\mathcal{G}(I|I). \tag{4.22}$$

This is nothing but a summation over all forests each of which contains a tree in which $E'$ is inserted at the root and $h$ is inserted at one of vertices, and other trees rooted with weighed $Lp'$. Therefore, to prove (4.21), we shall show that $G^{-1}_{ji}$ generates all the forests each of which contains trees that are rooted with weighed $Lp'$ except one tree that is made by decorating a spine rooted at the vertex $j$ and terminating at another vertex $i$. Namely, we establish

$$G^{-1}_{ji}=\frac{1}{\mathcal{G}}\sum_{I\subset\{1,\cdots,n\}}\prod_{\beta\neq j}^{|I|}Lp'_\beta\sum_{\substack{\langle kl\rangle\in F_I\\ j\to i}}\varphi_{lk}. \tag{4.23}$$

Once it is shown, it is obvious that the RHS of (4.21) coincides with its LHS.

Let us start with rewriting the Gaudin matrix $G_{ij}$ as $G_{ij}=Lp'_i\tilde{G}_{ij}$, where $\tilde{G}_{ij}$ is

$$\tilde{G}_{ij}=\delta_{ij}+\delta_{ij}\sum_{l\neq j}^n\tilde{\varphi}_{il}-(1-\delta_{ij})\tilde{\varphi}_{ij},\quad \tilde{\varphi}_{ij}=\frac{1}{Lp'_i}\varphi_{ij}. \tag{4.24}$$

It then follows that

$$LG^{-1}_{ji}p'_i=\tilde{G}^{-1}_{ji}=(-1)^{i+j}\frac{\tilde{G}(i|j)}{\tilde{\mathcal{G}}}, \tag{4.25}$$

thus

$$G^{-1}_{ji} = (-1)^{i+j} \prod_{\beta \neq i}^{n} Lp'_{\beta} \frac{\tilde{G}(i|j)}{\mathcal{G}}. \tag{4.26}$$

As proven in [89, 134], $\tilde{G}(i|j)$ can be written as

$$\tilde{G}(i|j) = (-1)^{i+j} \sum_{I \subset \{1,\cdots,n\}} \sum_{\substack{\langle kl \rangle \in F_I \\ i \to j}} \frac{1}{Lp'_l} \varphi_{lk}, \tag{4.27}$$

where we note that the weighs $\frac{1}{Lp'_l}$ are assigned to all the vertices *except* roots. Plugging (4.27) into (4.26), we realize that now the weights $Lp'_l$ are multiplied to only roots except the root with the vertex $j$, from which observation (4.23) follows. We note that a similar result was also obtained in a recent work for the XXZ spin 1/2 chain [135].

# Equations of state in generalized hydrodynamics

Dinh-Long Vu* and Takato Yoshimura*,†

* *Institut de Physique Théorique, CEA Saclay, Gif-Sur-Yvette, 91191, France*
† *Department of Mathematics, King's College London, Strand, London WC2R 2LS, U.K.*

We, for the first time, report a first-principle proof of the equations of state used in the hydrodynamic theory for integrable systems, termed generalized hydrodynamics (GHD). The proof makes full use of the graph theoretic approach to Thermodynamic Bethe ansatz (TBA) that was proposed recently. This approach is purely combinatorial and relies only on common structures shared among Bethe solvable models, suggesting universal applicability of the method. To illustrate the idea of the proof, we focus on relativistic integrable quantum field theories with diagonal scatterings and without bound states such as strings.

## 1 Introduction

Extending the notion of statistical mechanics to describe states that are far from equilibrium has been one of the foremost challenges in theoretical physics. Although a unified *modus operandi* to deal with a genuinely out of equilibrium state is still out of reach, transport in many-body systems can serve as a fertile testbed to study rich and sometimes counter-intuitive physics arising in non-equilibrium states. In particular, transport phenomena in one dimensional quantum systems have drawn a plethora of interest in recent years, due partially to spectacular advances in experiments that can now probe the dynamics of the quantum many-body systems in one dimension in a controlled manner [1, 2, 3]. From the theoretical point of view, transport in one dimension is somewhat special in that most of them are expected to be anomalous (non-diffusive) [4, 5, 6]. There is, however, a class of one dimensional quantum systems that exhibits a variety of transport types: integrable systems. It has been known that not only a seemingly likely case, ballistic transport [7, 8, 9], but other type of transports such as diffusive and super-diffusive transports can in fact occur in integrable systems [10, 11, 12, 13]. In order to provide a coherent understanding in the transport phenomena in integrable systems, a hydrodynamic approach that can account for an excess amount of conserved charges, coined generalized hydrodynamics (GHD), was recently proposed [14, 15]. GHD was originally

capable of describing only the dynamics at the Euler scale (leading contribution of the derivative expansion with respect to the space coordinates), but was later extended to capture the sub-leading (diffusive) effect [16]. GHD is not only able to describe an array of inhomogeneous dynamics [17, 18, 19, 20, 21, 23, 24, 25, 26], but is also amenable to coping with external potentials [28] which allows us to efficiently simulate cold atom gases in a confining potential [29]. Moreover applicability of GHD to classical integrable systems is also numerically confirmed [27]. Remarkably, it can even yield some exact results including exact Drude weights at any temperature [19, 25, 30]. Despite of its far-reaching power to predict complicated dynamics, at the Euler scale, the picture GHD gives is intuitively rather clear: when systems are in local equilibrium, quasi-particles propagate ballistically with the effective velocity $v^{\rm eff}(\theta; x, t)$. Therefore the functional form of the effective velocity, which can be regarded as the equations of state for GHD, determines the dynamics, and was first presented in [14, 15]. We note that a proof shown in [14] that exploited crossing symmetry only, is in fact incomplete as the proof assumed analyticity of some function in TBA, which is not necessarily true for some generalized Gibbs ensembles (GGEs). Thus a full proof of the equations of state is still missing in GHD. So far, the validity of GHD, which is equivalent to that of the effective velocity, has been numerically confirmed for spin chains such as the XXZ spin-$\frac{1}{2}$ chain [17, 18, 19, 20, 24, 26] and the Fermi-Hubbard model [25], and it is believed that GHD correctly captures the long-wavelength dynamics of any Bethe solvable systems. Nonetheless, a down-to-earth proof of $v^{\rm eff}(\theta)$ is still highly-desired to complete the program of GHD, and it is the purpose of this paper to report such a proof for relativistic integrable field theories with diagonal scatterings of one or more particle species.

Our strategy is essentially depending on form factor expansions by means of the LeClair-Mussardo formula [31]. The formula allows us to represent the expectation value of a local operator as an infinite series. This series is universal in the sense that the expectation values of two operators differ only in their connected form factors. The problem of evaluating the equations of state boils down to a direct comparison between the connected form factors of the charge and that of the current. Such comparison can be carried out by a well-known relation [32] between the connected form factors and the symmetric ones. Although this relation in its analytic form can be used to verify the current-average hypothesis for a few particles, which was presented in [14], it quickly becomes intractable. In order to provide a proof at full generality, we employ an equivalent formulation of graph expansion. The main idea is to apply the matrix-tree theorem to write Gaudin-like determinants and their minors as sums over trees. The latter are easy to control due to their simple combinatorial structure. Similar technique has been used in [33, 34, 35] and recently in [36, 37] to evaluate other observables such as partition function, correlation function and g-function.

The structure of the paper is the following: In section 2 we quickly summarize GHD and its equations of state. The proof for the current average is covered in section 3, which consists of four subsections. In 3.1 we present basic facts about form factors, in particular

the relation between connected and symmetric ones. In 3.2 we provide basic tools in graph theory. The proof for a theory with a single type of particle is completed in 3.3 and is extended in 3.4 to a theory with more than one type of particles. Section 4 closes our paper with perspectives.

Throughout this article, we shall focus on (1+1)-D relativistic integrable field theories with no bound states.

# 2 GHD and current average

As emphasized in the introduction, our motivation to obtain an explicit expression of the current average comes from GHD. Here we briefly recall how the equation of states in GHD is expressed in terms of quasi-particle basis.

GHD is a framework to study the dynamics of integrable systems at the Euler scale [14, 15][1]. At such scale, generically, many-body systems are expected to be in a state where *local entropy maximization* is realized. In such a state, physics is dominated by macroscopic processes protected by conserved charges, and the state potentially carry a current. In practice, this scale can be accessed by taking a scaling limit of infinitely many degrees of freedom (i.e. the ratio between a typical microscopic scale $l_{\rm mic}$, say the inter-particle length, and a typical macroscopic scale $l_{\rm mac}$ becomes zero: $\epsilon = l_{\rm mic}/l_{\rm mac} \to 0$) while scaling the space-time simultaneously $(x,t) \to (\epsilon^{-1}x, \epsilon^{-1}t)$, which amounts to focusing on physics occurring at an emergent large scale called the *fluid cell*. Note that depending on the exponent $\alpha$ of the scaling of $x$, $\epsilon^{-\alpha}x$, a different scaling limit can be obtained (e.g. diffusive scaling for $\alpha = 1/2$ and super diffusive scaling for $1/2 < \alpha < 1$). The powerful assumption of local entropy maximization then provides us an efficient way to evaluate correlation functions at the Euler scale [38]. In particular, the expectation value of a given local operator $\mathcal{O}$ is computed by $\langle \mathcal{O}(x,t)\rangle_{\rm Eul} = {\rm Tr}(\rho(x,t)\mathcal{O})$ with $\rho(x,t) = \exp(-\sum_i \beta_i(x,t)Q_i)/Z(x,t)$, where $Q_i = \int {\rm d}x\, q_i(x,0)$ are the conserved charges. This suggests that, at the Euler scale, in order to solve the macroscopic continuity equations $\partial_t\langle q_i(x,t)\rangle_{\rm Eul} + \langle j_i(x,t)\rangle_{\rm Eul} = 0$, one only has to know the equilibrium form of the averages of densities $\langle q_i\rangle_{\vec\beta}$ and currents $\langle j_i\rangle_{\vec\beta}$ as functions of Lagrange multipliers $\vec\beta$: the Euler scale averages are then simply $\langle q_i(x,t)\rangle_{\rm Eul} = \langle q_i\rangle_{\vec\beta(x,t)}$ and $\langle j_i(x,t)\rangle_{\rm Eul} = \langle j_i\rangle_{\vec\beta(x,t)}$.

In integrable systems, one-point functions in any generalized Gibbs ensemble (GGE) are conveniently represented in the quasi-particle basis. For instance, the density average of a conserved charge $Q_i$ reads [39]

$$\langle q_i\rangle = \sum_a \int {\rm d}\theta\, \rho_{{\rm p},a}(\theta) h_{i,a}(\theta), \tag{1}$$

where $\theta$ is a quasi-momentum that parametrizes quasi-particles, and $a$ specifies each particle species. Here, $h_{i,a}(\theta)$ is the one-particle eigenvalue of $Q_i$: $Q_i|\theta\rangle_a = h_{i,a}(\theta)|\theta\rangle_a$,

[1] See [16] for the recent extension of GHD to account for diffusive corrections to GHD.

and $\rho_{\mathrm{p},a}(\theta)$ is the density of particle [40] that can be computed within thermodynamic Bethe ansatz (TBA). Now, we need to know how $\langle j_i \rangle$ looks like in order to solve the macroscopic continuity equations. In [14, 15], the exact expression of $\langle j_i \rangle$ was proposed that

$$\langle j_i \rangle = \sum_a \int \mathrm{d}\theta \, \rho_{\mathrm{p},a}(\theta) v_a^{\mathrm{eff}}(\theta) h_{i,a}(\theta) \tag{2}$$

where $v_a^{\mathrm{eff}}$ is the velocity of excitation over an equilibrium state. It satisfies

$$v_a^{\mathrm{eff}}(\theta) = v_a^{\mathrm{gr}}(\theta) + \sum_b \int \mathrm{d}\theta' \frac{\varphi_{ab}(\theta - \theta') \rho_{\mathrm{p},b}(\theta)}{p_b'(\theta)} (v_b^{\mathrm{eff}}(\theta') - v_a^{\mathrm{eff}}(\theta)), \tag{3}$$

where $v_a^{\mathrm{gr}}(\theta)$ is the group velocity, and $\varphi_{ab}(\theta)$ is the differential scattering kernel that is related to the S-matrix of a given model as $\varphi_{ab}(\theta) = -\mathrm{id} \log S_{ab}(\theta)/\mathrm{d}\theta$. In [14], a proof for relativistic integrable quantum field theories with diagonal scatterings was provided using crossing symmetry. This proof, however, has a flaw in the sense that it implicitly assumes the analyticity of the source term $w(\theta) = \sum_i \beta_i h_i(\theta)$ that drives the Yang-Yang equation (see (19) for the definition), which is not necessarily guaranteed for some GGEs. For instance, in a nonequilibrium steady state generated by gluing two initially disconnected integrable systems at equilibrium, $w(\theta)$ actually has a jump as a function of $\theta$, hence nonanalytic [14]. We stress that our proof does not require the assumption of analyticity of $w(\theta)$, and therefore is applicable to arbitrary (local) GGEs. The current formula (2) has also been extended to the XXZ spin-$\frac{1}{2}$ chain where strings are present without proof but with numerical verifications [15]. The form of $v_a^{\mathrm{eff}}(\theta)$ can be in fact considered as equations of state for GHD. Recall that equations of state are relations that relate the density averages $\langle q_i \rangle$ and the current averages $\langle j_i \rangle$: $\langle j_i \rangle = \mathcal{F}_i(\{\langle q_k \rangle\})$. Since it is precisely what $v_a^{\mathrm{eff}}(\theta)$ is doing, making (2) different from (1) by its very appearance in (2), the functional form of the effective velocity determines the relation between the density and current averages. In the next section, we shall present the first-principle proof of (2). We note that the main idea of our proof, which is the form factor expansion, is same as the one presented in the appendix in [14]. The crucial difference is that, in our proof, we prove a statement (see (24) below) that is equivalent to the current formula (2) for any number of particles, while in [14], only the cases of a few numbers of particles were worked out. This generalization is made possible by making full use of the powerful techniques of graph theory in the same spirit as in [36]. This proof should serve as a first satisfactory proof of (2), but we expect that there is a yet another way of proving it, which is not needing any explicit use of relativistic / gallilean invariance.

Before embarking on the proof, let us conclude this section by introducing the dynamical equation of GHD. It immediately follows by plugging (1) and (2) into the macroscopic continuity equations. Using the completeness of the space of $Q_i$, it reads

$$\partial_t \rho_{\mathrm{p},a}(\theta) + \partial_x (v_a^{\mathrm{eff}}(\theta) \rho_{\mathrm{p},a}(\theta)) = 0. \tag{4}$$

This type of equation for the spectral parameter $\theta$ has been found in several different contexts. For instance, the hydrodynamic equation of the hard-rod gas is known to have a same form to (4) with a similar effective velocity as (3) [41]. This is in fact readily derived by a simple kinetic argument presented in [14, 41], providing the underlying physical picture as to why the effective velocity has to be of the form (3). Note that the classical soliton gases of the KdV equation are also governed by an equation similar to (4) on the large scale [42, 43].

# 3 The proof

## 3.1 LeClair-Mussardo formula

Let us suppose the theory we consider has $N$ particle species $a_i$ with masses $m_i$ each of which differ, and it has no internal degrees of freedom. The Hilbert space of a generic (1+1)-D relativistic quantum field theory has natural bases: asymptotic *in* and *out* states $|\theta_1, \cdots, \theta_n\rangle^{in,out}_{a_1,\cdots,a_n}$ parameterized by rapidities $\theta$, which in turn diagonalize all the conserved charges if the model is integrable (to fix the basis, we use the *out* state, i.e. the ordering $\theta_1 < \cdots < \theta_n$). Another salient feature of the model, due to integrability, is that the dynamics is governed by the S-matrices that are factorizable into the product of two-body scattering matrix $S(\theta_i, \theta_j) = S(\theta_i - \theta_j)$. The *form factor* (with $n$ particles) of a local operator $\mathcal{O}$ of the model is then defined by

$$F_{a_1,\cdots,a_n}(\theta_1, \cdots, \theta_n) = \langle \mathrm{vac}|\mathcal{O}(0)|\theta_1, \cdots, \theta_n\rangle_{a_1,\cdots,a_n} \tag{5}$$

which is expected to satisfy the following axioms [44]:
1. Relativistic invariance

$$F_{a_1,\cdots,a_n}(\theta_1 + \eta, \cdots, \theta_n + \eta) = e^{s\eta} F_{a_1,\cdots,a_n}(\theta_1, \cdots, \theta_n) \tag{6}$$

where $s$ is the spin of the operator $\mathcal{O}$.
2. Watson's equations

$$\begin{aligned} F_{a_1,\cdots,a_k,a_{k+1},\cdots,a_n}(\theta_1, \cdots, \theta_k, \theta_{k+1}, \cdots, \theta_n) = S_{a_k,a_{k+1}}(\theta_k - \theta_{k+1}) \\ \times F_{a_1,\cdots,a_{k+1},a_k,\cdots,a_n}(\theta_1, \cdots, \theta_{k+1}, \theta_k, \cdots, \theta_n) \end{aligned} \tag{7}$$

$$F_{a_1,\cdots,a_n}(\theta_1 + 2\pi\mathrm{i}, \cdots, \theta_n) = F_{a_2,\cdots,a_n,a_1}(\theta_2, \cdots, \theta_n, \theta_1) \tag{8}$$

3. Kinematic poles

$$-\mathrm{i}\operatorname*{Res}_{\theta\to\theta'} F_{a,b,a_1,\cdots,a_n}(\theta + \pi\mathrm{i}, \theta', \theta_1, \cdots, \theta_n) = \left(1 - \delta_{ab}\prod_{k=1}^{n} S_{a,a_k}(\theta - \theta_k)\right) F_{a_1,\cdots,a_n}(\theta_1, \cdots, \theta_n). \tag{9}$$

Note that if our model has bound states, the case which we do not consider here, there are additional *dynamical* poles on the imaginary axis within the strip $0 < \mathrm{Im}\,\theta_{ij} < \pi$. We further assume that form factors are meromorphic functions except poles that are dictated by the axioms mentioned. In what follows, for brevity, we shall focus on the case with one particle species.

The form factors generally serve as building blocks of more complicated matrix elements. Of particular interest for our purpose is the diagonal matrix element $\langle \overleftarrow{\theta} | \mathcal{O}(0) | \overrightarrow{\theta} \rangle$, where we introduced the shortened notation $| \overrightarrow{\theta} \rangle = |\theta_1, \cdots, \theta_n\rangle$ (and $\langle \overleftarrow{\theta} | = \langle \theta_1, \cdots, \theta_n|$). By use of the crossing relation, all form factors can be expressed in terms of the following form factor [32]

$$\begin{aligned} &F_{2n}(\theta_1 + \pi\mathrm{i} + \delta_1, \theta_2 + \pi\mathrm{i} + \delta_2, \cdots, \theta_n + \pi\mathrm{i} + \delta_n, \theta_n, \cdots, \theta_2, \theta_1) \\ &\quad = \prod_{i=1}^{n} \frac{1}{\delta_i} \sum_{i_1=1}^{n} \sum_{i_2=1}^{n} \cdots \sum_{i_n=1}^{n} f_{i_1,i_2,\cdots,i_n}(\theta_1, \cdots, \theta_n)\delta_{i_1}\delta_{i_2}\cdots\delta_{i_n} + \cdots, \end{aligned} \tag{10}$$

where $f_{i_1,i_2,\cdots,i_n}(\theta_1, \cdots, \theta_n)$ is completely symmetric with respect to a rearrangement of indices, and "$\cdots$" refers to all the terms that vanish upon taking $\{\delta_i\} \to 0$ in any order. This form factor, in fact, is not well-defined due to the presence of kinematic singularities, i.e. its value depends on the order of limits $\{\delta_i\} \to 0$. There are two common ways to eliminate such singularities: one is to keep only finite terms by getting rid of all the terms that are divergent when taking $\{\delta_i\} \to 0$ in (10), yielding the *connected* form factor [31]

$$F^{\mathrm{c}}_{2n}(\theta_1, \cdots, \theta_n) = \mathrm{FP} \lim_{\{\delta_k\}\to 0} F_{2n}(\theta_1 + \pi\mathrm{i} + \delta_1, \cdots, \theta_n + \pi\mathrm{i} + \delta_n, \theta_n, \cdots, \theta_1). \tag{11}$$

Another one is to take a uniform limit such that $\delta_i = \delta \to 0$ for all $i$ that gives rise to the *symmetric* form factor [32]

$$F^{\mathrm{s}}_{2n}(\theta_1, \cdots, \theta_n) = \lim_{\{\delta_k\}=\delta\to 0} F_{2n}(\theta_1 + \pi\mathrm{i} + \delta, \cdots, \theta_n + \pi\mathrm{i} + \delta, \theta_n, \cdots, \theta_1). \tag{12}$$

These two form factors play essential roles in our proof later, and they are in fact related by the following relation

$$F^{\mathrm{s}}_{2n}(\theta_1, \cdots, \theta_n) = \sum_{\substack{\alpha\subset\{1,\cdots,n\} \\ \alpha\neq\varnothing}} \mathcal{L}(\alpha|\alpha) F^{\mathrm{c}}_{2|\alpha|}(\{\theta_i\}_{i\in\alpha}) \tag{13}$$

where $|\alpha|$ denotes the cardinal of the subset $\alpha$ and $\mathcal{L}(\alpha|\alpha)$ is the principal minor obtained by deleting the $\alpha$ rows and columns of the following matrix

$$L(\theta_1, \cdots, \theta_n)_{jk} = \delta_{jk} \sum_{l\neq j} \varphi_{j,l} - (1 - \delta_{jk})\varphi_{j,k}, \tag{14}$$

where $\varphi_{i,j} = \varphi(\theta_i - \theta_j)$. Relation (13) can be obtained by considering two equivalent ways of writing the finite-volume diagonal matrix element $\langle \overleftarrow{\theta} | \mathcal{O}(0) | \overrightarrow{\theta} \rangle_V$ [32]

$$\sum_{\substack{\alpha \subset \{1,\cdots,n\} \\ \alpha \neq \varnothing}} F^{\mathrm{s}}_{2|\alpha|}(\{\theta_i\}_{i\in\alpha}) \mathcal{G}(\{\theta_i\}_{i\in\bar{\alpha}}) = \sum_{\substack{\alpha \subset \{1,\cdots,n\} \\ \alpha \neq \varnothing}} F^{\mathrm{c}}_{2|\alpha|}(\{\theta_i\}_{i\in\alpha}) \mathcal{G}(\alpha|\alpha), \tag{15}$$

where $\bar{\alpha}$ denotes the complementary of $\alpha$. On the left hand side, $\mathcal{G}(\theta_1, \cdots, \theta_n)$ is the determinant of the $n \times n$ Gaudin matrix

$$G(\theta_1, \cdots, \theta_n)_{jk} = \delta_{jk} \Big( V p'(\theta_j) + \sum_{l \neq j} \varphi_{j,l} \Big) - (1 - \delta_{jk}) \varphi_{j,k}, \tag{16}$$

where $p'(\theta)$ is the derivative of the momentum $p$ with respect to the rapidity $\theta$. On the right hand side, $\mathcal{G}(\alpha|\alpha)$ is the principal minor of $G$ obtained by deleting its $\alpha$ rows and columns, and $V$ is the system size. Since the equality (15) is algebraic, it must hold for whatever value of $V$. Thus let us take a limit $V \to 0$. By writing the matrix $G(\{\theta_i\}_{i\in\bar{\alpha}})$ as the sum of a matrix of the type (14) and a diagonal matrix, we can write its determinent as a sum over partitions of $\bar{\alpha}$

$$\mathcal{G}(\{\theta_i\}_{i\in\bar{\alpha}}) = \sum_{\substack{I \subset \bar{\alpha} \\ I \neq \varnothing}} \mathcal{L}(I|I) \prod_{i \in I} V p'(\theta_i). \tag{17}$$

Since $I$ is always a non-empty set, (17) necessarily vanishes when $V \to 0$ except when $\bar{\alpha} = \varnothing$, i.e. $\alpha = \{1, \cdots, n\}$. Hence the LHS of (15) becomes that of (13) under the limit. Together with an immediate observation that $\mathcal{G}(\alpha|\alpha) \to \mathcal{L}(\alpha|\alpha)$ with $V \to 0$, the relation (13) is established.

Having these in mind, we are now in a position to introduce the LeClair-Mussardo formula. The formula is a variant of spectral decomposition for the thermal (GGE) average of a local operator. It reads [31]

$$\langle \mathcal{O} \rangle = \frac{1}{Z} \mathrm{Tr}\, (e^{-\sum_i \beta_i Q_i} \mathcal{O}) = \sum_{l=0}^{\infty} \Big( \prod_{k=1}^{l} \int \frac{\mathrm{d}\theta_k}{2\pi} n(\theta_k) \Big) F^{\mathrm{c}}_{2l}(\mathcal{O}; \theta_1, \cdots, \theta_k) \tag{18}$$

where $Z$ is the partition function, and the filling function $n(\theta) = 1/(1 + e^{\varepsilon(\theta)})$ is given by the pseudo-energy $\varepsilon(\theta)$ that satisfies the Yang-Yang equation

$$\varepsilon(\theta) = \sum_i \beta_i h_i(\theta) - \int \frac{\mathrm{d}\theta'}{2\pi} \varphi(\theta - \theta') \log(1 + e^{\varepsilon(\theta')}). \tag{19}$$

This is a remarkable simplification in computing the GGE average of a local operator, but it still requires us to compute the connected form factor, which is always a formidable

task. Further, even if one manages to do so, carrying out the resummation is, in most cases, not feasible. Therefore, in practice, the formula is used with truncating after some terms; if excitation is small enough, this provides a fairly good approximation of the average.

Being said so, there are some known cases where one can evaluate the formula explicitly. One of such examples is the density of a conserved charge $Q = \int \mathrm{d}x\, q(x,0)$: the connected form factor of which is given by [39]

$$F^{\mathrm{c}}_{2n}(q;\theta_1,\cdots,\theta_n) = h(\theta_1)\varphi_{1,2}\cdots\varphi_{n-1,n}p'(\theta_n) + \text{perm}, \tag{20}$$

where perm. is understood as permutations with respect to the integer set $\{1,\cdots,n\}$. Putting this into (18), we obtain an alternative expression of (1) [39]

$$\langle q\rangle = \int \frac{\mathrm{d}p(\theta)}{2\pi} n(\theta)h^{\mathrm{dr}}(\theta), \tag{21}$$

where the dressing operation is defined for any function $f(\theta)$ as

$$f^{\mathrm{dr}}(\theta) = f(\theta) + \int \frac{\mathrm{d}\theta'}{2\pi}\varphi(\theta-\theta')n(\theta')f^{\mathrm{dr}}(\theta'). \tag{22}$$

In the main proof, we will observe that, in fact, the same structure holds for the current operator $j$ as well. Recalling (2), we can also recast it into the similar form and expand as

$$\begin{aligned}\langle j\rangle &= \int \frac{\mathrm{d}E(\theta)}{2\pi} n(\theta)h^{\mathrm{dr}}(\theta) \\ &= \sum_{l=0}^{\infty}\Bigg(\prod_{k=1}^{l}\int\frac{\mathrm{d}\theta}{2\pi}n(\theta_k)\Bigg)h(\theta_1)\varphi_{1,2}\cdots\varphi_{k-1,k}E'(\theta_k),\end{aligned} \tag{23}$$

where $E'(\theta)$ denotes the derivative of the energy $E$ with respect to the rapidity $\theta$. This suggests that if the connected form factor of $j$ takes the following form, then (2) follows:

$$F^{\mathrm{c}}_{2n}(j;\theta_1,\cdots,\theta_n) = h(\theta_1)\varphi_{1,2}\cdots\varphi_{n-1,n}E'(\theta_n) + \text{perm}, \tag{24}$$

which is the actual statement we are going to prove in order to establish (2).

## 3.2 Graphical representation

The relation (13) between the symmetric and connected form factors can be understood graphically. The matrix $L$ whose minors appear in this relation is a Laplacian matrix

$$L_{jk} = \delta_{jk}\sum_{l\neq j}\varphi_{j,l} - (1-\delta_{jk})\varphi_{j,k}. \tag{25}$$

It is the discretized Laplacian operator $\Delta$ on a graph in which a weight $\varphi_{j,k}$ is assigned to the edge connecting $j$ and $k$. Although $L$ has a vanishing determinant, as the elements on each row sum up to zero, its principal minors can be expressed as a sum over trees. This is the virtue of the matrix-tree theorem [45], also known as Kirchhoff theorem.[2]

**Definition 3.1** (Trees and forests)**.** *A tree is a connected graph without cycles. A forest is a set of trees.*

In this paper we are referring to undirected graphs which means there is no direction on the edges. The reason behind is the symmetric property of the scattering differential: $\varphi_{i,j} = \varphi_{j,i}$. In the non-symmetric case, the definition of (directed) trees should be modified [36].

**Theorem 3.1** (Weighted matrix-tree theorem)**.** *Let $\alpha$ be a subset of vertices $\{1, 2, \cdots, n\}$. Then we have*

$$\mathcal{L}(\alpha|\alpha) = \sum_{F\in\mathcal{F}_\alpha} \prod_{e\in F} \varphi_e, \tag{26}$$

*where the summation is performed over all forests of $n$ vertices each tree of which contains exactly one vertex from $\alpha$. The product runs over all edges of the forests.*

This is known as the all-minor version of the matrix-tree theorem. A particular case is given by considering principal minors of rank $n-1$ i.e. by taking $\alpha$ to be one-element subsets. The forests would then become trees.

Let us illustrate the theorem in the case of three particles, where (25) is given by

$$L = \begin{pmatrix} \varphi_{1,2}+\varphi_{1,3} & -\varphi_{1,2} & -\varphi_{1,3} \\ -\varphi_{2,1} & \varphi_{2,1}+\varphi_{2,3} & -\varphi_{2,3} \\ -\varphi_{3,1} & -\varphi_{3,2} & \varphi_{3,1}+\varphi_{3,2} \end{pmatrix}. \tag{27}$$

All the principal minors of rank 2 are equal: $\mathcal{L}(1|1) = \mathcal{L}(2|2) = \mathcal{L}(3|3) = \varphi_{2,1}\varphi_{3,1} + \varphi_{2,1}\varphi_{3,2} + \varphi_{2,3}\varphi_{3,1}$. These terms are exactly the three trees spanning three vertices, see Fig.1. Note that we are referring to **labelled** trees. In particular, the trees in Fig.1 are considered as being distinguished, despite their similar combinatorial structure. The principal minors of rank 1 are written as forests with two trees. For example, when $\alpha = \{2, 3\}$ we have $\mathcal{L}(\alpha|\alpha) = \varphi_{1,2} + \varphi_{1,3}$, as in Fig.2. The matrix-tree theorem provides a nice interpretation of the relation (13) between symmetric and connected form factors. For each subset $\alpha$ of $\{1, 2, ..., n\}$ we decorate the connected form factor $F^{\rm c}_{2|\alpha|}(\{\theta_i\}_{i\in\alpha})$ by trees growing out of the elements of $\alpha$. The decorations must guarantee that all $n$ vertices are covered.

[2]Matrix of the type (25) appeared in the work of Maxwell, one can therefore view the weights $\varphi_{jk}$ as the electric currents in a circuit.

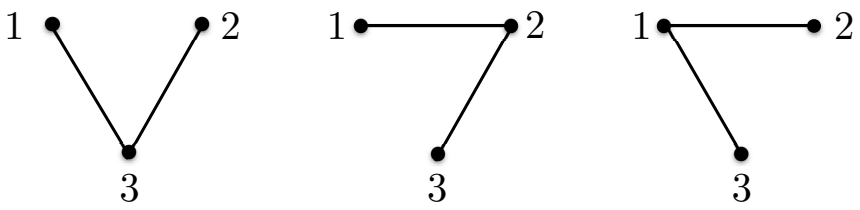


Figure 1: Trees associated with a minor of rank 2.


Figure 2: Forests associated with a minor $\mathcal{L}(\{2,3\}|\{2,3\})$.

### 3.3 Main proof: one type of particle

Here we present a graph theoretic proof for (24). Our proof consists of three steps:

- Obtain the symmetric form factor of the charge $F^{\rm s}_{2n}(q;\theta_1,\cdots,\theta_n)$ from the connected one (20) and the relation (13).
- Compute the symmetric form factor of the current $F^{\rm s}_{2n}(j;\theta_1,\cdots,\theta_n)$ from that of the charge, by using the continuity equation.
- Find the connected form factor of the curent from the symmetric one, by going from the left hand side to the right hand side of equation (13).

The first and the last step are done with help of the matrix-tree theorem 3.1.

In the first step, we represent the connected form factor of the charge

$$F^{\rm c}_{2n}(q;\theta_1,\cdots,\theta_n) = h(\theta_1)\varphi_{1,2}\cdots\varphi_{n-1,n}p'(\theta_n) + \text{perm}, \tag{28}$$

as $n!$ spines of length $n$ with the charge $h$ on one end and the momentum derivative $p'$ at the other end. Spines of length 1 with coinciding ends are allowed.

The corresponding symmetric form factor is obtained by decorating the spines with the trees, see Fig.3. Because the trees have different labelings and the spines come from different permutations, each term in the symmetric form factor is a (labelled) tree with two marked points, no tree appears more than once. Vice versa, each tree with two marked points can be decomposed to a spine and a forest. Indeed, the connectedness guarantees

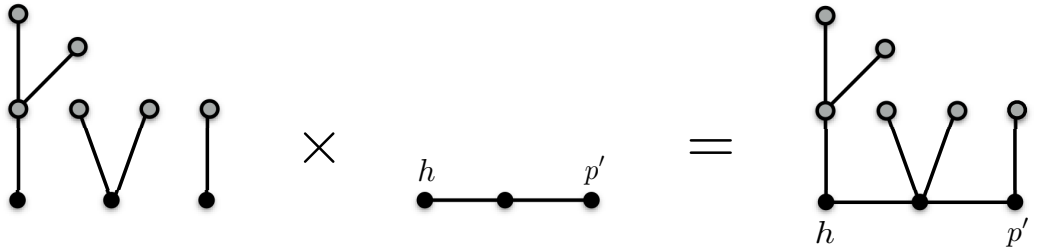


Figure 3: Pictorial representation of one of terms in the RHS of (13). Each term (forest) of $\mathcal{L}(\alpha|\alpha)$ and each term in $F^{\rm c}_{2|\alpha|}(\{\theta_i\}_{i\in\alpha})$ form a spanning tree by merging together at vertices $\alpha$ represented by black dots.

the existence of a path between the two marked points. Moreover, the uniqueness of this path is ensured by the non-existence of cycles. We conclude that the symmetric form factor of the charge is given by the sum over all the trees of $n$ vertices, with the weights $h$ and $p'$ inserted at two arbitrary vertices. This sum factorizes into the sum over the weights and the sum over the unmarked trees:

$$F^{\rm s}_{2n}(q;\theta_1,\cdots,\theta_n)=\sum_{j=1}^{n}h(\theta_j)\sum_{k=1}^{n}p'(\theta_k)\sum_{T\in\mathcal{T}}\prod_{e\in T}\varphi_e, \tag{29}$$

Here, $\mathcal{T}$ denotes the set of the trees of $n$ vertices. The sum over these trees are exactly given by the principal minor of rank $n-1$ of the matrix (25). For instance, in the case of three particles:

$$F^{\rm s}_{6}(q;\theta_1,\theta_2,\theta_3)=(h_1+h_2+h_3)(p'_1+p'_2+p'_3)(\varphi_{2,1}\varphi_{3,1}+\varphi_{2,1}\varphi_{3,2}+\varphi_{2,3}\varphi_{3,1})$$

We now turn to the second step. In order to relate (29) to the symmetric form factor of the current $F^{\rm s}_{2n}(j;\theta_1,\cdots,\theta_n)$, where $j$ satisfies the continuity equation $\partial_t q+\partial_x j=0$, we note that there is a relation between $F^{\rm s}_{2n}(q;\theta_1,\cdots,\theta_n)$ and $F^{\rm s}_{2n}(j;\theta_1,\cdots,\theta_n)$ which is a simple consequence of the continuity equation:

$$F^{\rm s}_{2n}(j;\theta_1,\cdots,\theta_n)=\frac{\sum_k E'(\theta_k)}{\sum_k p'(\theta_k)}F^{\rm s}_{2n}(q;\theta_1,\cdots,\theta_n), \tag{30}$$

where we recall $E(\theta)=m\cosh\theta$ and $p(\theta)=m\sinh\theta$. To see this, we first observe

$$\langle{\rm vac}|j(x,t)|\overrightarrow{\theta},\overleftarrow{\theta'}\rangle=e^{-{\rm i}m\sum_{k=1}^{n}\left[(\cosh\theta_k+\cosh\theta'_k)t-(\sinh\theta_k+\sinh\theta'_k)x\right]}\langle{\rm vac}|j(0,0)|\overrightarrow{\theta},\overleftarrow{\theta'}\rangle \tag{31}$$

and thus,

$$\langle{\rm vac}|\partial_x j(x,t)|\overrightarrow{\theta},\overleftarrow{\theta'}\rangle={\rm i}m\sum_{k=1}^{n}(\sinh\theta_k+\sinh\theta'_k)\langle{\rm vac}|j(x,t)|\overrightarrow{\theta},\overleftarrow{\theta'}\rangle. \tag{32}$$

Using this, it then follows that

$$\begin{aligned}
F^{\rm s}_{2n}(j;\theta_1,\cdots,\theta_n) &= \lim_{\delta\to 0}\langle {\rm vac}|j(x,t)|\overrightarrow{\theta},\overleftarrow{\theta'}\rangle \\
&= \lim_{\delta\to 0}\frac{-i}{m\sum_k(\sinh\theta_k+\sinh\theta'_k)}\langle {\rm vac}|\partial_x j(x,t)|\overrightarrow{\theta},\overleftarrow{\theta'}\rangle \\
&= \lim_{\delta\to 0}\frac{i}{m\sum_k(\sinh\theta_k+\sinh\theta'_k)}\langle {\rm vac}|\partial_t q(x,t)|\overrightarrow{\theta},\overleftarrow{\theta'}\rangle \\
&= \lim_{\delta\to 0}\frac{\sum_k(\cosh\theta_k+\cosh\theta'_k)}{\sum_k(\sinh\theta_k+\sinh\theta'_k)}\langle {\rm vac}|q(x,t)|\overrightarrow{\theta},\overleftarrow{\theta'}\rangle \\
&= \frac{\sum_k E'(\theta_k)}{\sum_k p'(\theta_k)}F^{\rm s}_{2n}(q;\theta_1,\cdots,\theta_n),
\end{aligned} \tag{33}$$

where we used the continuity equation when passing from the second line to the third line, and noted

$$\langle {\rm vac}|\partial_t q(x,t)|\overrightarrow{\theta},\overleftarrow{\theta'}\rangle = -{\rm i}m\sum_{k=1}^{n}(\cosh\theta_k+\cosh\theta'_k)\langle {\rm vac}|q(x,t)|\overrightarrow{\theta},\overleftarrow{\theta'}\rangle, \tag{34}$$

when moving from the third to the fourth line. Here, $\delta$ is defined as before in order to take the uniform limit $\theta'_j=\theta_j+\pi{\rm i}+\delta$.

Now, applying this relation to (29), it immediately follows that

$$F^{\rm s}_{2n}(j;\theta_1,\cdots,\theta_n)=\sum_{j=1}h(\theta_j)\sum_{k=1}E'(\theta_k)\sum_{T\in\mathcal{T}}\prod_{e\in T}\varphi_e, \tag{35}$$

which is nothing but the summation over all the trees of $n$ vertices, this time with $h$ and $E'$ inserted at two arbitrary points. By applying the same logic as in the first step, we can write this as a sum over spines and decorating trees

$$F^{\rm s}_{2n}(j;\theta_1,\cdots,\theta_n)=\sum_{\substack{\alpha\subset\{1,\cdots,n\}\\ \alpha\neq\varnothing}}\mathcal{L}(\alpha|\alpha)F^{\rm c}_{2|\alpha|}(j;\{\theta_i\}_{i\in\alpha}), \tag{36}$$

where the spines now have $h$ and $E'$ on two ends

$$F^{\rm c}_{2n}(j;\theta_1,\cdots,\theta_n)=h(\theta_1)\varphi_{1,2}\cdots\varphi_{n-1,n}E'(\theta_n)+{\rm perm.} \tag{37}$$

This is the desired formula for the current connected form factor. □

Our proof makes use of the matrix-tree theorem to express all the determinants and minors in the relation (13) between connected and symmetric form factors as sums over trees. We believe this is the natural language to understand this relation, as shown by the simplicity of the proof. One can of course argue that, because the matrix-tree theorem is

two-fold, quantities which are expressed in terms of trees can be written as determinants of some matrices as well. As mentioned above, this is indeed true for the symmetric form factor of the charge or the current. For instance, (29) can be equivalently written as

$$F^{\rm s}_{2n}(q;\theta_1,\cdots,\theta_n)=\mathcal{L}(1|1)\sum_{j=1}^{n}h(\theta_j)\sum_{k=1}^{n}p'(\theta_k) \tag{38}$$

where $\mathcal{L}(1|1)$ is the principal minor, obtained by deleting the first row and column of the $n\times n$ matrix (25). Interested readers are invited to derive (38), starting from (20) and (13) without using the matrix-tree theorem.

## 3.4 Main proof: more than one type of particle

Our method can be extended to a purely elastic scattering theory with $N$ types of particles $a=1,2,..,N$ of masses $m_a$. We illustrate it in the case of $T_2$ model [46, 47].

The underlying conformal field theory of this model is the minimal model $\mathcal{M}_{2,7}$ with central charge $c=-68/7$. It involves two nontrivial primary fields denoted by $\Phi_{1,2}$ and $\Phi_{1,3}$ with conformal dimensions

$$h_{1,2}=\bar{h}_{1,2}=-\frac{2}{7};\quad h_{1,3}=\bar{h}_{1,3}=-\frac{3}{7}.$$

The theory can be quantized on a cylinder of circumference $V$ with the corresponding conformal Hamiltonian

$$H_0=\frac{2\pi}{V}\big(L_0+\bar{L}_0-\frac{c}{12}\big).$$

The $T_2$ model is the perturbation of this theory by a positive parameter along the $\Phi_{1,3}$ direction

$$H=H_0+\lambda\int_0^V {\rm d}x\,\Phi_{1,3}(0,x), \tag{39}$$

More generally, $T_n$ models are perturbations of minimal models $\mathcal{M}_{2,2n+3}$ by the same operator. They can be realized as particular reductions of the sine-Gordon model [47].

The $T_2$ model is a massive integrable quantum field theory with the mass spectrum

$$\lambda=\kappa m_1^{2-2h_{1,3}},\quad m_2=2m_1\cos(\pi/5),$$

where $\kappa$ is a dimensionless constant. Its scattering information is encoded in the two-body scattering matrices

$$S_{11}(\theta)=\left\{\frac{2}{5}\right\}_\theta,\quad S_{12}(\theta)=\left\{\frac{1}{5}\right\}_\theta\left\{\frac{3}{5}\right\}_\theta,\quad S_{22}(\theta)=\left\{\frac{2}{5}\right\}_\theta^2\left\{\frac{4}{5}\right\}_\theta. \tag{40}$$

where

$$\{x\}_\theta \equiv \frac{\sinh\theta + i\sin\pi x}{\sinh\theta - i\sin\pi x} \quad .$$

Let us denote the two types of particle by $a = 1, 2$ with the corresponding energy and momentum $E_a$ and $p_a$. The thermodynamics of the model is driven by the TBA equations:

$$\epsilon_a(\theta) = \beta E_a(\theta) - \sum_b \int \frac{d\theta'}{2\pi} \varphi_{ab}(\theta - \theta') \log[1 + e^{\epsilon_b(\theta')}]$$

where $\varphi_{ab}$ is the logarithmic derivative of the scattering matrix: $\varphi_{ab}(\theta) = -i\partial_\theta \log S_{ab}(\theta)$. Unitarity again ensures that $\varphi$ is symmetric on its arguments:

$$S_{ab}(\theta)S_{ba}(-\theta) = 1 \Rightarrow \varphi_{ab}(\theta) = \varphi_{ba}(-\theta) \quad a, b \in \{1, 2\}. \tag{41}$$

The LM series for one point function of a local operator is a direct generalization of (18):

$$\langle \mathcal{O} \rangle = \sum_{l,m=0}^{\infty} \left( \prod_{j=1}^{l} \int \frac{\mathrm{d}\theta_j}{2\pi} n_1(\theta_j) \prod_{k=1}^{m} \int \frac{\mathrm{d}\vartheta_k}{2\pi} n_2(\vartheta_k) \right) F^{\mathrm{c}}_{2l,2m}(\mathcal{O}; \overrightarrow{\theta}, \overrightarrow{\vartheta}). \tag{42}$$

In this expression, $n_1$ and $n_2$ are the filling functions of each type of particle: $n_a = 1/(1 + e^{\epsilon_a})$, $\overrightarrow{\theta}$ and $\overrightarrow{\vartheta}$ denote the two sets of rapidities: $\overrightarrow{\theta} = \{\theta_1, \cdots, \theta_l\}$, $\overrightarrow{\vartheta} = \{\vartheta_1, \cdots, \vartheta_m\}$. The connected form factors are defined in a similar way as before:

$$\begin{aligned} F^{\mathrm{c}}_{2l,2m}(\overrightarrow{\theta}, \overrightarrow{\vartheta}) = \mathrm{FP} \lim_{\{\delta_k\}\to 0} F_{l,m,m,l}(&\theta_1 + \pi\mathrm{i} + \delta_1, \cdots, \theta_l + \pi\mathrm{i} + \delta_l, \\ &\vartheta_1 + \pi\mathrm{i} + \delta_{l+1}, \cdots, \vartheta_m + \pi\mathrm{i} + \delta_{l+m}, \vartheta_m, \cdots, \vartheta_1, \theta_l, \cdots, \theta_1). \end{aligned}$$

The symmetric form factor is obtained by taking the uniform limit: $\delta_k = \delta \to 0$ for all $k$. In particular, the relation between symmetric and connected form factor now becomes

$$F^{\mathrm{s}}_{2l,2m}(\overrightarrow{\theta}, \overrightarrow{\vartheta}) = \sum_{\substack{\alpha\subset\{1,\cdots,l\} \\ \beta\subset\{1,\cdots,m\}}} \mathcal{L}(\alpha, \beta|\beta, \alpha) F^{\mathrm{c}}_{2|\alpha|,2|\beta|}(\overrightarrow{\theta}_\alpha, \overrightarrow{\vartheta}_\beta). \tag{43}$$

where $\mathcal{L}(\alpha, \beta|\beta, \alpha)$ is the principal minor obtained by deleting the $\alpha$ rows and columns of the first diagonal block and $\beta$ rows and columns of the second diagonal block of the

following matrix

$$L(\overrightarrow{\theta}, \overrightarrow{\vartheta}) = \begin{pmatrix} A & B \\ C & D \end{pmatrix} \tag{44}$$

$$A_{ij} = \delta_{ij}\big[\sum_{k\neq i}^{l} \varphi_{11}(\theta_i - \theta_k) + \sum_{k=1}^{m} \varphi_{12}(\theta_i - \vartheta_k)\big] - (1-\delta_{ij})\varphi_{11}(\theta_i - \theta_j), \quad 1 \le i,j \le l$$

$$B_{ij} = -\varphi_{12}(\theta_i - \vartheta_j) \quad 1 \le i \le l, 1 \le j \le m$$

$$C_{ij} = -\varphi_{21}(\vartheta_i - \theta_j) \quad 1 \le i \le m, 1 \le j \le l$$

$$D_{ij} = \delta_{ij}\big[\sum_{k=1}^{l} \varphi_{21}(\vartheta_i - \theta_k) + \sum_{k\neq i}^{m} \varphi_{22}(\vartheta_i - \vartheta_k)\big] - (1-\delta_{ij})\varphi_{22}(\vartheta_i - \vartheta_j), \quad 1 \le i,j \le m$$

Despite its block structure, this matrix is still a Laplacian matrix as each of its rows sums up to zero. The matrix-tree theorem 3.1 is still valid, allowing us to write the principal minors $\mathcal{L}(\alpha, \beta|\beta, \alpha)$ as a sum over $(|\alpha| + |\beta|)$-forests of $l + m$ vertices. Each vertex now carries an index $a \in \{1, 2\}$ to indicate the type of particle it stands for. A branch connecting a particle of type $a$ and rapidity $\theta$ and another of type $b$ and rapidity $\vartheta$ carries a weight of $\varphi_{ab}(\theta - \vartheta)$. The symmetry of the scattering differential (41) indicates that the graphs are undirected.

We now turn our attention to the case of a conserved charge $Q$ which acts diagonally on the basis of multiparticle states:

$$\langle \overleftarrow{\vartheta}, \overleftarrow{\theta}\,|Q|\,\overrightarrow{\theta}, \overrightarrow{\vartheta}\rangle = \frac{1}{L}[h_1(\theta_1) + \cdots + h_1(\theta_l) + h_2(\vartheta_1) + \cdots + h_2(\vartheta_m)]\langle \overleftarrow{\vartheta}, \overleftarrow{\theta}\,|\,\overrightarrow{\theta}, \overrightarrow{\vartheta}\rangle. \tag{45}$$

The connected form factor for a state with $l$ particles of the first type and $m$ particles of the second type is given by the sum over $(l + m)!$ ways of distributing the particles on a spine with the charge $h$ on one end and $p'$ on the other end. Compared with the previous result (20), we now have to keep track of the particle type $a$, the scattering differential $\varphi_{ab}$ and the weight $h_a$ and $p'_a$ in each permutation. Explicitly we have:

$$\begin{aligned} &F^{\mathrm{c}}_{2l,2m}(q; \theta_1, \cdots, \theta_l, \vartheta_1, \cdots, \vartheta_m) \\ &= \sum_{\sigma \in S_{l+m}} p'_{\sigma_1}(\eta_{\sigma_1})\varphi_{\sigma_1\sigma_2}(\eta_{\sigma_1} - \eta_{\sigma_2}).....\varphi_{\sigma_{l+m-1}\sigma_{l+m}}(\eta_{\sigma_{l+m-1}} - \eta_{\sigma_{l+m}})h_{\sigma_{l+m}}(\eta_{\sigma_{l+m}}) \end{aligned} \tag{46}$$

where the notations are to be understood as follows

$$p_i = \begin{cases} p_1 \\ p_2 \end{cases}, \quad h_i = \begin{cases} h_1 \\ h_2 \end{cases}, \quad \eta_i = \begin{cases} \theta_i & \text{if } 1 \le i \le l \\ \vartheta_{i-l} & \text{if } l < i \le l+m \end{cases},$$

$$\varphi_{ij} = \begin{cases} \varphi_{11} & \text{if } 1 \le i,j \le l \\ \varphi_{12} & \text{if } 1 \le i \le l, l < j \le l+m \\ \varphi_{21} & \text{if } l < i \le l+m, 1 \le j \le l \\ \varphi_{22} & \text{if } l < i,j \le l+m \end{cases}.$$

All the arguments of the previous section are still valid, in particular the symmetric form factors for the charge is given by

$$F^{\mathrm{c}}_{2l,2m}(q;\theta_1,...,\theta_l,\vartheta_1,...,\vartheta_m) = \big[\sum_{j=1}^{l} h_1(\theta_j) + \sum_{k=1}^{m} h_2(\vartheta_k)\big]\big[\sum_{j=1}^{l} p_1'(\theta_j) + \sum_{k=1}^{m} p_2'(\vartheta_k)\big] \sum_{T\in\mathcal{T}} \prod_{e\in T} \varphi_e, \tag{47}$$

The last sum runs over all trees of $l+m$ vertices, $l$ of which is of type 1 and $m$ is of type 2. It is given by any principal minors of rank $l+m-1$ of the matrix (44). The connected form factor of the current is given by (46), with $p'$ replaced by $E'$.

# 4 Conclusions

In this article, we provided a graph theoretic proof of the equations of state used in GHD in the case of relativistic integrable quantum field theories without bound states. The proof applies to purely elastic scattering theories with one or multiple types of particles for which the corresponding LeClair-Mussardo formulae are known. Having the proofs for those cases, an obvious question would be if our approach can be applicable for theories where bound states and/or particles with internal degrees of freedom are present, such as the sine-Gordon model. This would be possible once we are able to extend the notion of connected form factor, or equivalently the LeClair-Mussardo formula for such theories. Such extension is still in development [48] and we leave it to future investigation.

We exemplified the graph theoretic idea using relativistic integrable quantum field theories, but it also works for the nonrelativistic case, such as the Lieb-Liniger model, through taking appropriate non-relativistic limits [49]. Extension of our method to spin chains seems to necessitate more investigation as much less is known about connected and symmetric form factors in spin chains [50, 51].

# 5 Acknowledgements

The authors would like to thank Benjamin Doyon and Balázs Pozsgay for useful discussions. D-L.V. thanks Didina Serban and Ivan Kostov for suggesting the graph expansion idea. T.Y. acknowledges the support from Takenaka Scholarship Foundation and the ERC grant NuQFT.

# References

[1] T. Kinoshita, T. Wenger and D. S. Weiss, "A Quantum Newton's Cradle", Nature **440**, 900-903 (2006).

[2] I. Bloch, J. Dalibard and S. Nascimbene, "Quantum simulations with ultracold quantum gases", Nature Physics **8**, 267-276 (2012).

[3] M. Gring, M. Kuhnert, T. Langen, T. Kitagawa, B. Rauer, M. Schreitl, I. Mazets, D. Adu Smith, E. Demler and J. Schmiedmayer, Relaxation and prethermalization in an isolated quantum system. Science **337**, 1318 (2012).

[4] A. Dhar, "Heat Transport in low-dimensional systems ", Adv. Phys. **57**, 457 (2008).

[5] Henk van Beijeren, "Exact results for anomalous transport in one-dimensional Hamiltonian systems", Phys. Rev. Lett. **108**, 180601 (2012).

[6] L. Bertini, A. De Sole, D. Gabrielli, G. Jona-Lasinio and C. Landim, "Macroscopic fluctuation theory", Rev. Mod. Phys. **87**, 593, (2015).

[7] X. Zotos, "Finite Temperature Drude Weight of the One-Dimensional Spin-1/2 Heisenberg Model", Phys. Rev. Lett. **82**, 1764 (1999).

[8] X. Zotos, F. Naef and P. Prelovšek, "Transport and conservation laws", Phys. Rev. B **55**, 11029 (1997).

[9] T. Prosen, "Open XXZ spin chain: Nonequilibrium steady state and strict bound on ballistic transport", Phys. Rev. Lett. **106**, 217206 (2011).

[10] J. Sirker, R.G. Pereira and I. Affleck, "Diffusion and ballistic transport in one-dimensional quantum systems", Phys. Rev. Lett. **103**, 216602 (2009).

[11] M. Ljubotina, M. Znidaric and T. Prosen, "Spin diffusion from an inhomogeneous quench in an integrable system", preprint `arXiv:1702.04210` (2017).

[12] Marko Medenjak, Christoph Karrasch, Tomaz Prosen, "Lower Bounding Diffusion Constant by the Curvature of Drude Weight, Phys. Rev. Lett. **119**, 080602 (2017).

[13] Enej Ilievski, Jacopo De Nardis, Marko Medenjak and Toma Prosen, "Super-diffusion in one-dimensional quantum lattice models ", `arXiv:1806.03288`.

[14] O. A. Castro-Alvaredo, B. Doyon and T. Yoshimura, "Emergent hydrodynamics in integrable quantum systems out of equilibrium ", Phys. Rev. X **6**, 041065 (2016).

[15] B. Bertini, M. Collura, J. De Nardis and M. Fagotti, "Transport in out-of-equilibrium XXZ chains: exact profiles of charges and currents", Phys. Rev. Lett. **117**, 207201 (2016).

[16] J. De Nardis, D. Bernard and B. Doyon, "Hydrodynamic Diffusion in Integrable Systems", `arXiv:1807.02414`.

[17] A. De Luca, M. Collura and J. De Nardis, "Nonequilibrium spin transport in integrable spin chains: Persistent currents and emergence of magnetic domains", Phys. Rev. B **96**, 020403(R) (2017).

[18] E. Ilievski and J. De Nardis, "On the microscopic origin of ideal conductivity",Phys. Rev. Lett. **119**, 020602 (2017). persistent currents and emergence of magnetic domains", Phys. Rev. B (2017)

[19] V.B. Bulchandani, R. Vasseur, C. Karrasch, J.E. Moore, "Bethe-Boltzmann Hydrodynamics and Spin Transport in the XXZ Chain", Phys. Rev. B **97**, 045407 (2018).

[20] V. B. Bulchandani, R. Vasseur, C. Karrasch and J. E. Moore, "Solvable hydrodynamics of quantum integrable systems", Phys. Rev. Lett. **119**, 220604 (2017).

[21] B. Doyon, T. Yoshimura and J.-S. Caux, "Soliton gases and generalized hydrodynamics", Phys. Rev. Lett. **120**, 045301 (2017).

[22] B. Doyon, J. Dubail, R. M. Konik and T. Yoshimura, "Large-Scale Description of Interacting One-Dimensional Bose Gases: Generalized Hydrodynamics Supersedes Conventional Hydrodynamics", Phys. Rev. Lett. **119**, 195301 (2017).

[23] B. Doyon, H. Spohn and T. Yoshimura, "A geometric viewpoint on generalized hydrodynamics", Nucl. Phys. B **926**, 570-582 (2017).

[24] L. Piroli, J. De Nardis, M. Collura, B. Bertini and M. Fagotti, "Transport in out-of-equilibrium XXZ chains: non-ballistic behavior and correlation functions", Phys. Rev. B **96**, 115124 (2017).

[25] E. Ilievski and J. De Nardis, "Ballistic transport in the one-dimensional Hubbard model: the hydrodynamic approach", Phys. Rev. B **96**, 081118 (2017).

[26] M. Collura, A. de Luca and J. Viti, "Analytic solution of the Domain Wall non-equilibrium stationary state", Phys. Rev. B **97**, 081111 (2018).

[27] A. Bastianello, B. Doyon, G. Watts and T. Yoshimura, "Generalized hydrodynamics of classical integrable field theory: the sinh-Gordon model", SciPost Phys. **4**, 045 (2018).

[28] B. Doyon and T. Yoshimura, "A note on generalized hydrodynamics: inhomogeneous fields and other concepts", SciPost Phys. **2**, 014 (2017).

[29] J-S Caux, B. Doyon, J. Dubail, R. Konik and T. Yoshimura, "Hydrodynamics of the interacting Bose gas in the Quantum Newton Cradle setup", `arXiv:1711.00873`.

[30] B. Doyon and H. Spohn, "Drude Weight for the Lieb-Liniger Bose Gas", SciPost Phys. **3**, 039 (2017).

[31] A. LeClair and G. Mussardo, "Finite temperature correlation functions in integrable QFT", Nucl. Phys. B, **552**, 624 (1999).

[32] B. Pozsgay and G. Takacs, "Form factors in finite volume II:disconnected terms and finite temperature correlators", Nucl.Phys. B **788**, 209 (2008).

[33] G.Kato and M.Wadati, "Graphical representation of the partition function of a one-dimensional delta-function Bose gas," J. Math. Phys., **42**, 4883 (2001).

[34] G.Kato and M.Wadati, "Partition Function for a 1-D delta-function Bose Gas", Phys. Rev. E **63** 036106 (2001).

[35] G.Kato and M.Wadati, "Direct calculation of thermodynamic quantities for the Heisenberg model," J. Math. Phys. **43**, 5060 (2002).

[36] I. Kostov, D. Serban and D. L. Vu, "TBA and tree expansion," `arXiv:1805.02591`.

[37] I. Kostov, D. Serban and D. L. Vu, "Boundary TBA, trees and loops," `arXiv:1809.05705` [hep-th].

[38] B. Doyon, "Exact large-scale correlations in integrable systems out of equilibrium", `arXiv:1711.04568`.

[39] H. Saleur, "A Comment on finite temperature correlations in integrable QFT," Nucl. Phys. B **567** (2000) 602 doi:10.1016/S0550-3213(99)00665-3 [hep-th/9909019].

[40] A. Zamolodchikov, "Thermodynamic Bethe ansatz in relativistic models. Scaling three state Potts and Lee-Yang models", Nucl. Phys. **B 342**, 695–720 (1990).

[41] C. Boldrighini, R. L. Dobrushin, and Yu. M. Sukhov, One-Dimensional Hard Rod Caricature of Hydrodynamics, J. Stat. Phys. **31**, 577 (1983).

[42] V. E. Zakharov, "Kinetic equation for solitons", Sov. Phys. JETP **33**, 538 (1971).

[43] G. A. El, A. M. Kamchatnov, M. V. Pavlov and S. A. Zykov, "Kinetic equation for a soliton gas and its hydrodynamic reductions", J. Nonlin. Sci. **21**, 151 (2011).

[44] F.A. Smirnov, "Form Factors in Completely Integrable Models of Quantum Field Theory" (World Scientific, Singapore, 1992); G. Mussardo, "Statistical Field Theory" (Oxford University Press, Oxford 2009)

[45] Seth Chaiken, "A Combinatorial Proof of the All Minors Matrix Tree Theorem", SIAM J. Alg. Disc. Meth. **3**, 319 (1982).

[46] A. Koubek, "Form-Factor Bootstrap and the Operator Content of Perturbed Minimal Models", Nucl.Phys. B **428**, 655 (1994).

[47] I.M. Szćsényi, G. Takács and G.M.T. Watts, "One-point functions in finite volume/temperature: a case study", JHEP **08**, 094 (2013).

[48] B. Pozsgay, W. V. van Gerven Oei and M. Kormos, J. Phys. A **45**, 465007 (2012).

[49] M. Kormos, G. Mussardo and A. Trombettoni, "Expectation Values in the Lieb-Liniger Bose Gas", Phys. Rev. Lett. **103**, 210404 (2009).

[50] L. Hollo, Y. Jiang and A. Petrovskii, "Diagonal form factors and heavy-heavy-light three-point functions at weak coupling", JHEP **09**, 125 (2015).

[51] Y. Jiang and A. Petrovskii, "Diagonal form factors and hexagon form factors", JHEP **07**, 120 (2016).

## 4.3 Semi-classical picture and flea gas

In this section, we review the contents of the paper [69]. My main contribution in this work is to check that the form of the effective velocity of hard-rod gases can be thought of a special case of that of GHD[4]. I also numerically solved the partitioning protocol for the Lieb-Liniger gas and provided a curve used in the paper.

One can acquire a considerable insight into the underlying structure in GHD by invoking an analogy with the hydrodynamics of classical rigid objects, i.e. hard rods [33,39,118]. A gas of hard rods consists of hard rods with the fixed length $d$, and the dynamics is such that upon two rods colliding each other, they simply exchange their velocities. This is equivalent to saying that the dynamics of hard rods is characterized by elastic scatterings between rigid segments. Its dynamics is so simple that it is amenable to rigorous mathematical analysis, and it was carried out intensively in 1980s. A remarkable upshot was that people could rigorously prove that hydrodynamics indeed *emerges* at late time and at the large scale (i.e. Euler scale); the model thereby serves as the first instance of a rigorous derivation of hydrodynamics [39]. It turns out that the resulting hydrodynamic equation takes a quite simple form. Let $\rho_{\rm rod}(v)$ be the density of rods with the velocity $v$. The Euler hydrodynamic equation for the hard rod gas reads [39]

$$\partial_t \rho_{\rm rod}(v) + \partial_x (v^{\rm eff}(v)\rho_{\rm rod}(v)) = 0, \tag{4.28}$$

where

$$v^{\rm eff}(v) = v + d\int {\rm d}w \rho_{\rm rod}(w)(v^{\rm eff}(v) - v^{\rm eff}(w)). \tag{4.29}$$

This is clearly the same as the equations of state in GHD (4.4) upon identifying $v^{\rm gr}(\theta)$ and $v$, and $\varphi(\theta-\alpha)$ and $-d$. The observation therefore suggests that, upon an appropriate alternation to the dynamics of a hard rods gas, one might obtain a classical system whose Euler scale dynamics precisely coincides with that of quantum integrable systems. This is indeed possible, and let us elaborate on how one achieve it. To this end, let us start with taking an alternative point of view on the hard rods dynamics. Namely, we put a *tracer particle* at the centre of each rod that traces the velocity of each rod. It can be considered as the quasi-particle of the system that indeed scatter elastically when the distance between two tracer particles becomes $d$. For instance, suppose that there are two hard rods equipped with tracers at $x_1$ and $x_2$ with velocities $v_1$ and $v_2$, respectively. Then, when $x_1 < x_2$ and $v_1 > v_2$, a collision occurs accompanied by trajectory shifts $x_1 \mapsto x_1 + d$ and $x_2 \mapsto x_2 - d$, which take place instantaneously (or within a microscopic time). A similar yet slightly different microscopic rule is to let two quasi-particles jump forward instantaneously with the distance $d$ when they meet at $x_1 = x_2$. These are two distinctive microscopic rules for the gas of tracer particles, but we expect that, at the macroscopic scale where Euler hydrodynamics becomes valid, they give rise to the same

[4]This was initially suggested by H. Spohn.

hydrodynamics. The latter implementation of the dynamics was named *flea gas algorithm*, and introduced in [69]. The flea gas algorithm can be straightforwardly generalized to a gas of quasi-particles that scatter with the velocity-dependent distance $d(v,w)$, which can be both positive and negative. Let us argue that the ensuing large scale dynamics can be identified as the Euler scale GHD. More precisely, we shall show that the average velocity of a probe quasi-particle labeled by its (bare) velocity $v$ after traveling for a large distance $\Delta x$ for a macroscopically large time $\Delta t$ is nothing but the GHD equations of state $v^{\rm eff}(v)$, i.e. $\Delta x = v^{\rm eff}(v)\Delta t$. First, during the travel, the contributions to the traveled distance $\Delta x$ can be decomposed into two parts; one of them comes from the consequence of propagating freely (without scatterings) while another is due to colliding with other quasi-particles. The former effect is immediate: it is simply given by $v\Delta t$, where $v$ can be considered as the group velocity of the quasi-particle. The latter requires a little more elaboration: we first note that, whenever the probe quasi-particle and a quasi-particle with the velocity $w$ scatters each other, the oriented jump distance of the probe particle is $\mathrm{sgn}\,(v-w)d(v,w)$. Since the number of quasi-particles with the velocity between $w$ and $w+\mathrm{d}w$ within the large volume $\Delta x$ is $\Delta x\,\mathrm{d}w\,\rho_{\rm cl}(w)$, where $\rho_{\rm cl}(w)$ is the quasi-particle density of the model, the total amount of jump distances due to hitting quasi-particles prescribed by the density $\rho_{\rm cl}(w)$ is $\Delta x\,\mathrm{d}w\,\rho_{\rm cl}(w)\mathrm{sgn}\,(v-w)d(v,w)$. A caveat here, however, is that the probe particle does not necessarily undergo the scatterings with all these particles (for instance, if the probe particle is located left to a particle with the velocity $w$ with $v^{\rm eff}(v)<v^{\rm eff}(w)$, then they never hit each other). The probability of encountering such scattering events can be estimated as $\Delta t|v^{\rm eff}(v)-v^{\rm eff}(w)|/\Delta x$. Therefore, the actual total traveled distance can be written as

$$\Delta x = v\Delta t + \int \mathrm{d}w\, d(v,w)\rho_{\rm cl}(w)(v^{\rm eff}(v)-v^{\rm eff}(w))\Delta t, \tag{4.30}$$

which entails

$$v^{\rm eff}(v) = v + \int \mathrm{d}w\, d(v,w)\rho_{\rm cl}(w)(v^{\rm eff}(v)-v^{\rm eff}(w)). \tag{4.31}$$

Upon appropriate identifications, this average velocity coincides with (4.4).

The above observation implies that the hydrodynamics of the classical flea gas implemented as above is the same as that of quantum integrable systems. This *quantum-classical correspondence* suggests a profound underlying structure behind the large scale dynamics of integrable systems. Namely, even if the microscopic model is quantum, at the Euler scale, quasi-particles behave like solitons in a sense that when two quasi-particles scatter, the only effect is the spatial displacement they experience, which is precisely how solitons scatter upon collisions. In fact, it has been known that a gas of particles that obeys the Korteweg-de Vries (KdV) equation can indeed be treated as the soliton gas with the effective velocity resembling (4.31) [101,136,137]. Therefore the above structure of the large scale dynamics seems to be universally shared among any models whose excitations are characterized by quasi-particles that scatter elastically.

It is also important to notice that the correspondence allows us to simulate the dy-

namics of *quantum* integrable systems using *classical* molecular dynamics, which turns out to be extremely efficient and useful [105, 106]. For the details on how to implement the algorithm, see our paper [69].

# Soliton gases and generalized hydrodynamics

Benjamin Doyon,[1] Takato Yoshimura,[1] and Jean-Sébastien Caux[2]

[1] *Department of Mathematics, King's College London, Strand, London WC2R 2LS, UK*
[2] *Institute for Theoretical Physics Amsterdam and Delta Institute for Theoretical Physics, University of Amsterdam, Science Park 904, 1098 XH Amsterdam, The Netherlands*

We show that the equations of generalized hydrodynamics (GHD), a hydrodynamic theory for integrable quantum systems at the Euler scale, emerge in full generality in a family of classical gases, which generalize the gas of hard rods. In this family, the particles, upon colliding, jump forward or backward by a distance that depends on their velocities, reminiscent of classical soliton scattering. This provides a "molecular dynamics" for GHD: a numerical solver which is efficient, flexible, and which applies to the presence of external force fields. GHD also describes the hydrodynamics of classical soliton gases. We identify the GHD of any quantum model with that of the gas of its soliton-like wave packets, thus providing a remarkable quantum-classical equivalence. The theory is directly applicable, for instance, to integrable quantum chains and to the Lieb-Liniger model realized in cold-atom experiments.

*Introduction.* It is widely believed and acknowledged that the late-time and large-scale dynamics of interacting systems, whether quantum or not, is well described by hydrodynamics. The applicability of hydrodynamics encompasses a large number of many-body systems, from classical gases and interacting quantum field theories [1, 2] where few hydrodynamic variables are necessary, to more exotic systems such as the classical hard-rod model [3]. Recently, the realm of hydrodynamics was extended to integrable quantum models by accounting for the infinity of nontrivial conservation laws they admit [4, 5]. On large (Eulerian) scales one assumes that fluid cells are in generalized Gibbs ensembles (GGE) [6]. The theory describing this was dubbed generalized hydrodynamics (GHD). It is applicable to many models, including quantum chains and field theory, and has been useful in many recent studies [7–11]. It has been applied [4] to the Lieb-Liniger model [12], thus can be used to describe the inhomogeneous dynamics in quasi-one-dimensional cold atom setups [13] such as that of the celebrated quantum Newton cradle [14].

In this paper, we show that the GHD equations also emerge as descriptions of *classical* gases. It is simple to see that a special case of GHD reproduces the equations, mathematically derived by Boldrighini, Dobrushin, Sukhovin in 1983 [3], for a gas of hard rods on the line colliding elastically (an observation used in [15] for the domain-wall problem). We show that a modification of the hard-rod dynamics leads to the general form of GHD found in integrable quantum systems. In the modified problem, point-like "quasi-particles" are subject to velocity-dependent spatial shifts upon colliding, generalizing the velocity tracers in the hard rod problem.

The classical gas problem is extremely easy to implement on the computer. This gives a "molecular dynamics" (MD) solver for GHD that is numerically efficient, that accounts for external forces, and that is flexible enough to offer the possibility of adding other effects such as integrability breaking and viscosity. MD solvers are known for their usefulness in low-temperature Fermi liquids, strongly-interacting gases and high-temperature/density plasmas, see e.g. [16–18]. The MD solver developed here offers better performance due to the stability of the integrable quasi-particles at the heart of the systems dynamics. It is free from limitations on temperature, interaction strength and density, only requiring Eulerian scales.

Velocity-dependent shifts upon scattering is a soliton-like feature, and equations of GHD form have in fact been found to describe classical soliton gases [19]. Wave packets of excitations in quantum models, although not strictly solitons, have also been observed to display such soliton-like features [20]. We identify the GHD of any quantum model with that of the gas of its soliton-like wave packets, thus providing a remarkable quantum-classical correspondence at the Euler scale. This means that, from the viewpoint of local averages in Eulerian hydrodynamics, all quantum effects can be accounted for by considering the two-body classical scattering of soliton-like wave packets.

*Generalized hydrodynamics.* Hydrodynamics is a theory for the dynamics of weakly inhomogeneous, non-stationary states of many-body physics. The principle of hydrodynamics is that of local entropy maximization. Local averages are thus related to each other in the same way they are in entropy-maximized states: the equations of state hold. Eulerian hydrodynamics (that is, hydrodynamics neglecting viscosity effects) is obtained simply by imposing the conservation laws for local averages of densities and currents. This thus transfers microscopic dynamics into a macroscopic dynamics for the local Lagrange parameters, or for any other hydrodynamic variables (parametrizations of the state). These concepts have recently been applied to one-dimensional integrable models [4, 5]. In this context, entropy maximization occurs with respect to infinitely many local and quasi-local conserved charges, leading to generalized Gibbs ensembles (GGEs) (for reviews see [6]). The hydrodynamic theory is referred to as generalized hydrodynamics (GHD).

In order to describe the equations of GHD, consider the quasi-particle description of Bethe ansatz integrable

models. A quasi-particle has a "rapidity" $\theta$ and a species $a$. The rapidity parametrizes the two fundamental characteristics of the model, the energy $E(\boldsymbol{\theta})$ and the momentum $p(\boldsymbol{\theta})$, which form the group velocity $v^{\rm gr}(\boldsymbol{\theta}) = E'(\boldsymbol{\theta})/p'(\boldsymbol{\theta})$ (here and below we use boldface letters for pairs of spectral parameter and particle type, $\boldsymbol{\theta} = (\theta, a)$, and the prime symbol ($'$) for rapidity derivatives $\mathrm{d}/\mathrm{d}\theta$). For instance, in relativistic (resp. Galilean) models one takes $\theta$ as the true rapidity (resp. the velocity). The interaction is characterized by the two-particle differential scattering phase, $\varphi(\boldsymbol{\theta}, \boldsymbol{\alpha})$. One represents a GGE state by its quasi-particle density $\rho_{\rm p}(\boldsymbol{\theta})$; the number of quasi-particles of type $a$ in the phase space element $[x, x + \mathrm{d}x] \times [p(\boldsymbol{\theta}), p(\boldsymbol{\theta}) + p'(\boldsymbol{\theta})\mathrm{d}\theta)]$ is $\rho_{\rm p}(\boldsymbol{\theta})\mathrm{d}\theta\mathrm{d}x$.

It was shown in [4, 5] that the infinity of hydrodynamic conservation laws of GHD lead to the following continuity equation:

$$\partial_t \rho_{\rm p}(\boldsymbol{\theta}) + \partial_x (v^{\rm eff}(\boldsymbol{\theta})\rho_{\rm p}(\boldsymbol{\theta})) = 0 \tag{1}$$

where the *effective velocity* $v^{\rm eff}(\boldsymbol{\theta})$ solves the equation

$$v^{\rm eff}(\boldsymbol{\theta}) = v^{\rm gr}(\boldsymbol{\theta}) + \int \mathrm{d}\boldsymbol{\alpha}\, \frac{\varphi(\boldsymbol{\theta}, \boldsymbol{\alpha})}{p'(\boldsymbol{\theta})}\, \rho_{\rm p}(\boldsymbol{\alpha})\, (v^{\rm eff}(\boldsymbol{\alpha}) - v^{\rm eff}(\boldsymbol{\theta})) \tag{2}$$

(here and below $\int \mathrm{d}\boldsymbol{\theta} = \sum_a \int_{\mathbb{R}} \mathrm{d}\theta$, and we suppress the explicit $x, t$ dependence for lightness of notation). The effective velocity $v^{\rm eff}(\boldsymbol{\theta})$ [4, 5, 21] serves as a velocity of the quasi-particle $\boldsymbol{\theta}$ in the fluid cell at $(x, t)$. The quasi-particle spectral density $\rho_{\rm p}(\boldsymbol{\theta})$ is a conserved fluid density. These equations were generalized to the presence of external inhomogeneous fields [7]. Here it is sufficient to recall the result for Galilean models (with particles of masses $m_a$) within a force potential $V(x)$:

$$\partial_t \rho_{\rm p}(\boldsymbol{\theta}) + \partial_x (v^{\rm eff}(\boldsymbol{\theta})\rho_{\rm p}(\boldsymbol{\theta})) - (\partial_x V/m_a)\partial_\theta \rho_{\rm p}(\boldsymbol{\theta}) = 0. \tag{3}$$

In the Lieb-Liniger (LL) model and other field theories, these equations were derived in [4, 7], and in the XXZ quantum spin chains in [5] (without force fields). The LL model is of particular interest and will be chosen below in order to give examples of our results. It represents Galilean-invariant interacting Bose gases, experimentally realizable [13]. In the repulsive regime, there is a single particle species, with differential scattering phase

$$\varphi(\theta, \alpha) = 2c/((\theta - \alpha)^2 + c^2) \qquad \text{(Lieb-Liniger)} \tag{4}$$

where $c$ is the coupling strength (see the Supplementary Material (SM) for the LL model in the attractive regime).

*Molecular dynamics: the classical flea gases.* The GHD equations are Euler-type hydrodynamic equations, requiring local entropy maximization (there is kinetic interpretation [5], which also implicitly requires local entropy maximization). An important problem in GHD is to numerically solve (1), (3). This is of particular interest for the LL model within a force field as this applies to cold atom gases, for instance in the quantum Newton cradle setup [14]. Euler-type equations are often solvable by using appropriate molecular dynamics (MD). This requires finding a particle dynamics whose entropy-maximized homogeneous states have the correct equations of state: the correct relations between currents and densities. As shown in [4], here this amounts to the relation (2) between the effective velocity and the quasi-particle density. We now develop a family of classical gases which, at the Euler scale, reproduce exactly (2) and the equations of GHD (1) and (3).

In order to make the argument clear, let us first recall the classical hard rod model [1, 3] and make connection with GHD (see also [15]). Rods (non-intersecting one-dimensional segments) of a fixed length $d$ move inertially at various velocities $v$ on the infinite line, except for elastic collisions at which they exchange their velocities. The emergence of hydrodynamic equations on large scales in this model for a large class of initial conditions was rigorously demonstrated [3]. Let $\rho_{\rm cl}(v)$ be the density of rods with velocity $v$ ($\rho_{\rm cl}(v)\,\mathrm{d}x\,\mathrm{d}v$ is the number of rod centers lying within the phase space element $[x, x + \mathrm{d}x] \times [v, v + \mathrm{d}v]$). The hydrodynamic equations read

$$\partial_t \rho_{\rm cl}(v) + \partial_x (v_{\rm cl}^{\rm eff}(v)\rho_{\rm cl}(v)) = 0, \tag{5}$$

where $v_{\rm cl}^{\rm eff}(v)$ satisfies [3]

$$v_{\rm cl}^{\rm eff}(v) = v + d \int \mathrm{d}w\, \rho_{\rm cl}(w)(v_{\rm cl}^{\rm eff}(v) - v_{\rm cl}^{\rm eff}(w)). \tag{6}$$

These are exactly the equations (2) and (1), in the Galilean case ($v = \theta$), with a single unit-mass particle species, with negative differential scattering length[1] $\varphi(v, w) = -d$, and with $\rho_{\rm p}(v) = \rho_{\rm cl}(v)$ and $v^{\rm eff}(v) = v_{\rm cl}^{\rm eff}(v)$. This simple observation suggests that if we allow the rods to collide more "softly", in such a way that $d$ becomes velocity dependent, the hydrodynamics of the emerging gas might be identical to that of GHD. With velocity-dependent rod lengths, neighboring rods of velocities $v$ and $w$ would exchange their velocities when their centers are at distance $d(v, w)$, as if rods were elastically contractible. However this simple-looking dynamics causes difficulties with respect to many-body scattering and for negative or non-symmetric lengths.

Consider instead a velocity-tracer, following the center of a rod of velocity $v$. This is a point-like quasi-particle, with trajectory that of a free particle except for jumps by a distance $d$ at rod collisions. Here rod collisions occur when the positions $x_1 < x_2$ of two quasi-particles satisfy $x_2 - x_1 = d$ and their velocities $v_1 > v_2$, and at this instant $x_1 \mapsto x_1 + d$ and $x_2 \mapsto x_2 - d$. Crucially, this means that every crossing of two quasi-particles' trajectories comes with such trajectory shifts, and this within

[1] In the quantum context, this corresponds to a purely exponential scattering phase, $S(\theta, \alpha) = e^{-\mathrm{i}d\,(\theta - \alpha)}$ [22]. In the large-$c$ region of the repulsive LL model, one also finds constant $\varphi(\theta, \alpha) \sim 2/c$, but this would correspond to negative rod lengths $d = -2/c$.

microscopic time. In fact, any dynamics with this property, independently of the microscopic details of the trajectory shifts, leads to the same hydrodynamics. We may thus modify the dynamics by proclaiming collisions to occur at $x_2 = x_1$, at which the involved quasi-particles instantaneously jump, like fleas, by a distance $d$. The jump is "forward": the quasi-particle on the left (right) jumps towards the right (left). This is easily generalizable to velocity-dependent jump lengths: a quasi-particle of velocity $v$ that enters in collision with one of velocity $w$ jumps by $d(v, w)$, forward if positive, backward if negative. Importantly, the jump lengths may be positive or negative, and need not be symmetric with respect to exchange of velocities. A jump is an infinitely-fast displacement, during which more collisions can occur, occasioning new jumps in a chain reaction that re-organizes the quasi-particles' positions in the local neighborhood. This is the classical "flea gas"; see the SM for the precise, somewhat subtle algorithm.

We now argue that this reproduces GHD. We are looking for the effective velocity $v_{\rm cl}^{\rm eff}(v)$ of a test quasi-particle of velocity $v$, defined through the actual distance that it travels in a macroscopic time $\Delta t$,

$$\Delta x = \Delta t\, v_{\rm cl}^{\rm eff}(v). \tag{7}$$

The gas is characterized by the density $\rho_{\rm cl}(w)$, and by standard arguments the continuity equation (5) holds. The quantity $\Delta x$ results from the linear displacements at velocity $v$, given by $\Delta t\, v$, along with the accumulation of jumps the quasi-particle undergoes as it travels through the gas. The oriented distance jumped due to hitting a quasi-particle that has velocity $w$ is $\mathrm{sign}(v-w)d(v,w)$. The average number of quasi-particles of velocity between $w$ and $w + \mathrm{d}w$ that has been crossed, is the total number $\mathrm{d}w\, \rho_{\rm cl}(w)\Delta x$ present within the length $\Delta x$, times the probability $\Delta t/\Delta x \times |v_{\rm cl}^{\rm eff}(v) - v_{\rm cl}^{\rm eff}(w)|$ that the test particle crosses such a quasi-particles in time $\Delta t$. Assuming that the effective velocity is monotonic with $v$ (see the SM), the total jumped distance is therefore

$$\int \mathrm{d}w\, d(v,w)\, \rho_{\rm cl}(w)\, \Delta t\, (v_{\rm cl}^{\rm eff}(v) - v_{\rm cl}^{\rm eff}(w)). \tag{8}$$

Equating (7) with the sum of $\Delta t\, v$ and (8) we find

$$v_{\rm cl}^{\rm eff}(v) = v + \int \mathrm{d}w\, d(v,w)\, \rho_{\rm cl}(w)\, (v_{\rm cl}^{\rm eff}(v) - v_{\rm cl}^{\rm eff}(w)). \tag{9}$$

Therefore the GHD equations (1), in the case of a single species, reproduce the hydrodynamics of the flea gas under the following identification:

$$\rho_{\rm cl}(v)\mathrm{d}v = \rho_{\rm p}(\theta)\mathrm{d}\theta, \quad v = v^{\rm gr}(\theta), \quad v_{\rm cl}^{\rm eff}(v) = v^{\rm eff}(\theta) \tag{10}$$

along with

$$d(v,w) = -\varphi(\theta,\alpha)/p'(\theta). \tag{11}$$

This is readily generalizable to many species, with, in (9), velocity parameters $v, w$ replaced by doublets $\boldsymbol{v} = (v, a)$, $\boldsymbol{w} = (w, b)$, and the driving velocity value $v$ replaced by $v^{\rm gr}(\boldsymbol{v})$. We recover (2) by reparametrization. It is clear that, if an external potential $V(x)$ affects the velocities $v$ of the quasi-particles of the flea gas so that there is an acceleration $\mathrm{d}v/\mathrm{d}t = -\partial_x V/m$, the continuity equation (3) holds.

*Domain of validity.* As any molecular dynamics, the flea gas reproduces the GHD equations only at the gas's Euler scale. Two sets of lengths determine this scale: (1) the inter-particle length $1/\rho$ ($\rho = \int \mathrm{d}\boldsymbol{v}\rho_{\rm cl}(\boldsymbol{v})$), and (2) the jump distance $d(\boldsymbol{\theta}, \boldsymbol{\alpha})$. We expect the Euler scale to be reached when these two lengths are much smaller than the variation length – the typical length over which $\rho$ varies. In this case, particles locally maximize entropy, as jumps do not send them away from their fluid cell and many jumps occur within a fluid cell. The flea gas cannot solve GHD away from such conditions. Of course, GHD only applies under similar conditions; for instance, in quantum models, variation lengths must be much bigger than the scattering length, determined by $\varphi(\boldsymbol{\theta}, \boldsymbol{\alpha})$.

*Numerical checks.* We have numerically simulated the classical gas corresponding to the LL model (4) with $c = 1$, $m = 1$. Besides being a model of experimental interest, the GHD of the LL model was studied in [4] at length, allowing benchmarking of the MD developed here. All verifications are done well within the strong coupling regime, far from either the Tonks-Girardeau or the free boson points. First, we have verified the form of the effective velocity by evaluating explicitly, in a homogeneous stationary gas with LL coupling parameter $\gamma = mc\rho^{-1} \approx 1.1$, the total displacement of a test quasi-particle divided by the time spent, and comparing with the result of solving numerically the integral equation (2). See Fig. 1a; the agreement is excellent. Second, we have implemented a domain wall initial condition in the LL model, and checked that its dynamics reproduces the self-similar solution derived in [4]. See Fig. 1b, as well as Fig. 3 in the SM. Again, these provide convincing evidence of the validity of the MD. Finally, we have implemented the "breathing motion" of the LL model occurring after a sudden change of frequency of a harmonic confining potential. This has been studied experimentally, with tDMRG and with conventional hydrodynamics, see [24]. As found in [11], GHD supersedes conventional hydrodynamics at nonzero temperature, and thus it is important to test the MD solver's validity in this case. The initial state, at temperature $T = 1$, is evolved within a wider harmonic potential. As expected, the density expands and contracts almost periodically. The observed period is slightly smaller than that of the evolution potential, as the interaction slows down the particles. We have simulated this setup using the flea gas, and directly verified the conservation equations (3), integrating over cells in phase-space-time. Without changing scattering and interparticle lengths, we have considered setups with 120 and 1200 particles. These have widely different variation lengths, affecting the accuracy of the hydrodynamic ap-

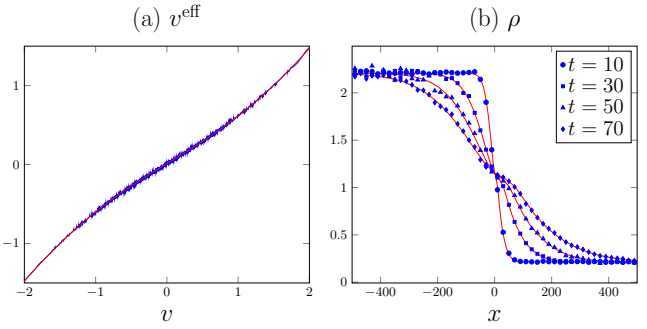


FIG. 1. GHD for the LL model with $m = 1$, $c = 1$ is simulated using the classical flea gas. (a) Truncated Gaussian distribution $\rho_{\rm cl}(v) = 0.5e^{-v^2}\chi(-3 < v < 3)$. Effective velocity evaluated using approx. 1500 trajectories over a time of 1200 (blue); using the formula (2) (red). (b) Density profile from domain wall initial condition, initial left and right temperatures 10 and 1/3 (resp.), at times $t = 10$, 30, 50, 70. Simulation with approx. 2400 quasi-particles (initial baths of lengths 1000, open boundary condition) averaged over 1000 samples (blue); exact self-similar solution (red).

proximation. With a gas of as little as 120 particles, we found (3) to be satisfied to 0.2-0.9%, and with 1200 particles, 0.08-0.16%. The accuracy is higher in central cells, away from the boundary of the density support where hydrodynamics is expected to fail. This quantifies the accuracy of the hydrodynamic approximation, and provides precise tests of how MD solves the GHD equations within force fields. See the SM for details.

*Quantum-classical dictionary.* The GHD equations were derived in quantum integrable models using quantum integrability. There is thus a quantum-classical dictionary, such as Eqs. (10) and (11). Further elements of the dictionary are as follows. The free space fraction is

$$\rho_{\rm free}(\boldsymbol{v}) = 1 - \int {\rm d}\boldsymbol{w}\, d(\boldsymbol{v},\boldsymbol{w})\rho_{\rm cl}(\boldsymbol{w}). \qquad (12)$$

In the hard rod gas, this is the fraction of a unit length where there is no rod at all; in the general case, that available omitting the distances jumped if forward, or adding them if backward (in the latter case the effect of quasi-particle scattering is to increase the space available). We recognize (12) as, up to a factor, the quantum *density of states* $\rho_{\rm s}(\boldsymbol{\theta})$ [23], $\rho_{\rm free}(\boldsymbol{v}) = 2\pi\rho_{\rm s}(\boldsymbol{\theta})/p'(\boldsymbol{\theta})$. The occupation function $n(\boldsymbol{\theta}) = \rho_{\rm p}(\boldsymbol{\theta})/\rho_{\rm s}(\boldsymbol{\theta})$ plays an important role in GHD, being the normal mode of the hydrodynamics [4, 5]. For it, we then have $\rho_{\rm cl}(\boldsymbol{v}){\rm d}v\,/\rho_{\rm free}(\boldsymbol{v}) = n(\boldsymbol{\theta})\,p'(\boldsymbol{\theta}){\rm d}\theta\,/(2\pi)$. The left-hand side is the classical number of quasi-particles per unit length of free space.

The classical picture helps us understand the form of the effective velocity. Let us write it as $v^{\rm eff}_{\rm cl}(\boldsymbol{v}) = (v^{\rm gr}(\boldsymbol{v}) - \int {\rm d}\boldsymbol{w}\, d(\boldsymbol{v},\boldsymbol{w})\rho_{\rm cl}(\boldsymbol{w})v^{\rm eff}_{\rm cl}(\boldsymbol{w}))/(1 - \int {\rm d}\boldsymbol{w}\, d(\boldsymbol{v},\boldsymbol{w})\rho_{\rm cl}(\boldsymbol{w}))$, and consider $d(v,w) < 0$. The gas *slows down* a test quasi-particle with respect to its "center of momentum", as it is affected by backwards jumps at collisions. There is thus a friction effect – the denominator – and a drag effect – the second term in the numerator, which were numerically noticed in [4] when studying steady states. Note also that the full dynamics is invariant under simultaneous scaling of space, time and jump lengths, but in the quantum problem a fundamental physical length scale arises due to $\hbar$ within the differential scattering phase.

*Soliton gases.* The above intriguing quantum-classical correspondence might be explained in terms of soliton gases. In classical soliton scattering, two solitons retain, asymptotically, their form and their speeds, the only change being in shifts of their trajectories. These shifts are velocity dependent, and thus the flea-gas Euler hydrodynamics might be the same as that of classical soliton scattering. Indeed, it turns out that equations of the GHD form, without force fields, were already found in recent studies of gases of solitonic modes of classical field theory [19]. In these studies an effective velocity emerge that is determined by the soliton's scattering shifts $d(v,w)$ as per (9). The integrability of the resulting equations was investigated, see also [25].

Why do gases of classical solitons have the same Euler hydrodynamics as that of quantum models? In the quantum context, it is known that quasi-particles excitations have soliton-like features. This was recently made numerically explicit by forming wave packets of quasi-particle excitations in the Heisenberg quantum chain [20]. It was seen that the trajectory shifts are given by the differential scattering phase of the quantum model. This exactly agrees with the relation (11) that we derived between the shift $d(v,w)$ and the differential scattering phase $\varphi(\theta,\alpha)$. Wave packets in quantum models are however *not* solitons: in the example of [20] for instance, they do not keep their shape but rather spread with time, as do wave packets of free fields. But this effect appears to be subleading: at the Euler scale, only the scattering shifts play a role. This explains why the Euler hydrodynamics of true classical solitons is the same as that of quantum models upon identifying the soliton-like features of quantum excitations, and is expected to be general. That quantum gases can be seen as the gas of their classical soliton-like wave packets gives, we believe, new insight into the large-scale dynamics of quantum models. It is also in agreement with the picture according to which multi-particle scattering processes are sequences of well separated two-body scattering processes, at the basis of the (generalized) thermodynamic Bethe ansatz [23].

*Conclusion.* We have developed a classical gas dynamics that reproduces, at the Euler scale, the equations of GHD for arbitrary differential scattering phase. This gives an efficient way of simulating full space-time dependent profiles solving GHD. It complements the exact "solution by characteristics" found in [9] and numerical methods [10, 11]. It is the first numerical procedure applicable in general states to the experimentally relevant case of the LL model in force fields. It shows that the GHD equations describe classical soliton gases, and pro-

vides a clear interpretation of friction and drag effects controlling the effective velocity. With the numerical technique developed here, the quantum Newton cradle setup [14] is now accessible, which it will be important to analyze.

The connection between GHD and soliton gases also has far-reaching implication. For instance, the integrable structures developed in the context of soliton gases [19] can now be used in quantum models, and may have connections with the solution by characteristics [9]. The GHD equation including for force fields was only derived in quantum models [7], it would be interesting to understand its meaning in classical soliton gases. The large-deviation theory of classical gases is also a problem of interest, especially its relation with that of quantum problems (see e.g. [26]). Soliton gases may be seen as wide generalizations of the semiclassical picture proposed in [27], and may lead to efficient ways of evaluating correlations in certain regimes.

Viscosity or other higher-derivative effects in the quantum problems will have many sources, including the finite scattering length taken into account by the classical gas, but also wave packet spreading. By appropriately modifying the classical algorithm, it might be possible to phenomenologically account for such corrections to GHD, as well as for integrability-breaking processes, which would otherwise be extremely difficult to numerically implement.

*Acknowledgment.* We thank Robert Konik and Herbert Spohn for useful discussions. Hospitality is acknowledged as follows: all authors thank SISSA and ICTP, Trieste (visits and workshop "Entanglement and non-equilibrium physics of pure and disordered systems", July 2016), BD and TY thank City University New York (workshop "Dynamics and hydrodynamics of certain quantum matter", March 2017), and TY thanks Tokyo Institute of Technology. TY is grateful for the support from the Takenaka Scholarship Foundation.

[1] H. Spohn, "Large Scale Dynamics of Interacting Particles" (Springer Verlag, Heidelberg, 1991).

[2] P. Nozieres and D. Pines, "The Theory of Quantum Liquids" (Benjamin, New York, 1966); S. Jeon and L. G. Yaffe, "From Quantum Field Theory to Hydrodynamics: Transport Coefficients and Effective Kinetic Theory", Phys. Rev. D **53**, 5799 (1996); A. G. Abanov, in Applications of Random Matrices in Physics, edited by E. Brezin, V. Kazakov, D. Serban, P. Wiegmann, and A. Zabrodin, NATO Science Series II: Mathematics, Physics and Chemistry, Vol. 221 (Springer, Dordrecht, 2006), pp. 139161; E. Bettelheim, A. G. Abanov, and P. Wiegmann, "Nonlinear Quantum Shock Waves in Fractional Quantum Hall Edge States", Phys. Rev. Lett. **97**, 246401 (2006); J. Bhaseen, B. Doyon, A. Lucas and K. Schalm, "Far from Equilibrium Energy Flow in Quantum Critical Systems", Nature Phys. **11**, 509 (2015); D. Bernard and B. Doyon, "A Hydrodynamic Approach to Non-Equilibrium Conformal Field Theories", J. Stat. Mech. **2016**, 033104 (2016).

[3] C. Boldrighini, R. L. Dobrushin and Yu. M. Sukhov, "One-Dimensional Hard Rod Caricature of Hydrodynamics", J. Stat. Phys. **31**, 577 (1983).

[4] O. A. Castro-Alvaredo, B. Doyon and T. Yoshimura, "Emergent Hydrodynamics in Integrable Quantum Systems Out of Equilibrium", Phys. Rev. X **6**, 041065 (2016).

[5] B. Bertini, M. Collura, J. De Nardis and M. Fagotti, "Transport in Out-of-Equilibrium XXZ Chains: Exact Profiles of Charges and Currents", Phys. Rev. Lett. **117**, 207201 (2016).

[6] A. Polkovnikov, K. Sengupta, A. Silva and M. Vengalattore, "Colloquium: nonequilibrium dynamics of closed interacting quantum system", Rev. Mod. Phys. **83**, 863 (2011); C. Gogolin and J. Eisert, "Equilibration, thermalisation, and the emergence of statistical mechanics in closed quantum systemsa review", Rep. Prog. Phys. **79**, 056001 (2016); J. Eisert, M. Friesdorf and C. Gogolin, "Quantum many-body systems out of equilibrium", Nature Phys. **11**, 124 (2015); F. Essler, M. Fagotti, "Quench dynamics and relaxation in isolated integrable quantum spin chains", J. Stat. Mech. **2016**, 064002 (2016); L. Vidmar, M. Rigol, "Generalized Gibbs ensemble in integrable lattice models", J. Stat. Mech. **2016**, 064007 (2016).

[7] B. Doyon and T. Yoshimura, "A note on generalized hydrodynamics: inhomogeneous fields and other concepts", preprint `arXiv:1611.08225` (2016).

[8] E. Ilievski and J. De Nardis, "On the microscopic origin of ideal conductivity", preprint `arXiv:1702.02930` (2017); M. Ljubotina, M. Znidaric and T. Prosen, "Spin diffusion from an inhomogeneous quench in an integrable system", preprint `arXiv:1702.04210` (2017); V. B. Bulchandani, R. Vasseur, C. Karrasch and J . E. Moore, "Bethe-Boltzmann hydrodynamics and spin transport in the XXZ Chain", preprint `arXiv:1702.06146` (2017); J. Dubail, J.-M. Stéphan, J. Viti and P. Calabrese, "Conformal field theory for inhomogeneous one-dimensional quantum systems: the example of non-interacting Fermi gases", SciPost Phys. **2**, 002 (2017); S. Sotiriadis, Equilibration in one-dimensional quantum hydrodynamic systems, preprint `arXiv:1612.00373` (2016).

[9] B. Doyon, H. Spohn and T. Yoshinura, "A geometric viewpoint on generalized hydrodynamics", preprint `arXiv:1704.04409`

[10] V. B. Bulchandani, R. Vasseur, C. Karrasch and J. E. Moore, "Solvable hydrodynamics of quantum integrable systems", preprint `arXiv:1704.03466`.

[11] B. Doyon, J. Dubail, R. Konik and T. Yoshimura, "Large-scale description of interacting one-dimensional Bose gases: generalized hydrodynamics supersedes conventional hydrodynamics", preprint `arXiv:1704.04151` (2017).

[12] E. H. Lieb and W. Liniger, "Exact analysis of an interacting Bose gas. I. The general solution and the ground state", Phys. Rev. **130**, 1605 (1963).

[13] M.A. Cazalilla, R. Citro, T. Giamarchi, E. Orignac and M. Rigol, "One dimensional bosons: from condensed matter systems to ultracold gases", Rev. Mod. Phys. **83**, 1405 (2011).

[14] T. Kinoshita, T. Wenger and D. S. Weiss, "A Quantum Newton's Cradle", Nature **440**, 900-903 (2006).

[15] B. Doyon and H. Spohn, "Dynamics of hard rods with initial domain wall state", preprint `arXiv:1703.05971` (2017).

[16] P. Lipavský, K. Morawetz and Václav Špička, "Kinetic equation for strongly interacting dense Fermi system", Ann. Phys. (Paris) **26**, 1 (2001).

[17] O. Goulko, F. Chevy and C. Lobo, "Boltzmann equation simulation for a trapped Fermi gas of atoms", New J. Phys. **14**, 073036 (2012).

[18] F. Graziani et al, "Large-scale molecular dynamics simulations of dense plasmas: The Cimarron Project", High Energy Density Physics **8**, 105 (2012).

[19] V. E. Zakharov, "Kinetic equation for solitons", Sov. Phys. JETP **33**, 538 (1971); G. A. El, "The thermodynamic limit of the Whitham equations", Phys. Lett. A **311**, 374 (2003); G. A. El and A. M. Kamchatnov, "Kinetic Equation for a Dense Soliton Gas", Phys. Rev. Lett. **95**, 204101 (2005); G. A. El, A. M. Kamchatnov, M. V. Pavlov and S. A. Zykov, "Kinetic equation for a soliton gas and its hydrodynamic reductions", J. Nonlin. Science **21**, 151 (2011).

[20] R. Vlijm, M. Ganahl, D. Fioretto, M. Brockmann, M. Haque, H.G. Evertz and J.-S. Caux, "Quasi-soliton scattering in quantum spin chains", Phys. Rev. B **92**, 214427 (2015).

[21] L. Bonnes, F. H. L. Essler and A. M. Läuchli, "Light-Cone, Dynamics after Quantum Quenches in Spin Chains", Phys. Rev. Lett. **113**, 187203 (2014).

[22] H. Grosse and G. Lechner, "Wedge-local quantum fields and noncommutative Minkowski space", JHEP **11**, 012 (2007).

[23] A. Zamolodchikov, "Thermodynamic Bethe ansatz in relativistic models. Scaling three state Potts and Lee-Yang models", Nucl. Phys. B **342**, 695 (1990); J. Mossel, J.-S. Caux, "Generalized TBA and generalized Gibbs", J. Phys. A **45**, 255001 (2012).

[24] S. Peotta and M. Di Ventra, "Quantum shock waves and population inversion in collisions of ultracold atomic clouds", Phys. Rev. A **89**, 013621 (2014); B. Fang, G. Carleo, A. Johnson and I. Bouchoule, "Quench-induced breathing mode of one-dimensional Bose gases", Phys. Rev. Lett. **113**, 035301 (2014); I. Bouchoule, S. S. Szigeti, M. J. Davis and K. V. Kheruntsyan, "Finite-temperature hydrodynamics for one-dimensional Bose gases: Breathing mode oscillations as a case study", Phys. Rev. A **94**, 051602 (2016).

[25] V. B. Bulchandani, "On classical integrability of the hydrodynamics of quantum integrable systems", preprint `arXiv:1706.06278` (2017).

[26] D. Bernard and B. Doyon, Conformal Field Theory Out of Equilibrium: A Review, J. Stat. Mech. **2016**, 064005 (2016).

[27] S. Sachdev and A. P. Young, "Low temperature relaxational dynamics of the Ising chain in a transverse field", Phys. Rev. Lett. **78**, 2220 (1997)


# Supplementary Material

## I. FLEA GAS ALGORITHM

The gas is represented by a chain of cells, each cell representing a quasi-particle $A$ and containing all necessary information pertaining to it (its velocity, its type, its position $A$.pos on the line), ordered from left to right. The procedure distance$(A, B)$ returns the oriented distance of the jump for a collision of $A$ against $B$ (it depends on the velocities and types of $A$ and $B$); it was denoted $d(\cdot, \cdot)$ in the text, and it is positive for forward jumps, negative for backward jumps. In order not to perform a given jump, associated to a give crossing, twice, we need to mark the pairs of quasi-particle at their first collision; marked pairs, if they collide another time, just past through each other. This is of course essential if jumps are backwards, and in general has the effect that under the re-organization of quasi-particles' positions in a neighborhood of a collision, the exact distance $d(\cdot, \cdot)$ has been jumped by every quasi-particle affected by a collision. A picture for possible collisions between quasi-particles with velocities $v$ and $w$ are depicted in the Fig.2, and a precise algorithm for the flea gas is as follows.

```
procedure Evolve:
Displace all until next collision;
Collide left-particle against right-particle;
repeat until evolution time has elapsed;
end.

procedure Collide A against B:
if marked (A,B):
  Exchange A, B in the chain
else:
  Mark (A,B);
  Jump A by distance(A,B);
  Jump B by −distance(A,B);
end.

procedure Jump A by D:
if D < 0 then side is left;
else side is right;
repeat:
  B := quasi-particle to the side of A;
  if B exists and |A.pos − B.pos| < |D|:
    D := D − B.pos + A.pos;
    A.pos := B.pos;
    if side is left:  Collide B against A;
    else:  Collide A against B;
  else:
    A.pos := A.pos + D;
    break;
end.
```

Above, side refers to the side within the chain. Note that, because of the recursive process (the chain reaction of collisions), the event Jump $A$ by distance$(A, B)$ may also affect the position of $B$. This is fine, as long as $B$ then jumps by the correct distance afterwards. Of course,

the choice of making $A$ jump before $B$ in the `Collide` procedure is arbitrary. Different orderings lead to different microscopic re-organizations of quasi-particles' positions at collisions, but to the same large-scale Euler hydrodynamics.

An acceleration due to an external field is implicitly implemented with the `Displace` procedure. There, the evolution of each quasi-particle changes, in general, both its position and its velocity, as per the usual physical laws for particles within external force fields. With an acceleration potential, it is possible that pairs of particles that collided, and thus were marked, meet again after a macroscopic time (for instance in a harmonic potential). We thus need to "unmark" marked pairs after a mesocopic time: a time that is larger than that characteristics of the microscopic dynamics, but smaller than typical macroscopic times after which particles can meet again. There is thus a "forgetting time" that needs to be set, and that depends on the detail of the external potential.

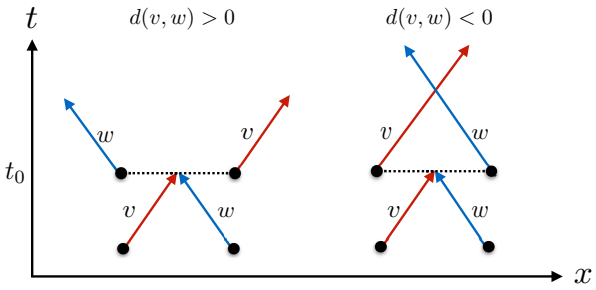


FIG. 2. A cartoon picture for collisions between quasi-particles with velocities $v$ and $w$. Upon a collision at time $t_0$, they move forward or backward depending on the sign of $d(v, w)$.

Other algorithms are possible. In particular, it is not necessary to perform jumps "instantaneously" at collisions; as long as the distance $d(\cdot, \cdot)$ is added to the trajectory in a microscopic time, the large-scale effect is the same. For instance, one may associate to each quasi-particle a "ghost velocity change" $\Delta v$, used for time evolution in order to add an appropriate distance, but not for the calculation of the jump distance (which uses the original spectral parameter and quasi-particle type). We choose an overall time $t_{\rm micro} > 0$. A quasi-particle either is in a "ghost" state ($\Delta v > 0$), or not ($\Delta v = 0$). We note the time $t_0$ of the start of a ghost state. Upon a collision of $A$ with $B$, we do $\Delta v := \Delta v + \Delta t/\texttt{distance}(A, B)$, so that within a time $\Delta t$, the correct distance is added. When entering a ghost state (at a collision), we set $\Delta t = t_{\rm micro}$, while for further collisions during the ghost state, we choose $\Delta t = t_{\rm micro} - t + t_0$, where $t$ is the time. The particle reverts to its normal state when $t - t_0 = t_{\rm micro}$.

## II. THE LIEB-LINIGER MODEL IN THE ATTRACTIVE REGIME

In first-quantized form, the Lieb-Liniger (LL) model is described by the Hamiltonian

$$H = -\frac{1}{2m}\sum_{j=1}^{N}\frac{\partial^2}{\partial x_j^2} + c\sum_{j_1<j_2}\delta(x_{j_1} - x_{j_2}). \tag{13}$$

With repulsive interaction, $c > 0$, the spectrum of Bethe excitations is composed of a single particles, and the differential scattering phase given by (4) (main text). The case of attractive interaction $c = -2\bar{c} < 0$ is however not simply obtained by replacing $c$ by $-2\bar{c}$ in (4) (main text). Instead, the spectrum of Bethe excitations is more complicated: it is composed of an infinity of Bethe strings, one for every positive length $j = 1, 2, 3, \ldots$. The attractive LL model is therefore classically implemented as a gas with infinitely-many species, representing the infinitely-many string lengths, all interacting with each other via a string-length- and velocity-dependent shift.

A thermodynamic Bethe ansatz analysis gives the following (we take $m = 1/2$ for simplicity). The energy and momentum functions, for a string of length $a$ with "pseudo-momentum" $\lambda$, are given by

$$E(\lambda, j) = j\lambda^2 - \frac{\bar{c}^2}{12}j(j^2 - 1), \quad p(\lambda, j) = j\lambda. \tag{14}$$

The velocity is therefore

$$v^{\rm gr}(\lambda, j) = 2\lambda \tag{15}$$

which allows us to parametrize energy and momentum functions in terms of velocities,

$$E(\boldsymbol{v}) = \frac{jv^2}{2} - \frac{\bar{c}^2}{12}j(j^2 - 1), \quad p(\boldsymbol{v}) = \frac{jv}{2}. \tag{16}$$

The differential scattering phase, expressed in the pseudo-momentum coordinates $\lambda$, is the following function:

$$\begin{aligned}&\varphi((\lambda, j), (\lambda', j'))\\ &= (1 - \delta_{j,j'})a_{|j-j'|}(\lambda - \lambda') + 2a_{|j-j'|+2}(\lambda - \lambda') + \ldots\\ &\quad \ldots + 2a_{j+j'-2}(\lambda - \lambda') + a_{j+j'}(\lambda - \lambda')\end{aligned} \tag{17}$$

where

$$a_j(\lambda) = \frac{j\bar{c}}{\lambda^2 + (j\bar{c}/2)^2}. \tag{18}$$

The above can be directly applied to the formulae presented in the main text, by taking pseudo-momenta $\lambda$ as "rapidities" (this is a good definition as the differential scattering phase depends on differences of pseudo-momenta), and identifying gas species $a$ with string lengths $j$.

## III. MONOTONICITY OF THE EFFECTIVE VELOCITY

Here we provide a demonstration that, under certain conditions on the differential scattering phase, the effective velocity is monotonic with $\theta$ (this is a fact that is used in the derivation in the main text).

Consider the case of a single particle in the spectrum:

$$v^{\rm eff}(\theta) = v^{\rm gr}(\theta) + \int {\rm d}\alpha\, \tilde\varphi(\theta,\alpha)\, \rho_{\rm p}(\alpha)\, (v^{\rm eff}(\alpha) - v^{\rm eff}(\theta)). \tag{19}$$

where $\tilde\varphi(\theta,\alpha) = \frac{\varphi(\theta,\alpha)}{p'(\theta)}$. Assume first that $\tilde\varphi(\theta,\alpha)$ is positive (and also that $\rho_{\rm p}(\theta)$ is positive) and that its derivative has the following sign (with $' = {\rm d}/{\rm d}\theta$):

$$(\theta-\alpha)\tilde\varphi'(\theta,\alpha) \le 0 \tag{20}$$

Assume also that $\theta$ parametrizes the group velocity in a monotonic fashion, $(v^{\rm gr})'(\theta) > 0$. Taking a derivative, we find

$$\begin{aligned}(v^{\rm eff})'(\theta) &= (v^{\rm gr})'(\theta) + \\ &+ \int {\rm d}\alpha\, \tilde\varphi'(\theta,\alpha)\, \rho_{\rm p}(\alpha)\, (v^{\rm eff}(\alpha) - v^{\rm eff}(\theta)) \; - \\ &- (v^{\rm eff})'(\theta) \int {\rm d}\alpha\, \tilde\varphi(\theta,\alpha)\, \rho_{\rm p}(\alpha)\end{aligned} \tag{21}$$

and thus

$$\begin{aligned}&\left(1 + \int {\rm d}\alpha\, \tilde\varphi(\theta,\alpha)\, \rho_{\rm p}(\alpha)\right) (v^{\rm eff})'(\theta) \\ &\quad = (v^{\rm gr})'(\theta) + \int {\rm d}\alpha\, \tilde\varphi'(\theta,\alpha)\, \rho_{\rm p}(\alpha)\, (v^{\rm eff}(\alpha) - v^{\rm eff}(\theta))\end{aligned}$$

Thanks to (20), the right-hand side of the latter equation is positive if $(v^{\rm eff})'(\theta) \ge 0$ for all $\theta$, and thus this latter condition is consistent with this integral equation. That is, if we assume that the solution is obtainable by recursion, starting with $(v^{\rm eff})'(\theta) = (v^{\rm gr})'(\theta)$, then the solution is monotonic. With decaying asymptotic for the particle density $\rho_{\rm p}(\alpha)$ it is easy to see that $v^{\rm eff}(\theta) \sim v^{\rm gr}(\theta)$ as $\theta \to \pm\infty$, and thus $v^{\rm eff}(\theta)$ covers full range of velocities.

All conditions, including (20), are satisfied in the Lieb-Liniger model and the sinh-Gordon model.

The condition on the sign of $\tilde\varphi(\theta,\alpha)$ may be relaxed, as long as

$$1 + \int {\rm d}\alpha\, \tilde\varphi(\theta,\alpha)\, \rho_{\rm p}(\alpha) > 0 \tag{22}$$

for all $\theta$.

## IV. ADDITIONAL NUMERICAL CHECKS

In the transport problem, in addition to the density, we have also verified numerically the accuracy of the current simulated by the classical flea gas as compared to the exact self-similar solution, in the Lieb-Liniger model. See Fig. 3. Again, the agreement is excellent, confirming the adequacy of the classical gas for representing GHD.

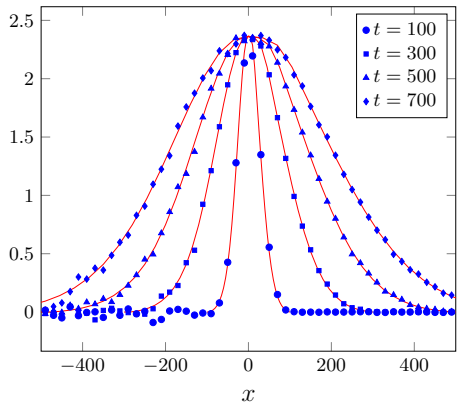


FIG. 3. GHD for the LL model with $m = 1$, $c = 1$ is simulated using the classical flea gas. Current profile from domain wall initial condition, initial left and right temperatures 10 and 1/3 (resp.), at times $t = 100, 300, 500, 700$. Simulation with approx. 2400 quasi-particles (initial baths of lengths 1000, open boundary condition) averaged over 1000 samples (blue); exact self-similar solution (red).

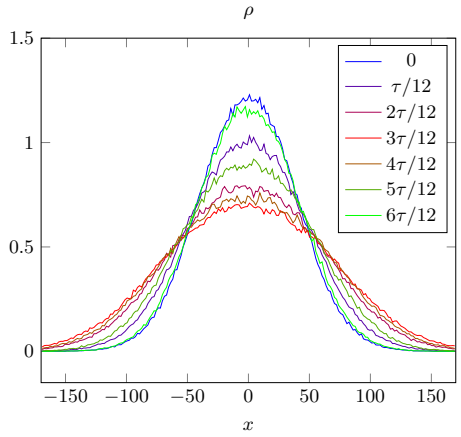


FIG. 4. Breathing motion of the LL model with $m = 1$, $c = 1$ occurring after change of frequency of a confining harmonic potential, simulated using the flea gas over half a period of the evolution potential. Colors go from blue (initial) to red (a quarter of a period) to green (half a period).

More interestingly, we have also simulated the "breathing motion" of the Lieb-Liniger model that is obtained after a change of the frequency of a harmonic potential. Consider adding a potential $V(x) = \omega_0^2 x^2/2$ to (13). The initial state is a thermal state within this potential, at temperature 1 (and throughout we keep $m = c = 1$). We then evolve this initial state within a wider potential, with $\omega = \omega_0/1.6$. The gas then expands and contracts in an almost periodic motion. The period is slightly larger than $\tau = 2\pi/\omega$ because of the interaction: particles are slowed down by the surrounding gas. See Fig 4 for an

illustration of half a period (this is the case $L = 100$ described below, with a sampling of 4000).

In order to verify the accuracy of the GHD equations (3) (main text), we have numerically evaluated its integral version: the result of integrating the left-hand side over a phase-space-time cell $\mathcal{C} = X \times T \times \Theta$, as $\int_{\mathcal{C}} \mathrm{d}x\, \mathrm{d}t\, \mathrm{d}\theta \times$(l.h.s. of GHD equations). Further, in order to verify how the accuracy is related to the length scales of the hydrodynamic approximation, we have considered two situations, with two different overall variation scales $L$ but with the same scattering length and the same range of interparticle distances.

We have chosen $L = 100$ and $L = 1000$. The initial particle density $\rho = \int \mathrm{d}\theta \rho_{\mathrm{cl}}(\theta)$ is supported mostly on $x \in [-L, L]$ and has a maximum 1.2 at the center $x = 0$. The central state at $x = 0$ is supported mostly on $\theta \in [-5, 5]$, and the evolution hamiltonian has period $\tau = 4L$. There are approximately $1.2L$ particles, and the "forgetting time" (see the description of the flea gas algorithm above) has been set to $\tau/10$. We have analyzed four types of cells: $|T| = L$ and $|T| = 3L$ (lengths of time of a quarter, and three quarter of a period), combined with $\Theta = \mathbb{R}$ and $\Theta = [-2, 2]$ (the full velocity space, and about half of the velocity support), in all cases choosing $|X| = L$. For $\Theta = \mathbb{R}$ we have looked at cells both around the center, $X = [-L/2, L/2]$, and nearer the boundary of the initial support, $X = [-4L/5, L/5]$, while for $\Theta = [-2, 2]$ we only consider the central cells. For each cell, we evaluated the relative error of the GHD equation, dividing by the total density and current on the boundaries of the cell (for simplicity we opted not to add the total force in the denominator):

$$E = \frac{\int_{X\times\Theta} \rho_{\mathrm{cl}}|_{\partial T} + \int_{T\times\Theta} (v^{\mathrm{eff}}\rho_{\mathrm{cl}})|_{\partial X} + \int_{X\times T} (-\partial_x V\, \rho_{\mathrm{cl}})|_{\partial\Theta}}{\int_{X\times\Theta} (\rho_{\mathrm{cl}}|_{T_+} + \rho_{\mathrm{cl}}|_{T_-}) + \int_{T\times\Theta} (|v^{\mathrm{eff}}\rho_{\mathrm{cl}}|_{X_+} + |v^{\mathrm{eff}}\rho_{\mathrm{cl}}|_{X_-})} \tag{23}$$

where $T_\pm$ and $X_\pm$ are the boundaries of $T = [T_-, T_+]$ and $X = [X_-, X_+]$, respectively. In all cases, we simulated the gas for a time $5\tau/4$ with $\Delta t = \tau/800$, and evaluated the average of $E$ over all cells with $T_-$ in the range from 0 up to $5\tau/4 - |T|$ (stepped by $\Delta t$). For finite-element approximations of integrals, we used this $\Delta t$, and $\Delta x = L/100$ and $\Delta\theta = 1/50$. The latter two also determine the sizes of fluid cells taken in order to evaluate densities. We used a sampling of 1000 for $L = 100$, and 100 for $L = 1000$ (in the latter case each fluid cell contains 10 times as many particles as in the former case, hence less sampling is necessary).

The results are as follows:

$X = [-L/2, L/2], |T| = L, \Theta = \mathbb{R}$ : 0.21% 0.10%
$X = [-L/2, L/2], |T| = 3L, \Theta = \mathbb{R}$ : 0.60% 0.10%
$X = [-4L/5, L/5], |T| = L, \Theta = \mathbb{R}$ : 0.31% 0.12%
$X = [-4L/5, L/5], |T| = 3L, \Theta = \mathbb{R}$ : 0.90% 0.16%
$X = [-L/2, L/2], |T| = L, \Theta = [-2, 2]$ : 0.23% 0.08%
$X = [-L/2, L/2], |T| = 3L, \Theta = [-2, 2]$ : 0.66% 0.08%

On the right-hand side, the first column of accuracies is for $L = 100$, the second is for $L = 1000$. The GHD equations are satisfied in all cases to quite high accuracy, showing that even for small numbers of particles, the hydrodynamic approximation is relatively accurate.

We note that the central cells probe regions of higher accuracy of the hydrodynamic approximation, as the particle density is higher and the actual variations of densities are lower. There are various trends in the accuracy, which are explainable as follows. (1) There is a large improvement from $L = 100$ to $L = 1000$, which is explained by the fact that as the variation length $L$ is increased, all other lengths being the same, the hydrodynamic approximation is improved. (2) In the case $L = 100$, accuracy is lost by taking cells with longer time span $|T|$; presumably because the larger errors due to the slight breaking of the hydrodynamic approximation accumulate. In the case $L = 1000$, there is no such loss in accuracy for the central cells, which might suggest that the finite accuracy, in this case, is mainly due to the finite-element approximation. For the boundary cell, which probes regions where the hydrodynamic approximation is less accurate, there is such a loss, but it is not as pronounced as in the case $L = 100$. (3) Accuracy is lost from the central cell to the boundary cell, again due to the fact that the hydrodynamic approximation looses is accuracy.

Thus the trends of the results are fully in agreement with the general expectations from hydrodynamic, and confirm the validity of the flea gas algorithm within force fields.

## 4.4 Low temperature dynamics of integrable systems

In this section, we review our work [70]. My main contribution in this work is to realize and explicitly show that 2HD (defined below) is actually equivalent to conventional hydrodynamics, which is a crucial observation that clarifies for the first time when conventional hydrodynamics can / cannot be applied to integrable systems. I also formulated the reduction of GHD equations to $2k$-HD equations with other authors, and numerically solved the 2HD equations, created some figures, and analyzed the behavior of their solutions.

The power of the GHD equation (4.5) is that the equation can predict the long-wavelength dynamics in which all the excitations from low-lying ones to highly-excitated ones participate. It is, however, always the case in equilibrium that only when low-lying excitations effectively contribute, a new low-temperature physics emerges, such as Luttinger liquids in one-dimensional gapless quantum systems [138]. In GHD, which is a tool to describe out-of-equilibrium physics, it turns out that the GHD equation indeed gets rather simplified when the dynamics stays in the vicinity of the ground state.

To illustrate the idea, let us consider the Lieb-Liniger model (4.12), which is a prototypical integrable system and is often used to characterize the dynamics of ultra-cold atom gases. The system is gapless, hence the ground state is constructed by filling the Fermi sea, i.e. the filling function (2.15) at $T = 0$ is given by $n(\theta) = \chi(\theta \in [-\theta_{\rm F}, \theta_{\rm F}])$, where $\chi$ is the indicator function [71]. Now, suppose that the system is driven out of equilibrium while staying close to the ground state during the dynamics. We then postulate that the filling function remains its form in the dynamics, or more generally, possesses the form of *zero-entropy state* that consists of $k$ distinctive dynamical Fermi seas, each of which is characterized by two dynamical Fermi velocities $\theta_j^-(x,t), \theta_j^+(x,t)$ [70]. Namely, we expect that the filling function can always be written as $n(\theta) = \chi(\theta \in \cup_{j=1}^k [\theta_j^-, \theta_j^+])$, which indeed gives a zero-entropy state. Plugging this into (4.6), we readily obtain the zero-entropy GHD equation [70]

$$\partial_t \theta_j^\pm + v_{\{\theta\}}^{\rm eff}(\theta_j^\pm)\partial_x \theta_j^\pm = 0, \tag{4.32}$$

where the effective velocity now resembles that of the zero-temperature Lieb-Liniger model

$$v_{\{\theta\}}^{\rm eff}(\alpha) = \alpha + \sum_j \int_{\theta_j^-}^{\theta_j^+} \frac{{\rm d}\gamma}{2\pi} \varphi(\alpha,\gamma)\rho_{\rm tot}(\gamma)(v_{\{\theta\}}^{\rm eff}(\alpha) - v_{\{\theta\}}^{\rm eff}(\gamma)), \tag{4.33}$$

where the dressed function $f^{\rm dr}(\theta)$ is defined by

$$f^{\rm dr}(\theta) = f(\theta) + \sum_j \int_{\theta_j^-}^{\theta_j^+} \frac{{\rm d}\alpha}{2\pi} \varphi(\theta,\alpha) f^{\rm dr}(\alpha). \tag{4.34}$$

We shall call the resulting zero-entropy hydrodynamics $2k$-HD. The above observation therefore indicates that, so long as the system remains in the space of zero-entropy states

in the course of time-evolution, the GHD equation for gapless integrable systems boil down to a simple finite-components coupled differential equations. Note that the zero-entropy GHD equation has only a finite number of components unlike the GHD equation parameterized by the continuous parameter $\theta$. This implies that $2k$-HD could develop *shocks*, which are solutions with sharp jumps. This is in stark contrast with the case in GHD where solutions of the GHD equation are made of a continuous family of contact discontinuities, which are free from any sharp (fine) structures. In ordinary fluid dynamics with finite component, the appearance of a shock is inevitable whenever the spatial profile of the system gets steeper, which amounts to the increase of entropy. Here is a crucial caveat: in contrast to conventional finite-components systems, the zero-entropy GHD never experiences any shock and the ensuing entropy generation. Rather, as soon as $2k$-HD develops sharp gradient, it immediately dissolves into $(2k+2)$-HD characterized by $k+1$ sets of dynamical Fermi seas (for instance, once 2HD creates a shock, it is taken over by 4HD). This is made possible by the arbitrarily large solution space of $2k$-HD, afforded by an infinite number of conservation laws. The mechanism behind the scenario is that, at the point when a shock is established in, say 2HD, the Fermi points $\theta^{\pm}$ get multivalued. To describe such multivalued Fermi points in a well-defined way, additional Fermi points are then employed so that a single Fermi point is assigned to each branch of a multivalued Fermi point. The dissolution of shocks was in fact already observed and analyzed in the free fermion model before [139–141], but our work shows that the same mechanism still holds in gapless quantum integrable systems [70].

Apart from the shock dissolution mechanism, it is noteworthy that 2HD can in fact be recast into the form of *conventional hydrodynamics* (CHD), which takes the standard form

$$\partial_t \rho + \partial_x (v\rho) = 0, \quad \partial_t v + v\partial_x v = -\frac{1}{m\rho}\partial_x \mathcal{P}, \tag{4.35}$$

where $\mathcal{P}(\rho)$ is the pressure at zero temperature, and is a function of $\rho$ only. The explicit mapping is presented in [70], whereby validating the use of CHD in describing the dynamics of the Lieb-Liniger model (of course, subject to the condition above) for the first time, solely from the principle of hydrodynamics. Until the discovery of GHD, CHD has been the main analytical tool to study the dynamics of the Lieb-Liniger model in the context of ultra-cold atoms [142–145], despite of the lack of justification. With the above observation, now we can justify the application of CHD in these studies so long as the system is close to the ground state and does not suffer from any shocks. Unless this condition is met, CHD generically fails to capture the dynamics correctly, and accordingly has to be superseded by GHD as evident from the recent experiment [106]. It is also worth pointing out that, specifically in the context of the low-temperature transport in the one-dimensional gapless systems, the effect of nonlinearity on top of the conventional Luttinger liquid was explored by means of nonlinear Luttinher liquid [146, 147]. Their results (spatio-temporal profile of local observables after the partitioning protocol near the ground state) are then confirmed to be agreeing with predictions from GHD and

numerics.

The validity of the $2k$-HD, and in particular the shock dissolution in passing from 2HD to 4HD, was confirmed against the flea gas simulation. Furthermore, the validity of 2HD until the appearance of shocks was corroborated against the stringent NRG-TSA ABACUS algorithm [148, 149].

# Large-scale description of interacting one-dimensional Bose gases: generalized hydrodynamics supersedes conventional hydrodynamics

Benjamin Doyon,[1] Jérôme Dubail,[2] Robert Konik,[3] and Takato Yoshimura[1]

[1] *Department of Mathematics, King's College London, Strand, London WC2R 2LS, UK*
[2] *CNRS & IJL-UMR 7198, Université de Lorraine, F-54506 Vandoeuvre-lès-Nancy, France*
[3] *Condensed Matter and Materials Science Division, Brookhaven National Laboratory, Upton, NY 11973 USA*

The theory of generalized hydrodynamics (GHD) was recently developed as a new tool for the study of inhomogeneous time evolution in many-body interacting systems with infinitely many conserved charges. In this letter, we show that it supersedes the widely used conventional hydrodynamics (CHD) of one-dimensional Bose gases. We illustrate this by studying "nonlinear sound waves" emanating from initial density accumulations in the Lieb-Liniger model. We show that, at zero temperature and in the absence of shocks, GHD reduces to CHD, thus for the first time justifying its use from purely hydrodynamic principles. We show that sharp profiles, which appear in finite times in CHD, immediately dissolve into a higher hierarchy of reductions of GHD, with no sustained shock. CHD thereon fails to capture the correct hydrodynamics. We establish the correct hydrodynamic equations, which are finite-dimensional reductions of GHD characterized by multiple, disjoint Fermi seas. We further verify that at nonzero temperature, CHD fails at all nonzero times. Finally, we numerically confirm the emergence of hydrodynamics at zero temperature by comparing its predictions with a full quantum simulation performed using the NRG-TSA-ABACUS algorithm. The analysis is performed in the full interaction range, and is not restricted to either weak- or strong-repulsion regimes.

***Introduction.*** Modern experiments with ultracold atoms confined in "cigar-shaped" traps [1, 2] or in atom chips [3] provide real-world implementations of one-dimensional (1d) many-body systems [4], and represent an important challenge for theoretical physics. Even though it is widely accepted that 1d clouds of bosonic atoms are described, at the microscopic scale, by the paradigmatic Lieb-Liniger (LL) model [5, 6], solving this model in experimentally relevant out-of-equilibrium inhomogeneous situations for more than a few dozens of atoms is a task that is out of the reach of modern theoretical methods, including state-of-the-art numerical ones.

Yet, it is a classic result of XX$^{\text{th}}$ century mathematical physics that, in its homogeneous, translation-invariant version at equilibrium, the LL model is exactly solvable by means of the Bethe ansatz [7], and its equation of state can be calculated exactly [8]. It then seems reasonable to use this equation of state as the basic input into a coarse-grained, hydrodynamic, approach, that is expected to be applicable as soon as typical lengths of variations of the local density are large enough as compared to inter-particle and scattering distances (the Euler scale) – in much the same way that classical hydrodynamics describes water waves. Such a "conventional hydrodynamic" (CHD) approach – defined in Eqs. (10) below –, has been used extensively in the cold atoms literature over the past decade [9–11], and has sometimes been viewed as a consequence of the Gross-Pitaevskii equation [6, 11] in the regime of small interaction strength.

However, a key physical feature of the LL model is overlooked in CHD: the fact that it admits infinitely many conservation laws. Indeed, CHD focuses only on a few quantities, like the particle density, the momentum density or the energy density. But the LL model possesses infinitely more conserved quantities. Those are not just a mathematical curiosity: they can have dramatic physical consequences, as illustrated by the quantum Newton cradle experiment [2]: the crucial observation of undamped oscillations in this experiment is connected with the lack of conventional thermalization [12].

The full connection between generalized thermalization and many-body dynamics was only recently uncovered [13, 14]. The fundamental precepts of hydrodynamics – the emergence of local entropy maximization – were used in systems with an infinite number of conservation laws in order to form the theory of generalized hydrodynamics (GHD). It is a type of Euler-scale hydrodynamics, but with an infinite-dimensional space of fluid states accounting for the large state manifold accessible by generalized thermalization. In practice, GHD consists in an infinite set of coupled continuity equations (one for each conserved charge), that can, at least in principle, be worked out with numerical solvers for non-linear partial differential equations.

In this letter, we show that GHD supersedes CHD. For this purpose, we focus on far-from-equilibrium waves emanating from a density accumulation in the LL model. The density waves are a good illustration for our purposes, but the main results and mechanisms are general. They have been studied in several ways in the past decade in the free Fermi gas [15], in the effective theory of the non-linear Luttinger liquid [18], and in the Calogero-Sutherland model [16], quantum Hall edges [17], and the LL model [10] using CHD. In particular, all these references – see also [11] – pointed out that the applicability of CHD was limited by the appearance of shocks. In this Letter, we show that GHD is the proper hydrodynamic framework to go beyond the latter.

We demonstrate that, only at zero temperature and for finite evolution times does CHD coincide with GHD. CHD being a finite-component hydrodynamics, it inevitably leads to "gradient catastrophes" and shock propagations thereon. In contrast, we show that at zero entropy, GHD decomposes into a hierarchy of instantaneously invariant finite-dimensional subspaces, whose exact hydrodynamic equations we establish. These are described by a multitude of Fermi seas, the stability of which is a consequence of integrability. We show that shocks dissolve as the system leaves the CHD subspace into a higher-dimensional reduction of GHD. No shock propagates in this process, as instead smoothness is reestablished. We note that an important practical consequence of the zero-entropy reduction is that the infinite system of coupled non-linear equations of GHD collapses to a finite number of equations that are computationally easy to solve, taking typically a few minutes on a laptop. We also numerically verify that at nonzero temperature, the GHD evolution, which necessitates the full infinite-dimensional space, is different from CHD at all times. In the density wave problem, a stark difference is that no sharp profile develops in GHD, while CHD based on the finite-temperature LL equations of state has gradient catastrophes. Finally, at zero temperature and using a local density approximation for the initial fluid state, we compare the hydrodynamic prediction for the space-time density profile with a simulation of the full quantum model obtained from the NRG-TSA-ABACUS algorithm [19–21], and find perfect agreement.

***GHD.*** The Hamiltonian of the repulsive LL model is

$$H = \int \mathrm{d}x \left( \frac{1}{2m} \partial_x \psi^\dagger \partial_x \psi + \frac{c}{2} \psi^\dagger \psi^\dagger \psi \psi \right), \quad c > 0 \quad (1)$$

for the complex bosonic field $\psi(x)$, where $m$ is the mass (we set $\hbar = 1$ throughout the manuscript). An inhomogeneous initial state $\langle \cdots \rangle$, to be specified below, is set to evolve unitarily with $H$.

Since the LL model is integrable, it admits infinitely many conservation laws $\partial_t q_i + \partial_x j_i = 0$. This includes the gas density $q_0 = \psi^\dagger \psi$, the momentum density $q_1 = -\mathrm{i}\psi^\dagger \partial_x \psi + h.c.$, and the energy density $q_2$ (the integrand in (1)). According to the principles of hydrodynamics, if averages of conserved densities $\langle e^{\mathrm{i}Ht} q_i(x) e^{-\mathrm{i}Ht} \rangle$ and currents $\langle e^{\mathrm{i}Ht} j_i(x) e^{-\mathrm{i}Ht} \rangle$ have smooth enough space-time profiles, they can be described by space-time dependent local states that have maximized entropy with respect to the conserved charges afforded by the dynamics. Eulerian hydrodynamics, which neglects viscosity effects and is valid at large scales, is formed of the ensuing macroscopic conservation laws. In integrable systems, entropy maximization leads to generalized Gibbs ensembles (GGEs) [12, 22] with (formal) density matrix $\rho_{\mathrm{GGE}} = e^{-\sum_i \beta_i Q_i}$, $Q_i = \int q_i(x) \mathrm{d}x$. Therefore, $\langle e^{\mathrm{i}Ht} \mathcal{O}(x) e^{-\mathrm{i}Ht} \rangle \approx \mathrm{tr}[\rho_{\mathrm{GGE}}(x,t)\mathcal{O}]$, where the only space-time dependence is in $\rho_{\mathrm{GGE}}(x,t)$. The macroscopic conservation laws of generalized hydrodyamics (GHD) are the infinite number of equations for the density averages $\mathtt{q}_i(x,t) = \mathrm{tr}[\rho_{\mathrm{GGE}}(x,t) q_i]$ and the current averages $\mathtt{j}_i(x,t) = \mathrm{tr}[\rho_{\mathrm{GGE}}(x,t) j_i]$:

$$\partial_t \mathtt{q}_i + \partial_x \mathtt{j}_i = 0. \quad (2)$$

The set of $\mathtt{q}_i$ fixes the GGE state, and thus can be seen as a set of fluid variables for GHD. In the manifold of GGE states, the currents $\mathtt{j}_i$ have a fixed functional form in terms of the densities $\mathtt{q}_i$: these are the equations of state, which fully determine the GHD model at hand.

An efficient treatment of hydrodynamics requires an appropriate choice of fluid variables. Instead of the $\mathtt{q}_i$, the most powerful fluid variables are obtained in terms of the emerging quasi-particles of the integrable model. In the repulsive LL model, there is a single quasi-particle species. The interaction in the LL model is fully described by the two-particle scattering matrix $S(\theta - \theta')$, a function of velocity differences. The object of importance is the differential scattering phase [7],

$$\varphi(\theta) = -\mathrm{i} \frac{\mathrm{d}}{\mathrm{d}\theta} \log S(\theta) = 2c/(\theta^2 + c^2). \quad (3)$$

The quasi-particle can be seen as a spinless real fermion, which is free in the Tonks-Girardeau (TG) limit $c = \infty$ (hard-core repulsion).

States $|\theta_1, \ldots, \theta_N\rangle$ are described by the velocities $\theta_k$ of the quasi-particles. Each conserved charge $Q_i$ is characterized by its one-particle eigenvalue $h_i(\theta) \propto \theta^i$, with $Q_i|\theta, \ldots, \theta_N\rangle = \sum_k h_i(\theta_k)|\theta_1, \ldots, \theta_N\rangle$. For instance, the particle number has eigenvalue $h_0(\theta) = 1$, the momentum $h_1(\theta) = p(\theta) = m\theta$, and the energy $h_2(\theta) = E(\theta) = m\theta^2/2$. In the thermodynamic limit, the eigenstates are expressed in terms of $\rho_{\mathrm{p}}(x,\theta)\mathrm{d}x\mathrm{d}\theta$, the number of quasi-particles in the phase-space region $[x, x + \mathrm{d}x] \times [m\theta, m(\theta + \mathrm{d}\theta)]$, leading to average densities $\mathtt{q}_i = \int \mathrm{d}\theta\, \rho_{\mathrm{p}}(\theta) h_i(\theta)$. The most convenient fluid variable is the occupation function $n(\theta) = \rho_{\mathrm{p}}(\theta)/\rho_{\mathrm{s}}(\theta)$, where $\rho_{\mathrm{s}}$ is the state density, $2\pi\rho_{\mathrm{s}}(\theta) = m + \int \mathrm{d}\alpha\, \varphi(\theta - \alpha)\rho_{\mathrm{p}}(\alpha)$. The density and current averages take the form [13],

$$\mathtt{q}_i = m \int \frac{\mathrm{d}\theta}{2\pi}\, n(\theta)\, h_i^{\mathrm{dr}}(\theta), \quad \mathtt{j}_i = m \int \frac{\mathrm{d}\theta\, \theta}{2\pi}\, n(\theta)\, h_i^{\mathrm{dr}}(\theta) \quad (4)$$

where the dressing operation is defined by

$$f^{\mathrm{dr}}(\theta) = f(\theta) + \int \frac{\mathrm{d}\alpha}{2\pi}\, \varphi(\theta - \alpha) n(\alpha) f^{\mathrm{dr}}(\alpha). \quad (5)$$

These establish a relation between the $\mathtt{j}_i$'s and the $\mathtt{q}_i$'s, and thus the equations of state. For the LL model they were derived in [13] by extending the theory of (generalized) TBA [20, 23].

It was realized in [13, 14] that demanding the continuity equations (2) together with the averages (4) implies the continuity equation at the level of quasi-particles:

$$\partial_t n(\theta) + v^{\mathrm{eff}}(\theta) \partial_x n(\theta) = 0, \quad (6)$$

where the effective velocity $v^{\rm eff}(\theta)$ is the velocity of elementary excitations [24]

$$v^{\rm eff}(\theta) = \frac{(E')^{\rm dr}(\theta)}{(p')^{\rm dr}(\theta)} = \frac{{\rm id}^{\rm dr}(\theta)}{1^{\rm dr}(\theta)} \tag{7}$$

with ${\rm id}(\theta) = \theta$. These are the GHD equations in terms of quasi-particle fluid variables in the LL model. Since $v^{\rm eff}(\theta)$ depends on the fluid state through the function $n$, these are nonlinear equations for an infinity of functions of space-time (one for each velocity $\theta$).

Some intuition into Eqs. (6), (7) can be gained by looking at the TG limit $c = \infty$. In this case, $n(\theta)$ is the fermion occupation number at each momentum $m\theta$, at position $x$. This is the Wigner function of the state [25] (the partial Fourier transform of the fermion-fermion correlator). The effective velocity is equal to the particle velocity, $v^{\rm eff}(\theta) = \theta$, and (6) simply reproduces the exact evolution equation for the Wigner function, a direct consequence of the Schrödinger equation, as exploited in [15, 26] (see also the Supplementary Material (SM)). The quasi-particle occupation $n(\theta)$ may thus be viewed as the generalization of the Wigner function to non-free-fermion systems, with time-evolution governed by GHD (6)-(7).

***Zero-entropy GHD.*** Natural initial conditions are ground states within inhomogeneous potentials $V(x)$,

$$H_V = \int {\rm d}x \left( \frac{1}{2m} \partial_x \psi^\dagger \partial_x \psi + \frac{c}{2} \psi^\dagger \psi^\dagger \psi \psi + V(x) \psi^\dagger \psi \right). \tag{8}$$

With a slowly varying potential, local averages are well described by a local-density approximation (LDA) [6]. LDA provides a GHD initial condition, a fluid of local zero-temperature states, which at every point $x$ is the ground state of $H + V(x)Q_0$. In this section, we observe that GHD equations give rise to finite-dimensional hydrodynamics when one restricts to the subspace of fluid states with zero entropy such as those. An analogous observation was made previously for free fermions [15] and for the Calogero-Sutherland model [16].

Recall that the occupation function at zero temperature is $n_{T=0}(\theta) = \chi(\theta \in [-\theta_{\rm F}, \theta_{\rm F}])$ (where $\chi$ is the indicator function) where $\theta_{\rm F}$ is the Fermi pseudo-velocity, which depends on the chemical potential. Let us consider the space of zero-entropy occupation functions which have exactly $2k$ jumps, characterized by $2k$ velocities $\cdots < \theta_{j-1}^+ < \theta_j^- < \theta_j^+ < \theta_{j+1}^- < \cdots$ bounding separate Fermi seas: $n(\theta) = \chi(\theta \in \cup_{j=1}^k [\theta_j^-, \theta_j^+])$. We show that under GHD evolution, any smooth fluid whose state lies in such a space at all positions $x$, stays so for short enough times. Time evolution leads to displacements of Fermi points. Thus at zero entropy, GHD is reduced to hydrodynamics with a finite number of fluid variables.

Indeed we have $\partial_x n(\theta) = -\sum_{\epsilon=\pm} \sum_{j=1}^k \epsilon \partial_x \theta_j^\epsilon \, \delta(\theta - \theta_j^\epsilon)$, and thus the time derivative $\partial_t n(\theta)$ is supported on the finite set of velocities $\theta_j^\pm$. A solution to (6) is therefore provided by setting $\theta_j^\pm = \theta_j^\pm(x,t)$ with

$$\partial_t \theta_j^\pm + v^{\rm eff}_{\{\theta\}}(\theta_j^\pm) \partial_x \theta_j^\pm = 0. \tag{9}$$

We expect the solution to (6) in the space of smooth fluid space-time functions to be unique, based on such rigorous results in related classical gases [27]. Thus it is given by solving (9) as long as no shock develops. Here, more explicitly, the effective velocity is $v^{\rm eff}_{\{\theta\}}(\alpha) = {\rm id}^{\rm dr}_{\{\theta\}}(\alpha)/1^{\rm dr}_{\{\theta\}}(\alpha)$ with the dressing operation $f^{\rm dr}_{\{\theta\}}(\alpha) = f(\alpha) + \sum_{j=1}^k \int_{\theta_j^-}^{\theta_j^+} {\rm d}\gamma \, \varphi(\alpha - \gamma) f^{\rm dr}_{\{\theta\}}(\gamma)$. The resulting equations (9) will be referred to as $2k$-hydrodynamics ($2k$HD).

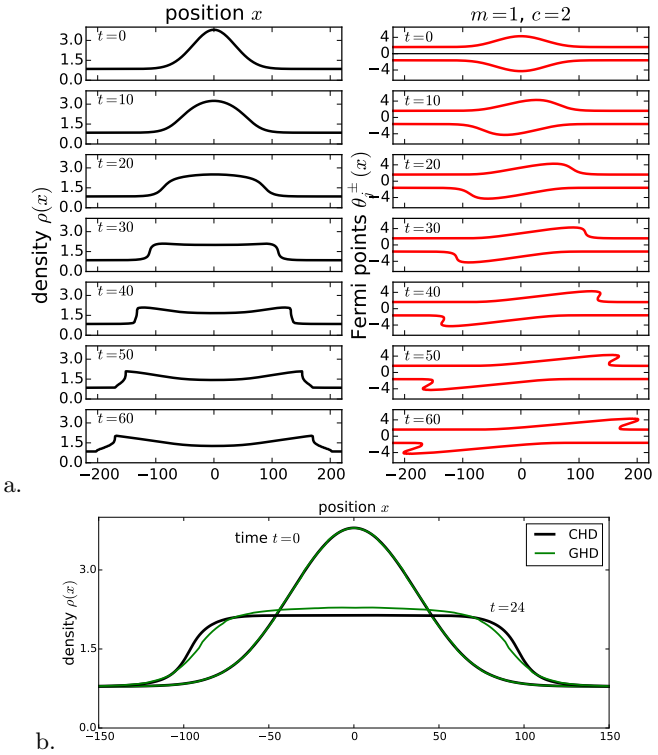


FIG. 1. (a) Left: density profile of LL gas suddenly released from a gaussian potential $V(x) = -5e^{-(\frac{x}{50})^2} - 1$. Right: Corresponding Fermi points $\theta_j^\pm(x)$. Initially, there are only $k = 2$ Fermi points, but after the shock at $t \simeq 37$, there is a region where the red curve is multi-valued, corresponding to $k = 4$ Fermi points. (b) Same setup at finite temperature: the initial state is obtained from LDA at temperature $T = 1$. After finite time, CHD quantitatively differs from GHD. Moreover, at a later time $t \simeq 35$, CHD has a shock (see the SM); in contrast, GHD has no shock.

Eqs (9) are Euler-type hydrodynamic equations for a fluid with finitely-many components. Finite-component fluids are expected to develop shocks. Therefore, Eqs (9) are expected to hold *only for finite times*. However, contrary to true conventional finite-component fluids, where viscosity effects, present beyond the Euler scale, dominate and produce entropy at shocks, the presence of infinitely-many conservation laws forbids sustained entropy production in GHD. Any shock instantaneously dissolves into the higher-dimensional solution space of GHD. More precisely, $2k$HD solutions become multivalued at the time of the appearance of the shock, but here

this multivaluedness is physically meaningful, representing a higher number of Fermi seas. Thus shocks in $2k$HD resolve by increasing the number of Fermi seas, passing to $(2k+2)$HD. We exemplify this in Fig. 1a, where after $t_{shock} = 37$ we begin to simulate, effectively, 4HD equations. This has previously been observed in free fermion models [15], thanks to an analysis based on the Wigner function; here it is generalized to the fully interacting LL model. We have also confirmed this shock dissolution mechanism of GHD in a nontrivial classical gas with the same hydrodynamic equations as those of the LL model [28].

***GHD and conventional hydrodynamics (CHD).*** Starting with a smooth fluid of local zero-temperature states, GHD reduces to 2HD, where every local fluid cell is the Galilean boost of a zero-temperature state. As a consequence, 2HD is in fact equivalent to the conventional hydrodynamics (CHD) of Galilean fluids,

$$\partial_t \rho + \partial_x (v\rho) = 0, \quad \partial_t v + v\partial_x v = -\frac{1}{m\rho}\partial_x \mathcal{P} \qquad (10)$$

where $\rho = \mathtt{q}_0$ is the fluid density and $\mathcal{P}$ is the pressure [30]. The first equation is conservation of mass, the second, of momentum. The pressure $\mathcal{P} = \mathcal{P}(\rho)$ gives the equations of state of the fluid, and here equals the momentum current $\mathtt{j}_1$ in the zero-temperature state with density $\rho$. The explicit equations of state are obtained from (4) and (5) (see SM [30]).

CHD has been used as an important tool in analyzing the dynamics of 1d Bose gases [9–11]. It has sometimes been presented as a consequence of the Gross-Pitaevskii equation [6]—itself valid only in the limit of small interaction strength $c$—, and it was never quite clear what exactly the range of validity of CHD was in the full interaction range of the LL model. Our analysis clearly shows that CHD is valid —in the sense that it coincides with GHD— *only at zero temperature*, and *before the first shock*. We conclude that, *in any other situation, CHD is not applicable and leads to quantitatively wrong results.* To illustrate this, a comparison of CHD at finite temperature and GHD is shown in Fig.1b; the initial state is the same in both cases (obtained from LDA at finite temperature), but one sees that the density profiles differ significantly at finite time; moreover, CHD has solutions up to a finite shock time, while GHD has no shocks and has solutions at arbitrarily long times [32].

***Comparison with microscopic simulation of the LL model.*** We consider evolution from the ground state of (8) with a background chemical potential $\mu_\infty$ perturbed by a Gaussian, $V(x) = -\mu_\infty - Ue^{-ax^2}$. The initial density profile accumulates around $x = 0$, and is asymptotically nonzero. Two procedures are compared: (1) the ground state is exactly evaluated using the NRG-TSA-ABACUS algorithm [20, 21, 34], and then evolved unitarily; and (2) the ground state is approximated using LDA, and this initial fluid state is evolved using 2HD (see the SM for a review of standard conditions for the hydrodynamic regime, which are fulfilled by the choice of parameters below). Fig. 2 provides the result for a choice of parameters corresponding to the local dimensionless coupling $\gamma(x) = mc/\rho(x)$ of the order of 1, thus the system is in an intermediate regime with nontrivial interactions being important. We observe that GHD is in excellent agreement with NRG-TSA-ABACUS numerics at almost all times except near the right and left boundaries at $t = 72$, and provides a substantially better approximation than linear sound waves (see the SM). It can also be seen that, since $v^{\rm eff}_{\{\theta\}}(\theta^+)$ is always greater than the background Fermi velocity corresponding to $\mu_\infty$, the propagation speed of 2HD is larger than that of the sound wave. It is remarkable that the complex (zero-temperature) dynamics of the LL gas is exactly described by 2HD, a simple set of differential equations.

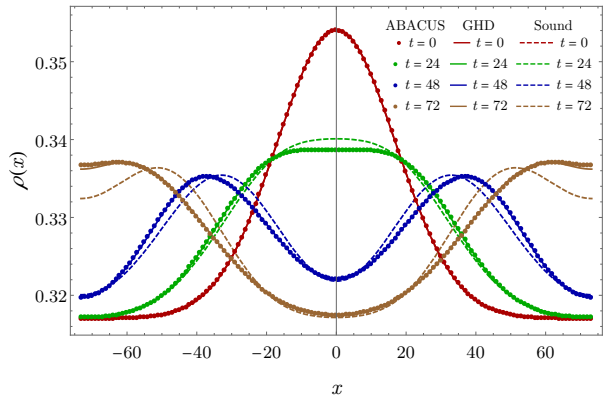


FIG. 2. The density profile under the evolution with $2m = 1$, $c = 1$, $U = 0.03$, $a = 1/576$, and a choice of $\mu_\infty$ such that there are $N = 48$ particles in the ground state. We use periodic boundary conditions. Points show NRG-TSA-ABACUS data, full line the GHD simulation, and dotted line a linear sound wave approximation.

At large times, discrepancies, though very tiny in the above graph, are expected to emerge. One reason is that, as explained above, shocks attempt to form, and as variations become larger, conditions for the hydrodynamic regime break down. Higher-derivative effects, such as viscosity, become more important. Recent observations in the related hard rod gas [42] suggest however that such higher-derivative effects play only a small role. Another cause for late-time discrepancy is that LDA is not exact. As higher-order charges are more sensitive to the large-scale variations of the potential, LDA gives an extremely good approximation to the particle density, but describes poorly densities of higher-order charges $Q_i$. As time passes, the effects of the latter under the full GHD evolution eventually breaks 2HD. An analysis of the Wigner function $n(\theta)$ at the free-fermion point $c = \infty$, where GHD is exact (no viscosity is neglected), gives further insight (see the SM).

***Conclusion.*** We showed that widely used conven-

tional hydrodynamics of the Lieb-Liniger model correctly describes interacting Bose gases, but that this holds only at zero temperatures and for finite times. We provided exact, simple hydrodynamic equations valid beyond gradient catastrophes, where no shocks are sustained. These are zero-entropy reductions of GHD, which are finite-component fluid equations easily solvable on a laptop. This suggests that fluids of integrable models avoid entropy production thanks to the large space of fluid states. We provided compelling evidence for the emergence of GHD in the LL gas in the limit of slow variations of the density profile. This provides a crucial dynamical extension of LDA that is valid beyond previously existing frameworks. As a future direction, it would be very interesting to apply our method to more experimentally relevant situations such as "Quantum Newton's cradle"-type protocol [2], known to be beyond the reach of CHD [11].

***Acknowledgements:*** We are extremely grateful to J.-S. Caux for access to the ABACUS software package without which the Lieb-Liniger simulations reported here would not have been possible. We thank B. Bertini, M. Fagotti, and H. Spohn for stimulating discussions, and the anonymous referees for useful comments. TY is grateful for the support from the Takenaka Scholarship Foundation and the hospitality at the Tokyo Institute of Technology. BD and JD thank the IESC Cargèse for hospitality. RMK's research effort here was supported by the U.S. Department of Energy, Office of Basic Energy Sciences, under Contract No. DE- AC02-98CH10886.

[1] H. Moritz, T. Stöferle, M. Köhl and T. Esslinger, "Exciting collective oscillations in a trapped 1d gas", Phys. Rev. Lett. **91**, 250402 (2003); T. Kinoshita, T. Wenger and D. S. Weiss, "Observation of a one-dimensional Tonks-Girardeau gas", Science **305**, 1125 (2004); T. Stöferle, H. Moritz, C. Schori, M. Köhl and T. Esslinger, "Transition from a strongly interacting 1d superfluid to a Mott insulator", Phys. Rev. Lett. **92**, 130403 (2004); A. Vogler, R. Labouvie, F. Stubenrauch, G. Barontini, V. Guarrera and H. Ott "Thermodynamics of strongly correlated one-dimensional Bose gases", Phys. Rev. A 88, 031603(R) (2013); F. Meinert, M. Panfil, M.J. Mark, K. Lauber, J.-S. Caux and H.-C. Nägerl, "Probing the excitations of a Lieb-Liniger gas from weak to strong coupling", Phys. Rev. Lett. **115**, 085301 (2015).

[2] T. Kinoshita, T. Wenger and D. S. Weiss, "A Quantum Newton's Cradle", Nature **440**, 900-903 (2006).

[3] J. Esteve, J.-B. Trebbia, T. Schumm, A. Aspect, C. I. Westbrook and I. Bouchoule, "Observations of Density Fluctuations in an Elongated Bose Gas: Ideal Gas and Quasicondensate Regimes", Phys. Rev. Lett. 96, 130403 (2006); A. H. van Amerongen, J. J. P. van Es, P. Wicke, K. V. Kheruntsyan and N.J. van Druten, "Yang-Yang Thermodynamics on an Atom Chip", Phys. Rev. Lett. **100**, 090402 (2008); B. Fang, G. Carleo, A. Johnson and I. Bouchoule, "Quench-Induced Breathing Mode of One-Dimensional Bose Gases", Phys. Rev. Lett. 113, 035301 (2014); T. Langen, S. Erne, R. Geiger, B. Rauer, T. Schweigler, M. Kuhnert, W. Rohringer, I. E. Mazets, T. Gasenzer and J. Schmiedmayer, "Experimental Observation of a Generalized Gibbs Ensemble", Science **348**, 207 (2015); B. Fang, A. Johnson, T. Roscilde and I. Bouchoule, "Momentum-Space Correlations of a One-Dimensional Bose Gas" Phys. Rev. Lett. 116, 050402 (2016).

[4] T. Giamarchi, "Quantum Physics in One Dimension" (Oxford University Press, Oxford), 2004.

[5] M. Olshanii, "Atomic Scattering in the Presence of an External Confinement and a Gas of Impenetrable Bosons", Phys. Rev. Lett. 81, 938 (1998).

[6] M.A. Cazalilla, R. Citro, T. Giamarchi, E. Orignac and M. Rigol, "One dimensional bosons: from condensed matter systems to ultracold gases", Rev. Mod. Phys. **83**, 1405 (2011).

[7] E.H. Lieb and W. Liniger, "Exact analysis of an interacting Bose gas. I. The general solution and the ground state", Phys. Rev. **130**(4), 1605 (1963); F. Berezin, G. Pokhil and V. Finkelberg, "Schrödinger equation for a system of 1d particles with point interaction", Vestnik MGU **1**, 21 (1964).

[8] C. N. Yang and C. P. Yang, "Thermodynamics of a One-Dimensional System of Bosons with Repulsive Delta-Function Interaction", J. Math. Phys. 10 , 1115 (1969).

[9] S. Stringari, "Dynamics of Bose-Einstein Condensed Gases in Highly Deformed Traps", Phys. Rev. A **58**, 2385 (1998); C. Menotti and S. Stringari, "Collective oscillations of one-dimensional Bose-Einstein gas in a time-varying trap potential and atomic scattering length", Phys. Rev. A **66**, 043610 (2002); P. Öhberg and L. Santos,"Dynamical transition from a quasi-one-dimensional Bose-Einstein condensate to a Tonks-Girardeau gas", Phys. Rev. Lett. **89**, 240402 (2002); P. Pedri, L. Santos, P. hberg and S. Stringari, "Violation of Self-similarity in the Expansion of a One-dimensional Bose gas", Phys. Rev. A 68, 043601 (2003); A. Campbell, D. Gangardt and K. Kheruntsyan, "Sudden Expansion of a One-Dimensional Bose Gas from Power-Law Traps", Phys. Rev. Lett. **114**, 125302 (2015); I. Bouchoule, S. S. Szigeti, M. J. Davis and K. V. Kheruntsyan, "Finite-temperature Hydrodynamics for One-dimensional Bose gases: Breathing-mode Oscillations as a Case Study", Phys. Rev. A **94**, 051602(R) (2016).

[10] B. Damski, "Shock waves in a one-dimensional Bose gas: From a Bose-Einstein condensate to a Tonks gas", Phys. Rev. A 73 (4), 043601 (2006); A.D. Sarishvili, I.V. Protopopov and D.B. Gutman, "Pulse propagation in interacting one dimensional Bose liquid", Phys. Rev. B **94**, 045110 (2016).

[11] S. Peotta and M. Di Ventra, "Quantum shock waves and population inversion in collisions of ultracold atomic clouds", Phys. Rev. A **89**, 013621 (2014).

[12] M. Rigol, V. Dunjko, V. Yurovsky and M. Olshanii, "Relaxation in a Completely Integrable Many-Body Quantum System: An Ab Initio Study of the Dynamics of the Highly Excited States of 1D Lattice Hard-Core Bosons", Phys. Rev. Lett. **97**, 050405 (2007); M. Rigol, V. Dunjko

and M. Olshanii, "Thermalization and its mechanism for generic isolated quantum systems", Nature **452**, 854-858 (2008).

[13] O. A. Castro-Alvaredo, B. Doyon and T. Yoshimura, "Emergent Hydrodynamics in Integrable Quantum Systems Out of Equilibrium ", Phys. Rev. X **6**, 041065 (2016).

[14] B. Bertini, M. Collura, J. De Nardis and M. Fagotti, "Transport in Out-of-Equilibrium XXZ Chains: Exact Profiles of Charges and Currents", Phys. Rev. Lett. **117**, 207201 (2016).

[15] E. Bettelheim, A.G. Abanov and P. Wiegmann, "Orthogonality Catastrophe and Shock Waves in a Nonequilibrium Fermi Gas", Phys. Rev. Lett. **97**, 246402 (2006); E. Bettelheim, A.G. Abanov and P.B. Wiegmann, "Quantum hydrodynamics and nonlinear differential equations for degenerate Fermi gas", J. Phys. A: Math. Theor. 41 392003 (2008); E. Bettelheim and L. Glazman, "Quantum Ripples Over a Semiclassical Shock", Phys. Rev. Lett. **109**, 260602 (2012); I.V. Protopopov, D.B. Gutman, P. Schmitteckert and, A.D. Mirlin, "Dynamics of Waves in one-dimensional Electron Systems: Density Oscillations Driven by Population Inversion", Phys. Rev. B **87**, 045112 (2013).

[16] A.G. Abanov and P. B. Wiegmann, "Quantum Hydrodynamics, the Quantum Benjamin-Ono Equation, and the Calogero Model", Phys. Rev. Lett. **95**, 076402 (2005); A.G. Abanov, E. Bettelheim and P. Wiegmann, "Integrable hydrodynamics of Calogero-Sutherland model: bidirectional Benjamin-Ono equation", J. Phys. A: Math. Theor. 42 135201 (2009).

[17] E. Bettelheim, A.G. Abanov and P. Wiegmann, "Nonlinear Quantum Shock Waves in Fractional Quantum Hall Edge States", Phys. Rev. Lett. **97**, 246401 (2006).

[18] I.V. Protopopov, D.B. Gutman, M. Oldenburg and A.D. Mirlin, "Dissipationless kinetics of one-dimensional interacting fermions", Phys. Rev. B **89**, 161104(R) (2014).

[19] J.-S. Caux, "Correlation functions of integrable models: a description of the ABACUS algorithm", J. Math. Phys. **50**, 095214 (2009); J.-S. Caux, P. Calabrese and N. Slavnov, "Dynamics of the attractive 1D Bose gas: analytical treatment from integrability", J. Stat. Mech. **2007** P01008 (2007); J.-S. Caux and P. Calabrese, "Dynamical density-density correlations in the one-dimensional Bose gas", Phys. Rev. A **74**, 031605 (2006).

[20] J.-S. Caux and R. M. Konik, "Constructing the generalized Gibbs ensemble after a quantum quench", Phys. Rev. Lett. **109**, 175301 (2012).

[21] R. M. Konik and Y. Adamov, "A Numerical Renormalization Group for Continuum One-Dimensional Systems", Phys. Rev. Lett. **98**, 147205 (2007).

[22] A. Polkovnikov, K. Sengupta, A. Silva and M. Vengalattore, "Colloquium: nonequilibrium dynamics of closed interacting quantum system", Rev. Mod. Phys. **83**, 863 (2011); C. Gogolin and J. Eisert, "Equilibration, thermalisation, and the emergence of statistical mechanics in closed quantum systems: a review", Rep. Prog. Phys. **79**, 056001 (2016); J. Eisert, M. Friesdorf, C and Gogolin, "Quantum many-body systems out of equilibrium", Nature Phys. **11**, 124 (2015); F. Essler and M. Fagotti, "Quench dynamics and relaxation in isolated integrable quantum spin chains", J. Stat. Mech. **2016**, 064002 (2016); L. Vidmar and M. Rigol, "Generalized Gibbs ensemble in integrable lattice models", J. Stat. Mech. **2016**, 064007 (2016).

[23] Al.B. Zamolodchikov, "Thermodynamic Bethe ansatz in relativistic models. Scaling three state Potts and Lee-Yang models", Nucl. Phys. B **342**, 695 (1990); J. Mossel and J.-S. Caux, "Generalized TBA and generalized Gibbs", J. Phys. A **45**, 255001 (2012).

[24] L. Bonnes, F.H.L. Essler and A.M. Läuchli, "Light-Cone dynamics after quantum quenches in spin chains", Phys. Rev. Lett. **113**, 187203 (2014).

[25] E. Wigner, "On the quantum correction for thermodynamic equilibrium", Phys. Rev. **40**, 749 (1932).

[26] E. Bettelheim and P. Wiegmann, "Universal Fermi distribution of semiclassical nonequilibrium Fermi states", Phys. Rev. B **84**, 085102 (2011).

[27] C. Boldrighini, R. L. Dobrushin and Yu. M. Sukhov, "One-dimensional hard rod caricature of hydrodynamics", J. Stat. Phys. **31**, 577 (1983)

[28] See Supplemental Material for a numerical check of the shock dissolution with the classical flea gas, which includes Ref. [29]

[29] B. Doyon, T. Yoshimura and J.-S. Caux, "Soliton gases and generalized hydrodynamics", `arXiv:1704.05482` (2017).

[30] See Supplemental Material for a proof of the equivalence, which includes Ref. [31].

[31] V. E. Korepin, N. M. Bogoliubov and A. G. Izergin,"Quantum Inverse Scattering Method and Correlation Functions", Cambridge University Press, 1993.

[32] See Supplemental Material for CHD at finite temperature, which includes Ref. [33].

[33] B. Doyon and H. Spohn, "Drude Weight for the Lieb-Liniger Bose Gas", `arXiv:1705.08141` (2017).

[34] See Supplemental Material for details of NRG-TSA-ABACUS algorithm, which includes Refs. [35–41]

[35] V. P. Yurov and Al. B. Zamolodchikov, "Truncated conformal space approach to scaling Lee-Yang model", Int. J. Mod. Phys. A **05**, 3221-3245 (1990); V. P. Yurov and Al. B. Zamolodchikov, "Truncated fermionic space approach to the critical 2D Ising model with magnetic field", Int. J. Mod. Phys. A **06**, 4557 (1991).

[36] A. J. A. James, R. M. Konik, P. Lecheminant, N. J. Robinson and A. M. Tsvelik, "Non-perturbative methodologies for low-dimensional strongly-correlated systems: From non-abelian bosonization to truncated spectrum methods", `arXiv:1703.08421` (2017).

[37] N. A. Slavnov, "Calculation of scalar products of wave functions and form factors in the framework of the algebraic Bethe ansatz", Theor. Math. Phys. **79**, 502 (1989); N. A. Slavnov, "Nonequal-time current correlation function in a one-dimensional Bose gas ", Theor. Math. Phys. **82**, 273 (1990).

[38] G. Feverati, K. Graham, P. A. Pearce, G. Zs. Tóth and G. M. T. Watts, "A renormalization group for the truncated conformal space approach", J. Stat. Mech. **2008**, P03011 (2008); G. Watts, "On the renormalisation group for the boundary truncated conformal space approach", Nucl. Phys. B **859**, 177 (2012).

[39] K. G. Wilson, "The renormalization group: Critical phenomena and the Kondo problem", Rev. Mod. Phys. **47** 773 (1975).

[40] R. M. Konik, "Exciton hierarchies in gapped carbon nanotubes", Phys. Rev. Lett. **106** 136805 (2011).

[41] G. P. Brandino, J.-S. Caux and R. M. Konik, "Glimmers of a quantum KAM theorem: insights from quan-

tum quenches in one-dimensional Bose gases", Phys. Rev. X **5**, 041043 (2015).
[42] B. Doyon and H. Spohn, "Dynamics of hard rods with initial domain wall state", preprint `arXiv:1703.05971` (2017).

# Supplementary material for "Large-scale description of interacting one-dimensional Bose gases: generalized hydrodynamics supersedes conventional hydrodynamics"

Benjamin Doyon,[1] Jérôme Dubail,[2] Robert Konik,[3] and Takato Yoshimura[1]

[1] *Department of Mathematics, King's College London, Strand, London WC2R 2LS, UK*
[2] *CNRS & IJL-UMR 7198, Université de Lorraine, F-54506 Vandoeuvre-lès-Nancy, France*
[3] *Condensed Matter and Materials Science Division, Brookhaven National Laboratory, Upton, NY 11973 USA*

## I. CONVENTIONAL HYDRODYNAMICS AND SOUND WAVE

### A. 2HD = CHD

In the set of zero-entropy states, GHD boils down to 2HD, the hydrodynamics of two conserved quantities described by Eq. (9) in the main text, with $k = 2$. Here we show that 2HD is equivalent to the conventional hydrodynamics (CHD) of Galilean fluids defined by Eqs. (10) in the main text.

First, Eq. (9) simplifies thanks to Galilean invariance. Let

$$v_{\rm F}(\theta) = v^{\rm eff}_{\{-\theta,\theta\}}(\theta) \tag{1}$$

be the equilibrium Fermi velocity, with Fermi pseudo-velocity $\theta$. Let $\Lambda = (\theta^+ - \theta^-)/2$ and $\eta = (\theta^+ + \theta^-)/2$. Shifting the integration variable by $\eta$ in the dressing operation, we obtain $f^{\rm dr}_{\{\theta^-,\theta^+\}} = \big(f \circ \iota_\eta\big)^{\rm dr}_{\{-\Lambda,\Lambda\}} \circ \iota_{-\eta}$ where $\iota_\eta(\theta) = \theta + \eta$ is the shift function. Using $\mathrm{id} \circ \iota_\eta = \mathrm{id} + \eta$ and $1 \circ \iota_\eta = 1$, we find $v^{\rm eff}_{\theta^-,\theta^+}(\alpha) = v_{\rm F}(\alpha - \eta) + \eta$, and with $v_{\rm F}(-\alpha) = -v_{\rm F}(\alpha)$ it follows that $v^{\rm eff}_{\{\theta^-,\theta^+\}}(\theta^\pm) = \pm v_{\rm F}(\Lambda) + \eta$. This leads to

$$\partial_t\theta^\pm + \Big((\theta^+ + \theta^-)/2 \pm v_{\rm F}\big((\theta^+ - \theta^-)/2\big)\Big)\partial_x\theta^\pm = 0. \tag{2}$$

That is, the hydrodynamics is completely determined by the functional form of the equilibrium Fermi velocity. Notice that the propagation velocity $\pm v_{\rm F}(\Lambda) + \eta$ of $\theta^\pm$ equals $\pm v_{\rm F}(\Lambda) + v$, where $v = \mathtt{j}_0/\mathtt{q}_0 = \mathtt{q}_1/\mathtt{q}_0 = \eta$ is the fluid velocity. This is a simple consequence of the Galilean velocity-addition formula. We note that this 2HD equation (2) was in fact already derived in [1], although the authors did not provide the interpretation that $\theta^\pm$ are "dynamical" Fermi pseudo-velocities.

Next, we observe that the equation of state of CHD – the relation between the pressure and the density in Eq. (10) in the main text – is obtained as follows. The pressure is given in two equivalent ways

$$\mathcal{P}(\rho) = m^2\int_{-\Lambda_\rho}^{\Lambda_\rho}\frac{{\rm d}\theta\,\theta}{2\pi}U(\theta) = -m^2\int_{\Lambda_\rho}^{\Lambda_\rho}\frac{{\rm d}\theta}{2\pi}\mathcal{E}(\theta) \tag{3}$$

where the function $U(\theta)$ and $\mathcal{E}(\theta)$ solve

$$U(\theta) = \theta + \int_{-\Lambda_\rho}^{\Lambda_\rho}\frac{{\rm d}\alpha}{2\pi}\varphi(\theta-\alpha)U(\alpha), \tag{4}$$

$$\mathcal{E}(\theta) = \frac{\theta^2}{2} - \frac{\mu(\Lambda_\rho)}{m} + \int_{-\Lambda_\rho}^{\Lambda_\rho}\frac{{\rm d}\alpha}{2\pi}\varphi(\theta-\alpha)\mathcal{E}(\alpha), \tag{5}$$

where $\mathcal{E}(\theta)$ is defined so that it satisfies $\mathcal{E}(\Lambda_\rho) = 0$ from which $\mu(\Lambda_\rho)$ is also fixed. The Fermi pseudo-velocity $\Lambda_\rho$ is determined by

$$\rho = m\int_{-\Lambda_\rho}^{\Lambda_\rho}\frac{{\rm d}\theta}{2\pi}V(\theta) \tag{6}$$

where the function $V(\theta)$ solves

$$V(\theta) = 1 + \int_{-\Lambda_\rho}^{\Lambda_\rho}\frac{{\rm d}\alpha}{2\pi}\varphi(\theta-\alpha)V(\alpha). \tag{7}$$

Observe that $U(\theta), V(\theta)/2\pi$, and $\mathcal{E}(\theta)$ are nothing but the dressed momentum, the density of state, and the pseudo-energy, respectively, at $T = 0$ with the Fermi pseudo-velocity $\Lambda_\rho$.

Using these expression, we can explicitly demonstrate that the CHD equations are recast into Eqs. (2). The derivative of the density $\rho(x,t) = \rho(\Lambda(x,t))$ with respect to $i$ ($i = x, t$) can be written in the following way

$$\partial_i\rho(\Lambda) = \partial_i\Lambda\frac{\partial\mu(\Lambda)}{\partial\Lambda}\frac{\partial\rho(\Lambda)}{\partial\mu(\Lambda)} = \partial_i\Lambda m v_{\rm F}(\Lambda)\kappa(\Lambda), \tag{8}$$

where $\kappa(\Lambda) := \partial\rho(\Lambda)/\partial\mu(\Lambda)$ is the compressibility. Here we also used $\partial\mu(\Lambda)/\partial\Lambda = m v_{\rm F}(\Lambda) = mU(\Lambda)/V(\Lambda)$ where the first equality can be shown by differentiating $\mathcal{E}(\Lambda) = 0$ with respect to $\Lambda$. Using an identity $\kappa(\Lambda) = V^2(\Lambda)/(\pi v_{\rm F}(\Lambda))$ [2], we obtain

$$\partial_i\rho(\Lambda) = \frac{\partial_i\Lambda m V^2(\Lambda)}{\pi}. \tag{9}$$

The density itself also bears a similar expression $\rho(\Lambda) = m v_{\rm F}(\Lambda)\rho_{\rm s}^2(\Lambda)/\pi$ in terms of $v_{\rm F}(\Lambda)$ and $V(\Lambda)$ [2]. An analogous manipulation on derivatives of the pressure $\mathcal{P}(\Lambda) = \mathcal{P}(\rho(\Lambda))$ is done using a thermodynamic relation $\partial\mathcal{P}/\partial\mu = \rho$, which readily follows from (3), yielding

$$\partial_i\mathcal{P}(\Lambda) = \partial_i\Lambda m v_{\rm F}(\Lambda)\rho(\Lambda). \tag{10}$$

The necessary ingredients are now ready; combining them and $v = \mathtt{j}_0/\mathtt{q}_0 = \eta$, the continuity equation and the Euler equation in Eq. (10) in the main text become, respectively,

$$\begin{aligned}\partial_t\Lambda + \eta\partial_x\Lambda + v_{\rm F}(\Lambda)\partial_x\eta = 0,\\ \partial_t\eta + \eta\partial_x\eta + v_{\rm F}(\Lambda)\partial_x\Lambda = 0,\end{aligned} \tag{11}$$

which are clearly equivalent to (2).

### B. Sound wave

When the fluid of the LL gas is in the linear-response regime, we can describe the fluid as a sound wave: expanding $\theta^{\pm}(x,t) = \pm\theta_{\rm F} + \delta\theta^{\pm}(x,t)$, where $\theta_{\rm F}$ is the Fermi-pseudo velocity of the unperturbed LL gas, the 2HD equation (2) becomes

$$\partial_t \delta\theta^{\pm}(x,t) \pm v_{\rm F}(\theta_{\rm F})\partial_x \delta\theta^{\pm}(x,t) = 0. \qquad (12)$$

This is the sound wave propagating with the Fermi velocity $v_{\rm F}(\theta_{\rm F})$, and describes the dynamics of the linear Luttinger liquid. Note that, in the LL gas, the Fermi velocity is same as the sound velocity $v_{\rm s} = \sqrt{\partial\mathcal{P}/\partial(m\rho)}$, which is readily confirmed.

### C. Conventional hydrodynamics at finite temperature

Here we explain how to generalize the CHD Eqs. (10) in the main text to the finite temperature case, needed to produce the data in Fig. (1.b) in the main text, see also Fig. 1 below.

To do CHD at finite temperature, one needs to keep track of three conserved quantities: the number of particles, the momentum, and the energy. These correspond to the three densities $\mathtt{q}_0$, $\mathtt{q}_1$ and $\mathtt{q}_2$ respectively. In principle, one can write three continuity equations for these densities, which can be recast in the more conventional form of Euler hydrodynamics

$$\begin{aligned} \partial_t n + \partial_x(nu) &= 0 \\ (\partial_t + u\partial_x)u &= -\tfrac{1}{\rho}\partial_x P \\ (\partial_t + u\partial_x)\tau + \tfrac{2}{3}(\partial_x u)\tau &= 0 \end{aligned} \qquad (13)$$

where $n$ is the particle density, $u$ is the local velocity of the fluid, $\tau$ is the kinetic energy, and $P$ is the pressure.

We find it more convenient, however, to work directly with the continuity equations

$$\partial_t \mathtt{q}_i + \partial_x \mathtt{j}_i = 0, \qquad i = 0,1,2, \qquad (14)$$

and with the Lagrange multipliers $\beta_0$, $\beta_1$ and $\beta_2$, such that the reduced density matrix at a point $(x,t)$ is approximated by the Generalized Gibbs Ensemble with three charges, $e^{-\beta_0 Q_0 - \beta_1 Q_1 - \beta_2 Q_2}$ where $Q_0 = N$ is the number of particles, $Q_1 = P$ is the momentum, $Q_2 = H$ is the Hamiltonian, and $\beta_2$ is the inverse temperature while $-\beta_0/\beta_2$ is the chemical potential. The occupation function $n(\theta)$ in this Generalized Gibbs Ensemble is obtained by solving the (Generalized) Thermodynamic Bethe Ansatz equations,

$$\begin{aligned} \frac{\varepsilon(\theta)}{T} &= \sum_{i=0,1,2} \beta_i q_i(\theta) - \int \frac{d\theta'}{2\pi}\varphi(\theta-\theta')\log[1+e^{-\frac{\varepsilon(\theta')}{T}}] \\ n(\theta) &= \frac{1}{1+e^{\frac{\varepsilon(\theta)}{T}}}, \end{aligned} \qquad (15)$$

where $q_0(\theta) = 1$, $q_1(\theta) = m\theta$, $q_2(\theta) = m\theta^2/2$. Then, using the results of Ref. [3], one gets

$$\begin{aligned} \frac{\partial \mathtt{q}_j}{\partial\beta_i} &= -\int \frac{d\theta}{2\pi}\rho_{\rm p}(\theta)(1-n(\theta))h_i^{\rm dr}(\theta)h_j^{\rm dr} \\ \frac{\partial \mathtt{j}_j}{\partial\beta_i} &= -\int \frac{d\theta}{2\pi}\rho_{\rm p}(\theta)v^{\rm eff}(\theta)(1-n(\theta))h_i^{\rm dr}(\theta)h_j^{\rm dr}. \end{aligned}$$

The CHD equations at finite temperature can then be written as

$$\sum_{j=0}^{2}\left[C_{ij}\partial_t\beta_j(x,t) + B_{ij}\partial_x\beta_j(x,t)\right] = 0, \qquad (16)$$

where

$$\begin{aligned} C_{ij} &= \int \frac{d\theta}{2\pi}\rho_{\rm p}(\theta)(1-n(\theta))h_i^{\rm dr}(\theta)h_j^{\rm dr} \\ B_{ij} &= \int \frac{d\theta}{2\pi}\rho_{\rm p}(\theta)v^{\rm eff}(\theta)(1-n(\theta))h_i^{\rm dr}(\theta)h_j^{\rm dr}. \end{aligned}$$

These are the equations we solve to produce the data for CHD at finite temperature in Fig. (1.b) in the main text and in Fig. 1.

## II. THE FREE FERMION CASE

Hydrodynamics of 1d free fermions has been studied thoroughly in the past decade [4, 5], with the conclusion that the leading role is played by the Wigner function. For the convenience of the reader, we now discuss the aspects of the free fermion case that shed light on GHD, in relation with the discussion in the main text; for full details about the free fermion case, the reader is referred to the original references [4, 5].

### A. GHD for free fermions, and the role of the Wigner function

In the Tonks-Girardeau limit $c \to \infty$, the bosons are impenetrable. Impenetrable bosons can be mapped to non-interacting fermions through the Jordan-Wigner mapping,

$$\Psi_{\rm F}^{\dagger}(x) := e^{i\pi\int_{y<x}\psi^{\dagger}(y)\psi(y)dy}\,\psi^{\dagger}(x)$$

and a similar relation for the annihilation operator $\Psi_{\rm F}$, such that they satisfy the canonical anticommutation relations $\{\Psi^{\dagger}(x),\Psi(x')\} = \delta(x-x')$ and $\{\Psi(x),\Psi(x')\} = \{\Psi^{\dagger}(x),\Psi^{\dagger}(x')\} = 0$. In terms of these operators, the Hamiltonian of the Lieb-Liniger model with $c \to +\infty$, or Tonks-Girardeau gas, is simply

$$H_{\rm TG} = \int dx\ \Psi_{\rm F}^{\dagger}(x)\left(-\frac{1}{2m}\partial_x^2\right)\Psi_{\rm F}(x). \qquad (17)$$

What is crucial here is that the hamiltonian is quadratic, so the particles created/annihilated by $\Psi_{\rm F}^{\dagger}/\Psi_{\rm F}$ propagate

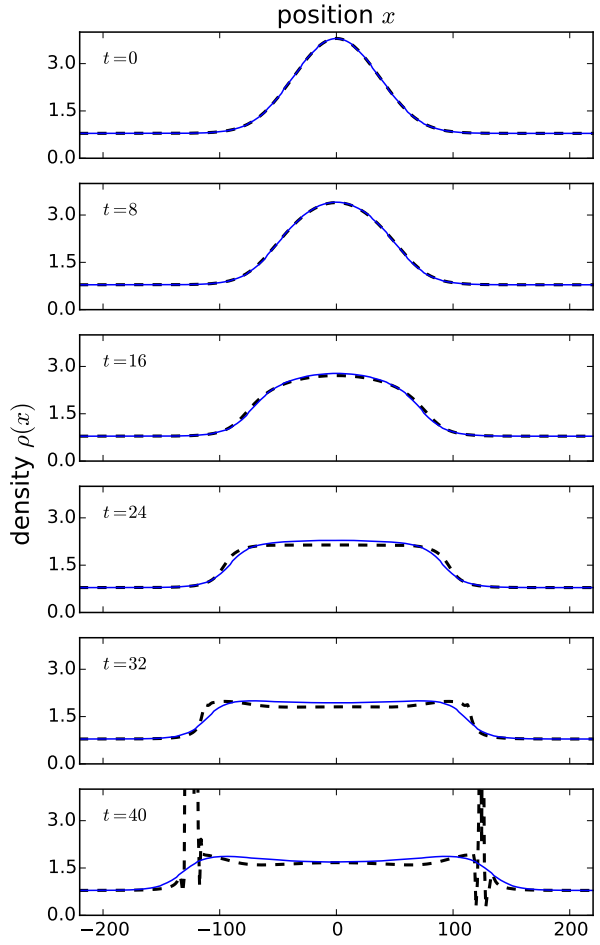


FIG. 1. Evolution of the density profile at temperature $T = 1$, with parameters $m = 1$, $c = 2$ and an initial potential $V(x) = -5e^{-(\frac{x}{50})^2} - 1$. The solution from CHD (black, dashed) is compared to the GHD solution (blue) obtained from the molecular simulation of the classical flea gas. We see that, already at $t = 24$, CHD differs significantly from GHD. We see CHD has a shock at $t \simeq 35$, and loses its validity after the shock. GHD has no shocks.

freely, and interact with other particles only through the Pauli principle—as they have fermionic statistics, unlike the original bosonic particles which entered the definition of the model—. There is no interaction energy, and this is of course a dramatic simplification. Thanks to translation invariance $H_{\rm TG}$ is diagonal in Fourier space,

$$H_{\rm TG} \;=\; \int \frac{dk}{2\pi}\frac{k^2}{2m}\Psi_{\rm F}^\dagger(k)\Psi_{\rm F}(k) \tag{18}$$

where $\Psi_{\rm F}^\dagger(k) := \int e^{ikx}\,\Psi_{\rm F}^\dagger(x)\,dx$.

Because the Hamiltonian is quadratic and diagonal in $k$-space, we see that for any function $h(.)$, one can construct a conserved charge

$$Q[h] \;:=\; \int \frac{dk}{2\pi}\,h(k)\Psi_{\rm F}^\dagger(k)\Psi_{\rm F}(k). \tag{19}$$

This provides a (continuous) family of commuting conserved charges,

$$[H, Q[h]] \;=\; [Q[h], Q[f]] \;=\; 0.$$

The associated charge density is

$$q[h](x) \;=\; \int dy\,h(y)\,\Psi^\dagger(x+\frac{y}{2})\Psi(x-\frac{y}{2}) \tag{20}$$

where $h(y) := \int \frac{dk}{2\pi}e^{iky}h(k)$ is the Fourier transform of $h(k)$. For an analytic function $h(k)$, the Fourier transform decays exponentially, so the charge density $q[h](x)$ is local in the sense that it has exponentially decaying tails.

If we allow ourselves to take $h(k) = \delta_{k_0}(k) \equiv \delta(k-k_0)$, then we obtain a charge density with tails that do not decay, but apart from that, the conserved charge $Q[\delta_{k_0}] = \frac{1}{2\pi}\Psi_{\rm F}(k_0)\Psi_{\rm F}^\dagger(k_0)$ is a perfectly decent conserved quantity. Of course, we see that it is nothing but the mode occupation at momentum $k_0$. The associated charge density reads [from now we drop the subscript '0' in '$k_0$']

$$q[\delta_k](x) \;=\; \frac{1}{2\pi}\int e^{iky}\Psi_{\rm F}^\dagger(x+\frac{y}{2})\Psi_{\rm F}(x-\frac{y}{2})dy\,. \tag{21}$$

The charge density $q[\delta_k]$ obeys the following evolution equation, with $v(k) = k/m$,

$$\partial_t q[\delta_k](x) \;:=\; \frac{1}{i}\,[H,\,q[\delta_k](x)] \;=\; -v(k)\,\partial_x q[\delta_k](x)\,, \tag{22}$$

which follows from a straightforward calculation using the Hamiltonian (18). Thus, we can identify the current operator associated to the density $q[\delta_k](x)$ as

$$j[\delta_k](x) = v(k)q[\delta_k](x), \tag{23}$$

such that the continuity equation $\partial_t q[\delta_k] + \partial_x j[\delta_k] = 0$ holds. Notice also that, by linearity, this gives a simple closed formula for the current associated to any charge density $q[h]$,

$$j[h] = \int \frac{dk}{2\pi}\frac{k}{m}h(k)q[\delta_k].$$

We stress that Eq. (22)-(23) is an exact formula that holds for the operators themselves; we have not taken any expectation values yet. It is also important to emphasize that this particularly simple form of the evolution equation is possible only because the problem is galilean invariant. If we were dealing with a lattice gas, the velocity would not simply be $v(k) = k/m$, and there would be additional terms generated by the bracket $[H, .]$ in Eq. (22).

In order to connect the simple exact result (23) for currents in the Tonks-Girardeau gas to the more general discussion of hydrodynamics in the main text, we need to turn to expectation values. Namely, we take expectation

values $\langle . \rangle$ in some initial state $|\psi_0\rangle$ (or some initial density matrix), such that the exact relation (22)-(23) becomes

$$\partial_t \mathtt{q}[\delta_k] + \partial_x \mathtt{j}[\delta_k] \;=\; 0 \qquad \text{with} \quad \left\{ \begin{array}{rcl} \mathtt{q}[\delta_k] & := & \langle q[\delta_k] \rangle \\ \mathtt{j}[\delta_k] & := & v(k) \langle q[\delta_k] \rangle \end{array} \right. . \tag{24}$$

In the language of the Thermodynamic Bethe Ansatz used in the main text, the quantity $\mathrm{q}[\delta_k]$ is nothing but the *density of particles* $\rho_\mathrm{p}$. In the main text, we chose to work with the occupation number $n(k) = \rho_\mathrm{p}(k)/\rho_\mathrm{s}(k)$, where $\rho_\mathrm{s}(k)$ is the state density. But in the Tonks-Girardeau limit, the latter is just a numerical constant, $\rho_\mathrm{s}(k) = 1/(2\pi)$, so we end up with

$$n(x,k) = \int dy e^{iky} \left\langle \Psi_\mathrm{F}^\dagger(x+y/2)\Psi_\mathrm{F}(x-y/2) \right\rangle . \tag{25}$$

The function $n(x,k)$ is an extremely well-known object in quantum mechanics: it is the *Wigner function*. Roughly speaking, the Wigner function represents the probability of finding a particle at position $(x,k)$ in phase space. It is an extremely useful tool because it allows to get a simple (semi-classical) picture of a quantum particle, or, as we are doing here, of a large collection of non-interacting particles.

In conclusion, in the Tonks-Girardeau limit, the GHD equations are nothing but the well-known evolution equation for the Wigner function,

$$\partial_t n(x,k,t) + v(k)\partial_x n(x,k,t) \;=\; 0, \tag{26}$$

which can be solved trivially in terms of the Wigner function of the initial state at $t = 0$,

$$n(x,k,t) \;=\; n(x - v(k)t, k, 0).$$

We are looking at this well-known equation in a slightly non-standard way though: for each $k$ we view $n(x,k)$, or $\rho_\mathrm{p}(x,k)$, as the expectation value of a single charge density $q[\delta_k]$ at position $x$. In that sense, Eq. (26) is an infinite set of continuity equations, one for each mode $k$.

### B. Initial Wigner function: deviation from LDA

This section is adapted from Bettelheim and Wiegmann [5].

In the main text, we focus on an initial state that is the ground state of the Hamiltonian with an external potential

$$H_\mathrm{TG} \;=\; \int dx \Psi_\mathrm{F}^\dagger(x) \left( -\frac{1}{2m}\partial_x^2 + V(x) \right) \Psi_\mathrm{F}(x). \tag{27}$$

It is the Wigner function of this ground state that enters the formalism of GHD. In the main text, it is obtained from LDA: in the limit where the variation of $V(x)$ is small at the interparticle distance, the system is locally translation invariant, so the Wigner function should be well approximated by the one of a Fermi sea with position-dependent Fermi momentum $k_\mathrm{F}(x) = \sqrt{-2mV(x)}$,

$$\begin{aligned} n_\mathrm{LDA}(x,k) &= \int \frac{dq}{2\pi} e^{-iqx} \left\langle \Psi_\mathrm{F}^\dagger(k+q/2)\Psi_\mathrm{F}(k-q/2) \right\rangle_{\text{F. sea}} \\ &= \Theta(k_\mathrm{F}(x) - k) - \Theta(-k_\mathrm{F}(x) - k), \end{aligned}$$

where $\Theta(.)$ is the Heaviside function. Thus, the initial occupation number $n(x,k)$ obtained from LDA is indeed of the form discussed in the main text, $n_\mathrm{LDA}(x,k) = 1$ if $k^-(x) < k < k^+(x)$, and $n_\mathrm{LDA}(x,k) = 0$ otherwise, for $k^+ = -k^- = k_\mathrm{F}$. The evolution from such an initial state is then governed by 2HD until a shock appears, which dissolves into 4HD, which itself dissolves into 6HD, and so on, as discussed in the main text.

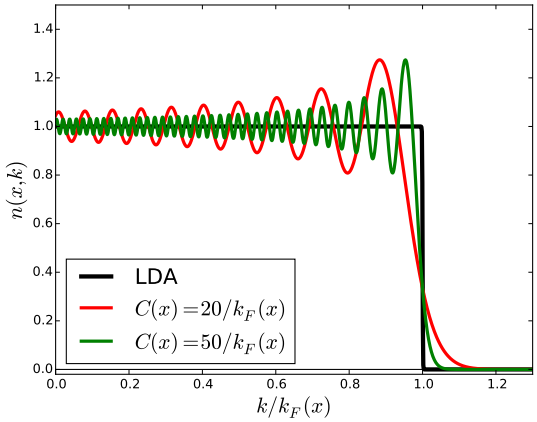


FIG. 2. Wigner function $n(x,k)$, plotted as a function of $k$ at fixed $x$. The result from LDA is plotted in black. The true Wigner function, however, is oscillating around $k_F(x)$ [5], with a period set by the length scale $C(x) := (k_\mathrm{F}''(x)/8)^{-1/3}$, as illustrated by the red and green curve, given by Eq. (29).

An important question that needs to be addressed is the accuracy of the approximation $n(x,k) = n_\mathrm{LDA}(x,k)$ in the initial state. An estimate of the ground-state propagator in real-space is [5]

$$\left\langle \Psi_\mathrm{F}^\dagger(x)\Psi_\mathrm{F}(x') \right\rangle = \frac{\exp\left(-i\int_{x'}^{x} k_\mathrm{F}(u)du\right)}{-2\pi i(x-x')} + \text{c.c.} \tag{28}$$

Expanding the argument of the exponential, one gets

$$\begin{aligned} &\left\langle \Psi_\mathrm{F}^\dagger(x+y/2)\Psi_\mathrm{F}(x-y/2) \right\rangle \\ &= \frac{\exp\left(-ik_\mathrm{F}(x)y - i\frac{y^3}{24}k_\mathrm{F}''(x)\right)}{-2\pi i y} + \text{c.c.} \end{aligned}$$

From this expression, one can calculate the Wigner function, and get a better result than the crude approximation $n_\mathrm{LDA}(x,k)$. For notational simplicity, we focus on the behavior of $n(x,k)$ for $k$ close to $k_\mathrm{F}(x)$, which is determined only by the first term in the propagator (so we

drop the c.c. term),

$$\begin{aligned} n(x,k) &= \int dy e^{iky} \left\langle \Psi_{\rm F}^\dagger(x+y/2)\Psi_{\rm F}(x-y/2)\right\rangle \\ &\simeq \int dy \frac{\exp\left(i(k-k_{\rm F})y - i\frac{y^3}{24}k_{\rm F}''\right)}{-2\pi i y} \\ &= C\int dq\, \Theta(k_{\rm F}-k+q)\,{\rm Ai}\,(Cq) \end{aligned} \tag{29}$$

where Ai(.) is the Airy function, and $C(x) := (k_{\rm F}''(x)/8)^{-1/3}$ is a new characteristic length scale. The convolution with the Airy function induces oscillations of $n(x,k)$ as a function of $k$, close to the Fermi point $k_{\rm F}(x)$, see Fig. 2.

This discussion shows that replacing the true initial Wigner function $n(x,k)$ by $n_{\rm LDA}(x,k)$ is a valid approximation only if the typical period of the oscillations is small compared to $k_{\rm F}(x)$, such that, when calculating average values of observables, integration over $k$ in the interval $[-k_{\rm F}, k_{\rm F}]$ kills the oscillatory terms. We thus arrive at the criterion $1/C(x) \ll k_{\rm F}(x)$ for the validity of LDA, or in terms of the local density $\rho(x)$,

$$\rho(x)^{-1} \ll C(x) \quad \Rightarrow \quad n(x,k) \simeq n_{\rm LDA}(x,k). \tag{30}$$

The deviation of the true Wigner function $n(x,k)$ from the LDA result $n_{\rm LDA}(x,k)$ affects the expectation values of charge densities $\mathfrak{q}[h]$. For the charges $q_j$ associated to $h(k) = k^j$, the direct calculation from Eq. (29), including the c.c. term, shows that

$$\begin{aligned} \mathfrak{q}_j(x) &= \int \frac{dk}{2\pi} n(x,k) k^j \\ &= \frac{i^j}{2\pi}\left(\frac{\partial^j}{\partial y^j}\frac{e^{-ik_{\rm F}y - i\frac{y^3}{3C^3}} - \text{c.c.}}{-iy}\right)_{y=0}. \end{aligned}$$

For the first few $j$'s, this gives

$$\begin{aligned} \mathfrak{q}_0(x) &= \frac{k_{\rm F}(x)}{\pi} \\ \mathfrak{q}_1(x) &= 0 \\ \mathfrak{q}_2(x) &= \frac{k_{\rm F}(x)^3}{3\pi} - \frac{2}{3\pi C(x)^3} \\ \mathfrak{q}_3(x) &= 0 \\ \mathfrak{q}_4(x) &= \frac{k_{\rm F}(x)^5}{5\pi} - \frac{4k_{\rm F}(x)^2}{\pi C(x)^3} \\ \mathfrak{q}_5(x) &= 0 \\ \mathfrak{q}_6(x) &= \frac{k_{\rm F}(x)^7}{7\pi} - \frac{10k_{\rm F}(x)^4}{\pi C(x)^3} + \frac{40k_{\rm F}(x)}{\pi C(x)^6} \end{aligned}$$

Interestingly, since $1/C(x)^3$ is a total derivative, when we integrate over $x$, we see that the expectation values of the total charges $\langle Q_j\rangle = \int dx \mathfrak{q}_j(x)$ remain unaffected by the oscillations of the Wigner function for $j \leq 3$. At the level of the expectation values of total charges, the deviation from the LDA result is seen only for $j \geq 4$.

## III. THE HYDRODYNAMIC REGIME

***The hydrodynamic regime.*** In classical systems, one assumes that local entropy maximization has occurred because of the fast motion of classical particles and small mean free path (separation of scales). Common wisdom then suggests that hydrodynamics emerges at large times. However, in quantum systems, the eigenstate thermalization hypothesis suggests that near-homogeneous, near-steady states are well approximated, from the viewpoint of local observables, by (generalized) Gibbs ensembles, and thus their dynamics by GHD. In effect, "molecular chaos" is already present within homogeneous and stationary states. One would therefore expect that time evolution from near-homogeneous, near-steady initial states is instantaneously well represented by GHD. It is possible to suggest, from physical intuition, quantitative criteria. Consider a state with density $\rho(x)$. The total variation, over an interval $d$, of the inter-particle length $l_{\rm int}(x) = 1/\rho(x)$ is $\Delta(x,d) = \max(|l_{\rm int}(x+y) - l_{\rm int}(x)| : y \in [0,d])$. On one hand, it is natural to require the relative total variation over $d$ to be small whenever $l_{\rm int}(x)$ is a significant proportion of $d$. That is, $\Delta(x,d)/l_{\rm int}(x)$ times $l_{\rm int}(x)/d$ is $\ll 1$; taking $d \to 0$, this is boils down to $|\partial_x l_{\rm int}(x)| \ll 1$, or equivalently $l_{\rm int}(x) \ll \rho(x)/|\partial_x\rho(x)|$. On the other hand, the scattering length $\varphi(\theta)/p'(\theta)$ should also be small. It is velocity dependent, and an upper bound is $l_{\rm scat} = \max(\varphi(\theta)/p'(\theta) : \theta \in \mathbb{R}) = 2/(mc)$. Scattering will occur in a relatively homogeneous region if $\Delta(x, l_{\rm scat})/l_{\rm int} \ll 1$, which boils down to $l_{\rm scat} \ll \rho(x)/|\partial_x\rho(x)|$. Thus, sufficient conditions for the validity of GHD should be

$$\max\{l_{\rm int}(x), 2/(mc)\} \ll \frac{\rho(x)}{|\partial_x\rho(x)|}. \tag{31}$$

## IV. THE NRG-TSA-ABACUS ALGORITHM

In order to describe the behavior of the Bose gas pre- and post-quench, we must deal with two problems: one, first finding the ground state of the gas in a one-body Gaussian potential, and then two, determining its post-quench evolution in time. As we will see, it is only the first that is non-trivial.

To find the pre-quench ground state, we employ the truncated spectrum approach, an approach first introduced by V. Yurov and A. Zamolodchikov to study simple perturbations of the conformal minimal models [6]. This approach in general enables the study of models of the form,

$$H = H_{integrable} + V_{pert}, \tag{32}$$

where $H_{integrable}$ will for us be the Lieb-Liniger model and $V_{pert}$ the one-body potential,

$$V_{pert} = V_0 \int_0^R dx e^{-ax^2}\hat{\rho}(x), \tag{33}$$

where $\hat{\rho}(x)$ is the density operator. The method employs the eigenstates of $H_{integrable}$ as a computational basis. The method presumes that we have complete control of this basis, knowing both the energies of the eigenstates as well the matrix elements of any relevant operator with respect to this basis. And in fact we do as the spectrum of the Lieb-Liniger as well as matrix elements of the density operator are computable. Because we are using the eigenstates of an interacting theory as a starting point for our numerics, we, at the very start, incorporate strong correlations into the problem. This, in principle, alleviates the numerical burden of solving the full Hamiltonian, at least in comparison of starting with a non-interacting basis. For a comprehensive review of truncated spectrum methods, see Ref. [7].

The essential idea behind the truncated spectrum approach is to order the eigenstates of $H_{integrable}$ by importance as determined by some metric. In its simplest form, this metric is their unperturbed energy. This (infinite) list of states is then truncated, keeping the most (N, say) important states (as measured by the metric). This list of states, $\{|E_i\rangle\}_{i=1}^{N}$, where state, $|E_i\rangle$, has energy, $E_i$, is then used to form the Hamiltonian matrix,

$$H_N = \begin{bmatrix} E_1 + \langle E_1|V_{\rm pert}|E_1\rangle & \langle E_1|V_{\rm pert}|E_2\rangle & \langle E_1|V_{\rm pert}|E_3\rangle & \dots & \langle E_1|V_{\rm pert}|E_N\rangle \\ \langle E_2|V_{\rm pert}|E_1\rangle & E_2 + \langle E_2|V_{\rm pert}|E_2\rangle & \langle E_2|V_{\rm pert}|E_3\rangle & \dots & \langle E_2|V_{\rm pert}|E_N\rangle \\ \langle E_3|V_{\rm pert}|E_1\rangle & \langle E_3|V_{\rm pert}|E_2\rangle & E_3 + \langle E_3|V_{\rm pert}|E_3\rangle & \dots & \langle E_3|V_{\rm pert}|E_N\rangle \\ \vdots & \vdots & \vdots & \ddots & \\ \langle E_N|V_{\rm pert}|E_1\rangle & \langle E_N|V_{\rm pert}|E_2\rangle & \langle E_N|V_{\rm pert}|E_3\rangle & \dots & E_N + \langle E_N|V_{\rm pert}|E_N\rangle \end{bmatrix} \tag{34}$$

This finite dimensional matrix can then be easily diagonalized and both the spectrum and matrix elements of the full theory determined.

To compute the energies, $E_i$, as well as the matrix elements, $\langle E_i|V_{\rm pert}|E_j\rangle$, for our perturbed Lieb-Liniger model, we employ ABACUS [8]. ABACUS is a software package that enables the efficient computation of these quantities. These are non-trivial because the determination of energy of an eigenstate, $|E_i\rangle$, involving $N$ particles necessitates the solution of N-coupled non-linear equations. These are known as the Bethe ansatz equations:

$$e^{ip_iL} = \prod_{j\neq i}^{N} \frac{p_i - p_j + ic/2}{p_i - p_j - ic/2}. \tag{35}$$

Here $p_i$ is the momentum associated with the $i-$th particle. To determine the matrix element $\langle E_i, \{p_i k\}_{k=1}^{N}|V_{\rm pert}|E_j, \{p_j k\}_{k=1}^{N}\rangle$, ABACUS uses a determinantal expression for this quantity first developed by N. Slavov [9].

The use of a simple truncation of the spectrum works exceedingly well for perturbations of simple conformal minimal models. However for more complicated models, there are strong truncation effects. To lessen these effects, a variety of strategies are available, both analytical [10] and numerical [11]. The approach we employ here is to adapt the numerical renormalization group [12] first developed by Kenneth Wilson for the study of quantum impurity problems. The basic idea is to perform a set of iterative exact diagonalizations where the most important states are taken into account in the first set of diagonalizations and successively less important states are taken into account in later diagonalizations. In this way the truncation level of the eigenspace of $H_{Lieb-Liniger}$ can be made much greater. Rather than employ a basis of $\sim 10^4$ states, one can operate with bases of sizes on the order of $\sim 10^5 - 10^6$.

The metric that determines which states in the computational basis are important need not be energy. In fact for the perturbed Lieb-Liniger model, the energy is not the most robust of metrics. We have instead developed an adaptive metric that uses the magnitude of matrix elements of $V_{pert}$ of an unperturbed state with the ground state of the full model (as computed using a small exact diagonalization) [13, 14]. This metric is much more efficient at determining which unperturbed states will be important for the full problem and enables the equivalent study of bases with $\sim 10^6 - 10^7$ states.

Using this approach we then arrive at the ground state of the gas in the Gaussian potential in the form

$$|\psi_{gs}\rangle = \sum_i c_i |E_i\rangle. \tag{36}$$

We are confident that this representation is an accurate one for several reasons. For our purposes here we did not need to consider a very strong Gaussian potential, nominally because we wished to mimic the zero temperature hydrodynamic limit. In past work, i.e. Refs. [13, 15], we considered stronger one-body potentials with larger number of particles and were able there to establish the robustness of the technique. Furthermore we are solely interested in the computing the ground state of the gas in the one-body potential. If we were in a position to need excited states, we would have to be more cautious.

Having the ground state in hand, Eqn. 36, we can then turn to the second problem, determining it's post-quench evolution in time. This in fact is trivial because the post-quench Hamiltonian is the Lieb-Liniger model

itself. Thus the time evolved state, $|\psi(t)\rangle$, is simply

$$|\psi_{gs}(t)\rangle = \sum_i c_i e^{-iE_i t}|E_i\rangle, \tag{37}$$

that is, because our computational basis is equal to the post-quench eigenbasis, the coefficients of expansion simply pick up phase factors that depend on the energies, $\{E_i\}$. It is worthwhile to stress that because we can compute $E_i$ to arbitrary accuracy, we can then evolve the state to arbitrary times without incurring phase errors.

While it is more difficult, we can also consider quenches where we quench from one one-body potential to another non-trivial potential. In such a case, we must compute using our NRG-TSA-ABACUS algorithm a large number of excited states post-quench so that we can expand the pre-quench ground state into the post-quench eigenbasis. This is however a tractable problem as demonstrated in Ref. [15] where quenches from parabolic to cosine potentials were studied. However it does place limits on the strength of the quench as well as the number of particles that can be treated.

## V. ADDITIONAL GRAPH

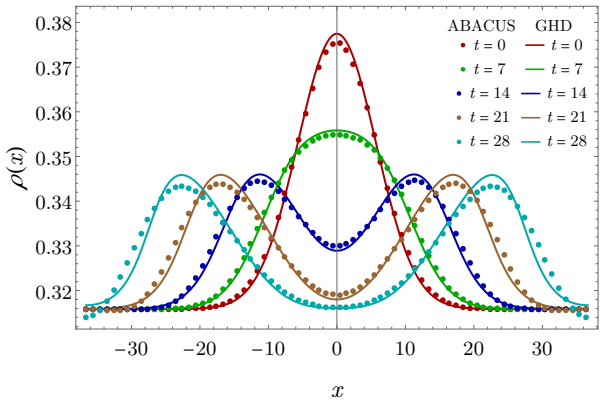


FIG. 3. The density profile under the evolution with $2m = 1$, $c = 1$, $U = 0.05$, $a = 1/64$, and a choice of $\mu_\infty$ such that there are $N = 24$ particles in the ground state. The agreement between the initial density obtained by LDA and NRG-TSA-ABACUS numerics is not good in the first place, and the disagreement grows as time is evolved.

In the main text, we showed a graph for curves with $\gamma$ being of order 1, which is an intermediate regime. It is then natural to ask how curves would look like in two extreme regimes: the TG regime ($\gamma \gg 1$) and the Gross-Pitaevskii regime ($\gamma \ll 1$). It turns out, however, that the qualitative behavior basically does not differ whatever the coupling constant is. Namely, with any coupling constant, an initial density accumulation splits into two bumps and each bump moves towards right/left with a same speed. Nonetheless, it is instructive to see how a density wave evolves when a trap potential is not smooth enough.

For this purpose, we use a LL gas with $c = 1$ as in Fig. 2 in the main text, and a potential $V(x) = -\mu_\infty - Ue^{-ax^2}$ with $U = 0.05$, $a = 1/64$, and $\mu_\infty$ is determined so that $N = 24$. In Fig. 3 we observe that the initial density prepared by LDA is already not agreeing with NRG-TSA-ABACUS numerics, that is, the initial state is not in the hydrodynamic regime defined by (31). This discrepancy is then amplified as time goes, and we also see that the height of the dots by NRG-TSA-ABACUS numerics is lowering. We expect that these effects are generated by the neglected higher conserved charges in preparing the LDA.

## VI. SHOCK DISSOLUTION OF 2HD INTO 4HD: A COMPARISON WITH THE CLASSICAL FLEA GAS

The mechanism of shock-dissolution elaborated in the main text can be further supported by a comparison with a molecular dynamics of GHD (classical flea gas) [17]. The flea gas algorithm was recently developed by making use of a surprising equivalence between dynamics of the hard rod-like model and GHD. A protocol with the same parameters as in Fig. 1 in the main text is compared against a simulation using the flea gas in Fig. 4, showing a perfect agreement. This confirms, in a non-trivial gas (although classical instead of quantum), that the shock dissolution mechanism proposed in the main text is correct.

## VII. SKETCH OF THE ALGORITHM FOR ZERO-ENTROPY GHD

In this section, we briefly sketch the algorithm that we use to solve zero-entropy GHD. It is the one we used, for instance, to produce the data plotted in Fig. 1.a in the main text.

The idea is to work with a finite set of curves in the $(x, \theta)$ plane, each of these curves being a set of points where the occupation function $n(x, \theta)$ jumps from 0 to 1. We call $\Gamma_j$, $j = 1, \ldots, p$ these different curves. For example, in Fig. 1.a, there are $p = 2$ curves, and they are both plotted in red.

Then we view the zero-GHD entropy equation (Eq. (9) in the main text) as an evolution equation for this set of curves. Namely, if $(x_j, \theta_j)$ is a point on the curve $\Gamma_j$, then after a small time $\delta t$, its new position is $(x_j + \delta x_j, \theta_j)$ where

$$\delta x_j = v^{\text{eff}}_{\{\theta\}}(\theta_j)\delta t. \tag{38}$$

The velocity $v^{\text{eff}}_{\{\theta\}}(\theta_j)$ is calculated from the set $\{\theta\}$ of all points that lie at the intersection between the vertical

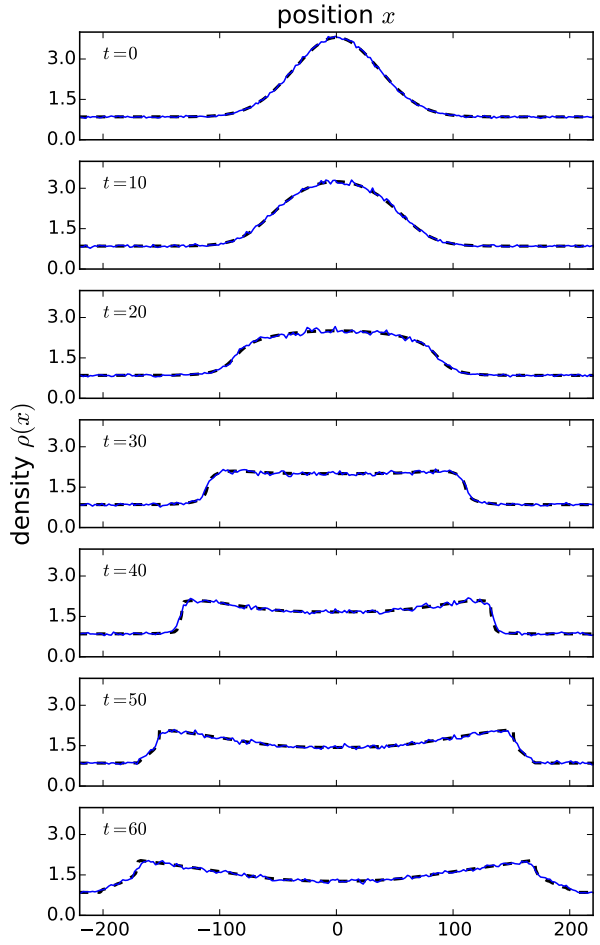


FIG. 4. Evolution of the density profile under the evolution with the same parameters as in Fig. 1 in the main text: $m = 1, c = 2$ and an initial potential $V(x) = -5e^{-(\frac{x}{50})^2} - 1$. We compare the data from Fig. 1 in the main text (here in black, dashed) to the classical flea gas (in blue).

line passing through $(x_j, \theta_j)$ and all the curves $\Gamma_{j'}$. It is obtained by solving the integral equation given in the main text, in the paragraph following Eq. (9).

This leads to the following algorithm. Numerically, each curve $\Gamma_j$ is encoded as the interpolation of some discrete set of points $(x_{j,a}, \theta_{j,a})$ for $a = 1, 2, \ldots$. The most basic version of the algorithm uses linear interpolation, but one can also use more refined interpolation schemes such as splines. To go from the configuration at time $t$ to the configuration at time $t + \delta t$, we do a loop over all the points labelled by $(j, a)$. For each point:

- we start by finding all the intersections between the vertical line at $x = x_{j,a}$ and all the curves $\Gamma_{j'}$ for $j' = 1, \ldots, p$. This gives us a set $\{\theta\}$.
- we order the elements of the set $\{\theta\}$ and label them as $\theta_1^- < \theta_1^+ < \theta_2^- < \cdots < \theta_k^- < \theta_k^+$.
- we calculate $\mathrm{id}^{\mathrm{dr}}_{\{\theta\}}(\theta_{j,a})$ and $1^{\mathrm{dr}}_{\{\theta\}}(\theta_{j,a})$. To do this, one needs to solve the linear integral problem $f^{\mathrm{dr}}_{\{\theta\}}(\alpha) = f(\alpha) + \sum_{q=1}^{k} \int_{\theta_q^-}^{\theta_q^+} d\gamma \varphi(\alpha - \gamma) f^{\mathrm{dr}}_{\{\theta\}}(\gamma)$. This is done by discretizing the integral, which leads to a matrix formulation of the problem, of the form $f^{\mathrm{dr}} = f + M \cdot f^{\mathrm{dr}}$ where $f$ and $f^{\mathrm{dr}}$ are finite-dimensional vectors.
- we evaluate the ratio $v^{\mathrm{eff}}_{\{\theta\}}(\theta_{j,a}) = \mathrm{id}^{\mathrm{dr}}_{\{\theta\}}(\theta_{j,a})/1^{\mathrm{dr}}_{\{\theta\}}(\theta_{j,a})$, and use it to calculate the new position of the point $(x_{j,a} + \delta x_{j,a}, \theta_{j,a})$ after $\delta t$, according to Eq. (38).

We find that the algorithm performs better if one reparametrizes the curves $\Gamma_j$ from time to time. Namely, it is possible that the distance between successive points $(x_{j,a}, \theta_{j,a})$ and $(x_{j,a+1}, \theta_{j,a+1})$ increases during the evolution, so that the initial discrete set of points does not provide a good description of the curve $\Gamma_j$ any longer. To avoid that, it is useful to chose a new discrete set points on the curve $\Gamma_j$ every once in a while, and then carry on with the evolution.


[1] A. D. Sarishvili, I. V. Protopopov and D. B. Gutman, "Pulse propagation in the interacting one-dimensional Bose liquid", Phys. Rev. B **94**, 045110 (2016).

[2] V. E. Korepin, N. M. Bogoliubov and A. G. Izergin, *Quantum Inverse Scattering Method and Correlation Functions* (Cambridge University Press, 1993).

[3] B. Doyon and H. Spohn, "Drude weight for the Lieb-Liniger Bose gas", `arXiv:1705.08141` (2017).

[4] E. Bettelheim, A.G. Abanov and P. Wiegmann, "Orthogonality catastrophe and shock waves in a nonequilibrium Fermi gas", Phys. Rev. Lett. **97**, 246402 (2006); E. Bettelheim, A.G. Abanov and P.B. Wiegmann, "Quantum hydrodynamics and nonlinear differential equations for degenerate Fermi gas", J. Phys. A: Math. Theor. 41 392003 (2008); E. Bettelheim and L. Glazman, "Quantum ripples over a semiclassical shock", Phys. Rev. Lett. **109**, 260602 (2012); I.V. Protopopov, D.B. Gutman, P. Schmitteckert and A.D. Mirlin, "Dynamics of waves in one-dimensional electron systems: density oscillations driven by population inversion", Phys. Rev. B **87**, 045112 (2013).

[5] E. Bettelheim and P. Wiegmann, "Universal Fermi distribution of semiclassical nonequilibrium Fermi states", Phys. Rev. B **84**, 085102 (2011).

[6] V. P. Yurov and Al. B. Zamolodchikov, "Truncated conformal space approach to scaling Lee-Yang model", Int. J. Mod. Phys. A **05**, 3221-3245 (1990); V. P. Yurov and Al. B. Zamolodchikov, "Truncated fermionic space approach to the critical 2D Ising model with magnetic field", Int. J. Mod. Phys. A **06**, 4557 (1991).

[7] A. J. A. James, R. M. Konik, P. Lecheminant, N. J. Robinson and A. M. Tsvelik, "Non-perturbative methodologies for low-dimensional strongly-correlated systems: From non-abelian bosonization to truncated spectrum methods", arXiv:1703.08421 (2017).

[8] J.-S. Caux, "Correlation functions of integrable models: a description of the ABACUS algorithm", J. Math. Phys. **50**, 095214 (2009).

[9] N. A. Slavnov, "Calculation of scalar products of wave functions and form factors in the framework of the algebraic Bethe ansatz", Theor. Math. Phys. **79**, 502 (1989); N. A. Slavnov, "Nonequal-time current correlation function in a one-dimensional Bose gas ", Theor. Math. Phys. **82**, 273 (1990).

[10] G. Feverati, K. Graham, P. A. Pearce, G. Zs. Tóth and G. M. T. Watts, "A renormalization group for the truncated conformal space approach", J. Stat. Mech. **2008** P03011 (2008); G. Watts, "On the renormalisation group for the boundary truncated conformal space approach", Nucl. Phys. B **859** 177 (2012).

[11] R. M. Konik and Y. Adamov, "A numerical renormalization group for continuum one-dimensional systems", Phys. Rev. Lett. **98**, 147205 (2007).

[12] K. G. Wilson, "The renormalization group: Critical phenomena and the Kondo problem", Rev. Mod. Phys. **47** 773 (1975).

[13] J.-S. Caux and R. M. Konik, "Constructing the generalized Gibbs ensemble after a quantum quench", Phys. Rev. Lett. **109**, 175301 (2012).

[14] R. M. Konik, "Exciton hierarchies in gapped carbon nanotubes", Phys. Rev. Lett. **106** 136805 (2011).

[15] G. P. Brandino, J.-S. Caux and R. M. Konik, "Glimmers of a quantum KAM theorem: insights from quantum quenches in one-dimensional Bose Ggases", Phys. Rev. X **5**, 041043 (2015).

[16] T. Kinoshita, T. Wenger and D. S. Weiss, "A quantum Newton's cradle", Nature **440**, 900-903 (2006).

[17] B. Doyon, T. Yoshimura and J.-S. Caux, "Soliton gases and generalized hydrodynamics", arXiv:1704.05482 (2017).

# Chapter 5

# Conclusion and outlook

## 5.1 Conclusion

In this thesis, we have investigated the structure and the application of generalized hydrodynamics, which is a hydrodynamic approach to study the large scale dynamics of integrable systems. The core idea of hydrodynamics is the emergence of mesoscopic scales called fluid cells at large scale, which are large enough compared to inter-particle length, yet small enough compared to macroscopic length scale, such as the variation of the fluid density. Each fluid cell is almost homogeneous within itself, and therefore states at space-time $(x, t)$ are expected to be specified completely by the average densities of conserved charges near $(x, t)$. The degree of homogeneity in the fluid cells can be characterized by the truncation in the derivative expansions of the average currents. If we assume the maximum homogeneity, then we can assume that the average currents at $(x, t)$ are functions of the average densities at $(x, t)$ only (this amounts to Euler hydrodynamics). Instead, if the system is is not homogeneous enough for Euler hydrodynamics to be adequately used, then how the average densities vary near $(x, t)$ also matters in determining the value of average currents at $(x, t)$. This is the idea of derivative expansion, and typically the first spatial derivative of average densities suffice (i.e. higher derivative corrections give rise to irrelevant effect).

The machinery of hydrodynamics can be straightforwardly applied to integrable systems as well by simply enumerating all the conserved charges possessed by the systems. Within the Euler scale, the problem then boils down to the determination of average currents and densities, namely equations of state. This turns out to be possible within the framework of thermodynamic Bethe ansatz (TBA), and the explicit TBA expression of average currents was provided in [45,46] for the first time. This immediately allowed us to write down the hydrodynamic equation (GHD equation) for intgrable systems. To illustrate how the GHD equation works, we derived the solution of the partitioning protocol, providing the prescription on how to numerically determine it. We then argued that the GHD equation can be in fact naturally extended to the case with external potentials, and

pointed out that it is particularly useful when studying the dynamics of the trapped Lieb-Liniger model, which is expected to describe the dynamics of ultra-cold atoms confined in one dimension.

Proving the emergence of GHD from the mechanical time-evolution is obviously a formidable task, and has not been achieved yet. Nonetheless, the TBA expression of the average currents can actually be nicely proven in the case of diagonally-scattering relativistic integrable field theories in a combinatorial manner. Following [67], we provided a graph theoretical proof of the average currents. The key idea was to compute the connected form factor for the current combinatorially, and then employ the LeClair-Mussardo formula to obtain the average currents. The connected (or symmetric) form factor is essentially the infinite-volume matrix element, but we also demonstrated the derivation of the finite-volume matrix element of the current.

Having established the theory on solid ground, we then introduced a surprising connection between GHD and the (Euler) hydrodynamics of one-dimensional classical rigid objects. Remarkably, there is a strong resemblance between the hydrodynamics of classical hard rod gases and GHD, and we noted that they can actually coincide subject to a slight but nontrivial modification to the former. The modification is simply to allow the rod length, which can also be though of as the jump length of velocity tracers upon hitting each other, to be velocity dependent. We termed a gas of classical particles that follows the dynamics dictated by velocity-dependent jumps flea gas. The correspondence between the hydrodynamics of the classical flea gas and that of quantum integrable systems is not something unpredictable indeed, but still implies an intriguing physical consequence: at large (Euler) scale, a gas of quantum integrable systems behave like that of classical solitons. In fact it has been known that the hydrodynamics of soliton gases following the KdV equation has the equations of state similar to (4.4) [137], and the observation we made provides a universal understanding on the nature of the hydrodynamics of soliton gases.

Finally, we specialized to the case where the system always remains close to the ground state throughout the dynamics. In this situation the GHD equation becomes substantially simpler, and boils down to a hydrodynamic equation with fluid variables being the finite number of dynamical Fermi momenta (when $2k$ Fermi momenta are involved, we call such hydrodynamics $2k$ HD). A crucial caveat here is that, despite of being a finite-component system, $2k$ HD does not suffer from any gradient catastrophe (i.e. shock). This is because whenever $2k$ HD experiences a sharp structure, the fluid can prevent it developing further by increasing the number of dynamical Fermi momenta to $2k+2$. This is possible thanks to the abundance of conserved charges, and the dissolution of shocks by passing from $2k$ HD to $2k+2$ HD is the characteristics of low-temperature dynamics of (gapless) integrable systems.

## 5.2 Open problems

GHD has been extremely successful at describing the large scale dynamics of integrable systems so far, and a numerous amount of research efforts has been made to unveil its profound structures. Being said so, there is still a variety of aspects that awaits further investigations.

One of them is the spin transport in the spin 1/2 isotropic Heisenberg chain at half-filling, which has been numerically found to exhibit superdiffusion. More precisely, it was numerically confirmed that the equilibrium spin-spin correlation function $\langle S^z(x,t)S^z(0,0)\rangle^c$ follows the Karder-Parisi-Zhang (KPZ) scaling with the dynamical exponent $\alpha = 3/2$ [150]. Subsequently, a phenomenological argument that supports superdiffusion was provided in [151, 152], and it was also analytically conjectured that in fact an additional non-Abelian symmetry of the system (e.g. $SU(2)$ spin symmetry) is the only requirement for quantum chains having KPZ scaling (i.e. integrability is not needed) [153]. However, the issue of the precise condition under which anomalous diffusion is realized in quantum chains is far from being settled, and with a recent numerical study that does not favor the above conjectured condition [154], it is still under intense scrutiny. Meanwhile, remarkably, the classical counterpart of the model, which is the Faddeev-Takhtajan chain, is also found to exhibit superdiffusion at half-filling [155]. This suggest that superdiffusion in isotropic quantum chains is not caused by quantum effects, and the mechanism of it is the same as in classical isotropic chains.

As explained in the main text, the full Navier-Stokes corrections to GHD are now available, by which diffusive spin transports observed in integrable systems so far would be captured. However superdiffusion is characterized by the divergence of the diffusion constant, hence the new prescription is called for in order to correctly describe such anomalous diffusion. A natural direction is then to combine GHD and NLFHD, which actually turns out to necessiate careful treatments [156].

Another direction could be to investigate how GHD emerges microscopically. This is of course rather nontrivial, and rigorous results are available only for hard-rod systems [39]. Instead of directly dealing with integrable mechanical many-body systems, it might be in fact useful to study something easier to handle but contains enough complexity. One of possible choices is the ball-box system (BBS) [157], which is a cellular automaton model, and known to be an ultra-discretized version of the KdV equation or the classical Toda chain [158]. The model has been shown to be integrable with surprisingly rich structures (see e.g. [158] for a detailed review on various aspects of the model). The structure of out-of-equilibrium dynamics of the model was also analyzed in a mathematically rigorous fashion [159].

# Bibliography


[1] P. W. Anderson, *More is different*, Science **177**(4047), 393 (1972), doi:10.1126/science.177.4047.393.

[2] L. Bertini, A. De Sole, D. Gabrielli, G. Jona-Lasinio and C. Landim, *Macroscopic fluctuation theory*, Rev. Mod. Phys. **87**, 593 (2015), doi:10.1103/RevModPhys.87.593.

[3] T. Kinoshita, T. Wenger and D. S. Weiss, *A quantum newton's cradle*, Nature **440**(7086), 900 (2006), doi:10.1038/nature04693.

[4] I. Bloch, J. Dalibard and W. Zwerger, *Many-body physics with ultracold gases*, Rev. Mod. Phys. **80**, 885 (2008), doi:10.1103/RevModPhys.80.885.

[5] A. Polkovnikov, K. Sengupta, A. Silva and M. Vengalattore, *Colloquium: Nonequilibrium dynamics of closed interacting quantum systems*, Rev. Mod. Phys. **83**, 863 (2011), doi:10.1103/RevModPhys.83.863.

[6] I. Bloch, J. Dalibard and S. Nascimbène, *Quantum simulations with ultracold quantum gases*, Nature Physics **8**, 267 EP (2012).

[7] S. Trotzky, Y.-A. Chen, A. Flesch, I. P. McCulloch, U. Schollwöck, J. Eisert and I. Bloch, *Probing the relaxation towards equilibrium in an isolated strongly correlated one-dimensional bose gas*, Nature Physics **8**, 325 EP (2012).

[8] M. Gring, M. Kuhnert, T. Langen, T. Kitagawa, B. Rauer, M. Schreitl, I. Mazets, D. A. Smith, E. Demler and J. Schmiedmayer, *Relaxation and prethermalization in an isolated quantum system*, Science **337**(6100), 1318 (2012), doi:10.1126/science.1224953.

[9] J. Bauer, C. Salomon and E. Demler, *Realizing a kondo-correlated state with ultracold atoms*, Phys. Rev. Lett. **111**, 215304 (2013), doi:10.1103/PhysRevLett.111.215304.

[10] M. Kanász-Nagy, Y. Ashida, T. Shi, C. u. u. u. u. P. m. c. Moca, T. N. Ikeda, S. Fölling, J. I. Cirac, G. Zaránd and E. A. Demler, *Exploring the anisotropic*

*kondo model in and out of equilibrium with alkaline-earth atoms*, Phys. Rev. B **97**, 155156 (2018), doi:10.1103/PhysRevB.97.155156.

[11] J. M. Deutsch, *Quantum statistical mechanics in a closed system*, Phys. Rev. A **43**, 2046 (1991), doi:10.1103/PhysRevA.43.2046.

[12] M. Srednicki, *Chaos and quantum thermalization*, Phys. Rev. E **50**, 888 (1994), doi:10.1103/PhysRevE.50.888.

[13] M. Rigol, V. Dunjko and M. Olshanii, *Thermalization and its mechanism for generic isolated quantum systems*, Nature **452**, 854 EP (2008).

[14] G. Biroli, C. Kollath and A. M. Läuchli, *Effect of rare fluctuations on the thermalization of isolated quantum systems*, Phys. Rev. Lett. **105**, 250401 (2010), doi:10.1103/PhysRevLett.105.250401.

[15] M. C. Bañuls, J. I. Cirac and M. B. Hastings, *Strong and weak thermalization of infinite nonintegrable quantum systems*, Phys. Rev. Lett. **106**, 050405 (2011), doi:10.1103/PhysRevLett.106.050405.

[16] M. Rigol, *Breakdown of thermalization in finite one-dimensional systems*, Phys. Rev. Lett. **103**, 100403 (2009), doi:10.1103/PhysRevLett.103.100403.

[17] J. Eisert, M. Friesdorf and C. Gogolin, *Quantum many-body systems out of equilibrium*, Nature Physics **11**, 124 EP (2015).

[18] C. Gogolin and J. Eisert, *Equilibration, thermalisation, and the emergence of statistical mechanics in closed quantum systems*, Reports on Progress in Physics **79**(5), 056001 (2016), doi:10.1088/0034-4885/79/5/056001.

[19] C. Gogolin, M. P. Müller and J. Eisert, *Absence of thermalization in nonintegrable systems*, Phys. Rev. Lett. **106**, 040401 (2011), doi:10.1103/PhysRevLett.106.040401.

[20] L. D'Alessio, Y. Kafri, A. Polkovnikov and M. Rigol, *From quantum chaos and eigenstate thermalization to statistical mechanics and thermodynamics*, Advances in Physics **65**(3), 239 (2016), doi:10.1080/00018732.2016.1198134.

[21] E. J. Heller, *Bound-state eigenfunctions of classically chaotic hamiltonian systems: Scars of periodic orbits*, Phys. Rev. Lett. **53**, 1515 (1984), doi:10.1103/PhysRevLett.53.1515.

[22] C. J. Turner, A. A. Michailidis, D. A. Abanin, M. Serbyn and Z. Papić, *Quantum scarred eigenstates in a rydberg atom chain: Entanglement, breakdown of thermalization, and stability to perturbations*, Phys. Rev. B **98**, 155134 (2018), doi:10.1103/PhysRevB.98.155134.

[23] V. Alba, *Eigenstate thermalization hypothesis and integrability in quantum spin chains*, Phys. Rev. B **91**, 155123 (2015), doi:10.1103/PhysRevB.91.155123.

[24] M. Rigol, V. Dunjko, V. Yurovsky and M. Olshanii, *Relaxation in a completely integrable many-body quantum system: An ab initio study of the dynamics of the highly excited states of 1d lattice hard-core bosons*, Phys. Rev. Lett. **98**, 050405 (2007), doi:10.1103/PhysRevLett.98.050405.

[25] M. Olshanii, *Atomic scattering in the presence of an external confinement and a gas of impenetrable bosons*, Phys. Rev. Lett. **81**, 938 (1998), doi:10.1103/PhysRevLett.81.938.

[26] V. Dunjko, V. Lorent and M. Olshanii, *Bosons in cigar-shaped traps: Thomas-fermi regime, tonks-girardeau regime, and in between*, Phys. Rev. Lett. **86**, 5413 (2001), doi:10.1103/PhysRevLett.86.5413.

[27] A. H. van Amerongen, J. J. P. van Es, P. Wicke, K. V. Kheruntsyan and N. J. van Druten, *Yang-yang thermodynamics on an atom chip*, Phys. Rev. Lett. **100**, 090402 (2008), doi:10.1103/PhysRevLett.100.090402.

[28] F. H. L. Essler and M. Fagotti, *Quench dynamics and relaxation in isolated integrable quantum spin chains*, Journal of Statistical Mechanics: Theory and Experiment **2016**(6), 064002 (2016), doi:10.1088/1742-5468/2016/06/064002.

[29] A. C. Cassidy, C. W. Clark and M. Rigol, *Generalized thermalization in an integrable lattice system*, Phys. Rev. Lett. **106**, 140405 (2011), doi:10.1103/PhysRevLett.106.140405.

[30] T. Prosen and E. Ilievski, *Families of quasilocal conservation laws and quantum spin transport*, Phys. Rev. Lett. **111**, 057203 (2013), doi:10.1103/PhysRevLett.111.057203.

[31] E. Ilievski, M. Medenjak and T. Prosen, *Quasilocal conserved operators in the isotropic heisenberg spin-1/2 chain*, Phys. Rev. Lett. **115**, 120601 (2015), doi:10.1103/PhysRevLett.115.120601.

[32] E. Ilievski, M. Medenjak, T. Prosen and L. Zadnik, *Quasilocal charges in integrable lattice systems*, Journal of Statistical Mechanics: Theory and Experiment **2016**(6), 064008 (2016), doi:10.1088/1742-5468/2016/06/064008.

[33] H. Spohn, *Large scale dynamics of interacting particles*, Texts and monographs in physics. Springer-Verlag, ISBN 9780387534916 (1991).

[34] M. Crossley, P. Glorioso and H. Liu, *Effective field theory of dissipative fluids*, arXiv e-prints arXiv:1511.03646 (2015).

[35] F. M. Haehl, R. Loganayagam and M. Rangamani, *The fluid manifesto: emergent symmetries, hydrodynamics, and black holes*, Journal of High Energy Physics **2016**(1), 184 (2016), doi:10.1007/JHEP01(2016)184.

[36] P. Glorioso, M. Crossley and H. Liu, *Effective field theory of dissipative fluids (ii): classical limit, dynamical kms symmetry and entropy current*, Journal of High Energy Physics **2017**(9), 96 (2017), doi:10.1007/JHEP09(2017)096.

[37] K. Jensen, R. Marjieh, N. Pinzani-Fokeeva and A. Yarom, *A panoply of Schwinger-Keldysh transport*, SciPost Phys. **5**, 53 (2018), doi:10.21468/SciPostPhys.5.5.053.

[38] T. Banks and A. Lucas, *Emergent entropy production and hydrodynamics in quantum many-body systems*, Phys. Rev. E **99**, 022105 (2019), doi:10.1103/PhysRevE.99.022105.

[39] C. Boldrighini, R. L. Dobrushin and Y. M. Sukhov, *One-dimensional hard rod caricature of hydrodynamics*, Journal of Statistical Physics **31**(3), 577 (1983), doi:10.1007/BF01019499.

[40] A. Benassi and J.-P. Fouque, *Hydrodynamical limit for the asymmetric simple exclusion process*, Ann. Probab. **15**(2), 546 (1987), doi:10.1214/aop/1176992158.

[41] D. Pines and P. Nozières, *The Theory of Quantum Liquids*, CRC Press, doi:10.4324/9780429492662 (2018).

[42] M. A. Cazalilla, R. Citro, T. Giamarchi, E. Orignac and M. Rigol, *One dimensional bosons: From condensed matter systems to ultracold gases*, Rev. Mod. Phys. **83**, 1405 (2011), doi:10.1103/RevModPhys.83.1405.

[43] M. Müller, J. Schmalian and L. Fritz, *Graphene: A nearly perfect fluid*, Phys. Rev. Lett. **103**, 025301 (2009), doi:10.1103/PhysRevLett.103.025301.

[44] A. Lucas and K. C. Fong, *Hydrodynamics of electrons in graphene*, Journal of Physics: Condensed Matter **30**(5), 053001 (2018), doi:10.1088/1361-648x/aaa274.

[45] O. A. Castro-Alvaredo, B. Doyon and T. Yoshimura, *Emergent hydrodynamics in integrable quantum systems out of equilibrium*, Phys. Rev. X **6**, 041065 (2016), doi:10.1103/PhysRevX.6.041065.

[46] B. Bertini, M. Collura, J. De Nardis and M. Fagotti, *Transport in out-of-equilibrium xxz chains: Exact profiles of charges and currents*, Phys. Rev. Lett. **117**, 207201 (2016), doi:10.1103/PhysRevLett.117.207201.

[47] H. Spohn, *Nonlinear fluctuating hydrodynamics for anharmonic chains*, Journal of Statistical Physics **154**(5), 1191 (2014), doi:10.1007/s10955-014-0933-y.

[48] H. Spohn, *Fluctuating Hydrodynamics Approach to Equilibrium Time Correlations for Anharmonic Chains*, pp. 107–158, Springer International Publishing, Cham, ISBN 978-3-319-29261-8, doi:10.1007/978-3-319-29261-8_3 (2016).

[49] B. Thielemann, C. Rüegg, H. M. Rønnow, A. M. Läuchli, J.-S. Caux, B. Normand, D. Biner, K. W. Krämer, H.-U. Güdel, J. Stahn, K. Habicht, K. Kiefer *et al.*, *Direct observation of magnon fractionalization in the quantum spin ladder*, Phys. Rev. Lett. **102**, 107204 (2009), doi:10.1103/PhysRevLett.102.107204.

[50] Z. Chen, J. de Gier, I. Hiki and T. Sasamoto, *Exact confirmation of 1d nonlinear fluctuating hydrodynamics for a two-species exclusion process*, Phys. Rev. Lett. **120**, 240601 (2018), doi:10.1103/PhysRevLett.120.240601.

[51] A. Das, K. Damle, A. Dhar, D. A. Huse, M. Kulkarni, C. B. Mendl and H. Spohn, *Nonlinear Fluctuating Hydrodynamics for the Classical XXZ Spin Chain*, arXiv e-prints arXiv:1901.00024 (2018).

[52] H. Castella, X. Zotos and P. Prelovšek, *Integrability and ideal conductance at finite temperatures*, Phys. Rev. Lett. **74**, 972 (1995), doi:10.1103/PhysRevLett.74.972.

[53] X. Zotos, F. Naef and P. Prelovsek, *Transport and conservation laws*, Phys. Rev. B **55**, 11029 (1997), doi:10.1103/PhysRevB.55.11029.

[54] X. Zotos, *Finite temperature drude weight of the one-dimensional spin-* 1/2 *heisenberg model*, Phys. Rev. Lett. **82**, 1764 (1999), doi:10.1103/PhysRevLett.82.1764.

[55] J. Sirker, *Spin diffusion and the anisotropic spin-*$\frac{1}{2}$ *heisenberg chain*, Phys. Rev. B **73**, 224424 (2006), doi:10.1103/PhysRevB.73.224424.

[56] J. Sirker, R. G. Pereira and I. Affleck, *Diffusion and ballistic transport in one-dimensional quantum systems*, Phys. Rev. Lett. **103**, 216602 (2009), doi:10.1103/PhysRevLett.103.216602.

[57] J. Sirker, R. G. Pereira and I. Affleck, *Conservation laws, integrability, and transport in one-dimensional quantum systems*, Phys. Rev. B **83**, 035115 (2011), doi:10.1103/PhysRevB.83.035115.

[58] T. Prosen, *Open xxz spin chain: Nonequilibrium steady state and a strict bound on ballistic transport*, Phys. Rev. Lett. **106**, 217206 (2011), doi:10.1103/PhysRevLett.106.217206.

[59] T. Prosen, *Exact nonequilibrium steady state of a strongly driven open xxz chain*, Phys. Rev. Lett. **107**, 137201 (2011), doi:10.1103/PhysRevLett.107.137201.

[60] B. Derrida, M. R. Evans, V. Hakim and V. Pasquier, *Exact solution of a 1d asymmetric exclusion model using a matrix formulation*, Journal of Physics A: Mathematical and General **26**(7), 1493 (1993), doi:10.1088/0305-4470/26/7/011.

[61] K. Mallick, *The exclusion process: A paradigm for non-equilibrium behaviour*, Physica A: Statistical Mechanics and its Applications **418**, 17 (2015), doi:https://doi.org/10.1016/j.physa.2014.07.046, Proceedings of the 13th International Summer School on Fundamental Problems in Statistical Physics.

[62] T. Prosen, *Exact nonequilibrium steady state of an open hubbard chain*, Phys. Rev. Lett. **112**, 030603 (2014), doi:10.1103/PhysRevLett.112.030603.

[63] E. Ilievski and T. Prosen, *Exact steady state manifold of a boundary driven spin-1 laisutherland chain*, Nuclear Physics B **882**, 485 (2014), doi:https://doi.org/10.1016/j.nuclphysb.2014.03.016.

[64] C. N. Yang and C. P. Yang, *Thermodynamics of a one dimensional system of bosons with repulsive delta function interaction*, Journal of Mathematical Physics **10**(7), 1115 (1969), doi:10.1063/1.1664947.

[65] A. Zamolodchikov, *Thermodynamic bethe ansatz in relativistic models: Scaling 3-state potts and lee-yang models*, Nuclear Physics B **342**(3), 695 (1990), doi:https://doi.org/10.1016/0550-3213(90)90333-9.

[66] I. Kostov, D. Serban and D.-L. Vu, *Tba and tree expansion*, In V. Dobrev, ed., *Quantum Theory and Symmetries with Lie Theory and Its Applications in Physics Volume 2*, pp. 77–98. Springer Singapore, Singapore, ISBN 978-981-13-2179-5 (2018).

[67] D.-L. Vu and T. Yoshimura, *Equations of state in generalized hydrodynamics*, SciPost Phys. **6**, 23 (2019), doi:10.21468/SciPostPhys.6.2.023.

[68] A. LeClair and G. Mussardo, *Finite temperature correlation functions in integrable qft*, Nuclear Physics B **552**(3), 624 (1999), doi:https://doi.org/10.1016/S0550-3213(99)00280-1.

[69] B. Doyon, T. Yoshimura and J.-S. Caux, *Soliton gases and generalized hydrodynamics*, Phys. Rev. Lett. **120**, 045301 (2018), doi:10.1103/PhysRevLett.120.045301.

[70] B. Doyon, J. Dubail, R. Konik and T. Yoshimura, *Large-scale description of interacting one-dimensional bose gases: Generalized hydrodynamics supersedes conventional hydrodynamics*, Phys. Rev. Lett. **119**, 195301 (2017), doi:10.1103/PhysRevLett.119.195301.

[71] E. H. Lieb and W. Liniger, *Exact analysis of an interacting bose gas. i. the general solution and the ground state*, Phys. Rev. **130**, 1605 (1963), doi:10.1103/PhysRev.130.1605.

[72] A. B. Zamolodchikov and A. B. Zamolodchikov, *Factorized s-matrices in two dimensions as the exact solutions of certain relativistic quantum field theory models*, Annals of Physics **120**(2), 253 (1979), doi:https://doi.org/10.1016/0003-4916(79)90391-9.

[73] V. E. Korepin, N. M. Bogoliubov and A. G. Izergin, *Quantum Inverse Scattering Method and Correlation Functions*, Cambridge Monographs on Mathematical Physics. Cambridge University Press, doi:10.1017/CBO9780511628832 (1993).

[74] J. Mossel and J.-S. Caux, *Generalized TBA and generalized gibbs*, Journal of Physics A: Mathematical and Theoretical **45**(25), 255001 (2012), doi:10.1088/1751-8113/45/25/255001.

[75] M. Fowler and X. Zotos, *Quantum sine-gordon thermodynamics: The bethe ansatz method*, Phys. Rev. B **24**, 2634 (1981), doi:10.1103/PhysRevB.24.2634.

[76] M. Takahashi and M. Suzuki, *One-Dimensional Anisotropic Heisenberg Model at Finite Temperatures*, Progress of Theoretical Physics **48**(6), 2187 (1972), doi:10.1143/PTP.48.2187.

[77] M. Takahashi, *One-Dimensional Heisenberg Model at Finite Temperature*, Progress of Theoretical Physics **46**(2), 401 (1971), doi:10.1143/PTP.46.401.

[78] M. Gaudin, *Thermodynamics of the heisenberg-ising ring for* $\Delta gt$; 1, Phys. Rev. Lett. **26**, 1301 (1971), doi:10.1103/PhysRevLett.26.1301.

[79] M. Takahashi, *Thermodynamics of One-Dimensional Solvable Models*, Cambridge University Press, doi:10.1017/CBO9780511524332 (1999).

[80] F. H. L. Essler, H. Frahm, F. Ghmann, A. Klmper and V. E. Korepin, *The One-Dimensional Hubbard Model*, Cambridge University Press, doi:10.1017/CBO9780511534843 (2005).

[81] A. Klümper, *Thermodynamics of the anisotropic spin-1/2 heisenberg chain and related quantum chains*, Zeitschrift für Physik B Condensed Matter **91**(4), 507 (1993), doi:10.1007/BF01316831.

[82] A. Klümper, *Integrability of quantum chains: Theory and applications to the spin-1/2 XXZ chain*, pp. 349–379, Springer Berlin Heidelberg, Berlin, Heidelberg, ISBN 978-3-540-40066-0, doi:10.1007/BFb0119598 (2004).

[83] J. Balog, *Field theoretical derivation of the tba integral equation*, Nuclear Physics B **419**(3), 480 (1994), doi:10.1016/0550-3213(94)90341-7.

[84] G. Kato and M. Wadati, *Graphical representation of the partition function of a one-dimensional -function bose gas*, Journal of Mathematical Physics **42**(10), 4883 (2001), doi:10.1063/1.1396836.

[85] G. Kato and M. Wadati, *Bethe ansatz cluster expansion method for quantum integrable particle systems*, Journal of the Physical Society of Japan **73**(5), 1171 (2004), doi:10.1143/JPSJ.73.1171.

[86] F. Woynarovich, *On the normalization of the partition function of bethe ansatz systems*, Nuclear Physics B **852**(1), 269 (2011), doi:https://doi.org/10.1016/j.nuclphysb.2011.06.015.

[87] I. Kostov, D. Serban and D.-L. Vu, *Boundary TBA, trees and loops*, arXiv e-prints arXiv:1809.05705 (2018).

[88] I. Kostov, D. Serban and D.-L. Vu, *Boundary entropy of integrable perturbed $SU(2)_k$ WZNW*, arXiv e-prints arXiv:1906.01909 (2019).

[89] S. Chaiken and D. Kleitman, *Matrix tree theorems*, Journal of Combinatorial Theory, Series A **24**(3), 377 (1978), doi:https://doi.org/10.1016/0097-3165(78)90067-5.

[90] F. A. Smirnov, *Form Factors in Completely Integrable Models of Quantum Field Theory*, WORLD SCIENTIFIC, doi:10.1142/1115 (1992).

[91] V. E. Korepin and N. A. Slavnov, *Form factors in the finite volume*, International Journal of Modern Physics B **13**(24), 2933 (1999), doi:10.1142/S0217979299002769.

[92] G. Mussardo, V. Riva and G. Sotkov, *Finite-volume form factors in semi-classical approximation*, Nuclear Physics B **670**(3), 464 (2003), doi:https://doi.org/10.1016/j.nuclphysb.2003.08.017.

[93] B. Pozsgay and G. Takács, *Form factors in finite volume i: Form factor bootstrap and truncated conformal space*, Nuclear Physics B **788**(3), 167 (2008), doi:https://doi.org/10.1016/j.nuclphysb.2007.06.027.

[94] B. Pozsgay and G. Takács, *Form factors in finite volume ii: Disconnected terms and finite temperature correlators*, Nuclear Physics B **788**(3), 209 (2008), doi:https://doi.org/10.1016/j.nuclphysb.2007.07.008.

[95] F. H. L. Essler and R. M. Konik, *Finite-temperature dynamical correlations in massive integrable quantum field theories*, Journal of Statistical Mechanics: Theory and Experiment **2009**(09), P09018 (2009), doi:10.1088/1742-5468/2009/09/p09018.

[96] F. H. L. Essler and R. M. Konik, *Finite-temperature lineshapes in gapped quantum spin chains*, Phys. Rev. B **78**, 100403 (2008), doi:10.1103/PhysRevB.78.100403.

[97] H. Saleur, *A comment on finite temperature correlations in integrable qft*, Nuclear Physics B **567**(3), 602 (2000), doi:https://doi.org/10.1016/S0550-3213(99)00665-3.

[98] J. D. Nardis, D. Bernard and B. Doyon, *Diffusion in generalized hydrodynamics and quasiparticle scattering*, SciPost Phys. **6**, 49 (2019), doi:10.21468/SciPostPhys.6.4.049.

[99] L. Piroli, J. De Nardis, M. Collura, B. Bertini and M. Fagotti, *Transport in out-of-equilibrium xxz chains: Nonballistic behavior and correlation functions*, Phys. Rev. B **96**, 115124 (2017), doi:10.1103/PhysRevB.96.115124.

[100] B. Doyon, *Exact large-scale correlations in integrable systems out of equilibrium*, SciPost Phys. **5**, 54 (2018), doi:10.21468/SciPostPhys.5.5.054.

[101] G. A. El, A. M. Kamchatnov, M. V. Pavlov and S. A. Zykov, *Kinetic equation for a soliton gas anditshydrodynamic reductions*, Journal of Nonlinear Science **21**(2), 151 (2011), doi:10.1007/s00332-010-9080-z.

[102] B. Doyon and J. Myers, *Fluctuations in ballistic transport from Euler hydrodynamics*, arXiv e-prints arXiv:1902.00320 (2019).

[103] C. M. Bender, *Introduction to pt-symmetric quantum theory*, Contemporary Physics **46**(4), 277 (2005), doi:10.1080/00107500072632.

[104] B. Doyon and T. Yoshimura, *A note on generalized hydrodynamics: inhomogeneous fields and other concepts*, SciPost Phys. **2**, 014 (2017), doi:10.21468/SciPostPhys.2.2.014.

[105] J.-S. Caux, B. Doyon, J. Dubail, R. Konik and T. Yoshimura, *Hydrodynamics of the interacting Bose gas in the Quantum Newton Cradle setup*, SciPost Phys. **6**, 70 (2019), doi:10.21468/SciPostPhys.6.6.070.

[106] M. Schemmer, I. Bouchoule, B. Doyon and J. Dubail, *Generalized hydrodynamics on an atom chip*, Phys. Rev. Lett. **122**, 090601 (2019), doi:10.1103/PhysRevLett.122.090601.

[107] B. Doyon, H. Spohn and T. Yoshimura, *A geometric viewpoint on generalized hydrodynamics*, Nuclear Physics B **926**, 570 (2018), doi:https://doi.org/10.1016/j.nuclphysb.2017.12.002.

[108] V. B. Bulchandani, R. Vasseur, C. Karrasch and J. E. Moore, *Solvable hydrodynamics of quantum integrable systems*, Phys. Rev. Lett. **119**, 220604 (2017), doi:10.1103/PhysRevLett.119.220604.

[109] C. Karrasch, D. M. Kennes and J. E. Moore, *Transport properties of the one-dimensional hubbard model at finite temperature*, Phys. Rev. B **90**, 155104 (2014), doi:10.1103/PhysRevB.90.155104.

[110] M. Ljubotina, M. Žnidarič and T. Prosen, *Spin diffusion from an inhomogeneous quench in an integrable system*, Nature Communications **8**, 16117 EP (2017).

[111] E. Ilievski, J. De Nardis, M. Medenjak and T. c. v. Prosen, *Superdiffusion in one-dimensional quantum lattice models*, Phys. Rev. Lett. **121**, 230602 (2018), doi: 10.1103/PhysRevLett.121.230602.

[112] J. De Nardis, D. Bernard and B. Doyon, *Hydrodynamic diffusion in integrable systems*, Phys. Rev. Lett. **121**, 160603 (2018), doi:10.1103/PhysRevLett.121.160603.

[113] A. Cortés Cubero and M. Panfil, *Thermodynamic bootstrap program for integrable qft's: form factors and correlation functions at finite energy density*, Journal of High Energy Physics **2019**(1), 104 (2019), doi:10.1007/JHEP01(2019)104.

[114] B. Doyon, *Finite-temperature form factors in the free majorana theory*, Journal of Statistical Mechanics: Theory and Experiment **2005**(11), P11006 (2005), doi: 10.1088/1742-5468/2005/11/p11006.

[115] B. Doyon, *Finite-temperature form factors: a review*, Symmetry, Integrability and Geometry: Methods and Applications (2007), doi:10.3842/sigma.2007.011.

[116] M. Medenjak, J. De Nardis and T. Yoshimura, *Diffusion from Convection*, arXiv e-prints arXiv:1911.01995 (2019).

[117] B. Doyon, *Diffusion and superdiffusion from hydrodynamic projection*, arXiv e-prints arXiv:1912.01551 (2019).

[118] B. Doyon and H. Spohn, *Dynamics of hard rods with initial domain wall state*, Journal of Statistical Mechanics: Theory and Experiment **2017**(7), 073210 (2017), doi:10.1088/1742-5468/aa7abf.

[119] B. Doyon and H. Spohn, *Drude Weight for the Lieb-Liniger Bose Gas*, SciPost Phys. **3**, 039 (2017), doi:10.21468/SciPostPhys.3.6.039.

[120] A. Bastianello, B. Doyon, G. Watts and T. Yoshimura, *Generalized hydrodynamics of classical integrable field theory: the sinh-Gordon model*, SciPost Phys. **4**, 45 (2018), doi:10.21468/SciPostPhys.4.6.045.

[121] B. Doyon, *Generalized hydrodynamics of the classical toda system*, Journal of Mathematical Physics **60**(7), 073302 (2019), doi:10.1063/1.5096892.

[122] H. Spohn, *Generalized gibbs ensembles of the classical toda chain*, Journal of Statistical Physics (2019), doi:10.1007/s10955-019-02320-5.

[123] V. B. Bulchandani, X. Cao and J. E. Moore, *Kinetic theory of quantum and classical toda lattices*, Journal of Physics A: Mathematical and Theoretical **52**(33), 33LT01 (2019), doi:10.1088/1751-8121/ab2cf0.

[124] X. Cao, V. B. Bulchandani and H. Spohn, *The GGE averaged currents of the classical Toda chain*, arXiv e-prints arXiv:1905.04548 (2019).

[125] A. De Luca, M. Collura and J. De Nardis, *Nonequilibrium spin transport in integrable spin chains: Persistent currents and emergence of magnetic domains*, Phys. Rev. B **96**, 020403 (2017), doi:10.1103/PhysRevB.96.020403.

[126] V. B. Bulchandani, R. Vasseur, C. Karrasch and J. E. Moore, *Bethe-boltzmann hydrodynamics and spin transport in the xxz chain*, Phys. Rev. B **97**, 045407 (2018), doi:10.1103/PhysRevB.97.045407.

[127] M. Collura, A. De Luca and J. Viti, *Analytic solution of the domain-wall nonequilibrium stationary state*, Phys. Rev. B **97**, 081111 (2018), doi:10.1103/PhysRevB.97.081111.

[128] E. Ilievski and J. De Nardis, *Ballistic transport in the one-dimensional hubbard model: The hydrodynamic approach*, Phys. Rev. B **96**, 081118 (2017), doi:10.1103/PhysRevB.96.081118.

[129] B. Bertini, L. Piroli and M. Kormos, *Transport in the sine-gordon field theory: From generalized hydrodynamics to semiclassics*, Phys. Rev. B **100**, 035108 (2019), doi:10.1103/PhysRevB.100.035108.

[130] M. Esposito, U. Harbola and S. Mukamel, *Nonequilibrium fluctuations, fluctuation theorems, and counting statistics in quantum systems*, Rev. Mod. Phys. **81**, 1665 (2009), doi:10.1103/RevModPhys.81.1665.

[131] J. Myers, M. J. Bhaseen, R. J. Harris and B. Doyon, *Transport fluctuations in integrable models out of equilibrium*, arXiv e-prints arXiv:1812.02082 (2018).

[132] B. Doyon, *Thermalization and pseudolocality in extended quantum systems*, Communications in Mathematical Physics **351**(1), 155 (2017), doi:10.1007/s00220-017-2836-7.

[133] B. Doyon, *Lower bounds for ballistic current and noise in non-equilibrium quantum steady states*, Nuclear Physics B **892**, 190 (2015), doi:https://doi.org/10.1016/j.nuclphysb.2015.01.007.

[134] P. Chebotarev and E. Shamis, *The Matrix-Forest Theorem and Measuring Relations in Small Social Groups*, arXiv Mathematics e-prints math/0602070 (2006).

[135] M. Borsi, B. Pozsgay and L. Pristyák, *Current operators in Bethe Ansatz and Generalized Hydrodynamics: An exact quantum/classical correspondence*, arXiv e-prints arXiv:1908.07320 (2019).

[136] G. El, *The thermodynamic limit of the whitham equations*, Physics Letters A **311**(4), 374 (2003), doi:https://doi.org/10.1016/S0375-9601(03)00515-2.

[137] G. A. El and A. M. Kamchatnov, *Kinetic equation for a dense soliton gas*, Phys. Rev. Lett. **95**, 204101 (2005), doi:10.1103/PhysRevLett.95.204101.

[138] T. Giamarchi, *Quantum Physics in One Dimension*, Oxford University Press, doi:10.1093/acprof:oso/9780198525004.001.0001 (2003).

[139] E. Bettelheim, A. G. Abanov and P. Wiegmann, *Orthogonality catastrophe and shock waves in a nonequilibrium fermi gas*, Phys. Rev. Lett. **97**, 246402 (2006), doi:10.1103/PhysRevLett.97.246402.

[140] E. Bettelheim and L. Glazman, *Quantum ripples over a semiclassical shock*, Phys. Rev. Lett. **109**, 260602 (2012), doi:10.1103/PhysRevLett.109.260602.

[141] I. V. Protopopov, D. B. Gutman, P. Schmitteckert and A. D. Mirlin, *Dynamics of waves in one-dimensional electron systems: Density oscillations driven by population inversion*, Phys. Rev. B **87**, 045112 (2013), doi:10.1103/PhysRevB.87.045112.

[142] P. Öhberg and L. Santos, *Dynamical transition from a quasi-one-dimensional bose-einstein condensate to a tonks-girardeau gas*, Phys. Rev. Lett. **89**, 240402 (2002), doi:10.1103/PhysRevLett.89.240402.

[143] P. Pedri, L. Santos, P. Öhberg and S. Stringari, *Violation of self-similarity in the expansion of a one-dimensional bose gas*, Phys. Rev. A **68**, 043601 (2003), doi:10.1103/PhysRevA.68.043601.

[144] A. S. Campbell, D. M. Gangardt and K. V. Kheruntsyan, *Sudden expansion of a one-dimensional bose gas from power-law traps*, Phys. Rev. Lett. **114**, 125302 (2015), doi:10.1103/PhysRevLett.114.125302.

[145] I. Bouchoule, S. S. Szigeti, M. J. Davis and K. V. Kheruntsyan, *Finite-temperature hydrodynamics for one-dimensional bose gases: Breathing-mode oscillations as a case study*, Phys. Rev. A **94**, 051602 (2016), doi:10.1103/PhysRevA.94.051602.

[146] B. Bertini, L. Piroli and P. Calabrese, *Universal broadening of the light cone in low-temperature transport*, Phys. Rev. Lett. **120**, 176801 (2018), doi:10.1103/PhysRevLett.120.176801.

[147] B. Bertini and L. Piroli, *Low-temperature transport in out-of-equilibrium XXZ chains*, Journal of Statistical Mechanics: Theory and Experiment **2018**(3), 033104 (2018), doi:10.1088/1742-5468/aab04b.

[148] J.-S. Caux, *Correlation functions of integrable models: A description of the abacus algorithm*, Journal of Mathematical Physics **50**(9), 095214 (2009), doi:10.1063/1.3216474.

[149] A. J. A. James, R. M. Konik, P. Lecheminant, N. J. Robinson and A. M. Tsvelik, *Non-perturbative methodologies for low-dimensional strongly-correlated systems: From non-abelian bosonization to truncated spectrum methods*, Reports on Progress in Physics **81**(4), 046002 (2018), doi:10.1088/1361-6633/aa91ea.

[150] M. Ljubotina, M. Žnidarič and T. c. v. Prosen, *Kardar-parisi-zhang physics in the quantum heisenberg magnet*, Phys. Rev. Lett. **122**, 210602 (2019), doi:10.1103/PhysRevLett.122.210602.

[151] S. Gopalakrishnan and R. Vasseur, *Kinetic theory of spin diffusion and superdiffusion in xxz spin chains*, Phys. Rev. Lett. **122**, 127202 (2019), doi:10.1103/PhysRevLett.122.127202.

[152] S. Gopalakrishnan, R. Vasseur and B. Ware, *Anomalous relaxation and the high-temperature structure factor of xxz spin chains*, Proceedings of the National Academy of Sciences **116**(33), 16250 (2019), doi:10.1073/pnas.1906914116.

[153] J. De Nardis, M. Medenjak, C. Karrasch and E. Ilievski, *Anomalous spin diffusion in one-dimensional antiferromagnets*, arXiv e-prints arXiv:1903.07598 (2019).

[154] M. Dupont and J. E. Moore, *Universal Spin Dynamics in Infinite-Temperature One-Dimensional Quantum Magnets*, arXiv e-prints arXiv:1907.12115 (2019).

[155] A. Das, M. Kulkarni, H. Spohn and A. Dhar, *Kardar-Parisi-Zhang scaling for the Faddeev-Takhtajan classical integrable spin chain*, arXiv e-prints arXiv:1906.02760 (2019).

[156] J. De Nardis, T. Yoshimura, M. Medenjak, E. Ilievski, B. Doyon and T. Sasamoto, *in preparation* .

[157] D. Takahashi and J. Satsuma, *A soliton cellular automaton*, Journal of the Physical Society of Japan **59**(10), 3514 (1990), doi:10.1143/JPSJ.59.3514.

[158] R. Inoue, A. Kuniba and T. Takagi, *Integrable structure of box–ball systems: crystal, bethe ansatz, ultradiscretization and tropical geometry*, Journal of Physics A: Mathematical and Theoretical **45**(7), 073001 (2012), doi:10.1088/1751-8113/45/7/073001.

[159] D. A. Croydon, T. Kato, M. Sasada and S. Tsujimoto, *Dynamics of the box-ball system with random initial conditions via Pitman's transformation*, arXiv e-prints arXiv:1806.02147 (2018).